UNIVERSITÀ DEGLI STUDI DI MILANO

PhD School in: Agriculture, Environment, Bioenergy – XXXII cycle

DiSAA - Department of Agricultural and Environmental Sciences - Production, Landscape, Agroenergy

GERMPLASM EVALUATION FOR SALT TOLERANCE IN *JAPONICA* RICE

AGR/13

PhD CANDIDATE: Michele Pesenti

TUTOR: Prof. Gian Attilio Sacchi

PhD PROGRAM COORDINATOR: Prof. Daniele Bassi

A.A. 2018 – 2019

INDEX

General abstract 3

Introduction 6

1. **Effects of salinity on soils** 7
2. **Effects of salinity on crops and tolerance mechanisms** 7
3. **Salt stress responses and tolerance in rice** 9
4. **Improving salt tolerance in rice** 16
5. **References** 18

Objectives and activities 22

Genome-wide association study of salinity tolerance during germination and seedling emergence from soil in rice (*Oryza sativa*, L.) 23

Genome-wide association study for salinity tolerance during growth in a panel of *japonica* rice (*Oryza sativa,* L.) accessions 73

Possible involvement of *OsTPP* genes in trehalose metabolism and starch mobilization during rice germination and seedling emergence under salt condition 118

General conclusions 144

General abstract

Soil salinity is one of the environmental constraints that affect crop cultivation worldwide. Among cereals, rice (*Oryza sativa* L.) is one of the most salt-sensitive although cultivars can differ in their response to salt stress. In European coastal rice areas, the salt wedge intrusion phenomenon caused by the rise in the sea levels consequent to the ongoing climate changes is provoking a tendency toward salinization in the adjacent paddy fields and coastal areas where rice is grown. Thus, the identification of rice cultivars tolerant to salt stress and the dissection of salt stress tolerance mechanisms are of high interest for European rice breeding.

Plant responses to salt stress are complex depending on the combination of the activity of many metabolic pathways and of the several involved genes, and thus they are difficult to control and/or engineer. Exploiting natural variation that occurs in worldwide genotypes may be a powerful approach to discover new genes and/or alleles involved in salt tolerance. Since salinity has many different effects on plants, several different tolerance mechanisms (osmotic tolerance, ion exclusion and/or tissue tolerance) exist. The predominance of a specific tolerance mechanism over others depends on salt stress intensity (severity x duration) and plant developmental stage.

Concerning *indica* rice subspecies, several QTLs and some genes involved in the phenotypic variability in response to salt stress have been identified and exploited in breeding programs for genetic improvement of élite varieties. On the contrary, in the case of *japonica* subspecies, far fewer informations are available.

General objective of this work is the discovery of novel molecular variability at different developmental stages in *japonica* rice cultivars resulting in tolerance to the mild salt stress conditionsreported for some European rice areas. In major detail, possible research deliverables are the identification of QTLs, alleles and/or molecular markers exploitable in future genetic improvement programs.

The stated goal was pursued by a Genome Wide Association Study (GWAS) using a panel of 277 accessions of *japonica* rice already genotyped-by-sequencing producing 31,421 SNPs.

The accession panel was subjected to a two-year phenotyping through the evaluation, at different growth stages, of traits [leaf visual injuries score (SES), tillering rate, plant height, flowering time, flag leaf chlorophyll index, and flowering time] sensitive to salt stress. For these activities, plants were grown in greenhouse environment, in pots filled with paddy soil maintained submerged and, starting from the 4^{th} leaf stage, subjected to about 5 dSm^{-1}soil electric conductivity (ECe) by the addition of adequate NaCl amounts. For all the measurements obtained from the two-years data, the Least Mean Square (LMS) were calculated. To be able to compare two-year data and different parameters with different range amplitudes, all data were standardized by Z-score transformation, and subjected to two-step cluster analysis, achieving a Core Collection of the 5 most tolerant and the 5 most susceptible varieties in response to salt stress.

Moreover, the seed germination dynamics and the seedling emergence rate were analyzed under high salt environment (150 mM NaCl for germination, and about 10 dSm^{-1} soil ECe for emergence) in a single-year experiment.

For each of the 277 rice accessions the effect of salt on each trait was evaluated in terms of Stress Susceptibility Index (SSI) evaluating the performance of a single accession in relation to the whole collection. An association analysis between the phenotyping and the GBS results was carried out using Tassel 3.0 to calculate a Mixed Linear Model (MLM). The critical p-values for assessing the significance of SNPs were calculated based on a False Discovery Rate (FDR) separately for each trait; a FDR cut-off of α 0.05 was used for determining significance. Currently, a total of 33 Marker-Trait Associations (MTAs) between SNPs and the analyzed salt stress-related traits have been identified. Several *loci* were subsequently identified by intersecting the MTAs with the genes annotated on the Nipponbare reference genome.

GWAS analysis carried out on germination and emergence parameters highlighted the presence of interesting associations between two markers and two *loci* in linkage disequilibrium with them: *Os09g0369400* and *Os07g0485000*, coding for a Trehalose 6-Phosphate Phosphatase 7 (*OsTPP7*) and a Trehalose 6-Phosphate Phosphatase 10 (*OsTPP10*), respectively, known to be involved in anoxia and salt stress response. Members of the *OsTPPs* family playing a role in the Trehalose-6P (T6P)/SnRK1 system that regulates the C-metabolism under stress conditions. Indeed, high levels of T6P inhibit the cell energetic metabolism that is, on the contrary, stimulated when T6P is dephosphorylated by TPPs activities. The possible involvement of *OsTPP7/10* in this regulative network and in the different salt sensitiveness of the different rice accessions has been investigated in two *japonica* accessions Olcenengo and SR113, salt tolerant and sensitive, respectively. The results obtained indicate that under salt condition (NaCl 150 mM) the coleoptile growth rate is less affected in Olcenengo where the T6P levels are quite lower than in SR113. The rate of growth in the controls appeared after 24 h from sowing and it was greater in Olcenengo than in SR113. Salt stress reduces coleoptile growth rate in each genotype but in SR113 the effect was more marked. In salt condition, Olcenengo showed a higher and earlier *OsTPP10* expression than SR113; this could trigger SnRK1 activity and thus the mobilization of starch (α-amylase activity), supporting the energy needed for seed germination and coleoptile elongation under salt stress. The data confirmed that in the general framework of stress tolerance, members of the *OsTPPs* family play a key role to overcome saline stress during the first stages of germination.

Moreover, on the basis of GWAS carried out on SES parameter, a QTL including a few genes that in the *indica* rice genome are localized within the major salinity tolerance-related QTL 'SalTol' have been identified. Among them, the gene encoding the vacuolar H^+-pyrophosphatase 6 (*OsOVP6*) is present. Since OsOVP6 activity is suggested to be important in the network of the transport activities concerning Na^+ and K^+ transmembrane movement related to plant salt stress susceptibility/tolerance, an in depth physiological approach evaluating this possibility has been conducted. Two *japonica* salt-tolerant varieties (Galileo and Virgo), one *japonica* rice variety (PL12) known to be salt-susceptible, and the salt-tolerant *indica* genotype FL478 (containing the 'SalTol' QTL) have been considered.

The Na^+/K^+ ratio, Na^+ influx and K^+ efflux, H^+ extrusion, cytosolic and vacuolar pH by in vivo ^{31}P-NMR techniques were evaluated in roots. The results obtained, together with the electrophysiological evaluation of the whole root Na^+ conductance, allow to define a picture that may explain the different salt tolerance observed among the genotypes analyzed. In this picture, *OsOVP6* plays a central role.

In general, good variability within the population was observed for all the analyzed parameters. Salt stress tolerance is a multi-genic complex trait, and GWAS has proven to be a powerful tool for detecting natural variation underlying complex traits in crops.

Through association analysis, several MTAs have been highlighted, with the identification of interesting *loci*, involved in the salt stress response. In particular, the idea of the function of two genes belonging to the *OsTPPs* family has been reinforced, confirming that in the general framework of salt tolerance, *OsTPPs* play a key role to overcome the stress during the germination stages. In this context, two varieties with contrasting behavior have been identified within the collection, Olcenengo and SR113, very tolerant and susceptible, respectively.

Moreover, the idea of the vacuolar H^+-pyrophosphatase function has been reinforced, too, since OsOVP6 activity is suggested to be important in the network of the transport activities concerning Na^+ and K^+ transmembrane movement related to plant salt stress tolerance.

Finally, by evaluating the overall performance of each genotype of the population in relation to each parameter measured along the two-years experiment, a "core collection" of the 5 most tolerant and the 5 most susceptible varieties has been identified.

Introduction

Crop production is threatened by several biotic and abiotic stresses causing dramatic worldwide yield losses (Pitman and Läuchli, 2002; Atkinson and Urwin, 2012). Abiotic stresses mainly include drought, heat, cold and soil salinity, and their negative influence on crops could increase in consequence to the expected global warming. This is particularly probable for what concerns soil salinity (Reddy et al., 2017).

A soil is generally defined as saline when the electrical conductivity (EC) of its paste extract (EC_e) exceeds 4 dS m^{-1} at 20°C and shows an exchangeable sodium percentage (ESP) equal to 15% (Jamil et al., 2011). When Na^+ and Cl^- are the predominant ions, the value of 4 dS m^{-1} corresponds to about 40 mM NaCl. In the presence of such EC values the yield of most cultivated plants is drastically reduced. Nevertheless, some species show significant yield contractions at soil EC_e values lower than 4 dS m^{-1} (Munns, 2005; Jamil et al., 2011).

Currently more than 20% of globally cultivated lands and 33% of irrigated agricultural lands are affected by salinity (Pitman and Läuchli, 2002). Furthermore, of concern is the fact that the areas at risk are increasing at a rate of about 10% per year due to the ongoing global climate change. If the climatic conditions will continue to change at this rate, it is estimated that by 2050 more than 50% of the total currently cultivated land will be salinized (FAO, 2008; Jamil et al., 2011).

Salinity in the soil can be due to both natural (primary salinity) and anthropogenic (secondary salinity) causes. Accretion of salts in the soil surface layers is caused by different factors in different geological and climatic regions (Reynolds et al., 2001). In coastal areas higher sea levels bring saline water further inland and/or promote salinization of surface watercourses by the so-called salt wedge ascent phenomenon (Smajgleet al., 2015). Low rainfall, high surface evapotranspiration, rock erosion and some exceptional events such as cyclones, that in coastal areas can reduce barriers between cultivated soils and sea, as happened in 2011 in Myanmar, may further complicate the situation.

Irrigation is the most important source of secondary salinity (Pannell and Ewing, 2006). The prolonged use of poor-quality water, exceedingly rich in salts (brackish), causes deterioration of the soil over time. The problem is drastically accentuated in areas where high evapotranspiration is present. Further sources of salinity of anthropic origin can derive from animal wastewater, fertilizer residues and wastewater from civil uses managed with poor attention.

1. Effects of salinity on soils

The general term "salinity" includes all the problems due to the salts present in the soil. More precisely, these soils are classifiable in three categories: **saline properly**, **sodic** (or alkaline), and **saline-sodic** (Shahid and ur Rahmam, 2010).

Saline soils are dominated by the presence of Na^+ cations, with electrical conductivity (EC) values greater than 4 dS m^{-1}, an ESP value of less than 15, and pH values lower than those of sodic soils. The **sodic** (or alkaline) **soils**, are characterized by the presence of high concentrations of carbonates and bicarbonates, with excess of Na^+ on the clay exchange sites. Usually, these soils are deficient in nitrogen, phosphorus and zinc, have pH values higher than 8.5 (in some cases even higher than 10.0), and an ESP higher than 15. Moreover, these soils present poor structure and poor hydraulic conductivity.

Table 1. Parameters distinguishing different saline soils

Kind of salinity	ECs (dS m^{-1})	ESP (%)	pH
Saline	> 4,0	< 15	< 8,5
Sodic	< 4,0	> 15	> 8,5
Saline-sodic	> 4,0	> 15	< 8,5

EC: Electrical Conductivity. The measurement of electrical conductivity, by means of a conductivity meter, allows the evaluation of the quantity of soluble salts present in the soil. Its value is directly proportional to the concentration of salts in the soil solution, and to the dissociability of the molecule, while it is inversely proportional to the molecular weight. EC is measured in dS m^{-1} or mS cm^{-1} (dS m^{-1} = mS cm^{-1}). ESP: Exchangeable Sodium Percentage. This value (calculable with the formula ESP = [Na] / CEC x 100) is useful for predicting phenomena of deterioration of the physical characteristics of the soil that may occur in response to sodium percentage increases in the soil solution. ([Na] = sodium concentration; CEC = Cation Exchange Capacity).

Salinization has negative effects on the soil, leading to de-flocculation and rise in pH value. At high concentrations Na^+ is adsorbed on the exchange surfaces of clay and organic colloids, replacing calcium and magnesium; this phenomenon leads to the disintegration of the soil structure and, in the long term, to its compaction (Richards, 1954; Kovda, 1977). Consequently, if plants are present, problems of radical hypoxia can arise due to the reduced permeability to oxygen of the soil and to the worsening of drainage. Moreover, the increase in pH values diminishes the solubility of some macro- and micro-elements and thus reduces their availability for plants (Kovda, 1977).

2. Effects of salinity on crops and tolerance mechanisms

Salt tolerance for crop plants means the ability to grow, albeit more slowly, and produce a harvestable yield without marked yield losses. Based on their salt tolerance, plants can be divided

into two groups: **halophytes** and **glycophytes**. Halophytes are very salt-tolerant plants normally found in brackish environments; in contrast, glycophytes are highly susceptible and live in environments where the salt concentrations in soils are low. Glycophytes tend to limit the flow of excess ions towards the shoot through a control at the level of the radical xylem, while halophytes tend to absorb and transport Na^+ ions more quickly to the aerial part of the plant, so that the roots normally have lower NaCl concentrations than the rest of the plant.

Salinity acts negatively on plant growth through some effects that rise shortly after its occurrence, and through other effects detectable in longer times. The earlier ones are defined as *shoot salt accumulation-independent effects,* the later ones are termed *ionic phase effects*, related to the toxic effects exerted by the ions, mainly Na^+ and Cl^-, that accumulate with the time in the tissues (Roy et al., 2014). The consequences of the *shoot salt accumulation-independent effects,* originally described by Munns and Tester (2008) as the *osmotic phase* of salt stress, primarily consist in the stomatal closure leading to an increase in leaf temperature (Sirault et al., 2009) and a marked reduction of the production of new leaves leading to a decreases in shoot elongation (Rajendran et al., 2009). The consequences of the *ionic phase effects* are damage to enzyme structure and activity leading to imbalances in the primary metabolic pathways and accumulation of Reactive Oxygen Species (ROS), in turn affecting structure and activity of macromolecules and membranes. The bulk of these effects, more evident on the older leaves that are subjected to premature senescence, has impacts on plant growth and development (Roy et al., 2014).

Due to the several and different effects of salt stress, many mechanisms have been evolved by plants to tolerate this unfavorable condition. A very clear synthesis of them has been reported by Roy et al., 2014 and by Ismail et al. (2014).

Osmotic tolerance

The mechanisms involved in this kind of tolerance are very far from being clarified. An involvement of signals perceiving salt condition in the soil, rapidly transduced in responses at the shoot level, has been hypothesized. Several experimental evidences pointed to ROS (Mittler et al., 2011; Formentin et al., 2018), long-distance chemical (i.e. Ca^{2+}) and/or electrical waves (Maischak et al., 2010), but further research is required to obtain a better understanding of osmotic tolerance. At cellular level, osmotic stress responses involve the ability to increase the value of the solute component of water potential (Ψ_π), in order to maintain a negative out-in gradient of water potential, and simultaneously an efficient hydraulic conductivity (L_p) of the plasma membrane.

Ion exclusion

This general mechanism is predominant in the root systems. It consists in the integrated regulation of the activity of several transporters that reduce the uptake of Na^+ and Cl^- into the root and/or promote their efflux from the root into the soil, their accumulation in the root cell vacuole and their retrieval from the root xylem. These mechanisms result in a limited root-to-shoot translocation of the two (toxic) ions preventing their accumulation at concentrations capable to affect negatively metabolism and development of the active tissues of the shoot.

Tissue tolerance

Tissue tolerance is substantially based on the activity of transport mechanisms able to compartmentalize in the cell apoplast and/or accumulate them in the vacuole the Na^+ and Cl^- ions coming from roots, and to counteract the osmotic consequences of this event through the synthesis of compatible solutes (proline, betaines, sucrose, trehalose, etc.) in the cytosol. Simultaneously, the possible excess of ROS generated by the residual amounts of Na^+ and Cl^- is counteracted by the stimulation of the cellular antioxidant systems.

The two last mechanisms (ion exclusion and tissue tolerance) should both be interpreted in the context of maintaining high tissue K^+/Na^+ ratios in plants under salt condition, and hence high cytosolic K^+/Na^+ ratios, a key salt tolerance trait (Shabala and Pottosin, 2014). Indeed, high external Na^+ competitively inhibits K^+ uptake and at high cellular concentrations Na^+ displaces K^+, affecting negatively its physiological functions, with consequent impairment of plant growth.

3. Salt stress responses and tolerance in rice

Oryza sativa and *Oryza glaberrima* are the cultivated species of the *Oryza* genus in the Poaceae family. In particular, *O. sativa* is a staple food for over one-half of the world population providing 50%–80% of the calories consumed for more than three billion people (Hoang et al., 2016 and references therein). Rice is cultivated in 114 out of the 193 Countries over the world in six continents, Asia, Africa, Australia, Europe, Latin America and North America for a total yearly acreage of about 170 million ha and a production of about approximately 480 million metric tons of milled grain (FAO, 2018). It has been evaluated that in the next years this amount should increase by about 1% $year^{-1}$ to meet the need for food of the world's increasing population. Soil salinity might

be one of the major obstacles to overcome, considering that rice is quite sensitive, and among the cereals the most sensitive one, to salt-induced stress (Munns and Tester, 2008). A threshold as low as of 3 dS m^{-1} for soil EC_e is reported to cause yield losses of about 10% in many cultivated varieties (USDA, 2016) whereas, generally, a soil is only considered saline (salt-affected) if it has an ECe (electrical conductivity of its saturation extract) above 4 dS m^{-1} (Rengasamy, 2006). Losses in the range of 40%-50% are recorded when the soil EC_e is higher than 7.0 dS m^{-1}(Umali, 1993).

Although rice is considered sensitive to salinity, some varieties, mainly belonging to the *indica* ssp., show a relative tolerance, whereas within the *japonica* ssp. this tolerance trait is less described and, probably, widespread (Bertazzini et al., 2018).

Among the physiological traits conferring salt tolerance, the growth vigour emerges as a relevant stress-avoidance mechanism (Yeo et al., 1990; Platten et al., 2013). Indeed, in fast-growing rice genotypes the concentrations of Na^+ observed in the shoot are usually lower (since the ion is diluted in the large biomass) than those in the slowly growing ones cultivated on the same soil. Nevertheless, this observation results in a general rule only under a mild stress condition, i.e., EC_e in the range 4-5 dS m^{-1} or no more than 60 mM NaCl when plants are grown in soil or in hydroponic conditions (Platten et al., 2013). Indeed, under more severe salt stress the influx of Na^+ is massive, overwhelming the dilution effect of growth and minimizing the differences due to different vigor. The ions present in the soil solution enter the root along with water through the apoplastic and symplastic pathways (Das et al., 2015). In the former case, ions move from celltocell through the intercellular spaces until they reach the xylem if along this path, they are not blocked by the Casparian strip and the suberin lamellae present at the exodermis and endodermis levels. The presence of the Casparian strip and suberin lamellae restrict the movement of ions forcing them towards the symplastic pathway, that requires the intervention of selective transport proteins (ion channels and/or carriers). In rice, as well as in other plants, non-negligible amounts of Na^+ from the soil solution may reach the xylem and thus the shoot only by the apoplastic pathway via a so-called bypass flow (Yeo et al. 1987; Krishnamurthiet al., 2009; 2011). This flow consists in a bypassing of the symplast in regions where the apoplastic barriers are underdeveloped or lacking, like in young roots and root tips or at the sites of origin of lateral roots. By screening 14-day-old seedlings of low- and high- Na^+-transporting Recombinant Inbred Lines (RILs) of rice, Faiyue et al. (2012) concluded that bypass flow contributes to the variability of Na^+ uptake in rice and that it should be considered an important trait contributing to salinity tolerance in this crop cereal. Since the composition, microstructure and localization of suberin may also have a great impact on the formation of efficient

barriers to water and solutes like Na^+, a correlation between these properties and variability in salt tolerance among rice genotypes is expected (Chen et al., 2011; Byrt et al., 2018). Recently, it has been demonstrated that the class II *Trehalose Phosphate Synthase (TPS)* gene family member *OsTPS8* controls salinity stress tolerance as well as several key agronomic traits in rice (Vishal *et* al., 2018). The authors suggest that OsTPS8 regulates suberin deposition in rice through an ABA signaling mechanism and outline the *OsTPS8*-mediated salinity tolerance as an alternative strategy for rice crop improvement.

The uptake of Na^+ at the root-soil boundary is believed to occur mainly through Non-Selective Cation Channels (NSCC), including the Cyclic Nucleotide-Gated Channels (CNGCs) and GLutamate Receptors (GLRs), as well as through some High affinity K^+ Transporters (HKTs) and K^+ channels including the *Arabidopsis* K^+ Transporter (AKT1), and the High-Affinity K^+ Transporter (HAK). At the root-soil boundary Na^+ is absorbed into the cells through some NSCC and aquaporin(s), whose activity is influenced by Ca^{2+}, K^+ channels and HKTs (Tester and Davenport, 2003; Plett and Møller, 2010; Hanin et al., 2016; Byrt, 2017). Depending on the external Na^+ concentration, some of these transport systems mediate the accumulation of tolerable amounts of Na^+ in the plants, while others introduce noxious quantities that seriously affect the growth of the plants (Horie et al., 2001, 2007; Suzuki et al., 2016a, b). Differences in salt tolerance among rice genotypes could be the result of differences in the expression of genes encoding these transporters or in the levels of the corresponding proteins.

Limitation of Na^+ uptake at the root level may result from the downregulation of genes encoding Na^+ influx channels at the soil-root boundary, and this phenomenon may lead to a salt-tolerant behavior. In rice the downregulation of the *OsCNGC1* gene encoding a nonselective Cyclic Nucleotide-Gated Channel confers to the *indica* cultivar FL478 a relatively high tolerance to salt stress compared to sensitive cultivars where the salt condition determines the upregulation of the gene (Senadheera et al., 2009). Coherently, Mekawy et al. (2014) reported that the salt-resistant behaviour of the *indica* Egyptian Yasmine cultivar was partially due to the downregulation of *OsCNGC1*.

Differently from what observed in *Arabidopsis thaliana*, where for an aquaporin protein, AtPIP2;1, a strong Na^+ conductance has been observed, no similar result has to date been reported in rice.

According to their specificity character, the members of the HKTs family are grouped in two classes with different selectivity due to the polypeptide motif forming the pore: class I (motif SGGG),

showing specificity for Na^+, and class II (motif GGGG), present only in monocots, showing specificity for Na^+ and K^+ since it operates by a Na^+-K^+ cotransport mechanism.

With the exception of OsHKT2;1, in rice the class I HKTs, operating by a H^+ co-transport mechanism, are localized mainly at the xylem/symplast boundary of roots and shoots, where they mediate the retrieval of Na^+ from the xylem vessels to the xylem parenchyma cells. OsHKT2;1 is active at the plasma membrane of the epidermis where it mediates the influx of Na^+ into the root cells making rice quite sensitive to salt-stress, as demonstrated by Horieand colleagues who were able to improve the tolerance of rice to salinity by downregulating *OsHKT2;1* (Horie et al., 2007). In the salt-tolerant Pokkali cultivar, but not in the salt-sensitive Nipponbare, presence of *OsHKT2;2*, a close homologue of *OsHKT2;1*, determined a higher permeability to K^+ that has been suggested to play a role in the salt-tolerant character of Pokkali (Horie et al., 2001). Investigation of 49 rice cultivars showing different levels of salt tolerance allowed to identify an additional HKT, defined *No-OsHKT2;2/1*, in the highly salt tolerant Nona Bokra genotype. This HKT isoform is highly expressed in roots, shows a strong permeability to Na^+ but, different than OsHKT2;1, also to K^+ even when external Na^+ concentration is high (Oomen et al., 2012).

In the root cells of rice operates an active transporter that mediates the efflux of Na^+ into the external medium and is considered a major mechanism by which the root cells restrain the rise in Na^+ concentrations in the cytosol. This transport system is based on the activity of the H^+/Na^+ antiporter OsSOS1 (El Mahi et al., 2019), the functional homolog of the *A. thaliana* Salt Overly Sensitive1 (SOS1) protein. At the level of the epidermal cells OsSOS1 extrudes Na^+ into the external medium, i.e., the soil solution, whereas at the level of the xylem parenchyma cellsOsSOS1represents the loading system of Na^+ into the xylem.

The SOS pathway is a three-component system that regulates the homeostasis of Na^+ and salt tolerance in plants (Shi et al., 2002, 2003; Oh et al., 2009, 2010; Shang et al., 2012; Ji et al., 2013; Ma et al., 2014; Katschnig et al., 2015). One component of this system is the Ca^{2+}-binding protein SOS3 located on the plasma membrane. SOS3 senses the cytosolic Ca^{2+}concentration waves induced by the uptake of Na^+ by binding the bivalent cation. The Ca-SOS3 complex is recruited at the plasmalemma where it binds the second component of the system, the SOS2 Ser/Thr protein kinase, that is activated and becomes capable to phosphorylate SOS1, stimulating it to extrude Na^+ by a Na^+/H^+ antiporter mechanism. A similar system exists also in the leaf cells, even if structural differences are observed concerning SOS3. Although not all the experimental evidences available are consistent, it is suggested that the SOS system active in the apical meristematic cells, as well as

in the root undifferentiated zone, is actually involved in limiting the total Na^+ concentration in the root. Indeed, in the stele the system is involved in Na^+ xylem loading (Assaha et al., 2017).

Limiting the concentration of Na^+ in the xylem is crucial for salt stress tolerance. QTL analysis of rice revealed that the *SKC1* locus, which is involved in the determination of a higher K^+/Na^+ ratio in shoots, corresponds to the *OsHKT1;5* gene encoding a Na^+-selective transporter. Loss-of-function *OsHKT1;5* mutants trigger a massive accumulation of Na^+ in shoots when roots are salt-stressed. In the roots, the OsHKT1;5 protein has been localized at the plasma membrane of the cells that surround the xylem, where by a H^+/Na^+ antiport mechanism (protons direct inward the cell and Na^+ outward) it mediates the retrieval of Na^+ from the xylem vessels. The same protein is also present at the plasmalemma of xylem parenchyma cells in leaf sheaths, where it is involved in the unloading of Na^+ from the xylem. The protein is also present at the plasma membrane of the phloem parenchyma cells of diffuse vascular bundles in basal nodes where it mediates the exclusion of Na^+ from the phloem in order to prevent the transfer of the ion to the young leaf blades (Kobayashi et al., 2017). These findings suggest that the function of OsHKT1;5, whose gene expression is upregulated under salt stress, plays crucial roles in salt tolerance throughout different growth stages of rice, including the protection of the next seed generation as well as of vital leaf blades under salt stress. In the reproductive growth stage OsHKT1;4, another transporter belonging to the class I HKT family, assumes a dominant role in Na^+ exclusion from leaf blades (Suzuki et al, 2016b).
Generally speaking, differential expression levels of HKTs and differential kinetic characteristics (i.e., Na^+ affinity) among plant genotypes can underlie different tolerance through Na^+ exclusion from the leaves. Clear suggestions in this respect have been reported mainly for solanaceous species (Assah et al., 2015) whereas for rice less information is currently available.

The Na^+ ions that reach the leaves need to be rapidly redistributed to prevent hampering of metabolic processes due to their accumulation in the leaf blades. The ability of rice varieties to remobilize Na^+ from the leaf blades towards the sheaths, as well as to accumulate Na^+ in older leaves and structural shoot tissues, could promote the capability for plant survival and regular growth under salt stress.

A prerequisite for salt stress tolerance is the ability of plants of maintaining, in both root and shoot cells, a high cytosolic K^+/Na^+ ratio even when growing on saline soils (Maathuis and Amtmann, 1999; Anschütz et al., 2014) Indeed, a correct K^+/Na^+ ratio ensures optimal cellular metabolic functions whereas the competitive inhibition of K^+ uptake by Na^+ leads to an interference of Na^+ on many K^+-dependent processes, and thereby to their inhibition. The replacement of K^+ with Na^+ at

the binding sites of several enzymes causes inhibition of their activity and disturbance of the metabolic processes in which they are involved is just one of the possible mechanisms of Na^+-K^+ interference (Munns and Tester, 2008). The influx of large amounts of Na^+ into the cells produces a significant depolarization of the transmembrane electric potential, a condition that promotes a massive K^+ efflux from the cell into the apoplast through the depolarization-activated K^+ Outward Rectifier channels (KOR) such as GORK (Jayakannan et al., 2013). The K^+ efflux induced by Na^+ influx worsens the cytosolic K^+/Na^+ ratio, exacerbating the toxic effects of Na^+. SOS1, by actively extruding from the cells into the apoplast part of the Na^+ taken up, represents an important mechanism contributing to Na^+ tolerance. In xylem parenchyma cells, this extrusion will lead to the loading of Na^+ into the xylem depending on the external Na^+ concentration (Shi et al., 2000; Mangano et al., 2008; Hamam et al., 2016).

Vacuolar sequestration of Na^+ is another very important strategy in regulating the accumulation of Na^+ in the cytosol. This activity is sustained by a Na^+/H^+ antiporter (HNX) localized at the tonoplast. Under low Na^+ concentrations, NHX operates as an H^+/K^+ antiporter with non-concurrent Na^+ permeability, and only at high Na^+ concentrations NHX operates as H^+/Na^+ antiporter. Several NHX isoforms have been described, differing in localization and/or structural aspects affecting their kinetic characteristics. In rice, five genes encoding different NHX transporters have been identified. The NHX-mediated Na^+ sequestration into the vacuole is associated with the activity of K^+ channels present at the tonoplast and known as Two-Pore K^+ channels (TPKs), that under salt stress mediate a release of K^+ towards the cytosol ameliorating the K^+/Na^+ ratio in this compartment. Interestingly, vacuolar TPKs channels can act as intracellular osmosensors probably involved also in the osmotic responses to salt stress. Retention in the vacuole of the sequestered Na^+ has been proposed as an efficient key mechanism of stress tolerance whenever its activity is accompanied with a reduced Na^+ leakage back to the cytoplasm mediated by Fast Vacuolar (FV) and Slow Vacuolar (SV) channels permeable to this ion (Isayenkov et al., 2010; Bonales-Alatorre et al., 2013a; Pottosin and Dobrovinskaya, 2014). In other words, sequestration of Na^+ in the vacuole without preventing its leaking back into the cytosol would be only partially helpful to achieve stress tolerance. To date, the activity and the role of both SV and FV Na^+ permeable channels in rice are not yet clarified.

Vacuolar $Na^+(K^+)/H^+$ exchange activities are energy-dependent. Under salt stress, they consume energy that could be otherwise used for metabolic activities (Hamam et al., 2016). In a salt-tolerant soybean genotype (S111-9) it has been shown that under salt stress an over-production

of ATP results from the activation of the plastidial NADPH-dependent Cyclic Electron Flow (CEF). This extra-ATP production sustains the vacuolar H^+-ATPase in pumping H^+ into the vacuole, thereby generating an outward (from the vacuole into the cytoplasm) proton gradient used to energize the sequestration of Na^+ in the vacuole (He at al., 2015). To date, at our best knowledge no similar mechanism has been demonstrated to exist in rice. A vacuolar H^+-Pyrophosphatase (H^+-PPase, VP) located at the tonoplast is a key element in sustaining the electrochemical potential gradient of H^+ between the cytoplasm and the vacuole, fueling the exchange of Na^+/H^+ through NHX (Zhao et al., 2006). Transgenic rice plants expressing the *A. thaliana AtHKT1;1* gene showed higher fresh weight under salinity stress, due to a lower concentration of Na^+ in the shoots. In the same plants, the root-to-shoot transport of Na^+ was also reduced consequent to an upregulation of *OsHKT1;5*. The consequent increase in the root Na^+ concentration observed in these plants was accompanied by the expression of three genes (*OsOVP4*, *OsOVP5*, and *OsOVP6*) encoding three different V-H^+-PPase isoforms, that resulted upregulated in Na^+-treated roots (Plett et al., 2010). Taken as whole, these data suggest the existence of a regulative network controlling the process of Na^+ sequestration into the vacuole. A clear definition of the genic elements that participate in this network, as well as the possible existence of allelic variations among rice genotypes showing different salt tolerance, could be particularly interesting.

Salt-induced ionic stress determines the overproduction of Reactive Oxygen Species (ROS) such as superoxide radicals (O_2^-), hydrogen peroxide (H_2O_2), and hydroxyl radicals (OH^-). Upon increase in the levels of these compounds, oxidative damage in cells and organelles due to the degradation of membranes, proteins, enzymes, and nucleic acids is observed (Abogadallah, 2010; Sharma et al., 2012). The activity of mechanisms controlling the cellular homeostasis of ROS can contribute to limit the risks of their accumulation induced by stress. Several enzymatic (superoxide dismutase, peroxidases, catalases, glutathione reductase and glutathione-S-transferase) and non-enzymatic (ascorbate, reduced glutathione) scavengers are involved in mitigating ROS-induced damage in plants under salt stress (You and Chan, 2015; Del Rıo and Lopez-Huertas, 2016;). Evaluation of ROS accumulation and of their damaging effects for the peroxidation of membrane lipids is used for phenotyping salt tolerance in cereals. The identification of ABA-dependent, ABA-independent and Ca^{2+}-mediated responses eventually resulting in reduced ROS accumulation under salt stress, as well as of the relationship between the efficiency of such mechanisms and salt tolerance in different rice genotypes are progressively increasing (Reddy et al., 2017 and references

therein; Asano et al. 2012; Schmidt et al., 2013; Campo et al, 2014; Yang and Guo, 2018). A role of ROS in stabilizing the activity of the SOS1 transporter has been described in *A. thaliana* (Chung at al., 2008).

The accumulation of compatible solutes such as proline, glycine betaine or trehalose is considered an effective strategy for the protection of plants, including rice, from salinity (Bohnert and Shen, 1999). Differential expression and/or posttranscriptional activation of key enzymes in the biosynthetic pathways of these molecules, either naturally observed among rice germplasm or induced by transgenic approaches, have been shown to be related to the acquisition of salt tolerance traits (Su et al., 2006; Karthikeyan et al., 2011; Li et al., 2011).

4. Improving salt tolerance in rice

Most of the recent breeding approaches aimed at obtaining salt-tolerant rice cultivars consist in the introgression of determinant salt-tolerance genetic traits in elite cultivars important under both the agronomical and the market point of view. The complexity of the salt-tolerance trait, that requires the combination of several independent and/or interdependent mechanisms and metabolic pathways, slows down the breeding programs and often makes difficult the obtainment of satisfactory results (Ismail and Horie, 2017; Cohen and Leach, 2019). The identification and successive use of molecular markers somehow related to salt tolerance are the basis of the so-called Marker-Assisted Selection (MAS) that can potentially speed up the breeding programs. The existence of allelic variation in the genes of interest provides useful tools for MAS.

Although *O. sativa* is considered sensitive to salinity, some traditional cultivars and landraces (mainly belonging to the *indica* ssp.), endowed with a good degree of tolerance, have been identified. The *indica* varieties Nona Bokra and Pokkali are part of this group thanks to the presence of, respectively, *OsHKT2;1/2* and *OsHKT2;2*, the two transporters responsible for maintaining a low ratio Na^+/K^+ at a symplastic level (Hamamoto et al., 2015). Studies have therefore been conducted to identify the genomic traits responsible for this feature, in order to include them in genetic improvement programs involving other varieties of commercial interest.

Through the crossing of Pokkali with the (susceptible) IR29 variety, it has been possible to produce 140 lines known as RILs (Recombinant Inbred Lines) which, after genotyping, showed on chromosome 1 the QTL (Quantitative Traits Locus) called *Saltol*, recognized as one of the major modulators responsible for the Na^+/K^+ ratio within the culm (Lin et al.,2004; Ren et al., 2005; Thomson et al., 2010; Platten et al., 2013). Still by means of the production of RILs, obtained by

crossing Nona Bokra with the susceptible variety Koshihikari (*japonica*), other QTLs have been identified, *e.g.*, qSKC7 and qSNC7, respectively involved in the regulation of the K^+ and Na^+ concentration mechanisms in the culm (Lin et al., 2004).Recently, a clear correspondence between the *SKC1* locus and the OsHKT1;5 transporter has been observed, involved in the maintenance of a low Na^+/K^+ ratio in the epigeal part of the plant (Kobayashi et al., 2017).

Several efforts have been developed for the introgression of *Saltol* in salt sensitive elite varieties belonging to *indica* or *japonica* subspecies. These activities take advantage by the identification of robust *Saltol* associated molecular markers useful to speed up the breeding programs adopting MAS approaches. Nevertheless, limits in the *Saltol* based approaches are that it is effective at early vegetative stage of the plant, that however is a very salt sensitive stage. Currently lesser information on genomic determinants involved on rice salt tolerance at reproductive stage, which is crucial for improving rice productivity under salt stress, are available. Therefore, STRS is an important trait for stable rice production in salt affected areas. Only a limited number of QTLs for STRS have been mapped using low-density SSR markers (Reza et al., 2013; Hossain et al., 2015). Recently Tiwari et al. (2016) by bulked segregant analysis using high density SNP array identified new interesting QTLs and candidate genes for stress susceptibility index (SSI) for grain yield in the sodicity tolerant *indica* rice variety CSR11.

As a general consideration it possible to state that only few studies have so far been conducted for the identification of traits responsible for salt tolerance in the varieties of the ssp. *japonica*; it will therefore be of great interest to carry out studies aimed at identifying QTLs, molecular markers, genes and their alleles involved in the salt tolerance traits in japonica cultivar. In fact, this subspecies supplies almost all the rice production in Europe and in other areas with temperate climate that, as consequences of the ongoing climatic changes are progressively subjected to mild salinization of soils. In this context, the development of new and innovative genetic sequencing techniques (NGSs) and of bioinformatic tools is providing the possibility of analyzing rapidly and in deep very large population with the objective to obtain these kinds of information and knowledge. On this way the adoption of Genome wide association study for discovering genetic determinant of complex quantitative traits, such as salt tolerance is, in crop is proving to be very efficient (Huang and Han, 2014; Volante et al., 2017; Liu and Yan, 2019).

5. References

Abogadallah, G.M. (2010). Insights into the significance of antioxidative defense under salt stress. *Plant Sign.Behav.* 5, 369-374, doi: 10.4161/psb.5.4.10873.

Anschütz, U., Becker, D., and Shabala, S. (2014). Going beyond nutrition: regulation of potassium homoeostasis as a common denominator of plant adaptive responses to environment. *J. Plant Physiol*. 171, 670–687, doi:10.1016/j.jplph.2014.01.009.

Asano, T., Hayashi, N., Kobayashi, M., Aoki, N., Miyao, A., Mitsuhara, I., Ichikawa, H., Komatsu, S., Hirochika, H., Kikuchi, S. and Ohsugi. R. (2012). A rice c.alcium-dependent protein kinase OsCPK12 oppositely modulates salt-stress tolerance and blast disease resistance. *Plant J.* 69, 26–36.

Assaha, D. V., Mekawy, A. M. M., Ueda, A. and Saneoka, H. (2015). Salinity induced expression of *HKT* may be crucial for Na^+ exclusion in the leaf blade of huckleberry (*Solanumscabrum* Mill.), but not of eggplant (*Solanum melongena* L.). *Biochem. Biophys. Res. Commun*. 460, 416–421, doi: 10.1016/j.bbrc.2015.03.048

Assaha, D.V.M., Ueda, A., Saneoka. H., Al-Yahyai, R. and Yaish, M.W. (2017). The Role of Na^+ and K^+ transporters in salt stress adaptation in glycophytes. *Front. Physiol.* 8, 509, doi:10.3389/fphys.2017.00509.

Atkinson, N. J. and Urwin, P. E. (2012). The interaction of plant biotic and abiotic stresses: from genes to the field. *J. Exp. Bot.* 63, 3523–3543.

Bertazzini, M., Sacchi, G.A. and Forlani, G. (2018).A differential tolerance to mild salt stress conditions among six Italian rice genotypes does not rely on Na^+ exclusion from shoots. *J. Plant Physiol.* 226, 145-153.

Bohnert, H.J. and Shen, B. (1999). Transformation and compatible solutes. *Sci. Hort.* 78, 237–260.

Bonales-Alatorre, E., Shabala, S., Chen, Z.-H. and Pottosin, I. (2013). Reduced tonoplast fast-activating and slow-activating channel activity is essential for conferring salinity tolerance in a facultative halophyte, quinoa. *Plant Physiol.* 162, 940–952, doi: 10.1104/pp.113.216572.

Byrt C.S., Zhao, M.C., Kourghi, M., Bose, J., Henderson, S.W., Qiu, J.E., Gilliham, M., Schultz C., Schwarz, M., Ramesh S.A. et al. (2017). Non-selective cation channel activity of aquaporin AtPIP2;1 regulated by Ca^{2+} and pH. *Plant Cell Environ.* 40, 802–815.

Byrt, C.S., Munns, R., Burton, R.A., Gilliham, M. and Wege, S., (2018). Root cell wall solutions for crop plants in saline soils. *Plant Sci.* 269, 47-55.

Campo, S., Baldrich, P., Messeguer, J., Lalanne, E., Coca, M. and San Segundo, B. (2014). Overexpression of a calcium-dependent protein kinase confers salt and drought tolerance in rice by preventing membrane lipid peroxidation. *Plant Physiol.* 165, 688–704.

Chen, T., Cai, X., Wu, X., Karahara, I., Schreiber, L. and Lin, J. (2011). Casparian strip development and its potential function in salt tolerance. *Plant Signal. Behav*. 6, 1499–1502. doi: 10.4161/psb.6.10.17054.

Chung, J.S., Zhu, J-K., Bressan, R.A., Hasegawa, P.M. and Shi, H. (2008). Reactive oxygen species mediate Na^+-induced *SOS1* mRNA stability in *Arabidopsis*. *Plant J.* 53, 554-568.

Cohen, S.P. and Leach, J.E. (2019). Abiotic and biotic stresses induce a core transcriptome response in rice. *Sci. Rep*. 9, 6273.

Das, P., Nutan, K. K., Singla-Pareek, S. L., Pareek A. (2015). Oxidative environment and redox homeostasis in plants: Dissecting out significant contribution of major cellular organelles. *Front Environ. Sci.*, 2, 70.

Del Rio, L. and Lópes-Huertas (2016). ROS generation in peroxixomes and its role in cell signaling. *Plant Cell Physiol*. 57, 1364-1367, https://doi.org/10.1093/pcp/pcw076.

El Mahi, H., Pérez-Hormaeche, J., De Luca, A., Villalta, I., Espartero, J., Gámez-Arjona, F., Fernández, J.L., Bundó, M., Mendoza, I., Mieulet, D., Lalanne, E., Lee, S-Y., Yun, D-J., Guiderdoni, E., Aguilar, M., Leidi, E.O., Pardo, J.M. and Quintero, F.J. (2019). A critical role of sodium flux via the plasma membrane Na^+/H^+exchanger SOS1 in the salt tolerance of rice. *Plant Physiol.* 180, 1046-1065.

FAO (2008). Land and plant nutrition management service. http://fao.org/agb/agl/agl1/.

FAO (2018). Rice market monitor. http://www.fao.org/3/I9243EN/i9243en.pdf.

Faiyue, B., Al-Azzawi, M.J. and Fowers, T.Y. (2015). A new screening technique for salinity resistance in rice (*Oryza sativa L.*) seedlings using bypass flow. *Plant Cell Environ.* 35, 1099–1108.

Formentin, E., Sudiro, C., Perin, G., Riccadonna, S., Barizza, E., Baldoni, E., Sacchi G.A., et al. (2018). Transcriptome and cell physiological analyses in different rice cultivars provide new insights into adaptive and salinity stress responses. *Front. Plant Sci.* 9, 204.

Hanin, M., Ebel, C., Ngom, M., Laplaze, L. and Masmoudi, K. (2016). New insights on plant salt tolerance mechanisms and their potential use for breeding. *Front. Plant Sci.* 7, 1787, doi: 10.3389/fpls.2016.01787.

Hamam, A. M., Britto, D. T., Flam-Shepherd, R. and Kronzucker, H. J. (2016). Measurement of differential Na^+ efflux from apical and bulk root zones of intact barley and *Arabidopsis* plants. *Front. Plant Sci*. 7, 272, doi: 10.3389/fpls.2016.00272.

Hamamoto, S., Horie, T., Hauser, F., Deinlein, U., Schroeder, J.I. and Uozumi, N. (2015) HKT transporters mediate salt stress resistance in plants: from structure and function to the field. *Curr. Opin. Biotechnol.* 32, 113-120.

He, Y., Fu, J., Yu, C., Wang, X., Jiang, Q., Hong, J., Lu, K., Xue, G., Yan, C., James, A., Xu, L., Chen, J. and Jiang, D. (2015). Increasing cyclic electron flow is related to Na^+ sequestration into vacuoles for salt tolerance in soybean. *J. Exp. Bot.* 66, 6877–6889.

Hoang. T.L.M., Tran, .C., Nguyen T.K.T., Williams, B., Wurm, P., Belairs, S. and Mundree, S. (2016). Improvement of salinity stress tolerance in rice: challenges and opportunities. Agronomy, 6, 54; doi:10.3390/agronomy6040054.

Horie, T., Costa, A. Kim, T.H. Han, M.J. Horie, R. Leung, H.Y. Miyao, A. Hirochika, H. An, G. Schroeder, J.I. (2007). Rice OsHKT2;1 transporter mediates large Na^+ influx component into K^+-starved roots for growth. *EMBO J.* 26, 3003–3014.

Horie, T., Yoshida, K., Nakayama, H., Yamada, K., Oiki, S. and Shinmyo, A. (2001). Two types of HKT transporters with different properties of Na^+ and K^+ transport in *Oryza sativa*. *Plant J.* 27, 129–138.

Hossain, H., Rahman, M.A., Alam, M.S. and Singh, R.K. (2015). Mapping of Quantitative Trait Loci associated with reproductive-stage salt tolerance in rice. *J. Agro. Crop Sci.* 201, 17–31.

Huang, X. and Han, B. (2014). Natural variation and genome-wide associations studies in crop plants. *Annu. Rev. Plant Biol.* 65, 531-551.

Isayenkov, S., Isner, J. C. and Maathuis, F. J. (2010). Vacuolar ion channels: roles in plant nutrition and signalling. *FEBS Lett.* 584, 1982–1988. doi: 10.1016/j.febslet.2010.02.050

Ji, H., Pardo, J.M., Batelli, G., Van Oosten, M.J., Bressan. R.A. and Li, X. (2013) The salt overly sensitive (SOS) pathway: established and emerging roles. *Mol. Plant* 6, 275–286.

Ismail, A.M., Takeda, S. and Nick, P. (2014). Life and death under salt stress: same players, different timing? J. Exp. Bot. 65, 2963–2979, https://doi.org/10.1093/jxb/eru159

Ismail, A.M. and Horie, T. (2017). Genomics, physiology, and molecular breeding approaches for improving salt tolerance. *Annu. Rev. Plant Biol.* 68, 405–34.

Jamil, A., Riaz, S., Ashraf, M. and Foolad, M. R. (2011). Gene expression profiling of plants under salt stress. *Crit. Rev. Plant Sci.* 30, 435-458.

Jayakannan, M., Bose, J., Babourina, O., Rengel, Z. and Shabala, S. (2013). Salicylic acid improves salinity tolerance in Arabidopsis by restoring membrane potential and preventing salt-induced K^+ loss via a GORK channel. *J. Exp. Bot.* 64, 2255–2268, doi: 10.1093/jxb/ert085.

Karthikeyan, A., Pandian, S.K. and Ramesh, M. (2011). Transgenic indica rice cv. ADT43 expressing a δ1-pyrroline-5-carboxylate synthetase (*P5CS*) gene from *Vigna aconitifolia* demonstrates salt tolerance. *Plant Cell Tiss. Org. Cult.* 107, 383–395.

Katschnig, D., Bliek, T., Rozema, J., and Schat, H. (2015). Constitutive high level *SOS1* expression and absence of *HKT1;1* expression in the salt accumulating halophyte *Salicornia dolichostachya*. *Plant Sci.* 234, 144–154. doi: 10.1016/j.plantsci.2015.02.011

Kobayashi, N.I., Yamaji, N., Yamamoto, H., Okubo, K., Ueno, H., Costa, A., Tanoi, K., Matsumura, H., Fujii-Kashino, M., Horiuchi, T., Nayef, M.A., Shabala, S., An, G., Ma, J.F. and Horie, T. (2017). OsHKT1;5 mediates Na^+ exclusion in the vasculature to protect leaf blades and reproductive tissues from salt toxicity in rice. *Plant J.* 91, 657-670, doi: 10.1111/tpj.13595.

Kovda, V.A. (1977). Arid land irrigation and soil fertility: problems of salinity, alkalinity, compaction. *In* Arid Land Irrigation in Developing Countries: Environmental Problems and Effects, E.B. Wothington ed, pp 211-235, Pergamon Press, U.S.A., https://doi.org/10.1016/C2013-0-02879-4.

Krishnamurthy, P., Ranathunge, K., Franke, R., Prakash, H.S., Schreiber, L. and Mathew, M.K. (2009). The role of root apoplastic transport barriers in salt tolerance of rice (*Oryza sativa* L.). *Planta*, 230, 119–134. doi: /10.1007/s00425-009-0930-6.

Krishnamurthy, P., Ranathunge, K., Nayak, S., Schreiber, L. and Mathew, M.K. (2011). Root apoplastic barriers block Na^+ transport to shoots in rice (*Oryza sativa* L.). *J. Exp. Bot.* 62, 4215–4228, doi: 10.1093/jxb/err135.

Li, H.W., Zang, B.S., Deng, X.W. and Wang, X.P. (2011). Overexpression of the trehalose-6-phosphate synthase gene *OsTPS1* enhances abiotic stress tolerance in rice. *Planta* 234, 1007–1018.

Lin, H.X., Zhu, M.Z., Yano, M., Gao, J.P., Liang, Z.W., Su, W.A., et al. (2004). QTLs for Na^+ and K^+ uptake of the shoots and roots controlling rice salt tolerance. Theor. Appl. Genet. 108, 253–60.

Liu, H. and Yan, J. (2019). Crop genome-wide association study: a harvest of biological relevance. *Plant J.* 97, 8–18

Ma, L., Zhang, H., Sun, L., Jiao, Y., Zhang, G., Miao, C., et al. (2011). NADPH oxidase AtrbohD and AtrbohF function in ROS-dependent regulation of Na^+/K^+ homeostasis in *Arabidopsis* under salt stress. *J. Exp. Bot.* 63, 305–317. doi: 10.1093/jxb/err280.

Maathuis, F. J. and Amtmann, A. (1999). K^+ nutrition and Na^+ toxicity: the basis of cellular K^+/Na^+ ratios. *Ann. Bot.* 84, 123–133. doi: 10.1006/anbo.1999.0912.

Maischak, H., Zimmermann, M.R., Felle, H.H., Boland, W., Mitho¨fer, A. (2010). Alamethicin-induced electrical long distance signaling in plants. *Plant Sig. Behav.* 5, 988-990.

Mangano, S., Silberstein, S. and Santa-María, G. E. (2008). Point mutations in the barley HvHAK1 potassium transporter lead to improved K^+-nutrition and enhanced resistance to salt stress. *FEBS Lett.* 582, 3922–3928, doi: 10.1016/j.febslet.2008.10.036

Mekawy, A., Dekoum, A., Hiroyuki, Y., Yuma, T., Akihiro U. and Hirofumi S. (2014). Growth, physiological adaptation, and gene expression analysis of two Egyptian rice cultivars under salt stress. *Plant Physiol. Biochem.* 87, 17-25, doi:10.1016/j.plaphy.2014.12.007.

Mittler, R., Vanderauwera, S., Suzuki, N., Miller, G. A. D., Tognetti, V. B., Vandepoele, K. et al. (2011). ROS signaling: the new wave? *Trends Plant Sci.* 16, 300-309.

Munns, R. (2005). Genes and salt tolerance: bringing them together. *New Phytol.* 167, 645–663.

Munns, R. and Tester, M. (2008). Mechanisms of salinity tolerance. *Annu. Rev. Plant Biol.* 59, 651-681.

Oh, D-H., Leidi, E., Zhang, Q., Hwang, S-M., Li, Y., Quintero, F.J., Jiang, X., D'Urzo, M.P., Lee, S.Y., Zhao, Y., et al (2009) Loss of halophytism by interference with SOS1 expression. *Plant Physiol* 151, 210–222.

Oh, D-H., Lee, S.Y., Bressan, R., Yun, D-J., and Bohnert, H.J. (2010). Intracellular consequences of SOS1 deficiency during salt stress. *J. Exp. Bot.* 61, 1205–1213. doi: 10.1093/jxb/erp391

Oomen, R. J., Benito, B., Sentenac, H., Rodríguez-Navarro, A., Talón, M., Véry, A. A., and Domingo, C. (2012). HKT2; 2/1, a K^+-permeable transporter identified in a salt-tolerant rice cultivar through surveys of natural genetic polymorphism. Plant J. 71, 750-762.

Pannell, D. J. and Ewing, M. A. (2006). Managing secondary dryland salinity: options and challenges. *Agri. Water Management* 80, 41-56.

Pitman, M. G. and Läuchli, A. (2002). Global impact of salinity and agricultural ecosystems. In *Salinity: environment-plants-molecules,* pp. 3-20. Springer, Dordrecht.

Platten J. D., Egdane, J. A., Ismail, A. M. (2013). Salinity tolerance, Na^+ exclusion and allele mining of *HKT1;5* in *Oryza sativa* and *Oryza glaberrima*: many sources, many genes, one mechanism? *BMC Plant Biol.* 13, 32.

Plett, C.D. and Møller I.S. (2010). Na^+ transport in glycophytic plants: what we know and would like to know. *Plant Cell Environ.* 33, 612-26. doi: 10.1111/j.1365-3040.2009.02086.x

Plett, D., Safwat, G., Gilliham. M., SkrumsagerMøller, I., Roy, S. et al. (2010). Improved salinity tolerance of rice through cell type-specific expression of *AtHKT1;1*. *PLoS ONE* 5, e12571, doi:10.1371/journal.pone.0012571.

Pottosin, I. and Dobrovinskaya, O. (2014). Non-selective cation channels in plasma and vacuolar membranes and their contribution to K^+transport. *J. Plant Physiol.* 171, 732–742, doi: 10.1016/j.jplph.2013.11.013

Rajendran, K., Tester, M. and Roy, S. J. (2009). Quantifying the three main components of salinity tolerance in cereals. *Plant Cell Environ.* 32, 237-249.

Reddy, I.N.B.L., Kim, B-K., Yoon I-S, Kim K-H and Kwon, T-R. (2017). Salt tolerance in rice: focus on mechanisms and approaches. *Rice Sci.* 24, 123-144.

Ren, Z.H., Gao, J.P., Li, L.G., Cai, X.L., Huang, W., Chao, D.Y., et al. (2005). A rice quantitative trait locus for salt tolerance encodes a sodium transporter. *Nature Genet.* 37, 1141–6

Reynolds, M.P., Ortiz-Monasterio, J.I. and Mc Nab, A. (2001). Application of physiology in wheat breeding. Mexico, D.F.: CIMMYT.

Reza, M., Mendioro, M.S., Diaz, G.Q., Gregorio, G.B. and Singh, R.K. (2013). Mapping Quantitative Trait Loci associated with yield and yield components under reproductive stage salinity stress in rice (*Oryza Sativa*). J. Genetics 92, 433–443.

Richards, L. A., ed. (1954). Diagnosis and Improvement of Saline and Alkali Soils. U.S. Department Agriculture Handbook 60. U.S. Gov. Printing Office, Washington, DC.

Roy, S.J., Negrao, S. and Tester, M. (2014). Salt resistant crop plants. *Curr. Opin. Biotechnol*. 26, 115-124.

Schmidt, R., Mieulet, D., Hubberten, H.M., Obata, T., Hoefgen, R., Fernie, A. R., Fisahn, J., Segundo, B.S., Guiderdoni, E., Schippers, J.H.M. and Mueller-Roebe, B. (2013). Salt-responsive *ERF1* regulates reactive oxygen species-dependent signaling during the initial response to salt stress in rice. *Plant Cell* 25, 2115–2131.

Senadheera, P., Singh, R.K. and Maathuis, F.J.M. (2009). Differentially expressed membrane transporters in rice roots may contribute to cultivar dependent salt tolerance. J. Exp. Bot. 60, 2553-63.

Shabala, S. and Pottosin, I. (2014). Regulation of potassium transport in plants under hostile conditions: implications for abiotic and biotic stress tolerance. *Physiol. Plant.* 151, 257-279.

Shahid, S.A. and ur Rahman, K. (2010). Soil Salinity Development, Classification, Assessment, and Management in Irrigated Agriculture. *In*: Handbook of Plant and Crop Stress, M. Pessarakaly ed., pp 23-39, CRC Press.

Shang, G., Li, Y., Hong, Z., Liu, C. L., He, S. Z., and Liu, Q. C. (2012). Overexpression of SOS genes enhanced salt tolerance in sweetpotato. *J. Integr. Agr.* 11, 378–386. doi: 10.1016/S2095-3119(12)60022-7.

Sharma, P., Jha, A.B., Dubey, R. S. and Pessarakli, M. (2012). Reactive oxygen species, oxidative damage, and antioxidative defense mechanism in plants under stressful conditions. *J. Bot*. doi:10.1155/2012/217037.

Shi, H., Ishitani, M., Kim, C. and Zhu, J.-K. (2000). The *Arabidopsis thaliana* salt tolerance gene SOS1 encodes a putative Na^+/H^+ antiporter. *Proc. Natl. Acad. Sci. U.S.A.* 97, 6896–6901, doi: 10.1073/pnas.120170197.

Shi, H., Quintero, F.J., Pardo, J.M. and Zhu, J.K. (2002). The putative plasma membrane Na+/H+ antiporter SOS1 controls long-distance Na^+ transport in plants. *Plant Cell* 14, 465–477.

Shi, H., Lee, B.H., Wu, S.J. and Zhu, J.K. (2003) Overexpression of a plasma membrane Na^+/H^+ antiporter gene improves salt tolerance in *Arabidopsis thaliana*. Nature Biotech. 21, 81–85.

Sirault, X. R., James, R. A. and Furbank, R. T. (2009). A new screening method for osmotic component of salinity tolerance in cereals using infrared thermography. *Func. Plant Biol.* 36, 970-977.

Smajgl, A., Toan, T. Q., Nhan, D. K., Ward, J., Trung, N. H., Trí, L. Q. et al. (2015). Responding to rising sea levels in the Mekong Delta. *Nature Climate Change*, 5(2), 167.

Su, J., Hirji, R., Zhang, L., He, C.K., Selvaraj, G. and Wu, R. (2006). Evaluation of the stress-inducible production of choline oxidase in transgenic rice as a strategy for producing the stress-protectant glycinebetaine. *J. Exp. Bot.* 57, 1129–1135.

Suzuki, K., Costa, A., Nakayama, H., Katsuhara, M., Shinmyo, A. and Horie, T. (2016a). OsHKT2;2/1-mediated Na^+ influx over K^+ uptake in roots potentially increases toxic Na^+ accumulation in a salt-tolerant landrace of rice Nona Bokra upon salinity stress. *J. Plant Res.* 129, 67–77.

Suzuki, L., Yamaji, N., Costa, A., Okuma, E., Kobayashi, N.I., Kashiwagi, T., Katsuhara, M., Wang, C., Tanoi, K., Murata, Y., Schroeder, J.I., Ma, J.F., and Horie, K. (2016b). OsHKT1;4-mediated Na^+ transport in stems contributes to Na^+ exclusion from leaf blades of rice at the reproductive growth stage upon salt stress. BMC Plant Biol. 16:22, doi10.1186/s12870-016-0709-4.

Tester, M. and Davenport, R. (2003). Na^+ tolerance and Na^+ transport in higher plants. *Ann. Bot*. 91, 503–527.

Thomson, M.J., de Ocampo, M., Egdane, J., Rahman, M.A., Sajise. A. G., Adorada, D. L., Tumimbang-Raiz, E., Blumward, E., Seraj, Z. I., Singh, R. K., Gregorio, G.B., Ismail, A. M. (2010). Characterizing the *Saltol*quantitative trait locus for salinity tolerance in rice. *Rice* 3, 148–160.

Tiwari, S., Sil, K., Kumar, V., Singh, B, Rao, A., Mithra, S.V.A. et al. (2016). Mapping QTLs for salt tolerance in rice (*Oryza sativa* L.) by bulked segregant analysis of Recombinant Inbred Lines using 50K SNP chip. *PLoS ONE* 11, e0153610, doi:10.1371/journal.pone.0153610.

Umali, D.L. (1993). Irrigation-Induced Salinity a Growing Problem for Development and the Environment. The Word Bank: Washington, DC, USA, 1993.

United States Department of Agriculture (2016). Bibliography on Salt Tolerance. Fibres, Grains and Special Crops; Brown, G.E., Jr., Ed.; Salinity Laboratory, USDA Research Service: Riverside, CA, USA. http://www.Ars.Usda.Gov/services/docs.Htm?Docid=8908.

Vishal, B., Krishnamurthy, P., Ramamoorthy, R. and Kumar, P.P. (2018). *OsTPS8* controls yield-related traits and confers salt stress tolerance in rice by enhancing suberin deposition. *New Phytol*. 221, 1369-1386. doi: 10.1111/nph.15464.

Yang, Y. and Guo, Y. (2018). Unraveling salt stress signaling in plants. J. *Integr. Plant Physiol.* 60, 796-804.

Yeo A.R., Yeo M.E. and Flowers, T.J. (1987). The contribution of an apoplastic pathway to sodium uptake by rice roots in saline conditions. *J. Exp. Bot.* 38, 1141–1153.

Yeo, A. R., Yeo, M. E., Flowers, S. A. and Flowers, T. J. (1990). Screening of rice (*Oryza sativa*) genotypes for physiological characters contributing to salinity resistance, and their relationship to overall performance. *Theor. Appl. Genet.*, 79, 377–384.

You, J. and Chan, Z. (2015). ROS regulation during abiotic stress responses in crop plants. Front. Plant Sci. 6, 1092, doi:10.3389/fpls.2015.01092.

Zhao, F-Y., Zhang, X-J., Li, P-H., Zhao, Y-X. and Zhang, H. (2006). Co-expression of the *Suaeda salsa SsNHX1* and *Arabidopsis AVP1* confer greater salt tolerance to transgenic rice than the single *SsNHX1*. *Mol. Breed.* 17, 341-353.

Objectives and activities

General objectives of the PhD activity here reported were:

- The identification of the natural variation existing for salt-tolerance traits at different plant developmental stages within a panel of 277 accessions of *japonica* rice.
- The discovery of novel molecular variability at different developmental stages in *japonica* rice cultivars resulting in tolerance to the mild salt stress conditions (soil EC 4-5 dS m^{-1}) reported for some European rice areas. In major detail, possible research deliverables are the identification of QTLs, alleles and/or molecular markers exploitable in future genetic improvement programs. The stated goals are pursued by Genome Wide Association Studies (GWAS) using the 277-rice japonica rice accession already genotyped-by-sequencing.

For achieving the stated goals, the activities following listed were carried out.

- Phenotyping of the rice panel consisting in: i) the two-years evaluation along plant different growth stages (germination and seedlings emergence, vegetative phase, reproductive phase), of traits (maximum germination percentage, kinetics of germination, leaf visual injuries score, plant height, flag leaf chlorophyll content and flowering time]related to salt stress responses after growing plant on soil under mild salinity (EC_e of about 4-5 dS m^{-1}); b) evaluation of the seed germination dynamics and the seedling emergence rates under high salt environment (150 mM NaCl for germination, and 9-10 dS m^{-1} EC for emergence) in a single-year experiment.
- GWAS study according to a Mixed Linear Model using the phenotyping data and the GBS data consisting in about 31.5 SNPs identifying significant phenotype-genotype MTA (Marker Traits Associations).
- Haplotype analyses of the most strong/interesting markers emerging from GWAS.
- Preliminary molecular and biochemical evaluation of some putative genes involved in salt tolerance included in the genomic segments in linkage disequilibrium with same of the most interesting MTAs emerging from GWAs.
- Preliminary field evaluation of two most salt tolerant accessions emerging from the phenotyping activities.

This thesis is structured in three successive scientific manuscripts currently under evaluation, or in a short time ready to be submitted to scientific journals.

Genome-wide association study of salinity tolerance during germination and seedling emergence from soil in rice (*Oryza sativa*, L.)

Michele Pesenti[1], Gabriele Orasen[1‡], Noemi Negrini[1], Silvia Morgutti[1], Fabio Francesco Nocito[1], Alessandro Tondelli[2] and Gian Attilio Sacchi[1]*

[1] DiSAA – Dipartimento di Scienze Agrarie e Ambientali, Università degli Studi di Milano, via Celoria 2, I-20133 Milano, Italy.
‡ Bertone Sementi. Strada Cacciolo 35, Terruggia Monferrato I-15030, Italy (current address).
[2] CREA - Consiglio per la Ricerca in Agricoltura e l'Analisi dell'Economia Agraria - Research Centre for Genomics and Bioinformatics, Via San Protaso 302, I-29107 Fiorenzuola d'Arda, Piacenza, Italy.

Abstract: A panel of 274 japonica rice accessions was evaluated for traits associated with salt susceptibility (SSI) at the germination and seedling emergence stages. Five traits describing the kinetic of seed germination were evaluated in control and salt conditions (150 mM NaCl): i) maximum percentage of germination (G_{max}); *ii*) time to reach 50% of G_{max} ($t_{50\%}$); *iii*) uniformity of 25-75% of germination (U_{25-75}); *iv*) area under the cumulative germination curve (AUC); *v*) emergence rate (ER). Two accessions, Olcenengo and SR113, showing the highest and the lowest levels of tolerance evaluated by means of the Susceptibility Score Index (SSI), respectively, were identified. GWA analyses of the phenotypic traits and 31,550 SNP markers obtained by GBS identified 28 significant MTAs related to germination kinetic and seedling emergence from soil. The analysis of the genes annotated in the Nipponbare reference sequence and included in the regions associated to the trait's variability detected allowed to highlight several candidate gens. For three of them (*OsTPP10*, OsACC1 and *OsBAT1)* a possible involvement in the observed traits is discussed. The results provide useful material and genetic information for developing molecular markers for improving rice salt tolerance in future breeding, as well as new evidences for molecular dissection of salt tolerance in rice.

Keywords: *Oryza sativa* L., germination, seedling emergence, salt tolerance, GWAS

Abbreviation: AUC, area under cumulative germination curve; ER, seedling emergence rate, G_{max}, maximum percentage of germination; GWAS, genome wide association studies; QTLs, quantitative trait loci; QTNs: quantitative traits nucleotides; ST, salt tolerance; SSI: salt tolerance stress index; $t_{50\%}$, time to reach 50% of G_{max}; U_{25-75}, uniformity of 25-75% germination

1. Introduction

About 20% of cultivated lands is affected by soil salinity due to relative high concentrations of soluble cations (mainly Na^+, K^+ and Mg^{2+}) and anions (mainly Cl^- and SO_4^{2-}). Other than natural causes consisting in the infiltration of sea water into the groundwater corps in the coastal areas a continuous and excessive use of mineral fertilizers and irrigation water of scarce quality are constantly causing the increase in salinity of several other soils (Tanji et al., 2002; Appelo and Postma, 2004). It is expected that the ongoing global warming, through the increases in average air temperature and lower availability of water, will further contribute to soil salinization.

Soil salinity constitutes one of the most important stress conditions limiting plant growth and crop yield (Machado and Serralheiro, 2017). Both high soil osmotic characteristics, that reduce the availability of water for plants, and onset of toxic effects on cell metabolism induced by the ionic imbalance, due to excessive absorption of ions are at the basis of the dramatic damages produced on crops by soil salinity. Rice (*Oryza sativa* L.) is considered, among the most important staple foods, quite sensitive to salt stress although a good genetic variability among its subspecies and genotypes exists. Even a soil electric conductance of about 3 dS m^{-1} is considered a threshold above which rice yield is usually affected negatively (Reddy et al., 2017), whereas in wheat and especially in barley higher thresholds, of about 6 dS $m^{-1}$and 8 dS m^{-1}, respectively, are reported (Munns and Tester, 2008).

Salt response is not univocal throughout the life cycle of the plant. In rice, a specific line may be tolerant in one stage and sensitive in another (Hoang et al., 2016 and references therein). The different responses are also genotype-related: different genotypes can be more tolerant to salinity stress at reproductive and grain filling stages than at the germination and vegetative ones, or relatively tolerant during germination, active tillering, and towards maturity, but sensitive during early seedling and reproductive stages (Heenan et al., 1988, Flowers and Yeo, 1981).

A crucial prerequisite for crop establishment is a rapid and uniform seed germination. High soil salinity, mainly due to exceedingly high levels of Na^+ and Cl^-, affects the germination process by diminishing the external water osmotic potential that in turn decreases the seed capability to absorb water. Therefore, salinity enforces the resting status of the seed inhibiting, together with water absorption, also the metabolic reactivation that accompanies the early phases of germination (Luan et al., 2014; Hannachi and van Labeke, 2018). In addition to the osmotic effect, in glycophytes the accumulation of ions (with particular regard to Na^+) negatively affects seed germination through specific toxic effects on cell metabolism (Daszkowska-Golec, 2011). A relatively low sensitiveness of

rice to salt at the germination stage is commonly reported (Heenan et al., 1988, Flowers and Yeo, 1981), also because in the lowland rice system, that represents the most largely adopted cultivation technique, seeds are sown after field submersion, i.e., when the salts potentially accumulated in the soil are diluted. In order to prevent excessive water consumption, water saving techniques have been developed for the cultivation of rice (Farooq et al., 2011). Most of them involve direct seed sowing on dry soil, and flooding is postponed at the 4^{th}-5^{th} leaf stage. In this case the availability of rice genotypes able to germinate uniformly and emerge from soil under salt condition proves necessary.

In this context, understanding the genetic factors that determine seed germination and early seedling vigor is surely helpful to improve the yield potential and stability of the crop. To exploit efficiently the genetic diversity of salt tolerance in breeding programs, it is important to identify quantitative trait loci (QTL)/quantitative trait nucleotides (QTN)/genes for this trait at the seed germination and seedling stages so that a marker-assisted breeding approach can be made easier. The very complex process of seed germination (Rajjou et al., 2012) has been recently addressed to, under both control and stress conditions, by Genome-Wide Association Studies (GWAS) in several plant materials (Hatzig et al., 2012, Zhang et al., 2016, Li et al., 2018). The GWAS approach is extremely powerful to explain the genetic basis of agronomic traits controlled by many genes, allowing to identify valuable natural variations in trait-associated loci, as well as allelic variations in candidate genes underlying quantitative and complex traits (Huang et al., 2011; Zhao et al., 2011).

Most studies aimed at defining genetic traits involved in salt tolerance at the germination stage limit the evaluation to the effects of this stress on the total percent of germination. Nevertheless, information about the responses of specific accessions to external variables in terms of kinetics and uniformity of germination are essential parameters for evaluating a seed population, with particular regard to traits related to stress tolerance. Thus, the performance of a seed lot can be better evaluated by gathering cumulative germination data (Joosen et al., 2010). Screens for natural variation to salt stress in *A. thaliana* conducted by the evaluation of cumulative germination curves rather than the only total percent of germination allowed the identification of loci involved in salt tolerance *(*Joosen et al., 2010*)*. To our knowledge, a similar approach has been never developed in rice. In the present study, a panel of 274 diverse *japonica* rice accessions and about 32,000 high-density SNPs have been exploited to conduct an association analysis to identify candidate genes and haplotypes potentially associated with salt tolerance and to reveal the genetic bases of salt tolerance at the germination and seedling emergence stages. The results open

interesting perspectives on the approach exploitable for elucidating the genetic bases of salt tolerance in rice, potentially appreciable for use in future programs of rice genetic improvement.

2. Materials and Methods

2.1. Plant material

The accession panel used in the study included 274 *Oryza sativa* L. varieties, ssp. *japonica*, from the Rice Germplasm Collection maintained at the CREA-Research Centre for Cereal and Industrial Crops in Vercelli, Italy (Tab. S1). The panel was composed of 68 tropical *japonica* and 206 temperate *japonica* accessions (see below). Most (144) of these accessions were developed in Italy, 32 from USA, 25 from Portugal, 19 from Spain, 10 from Bulgaria, 9 from Argentina, 6 from France and the remaining were developed elsewhere but considered well adapted to the Italian agro-climatic conditions (Volante et al., 2017; Orasen, 2018).

2.2. Phenotyping

Two kinds of experiments were conducted to record rice phenotypes in response to salt stress conditions: a lab experiment on 274 rice accessions for germination traits and a greenhouse experiment on the same accessions for seedling emergence rate.

For germination phenotyping in the salt stress condition, seeds were surface-sterilized with a sodium hypochlorite:water (2:1, v:v) solution for 20 min and then rinsed with abundant distilled water. Thirty seeds per each variety and four varieties per plate (total 120 seeds) were sown in square Petri dishes with lid (Corning® Square Bioassay dishes L×W×H 245×245×25 mm; Sigma Aldrich, Italy) on two layers of filter paper wetted with 40 mL of ddH_2O (controls) or 150 mM NaCl solution, to simulate severe salt-stress conditions. Trials were conducted in triplicate per each condition. The Petri dishes were placed in a thermoregulated (26 °C) growth chamber under continuous dark with 95% relative humidity. At the desired times the number of germinated seeds was checked, starting from 24 h after sowing and up to 144 h (6 d) of incubation. Germination was considered complete when the embryo structures penetrated the surrounding teguments (S1 stage: Counce et al., 2000). Cumulative germination data and time intervals were uploaded in the Microsoft Excel script module "Germinator_curve-fitting1.0.xls", a Solver add-in of the GERMINATOR package (Joosen et al., 2010) that, by using the four-parameter Hill function (El-Kassaby et al., 2008), performs the germination curve fitting and extracts the various germination parameters. The Germinator curve fitting script calculates averages and standard errors for

repeated samples, performs Student's *t*-test, and provides a formatted output including graphs for the different germination parameters. The biologically relevant parameters considered were: maximum percentage of germination (G_{max}), time to reach 50% of maximum germination (t_{50}), uniformity of germination (U_{25-75}, expressed as the time interval between 25% and 75% of viable seeds to germinate), and area under the curve (AUC, i.e., the integration of the fitted curve between t = 0 and a user-defined endpoint x). AUC combines information of the three previous parameters.

For phenotyping of seedling emergence rate (ER) in salt stress conditions, trials were conducted growing the seeds in water-saturated soil at the DiSAA greenhouse of the Milan University in Tavazzano (Lodi, Italy; 45°18'35.60" N, 9° 30'3.06"E). Twenty seeds per each genotype were sown (May 16, 2016) at 2-cm depth in black pots (170 mm diameter, 200 mm height) with drainage holes containing about 10 kg of paddy soil. The pots were placed inside larger pots (250 mm diameter, 260 mm height) with a closed base to simulate the waterlogged conditions of rice fields. Salt treatment was applied before sowing by adding 3 L of 100 mM NaCl to the inner pot plus an equal volume of the same solution to the larger pot, to a final concentration of 100 mM NaCl in the soil solution (saturated paste extract maintained at about 10 dS m^{-1} EC_e). In the control condition, the EC_e value of the non-saline waterlogged soil was approx. 1 dS m^{-1}. Four replicates per each condition and genotype were performed. Twenty-three d after sowing, the emerged seedlings were counted.

For each trait considered at the different developmental stages considered, the responses of the genotypes to salt stress were also expressed in terms of Stress Susceptibility Index (SSI) calculated, according to Fischer and Maurer (1978), as: SSI = (1 - Y_s/Y_p) / D, where Y_s = mean performance of a genotype under stress; Y_p = mean performance of the same genotype without stress; D (stress intensity) = 1 - (mean Y_s of all genotypes / mean Y_p of all genotypes) (Shi et al., 2017; Morton et al., 2019).

2.3. Statistical analysis of phenotypic data

Descriptive statistical parameters, as well as the plot boxes describing for each evaluated parameter and condition their distribution within the rice collection were obtained by SigmaPlot version 11.0. Analysis of variance (ANOVA) was carried out by the "aov" function in R environment to assess significance of genotypes (G) and replicates within each condition (Control and 150 mM NaCl for germination phenotyping and 100mM NaCl for seedling emergence rate).

The existence of correlations among the traits were determined evaluating the Pearson coefficients by the SigmaPlot.11 software.

Frequency distributions of phenotypic data were tested for normality using the Shapiro–Wilk function in R environment. Analysis of variance (ANOVA) was performed using the "aov" function in R environment to assess significance of genotypes (G), year (E), genotype year interaction (GE) and replicates within each environment (PF and LW). Components of phenotypic variances were estimated by fitting a mixed model by the Restricted Maximum Likelihood method, considering G, E and GE as random factors.

Broad sense heritability (H) was calculated according to the formula (Nyquist, 1991):

$$H = \sigma^2G/[\sigma^2G + (\sigma^2GE/E) + (\sigma^2e/rE)$$

where σ^2G is the genetic variance, σ^2GE is the genotype per environment interaction variance, σ^2e is the residual variance, E is the number of environments and r the number of replicates.

2.4. Genotypic data and genetic diversity analysis

The panel was genotyped-by-sequencing (GBS) following the pipeline described elsewhere (Biscarini et al. 2016; Volante et al. 2017). The set of molecular markers provided by the GBS analysis at Cornel University included 246,084 SNPs, which were located on the Os-Nipponbare-Reference-IRGSP-1.0 pseudomolecule assembly (Kawahara et al., 2013). The original SNP dataset was filtered by the program PLINK1 (Purcell et al., 2007) to avoid the biased detections due to rare alleles. Markers with a call rate value lower than 95% and with minimum allele frequency (MAF) lower than 5% were discarded. After filtering for call rate and MAF, a total number of 31,550 SNPs was subsequently used for the GWAS analyses.

In order to investigate the population structure, three different approaches (Principal Component Analysis, phylogenetic clustering, and Bayesian model-based analysis), were adopted. The PCA analysis were developed with the Adegenet package 2.0.0 of R software (Jombart and Collins, 2015). A phylogenetic tree or Neighbour-joining tree was constructed using a shared allele index based on a dissimilarity matrix estimated from the SNP dataset through Ape and Phyclust R package. The Bayesian model-based analysis was performed with the Structure software v2.3.4 (Pritchard et al., 2000), with a sub-set of 5,000 random SNPs marker. The parameters used in this analysis were: presence of admixture, allele frequencies correlated, burn-in period of 10,000 iterations, followed by 20,000 Monte Carlo Markov Chain (MCMC) replications, K levels from 1 to 10, 5 runs per K value. For the choice of the best number of clusters (K), the Evanno method of Δk

was used, implemented in the free software Structure Harvester (Earl and von Holdt, 2012). Once defined the most probable K value, a final single run was performed using the same parameters listed above, except for burn-in period of 100,000 iterations and 200,000 Monte Carlo Markov Chain (MCMC) replications. Accessions with a minimum membership of 0.7 were assigned to a subpopulation, while the remaining were considered as admixed. The phylogenetic tree, represented with iTOL (http://itol.embl.de/) was implemented with the results of the Structure analysis, together with the information relative to the varieties of the panel.

2.5. Linkage disequilibrium analysis

The computation of pairwise Linkage Disequilibrium (R2) among 5000 randomly selected markers was performed with the R package "LDcorSV v1.3.1" (Mangin et al., 2012), using the Structure membership matrix as a covariate. The values were averaged in 10 kb windows as in (Biscarini et al., 2016). For each distance class, a mean value was obtained from the data of the 12 chromosomes; the resulting values were plotted against physical distance and fitted to a second-degree LOESS curve using an R script (Cleveland, 1979; Marroni et al., 2011). A critical value of 0.2 was set as R2 between unlinked loci. The physical distance corresponding to a LOESS curve value of 0.2 was assumed as LD decay in the rice panel (Volante et al., 2017). The chromosome-wise local LD was calculated with the program Haploview v4.2 (Barrett et al., 2005). LD blocks were defined using the default settings, i.e. the method by (Gabriel et al., 2002), assuming 0.7 and 0.98 as D' lower and upper minima for strong LD, respectively, and the blocks have been numbered to facilitate identification.

2.6. Genome wide association studies

For the Genome-Wide Association analysis (GWAS), we calculated the least-square means for the seedling emergence rate (ER), and a standard average, for AUC, G_{max} and $t_{50\%}$.

A total number of 31,550 SNPs obtained through the filtering by PLINK1 software, were used for the association mapping analysis performed with the program Tassel v5.2.0, using a Mixed Linear Model (MLM) that includes the kinship matrix (K) as random effect to consider the population stratification. The program was run with the following parameters: no compression, genetic and residual variance estimated for each marker (P3D OFF).

For each marker a p-value of the association to the phenotypic traits was calculated; the significance threshold to declare a marker as associated was set to 0.05, after correction for multiple

testing using the false discovery rate (FDR) method according to (Benjamini and Hochberg, 1995). Manhattan plots and Q-Q plots of each trait were drawn using the R package "qqman" (Turner, 2014). The chromosome-wise local LD was calculated with the program Haploview v4.2 (Barrett et al., 2005). LD blocks were defined using the default Haploview settings, i.e., the method by Gabriel et al. (2002). The regions associated to each trait were aligned with the results of the Haploview analysis, in order to detect adjacent associations possibly tagging a single LD block. The regions defined by the peak marker/region positions including 100 kbp upstream and downstream (corresponding to an average LD decay of 0.5 estimated on the LOESS curve described above, as a trade-off between accuracy and power of the analysis) were screened to search for candidate genes underlying each trait. All gene models within these intervals were extracted from the annotation of *Oryza sativa* reference sequence (Os-Nipponbare-Reference-IRGSP-1.0)

2.7. Allele phenotypic effects

In according to Mei et al. (2013), the phenotypic effect of the allele was estimated through comparison between the average phenotypic value over accessions with the specific allele and that of all accessions:

$$a_i = \frac{\sum x_{ij}}{n_i} - \sum N_k / n_k$$

where a_i is the phenotypic effect of the i^{th} allele; x_{ij} is the phenotypic value over the j^{th} accession with the i^{th} allele; n_i is the number of accessions with the i^{th} allele; N_k is the phenotypic value over all accessions; n_k is the number of accessions. If the value of a_i is higher than 0, the allele is considered to have a positive effect, if it is lower than 0, it corresponds to a negative allele. The favorable alleles were then identified according to the breeding objective of each target trait.

3.Results

3.1. Phenotypic variation and trait correlations

Excluding G_{max}, a marked significant phenotypic variation in response to salt stress was observed for all the traits measured in the rice panel at both the germination and the seedling emergence rate (ER) stages (Table 1 and Figures 1-5).

Table1. Distribution of germination kinetic parameters and seedling emergence rate of the 274 *japonica* rice accessions in control and saline conditions. Cv: variability coefficient.

	Means ± SD		Range		CV	
	Control	Salt	Control	Salt	Control	Salt
G_{max} (%)	96.3 ± 3.3	92.2 ± 5.9	100 – 77.8	100 – 66.7	3.4	6.4
$t_{50\%}$ (h)	32.0 ± 5.2	54.0*± 10.3	49.0 – 19.2	91.4 – 29.8	16.3	19.0
$U_{25\text{-}75}$ (h)	9.3 ± 2.6	19.1* ± 6.2	16.3 – 2.7	45.1 -3.9	27.9	32.5
AUC (cm^2)	105.6 ± 2.6	80.2* ± 13.3	121.9 - 33.2	108.7 – 33.3	2.5	16.6
ER (%)	64.5 ± 11.9	17.2*± 10.9	95.0 – 17.5	58.8 - 0.0	18.4	61.9

Considering the panel as a whole the presence of 150 mM NaCl did not significantly affect its G_{max} average value with respect to that observed in the control condition (Table 1 and Fig. 1A). Nevertheless, the salt condition amplified the range of the G_{max} values indicating that the environmental constraint enhanced the differences existing among the accessions. The SSI values observed were distributed around 1.00 (absence of salt effect). In Supplemental Table 2, the most- and the less salt-sensitive accessions can be identified on the basis of the values of the SSI for G_{max}. For some accessions, the values of G_{max} seemed to be higher under the salt condition, so that the values of SSI resulted negative. However, in these cases by comparing the G_{max} values in the two germination conditions, no statistically significant differences resulted.

The average values of $t_{50\%}$ within panel resulted significantly increased (+ 69%) by the salt treatment (Tab. 1). Consistently, the distribution of the values of the kinetic parameter resulted strongly modified by salt (Fig. 2).

The salt effect was evident considering the SSI distribution. Several accessions proved to be marginally or not affected by the imposed stress condition, suggesting a tolerance to salt assuming that $t_{50\%}$ is increased in stressful conditions. In the Supplemental Table 2 the most- and the less salt-sensitive accessions can be identified based on high and low SSI values, respectively.

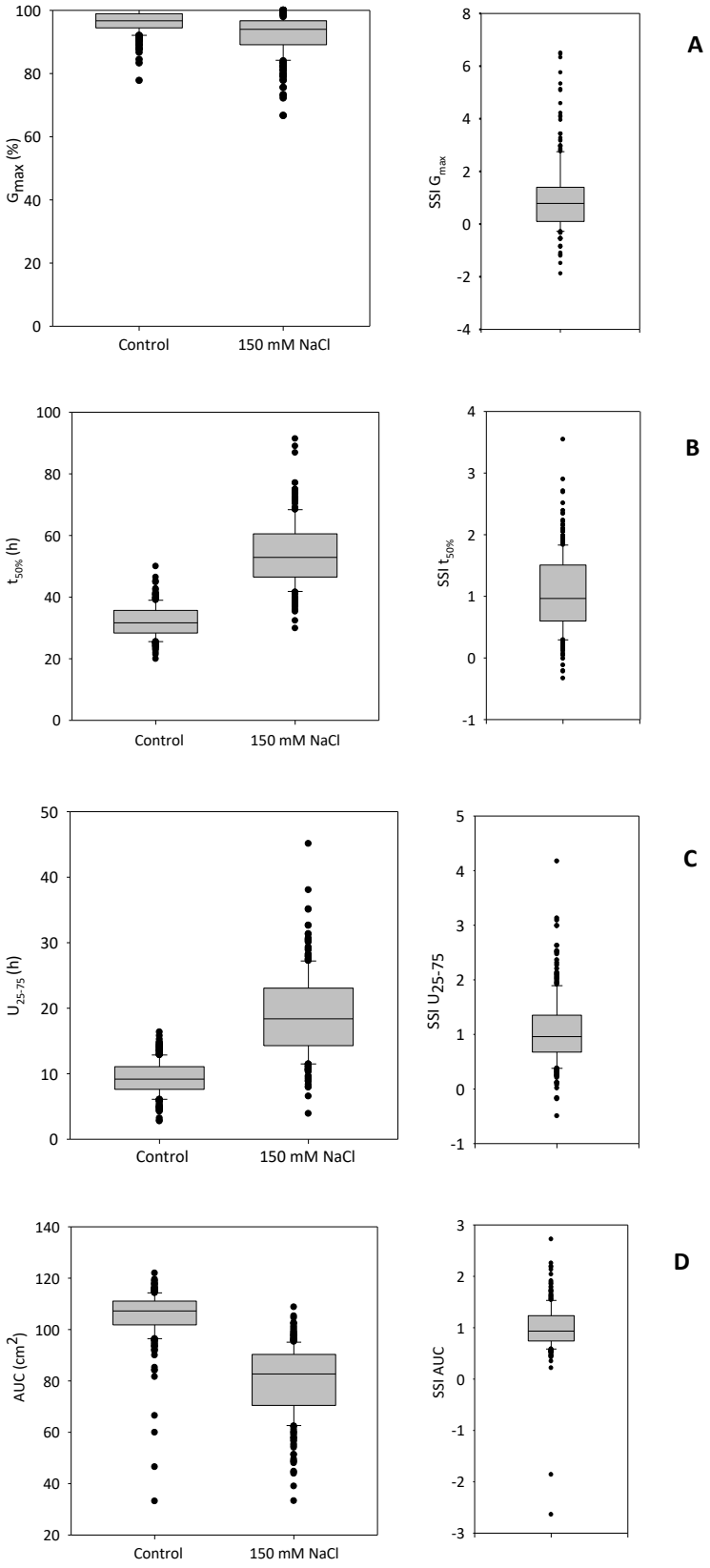

Figure 1. Box plots of germinations traits (left) and their relative SSI (right) values indicating the variability within the rice panel germinating under control and 150 mM NaCl conditions. Plots show the median, 10th, 25th, 75th and 90th percentiles as vertical boxes with error bars. A: G_{max}; B: $t_{50\%}$; C: $U_{25\text{-}75}$; D: AUC.

Within the studied rice panel, for each accession the uniformity of seed germination was evaluated considering the time span (h) necessary so that the percentage of germination increases from 25% to 75% (U_{25-75}; the higher U_{25-75}, the lower germination homogeneity). The values of this parameters considering the panel as a whole was affected by salt, doubling compared to the controls (Tab. 1,). As shown in Fig. 1C, the germination in the presence of 150 mM NaCl other than a lower uniformity in the kinetics of germination, caused a larger variability of this character within the rice panel. For some accessions (Table S2) an interesting outliner behavior was observed, showing SSI negative values that indicated a strong salt tolerance or even a salt-stimulating effect meaning that under 150 mM NaCl the seeds showed a higher uniformity of germination.

The area under the cumulative germination curve (AUC) provides a value that combines information yielded by G_{max}, t_{50} and the uniformity of germination (U_{25-75}). This parameter is therefore largely used to describe the effect of environmental variables on the germination kinetics of a seed lot (Joosen et *al*., 2010). The salt condition determined a reduction (-24%) of this area for most of the rice accessions of the tested panel (Tab. 1 and Fig. 1.D). Interestingly, assuming the reduction of AUC as a proxy of salt sensitiveness, a few accessions showed strongly negative values of SSI, indicating, in addition to their salt tolerance, an overall rapid kinetics of germination under salt condition (Fig. 1D).

For phenotyping of seedling emergence rate (ER) in salt stress conditions, the emerged seedlings were counted twenty-three days after sowing. Rice germination under anoxia in flooded soils is characterized by a longer coleoptile and delay in radicle emergence (Magneschi and Perata, 2009). A more vigorous (extension x rapidity) coleoptile growth is considered a trait by means of which rice genotypes can be classified as relatively able to overcome adverse metabolic conditions induced by abiotic stress such as anoxia (Kretzschmar et al., 2015; Nghi et al., 2019).

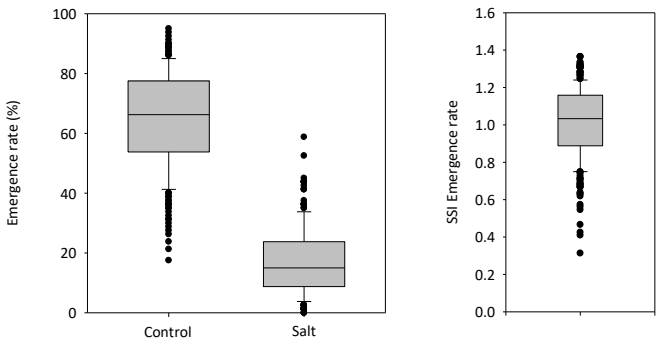

Figure 5. Box plots of ER (left) and SSI of ER (right) values indicating the variability within the *japonica* rice panel germinating in flooded soil under control and salt (9 dS m^{-1}) conditions. Plots show the median, 10th, 25th, 75th and 90th percentiles as vertical boxes with error bars.

In the time considered (23 d after sowing), ER in aerobic soil was very close to 90% for all the accessions (data not shown). As shown in Table 1 and Figure 5, the hypoxic condition allowed to the rice panel under investigation a wide capacity to emerge from the soil. When hypoxia was accompanied by severe salinity, the values of ER drastically dropped (Tab. 1, Fig. 2). Considering the panel as a whole, on average, the ER decrease was of about -73%. However, within the panel, quite variable values of SSI for salt stress under flooding were observed for this parameter.

The frequency distributions of phenotypic classes indicate that these traits are quantitative and continuous, suggesting a complex genetic control (Figure S1).

The results of the statistical analysis on the significance of variance estimates related to accession, treatment (control and salt condition) and their interactions are reported in Supplemental Table S3. The ANOVA results showed that genetic differences among accessions explained from 62.7% to 81.3% of the phenotypic variance for the traits at germination and seedling emergence. The values of the broad sense hereditability calculated for each trait within the rice panel in both the experimental condition ranged between a maximum value of 0.90 for $t_{50\%}$ in the control to 0.29 for ER in under salt stress (Table S4)

Strong correlations were observed between each couple of germination parameters in the case of both control and salt conditions (Table S5). In major detail, in both the conditions the existence of significant negative correlation resulted for the couples of traits $t_{50\%}/G_{max}$, $t_{50\%}$/AUC and $U_{25\text{-}75}$/AUC, whereas a significant positive correlation was observed for the couple $t_{50\%}/U_{25\text{-}75}$. Concerning the couple $G_{max}/U_{25\text{-}75}$ the positive correlation observed under control condition became negative under salt stress, whereas in the case of the cople G_{max}/AUC the negative correlation observed under control condition, became positive under salt.

By grouping the accessions according to the 10^{th} lowest and 90^{th} highest percentile of the SSI values, for two accessions every parameter always fell in the same percentile group: Olcenengo in the lowest and SR113 in the highest, respectively (Table S2). Considering the germination and the seedling emergence behavior, these results suggest that these two accessions can be considered as the most tolerant (Olcenengo) and the most sensitive (SR113) ones.

In this study four seed germination-related traits (G_{max}, $t_{50\%}$, $U_{25\text{-}75}$ and AUC) and 1 seedling growth-related trait (ER) were evaluated under salt stress and control conditions. In this study, the protrusion of the radicle through the endosperm and seed coat has been considered the completion of rice seed germination under oxic condition (as in Bewley, 1997). Usually, the total percent germination is considered for describing the germination performance of batches of seed.

Nevertheless, the information deriving from this parameter do not include rate and uniformity of germination that are two important properties for testing responses of seeds to environmental abiotic stresses (Joosen et al., 2010). Thus, cumulative germination curve (germination at various time) were considered. The G_{max} values did not result, on average basis, influenced by the stress treatment within the population. Nevertheless, all the other parameters (among them correlated, Table S3) resulted significantly affected: $t_{50\%}$, U_{25-75} and AUC highlighted genetic variability at 150 mM NaCl within the rice panel. It is known that salt tolerance is realized via distinct pathways depending on salt concentrations (Munnik et al., 1999). Indeed, cumulative germination data highlighted differences within populations that simple endpoint germination evaluation might not highlight.

The intensity of the salt stress adopted (150 mM NaCl) is coherent with the increasing trend in European rice system to adopt the sowing on dry soil technique. Indeed, values of soil electrical conductance (EC) in the range10-15 dS m^{-1}(corresponding to about 100-150 mM NaCl) are expected for dry soils exposed to salinity risks.

Under anoxic condition, rice seed germination occurs first trough the extrusion of embryo from the coats and the elongation of the coleoptile and then thought the root growth and development (Magnaschi e Perata, 2009). Recently, the natural variation existing within the same *japonica* rice accessions concerning the coleoptile length that conditions the seedling emergence rate from the soil under anoxic condition has been described (Nghi et al., 2019). Combination of salt stress with anoxic conditions exacerbates the constraints to seedling emergence from soil that, at the adopted soil salinity (~ 9 dS m^{-1}), and dramatically reduced ER (Table 1 and Figure 5). Nevertheless, in the drastic condition imposed an interesting natural variation for the traits exist within the panel considered. The lack of correlations between ER and each of the germination-related parameters (Table S3) suggests that the process controlling rice seed germination under salt stress and oxic condition are quite different to those involved in seedling emergence under salt stress an anoxic condition.

3.2. Genotypic data and genetic diversity analysis

The initial panel of 246,084 SNPs resulting for the *japonica* rice accessions (Biscarini et al., 2016; Volante et al., 2017) was filtered by PLINK2.0 providing the following panels: a) a subset of 5,000 random SNP markers (416 markers/chromosome) was used for investigating the genetic stratification (structure analysis); b) a subset of 31,550 SNPs showing the call rate 95% and MAF 5%

was used for LD and GWA analyses. The subset of markers used for the association analyses showed an average density of about 11.9 kbp/marker (ranging from 7 for chromosome 10 to 18.7 for chromosome 3). In this subset, the percentage of markers mapped on genic regions was about 51.8%, on average (data not shown).

In the structure analysis, the Evanno curve suggested a *K* = 2 as the ideal solution. In this definitive analysis, neighbor-joining tree and the structure K groups were graphically implemented with iTool in a single image (Fig. 6). The final analysis therefore suggested the following breakdown (with membership > 0.7): a) K1- 48 accessions predominantly belonging to the tropical japonica group; b) K2- 195 accessions belonging to the temperate japonica group; c) 31 accessions were classified as admixed. Any particular relationship between sensitiveness/tolerance to salt stress and belonging to one of this three groups was observed within the rice panel.

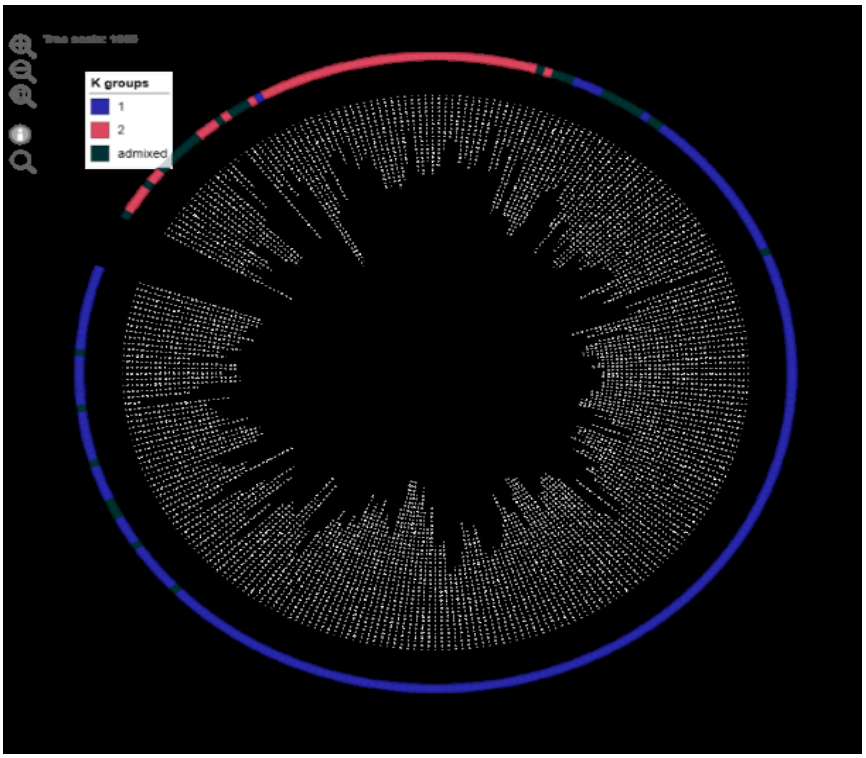

Figure 6. Neighbor-joining tree, overlapped with structure analysis. The blue circles on each branch show the results of the bootstrap analysis, when higher than 0.7.

The pairwise SNP Linkage Disequilibrium (LD) among the 31,550 SNPs was estimated as the correlation between pairs of alleles across a pair of markers (r^2) and was calculated with the R software (LDcoreSV package) for the whole population and for the temperate and tropical sub-populations ((Table 2). The mean r^2 dropped below 0.2 at approximately 900 kb inter-marker distance, ranging from 355 kbp for chromosome 11 to 1,295 kbp for chromosome 8, and the two subpopulations showed comparable LD decay (according to Volante et al. (2017).

An Haploview analysis performed on the panel (Table 2) divided the genome into 1497 linkage blocks, i.e., the blocks in which the markers are in linkage disequilibrium with each other, showing a D' of at least 0.7, in accordance to the coefficients of Gabriel et al. (2002). The analysis identified a number of LD blocks ranging from 54 for chromosome 5 to 277 for chromosome 11.

Table 2. A) LD decay in each chromosome for the whole population, temperate *japonica* and tropical *japonica* subgroups; B) LD blocks in each chromosome as calculated by Haploview.

A)

Chrom. #	Total	Temperate	Tropical
1	645	975	975
2	715	955	855
3	905	1105	1105
4	945	935	935
5	1055	1245	1245
6	625	755	755
7	1215	1475	1475
8	1295	1695	1695
9	945	1055	1055
10	1055	1675	1675
11	355	495	495
12	1185	1595	1595
Average	911.7	1163.3	1150

B)

Chrom. #	Blocks
1	162
2	152
3	81
4	154
5	54
6	109
7	104
8	141
9	62
12	117
11	277
12	84
Total	1497

3.3. GWAS analyses for salt stress-tolerance-related traits

For each phenotypic trait evaluated within the rice accessions grown under control or salt condition, as well as for the corresponding SSI values, GWAS was performed. For all the analyzed traits, both Manhattan and Q-Q plots resulting by the Tassel program in MLM configuration are reported in the Figures 7-10.

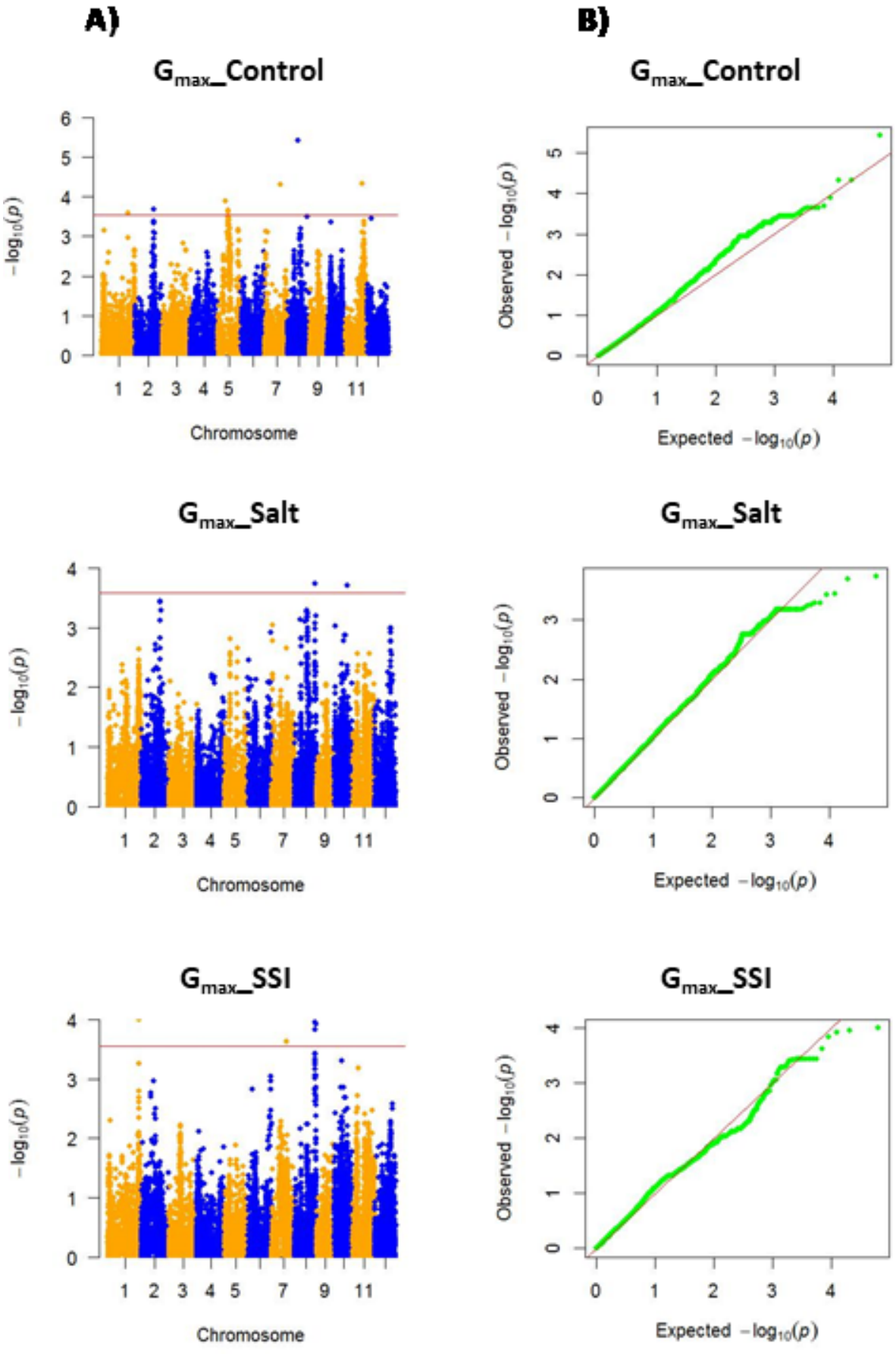

Figure 7. Manhattan (A) and Q-Q plot (B) concerning the parameter G_{max}.

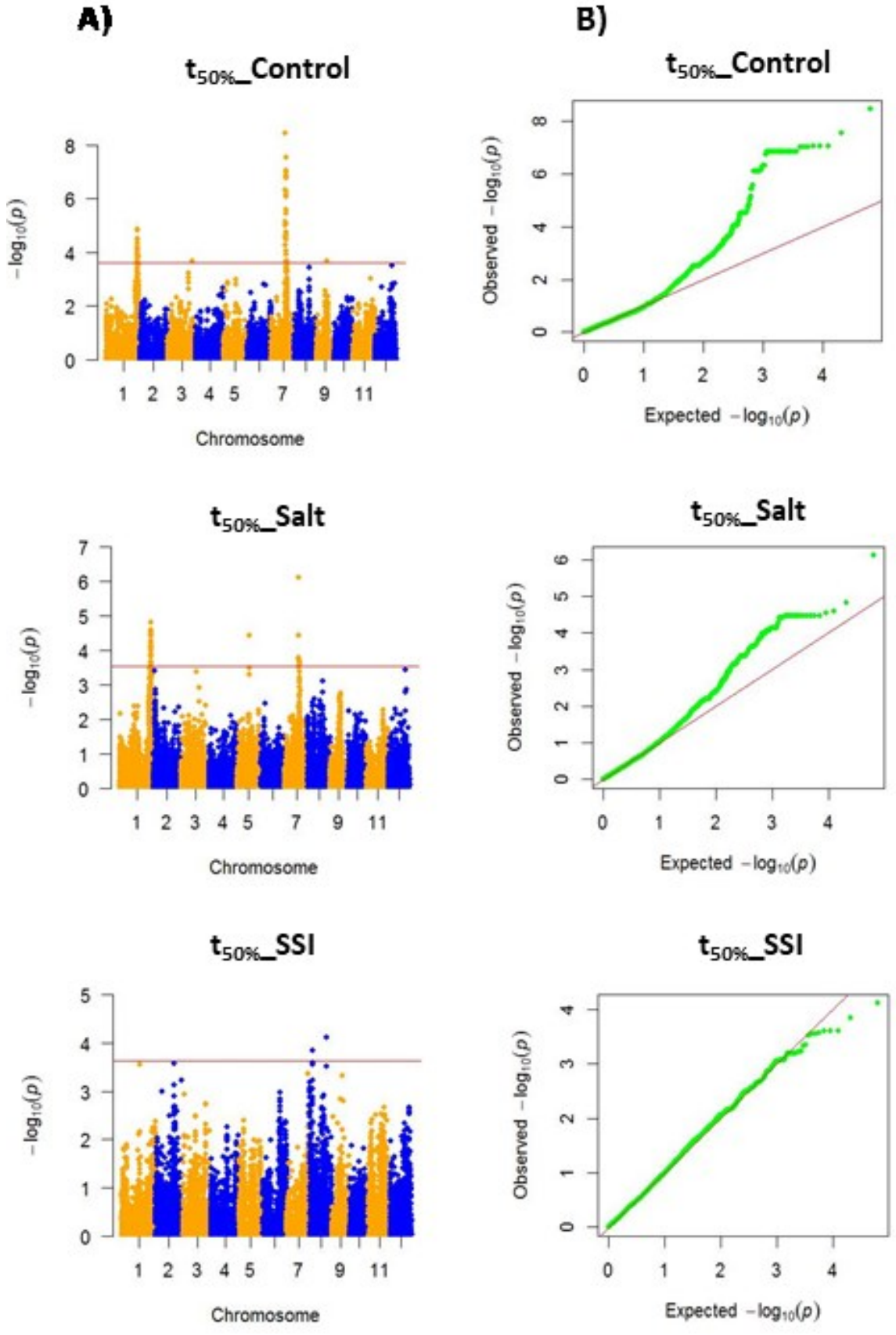

Figure 8. Manhattan (A) and Q-Q plot (B) concerning the parameter $t_{50\%}$.

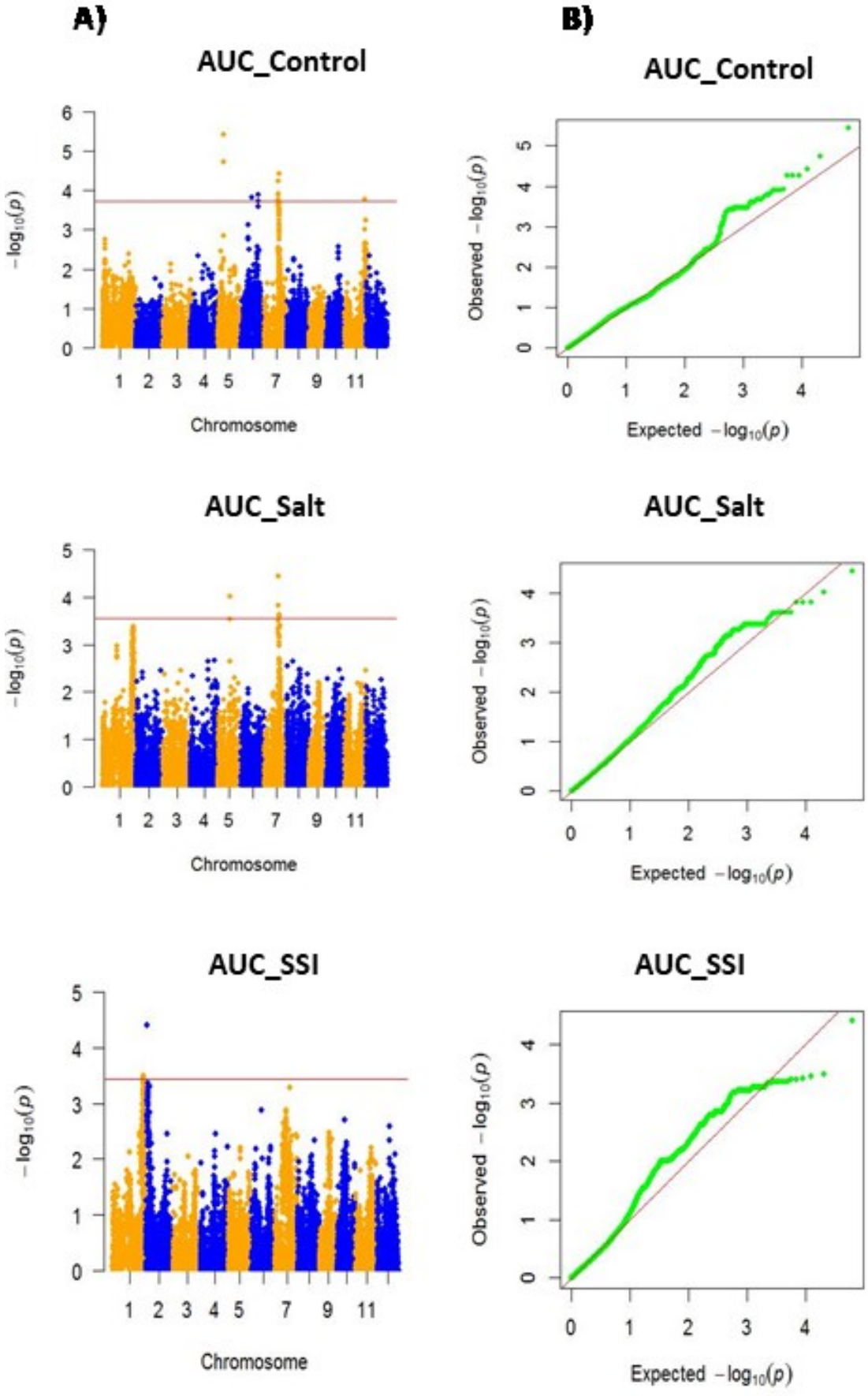

Figure 9. Manhattan (A) and Q-Q plot (B) concerning the parameter AUC.

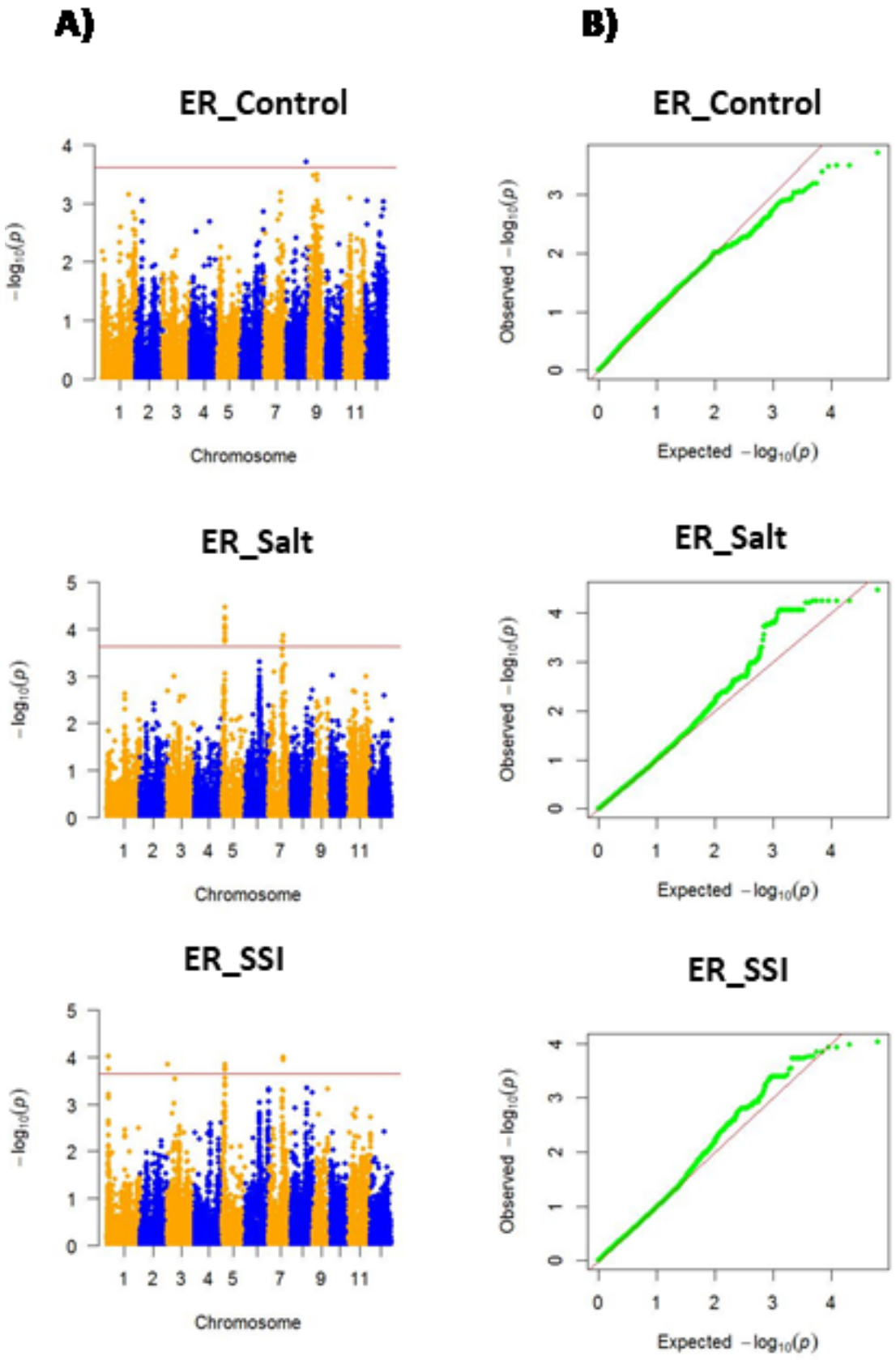

Figure 10. Manhattan (A) and Q-Q plot (B) concerning the parameter ER.

Several significant marker-trait associations (MTAs) were identified for the phenotypic parameters considered. In Table 3, the most significant associations (−log(p−value) > 3) detected in the GWAS study are listed, where the most significant SNP is reported, together with the number of additional significant SNPs (N. SNPs) and the and the start (bp), the end (bp) and related length (bp) of the linkage block including them.

A total number of 28 significant MTAs were identified having a –log (p) value in the range 3.46-8.46. The lowest number (1) of significant association was detected on chromosomes 02, 03, 09 and 10, the highest (5) on chromosome 05. for AUC_SSI and ER_C, the highest number (10) for $t_{50\%}$_C, respectively. Some positive associated MTAs resulted only in the case of specific traits and growth conditions, other MTAs resulted in common among the different parameters and/or conditions. The latter ones probably influence the different traits.

Detailing for single parameter the analyses detected: a) in the case of G_{max} 17 SNPs and seven MTAs (four specific for the controls, one specific for the salt condition, one specific for SSI, five in common between the control and the salt conditions; b) in the case of $t_{50\%}$ 155 SNPs and thirteen MTAs (five specific for the controls, one specific for the salt condition, one specific for SSI, one in common between the salt condition and the s SSI value, and one in common between the controls and the salt condition; c) in the case of $U_{25\text{-}75}$ any significant MTA was detected; d) in the case of AUC 24 SNPs and nine MTAs (five specific for the controls, one specific for the salt condition, one specific for SSI and two in common between the controls and the salt condition; e) in the case of ER 49 SNPs and six MTAs (one specific for the controls, two specific for the salt condition, one specific for SSI, and one in common between the salt condition and SSI value; Figure 10). Finally, five MTAs were detected in common between AUC and G_{max}, ER and t_{50}, AUC, ER and t_{50}, AUC and t_{50}, t_{50} and G_{max}.

3.4. Candidate genes

Several interesting candidate genes were found in the Nipponbare genomic regions where associations for physiology-related traits were detected. In the following lines details about three of these genes resulting particularly interesting are reported.

- *Os07g0485000*–The gene is included in the region associated to AUC-C, AUC-S, t_{50}-C, t_{50}-S, ER-S highlighted by the MTA 753 on the chromosome 07. *OsTTP10*, which transcript had been reliably detected in the endosperm of rice seeds (Galland et al. 2017), is one of the nine members of *OsTPP* gene family (Fernandez at al., 2010). Functional genomics approaches have shown that

some members as OsTPP1, OsTTP2, and OsTTP7 encode for the enzyme trehalose 6-phosphate phosphatase (T6P) (Shima et al., 2007; Ge et al., 2008; Kretzschmar et al., 2015) that dephosphorylate the signal molecule trehalose 6-P (T6P), an energy sensor that determines anabolism or catabolism depending on local sucrose availability by modulating the SnRK1 (Sucrose non-fermenting-1-related protein kinase 1; Hardie, 2000)-dependent α-amylase enzyme activity , plays a central role in the early phases of seed germination, and it's a main target of the T6P/SnRK1 system. Moreover, recently it has been shown as *OsTPP7,* another member of *OsTTP* gene family is crucial for rice coleoptile elongation under anoxic condition, further supporting a role of these genetic elements in seed and seedling responses to adverse environmental conditions (Kretzschmar et al., 2015; Nghi et al, 2019). Further investigation focused both on the *OsTTP10* function and on the presence of eventual allelic variants in the elements of the rice panel showing opposite salt sensitiveness: Olcenengo and SR113 the most tolerant and the most sensitive, respectively, currently under investigation, will clarify the role of this family members in conferring altered salt tolerance.

- *Os08g0157600* - This gene, is included in the region associated with $t_{50\%}$-SSI MTA 829 on chromosome 08. It codifies for a homeodomain-like containing protein (OsACC1: Oryza sativa Circadian Clock Associated 1) which mRNA expression resulted to be more than 20-fold higher in rice seedling after a drought treatment (Nakashima et al., 2014), The OsACC1 protein is a transcription factor with a single MYB DNA-binding domain at its N-terminal end and it is an element of the putative clock-associated components of rice (Muramaki et al., 2007).
- *Os01g0911100* - This gene named as *OsBAT1 is* included in the region highlighted by the MTAs 128 on chromosome 01, overlapping with G_{max}-SSI, AUC-SSI, t_{50}-C, t_{50}_S. *OsBAT1* is the rice homologous of the human gene codifying for BAT1 (leukocyte antigen-B associated transcript 1) a DExD/H-box protein involved in messenger RNA (mRNA) splicing (Tuteja et al., 2015). In rice OsBAT1 is localized in the nucleus gene and in the plasma membrane. Rice overexpressing OsBAT1 show tolerance to high salinity (200 mM NaCl) stress and this effect was related to a consequent up-regulation of stress-responsive genes of different pathways including the spliceosome (Tuteja et al., 2015).

3.5. Haplotype analysis

Phenotypic effects of each allele for the two associated loci detected in more than one environment were measured according to the method described by Mei *et al.* (2013). Several favorable and unfavorable alleles have been identified (Table 4), in particular, for one allele on

chromosome 07, at the same locus five alleles for AUC-C and three alleles for AUC-S, eight alleles for t_{50}-C and t_{50}-S, and one allele for the ER-C were identified. In the case of $t_{50\%}$-SSI an allele with a slight negative effect was identified on the chromosome 08.

Table 3. Individual MTAs emerging from association and Haploview analyses. Each MTAs is represented by the related marker, the peak marker (SNP marker with the highest -log10 (p) value), the chromosome number, the number of related SNPs and the length (bp) of the linkage block including it.

TRAIT	CONDITION or SSI	PEAK MARKER (bp)	-log(p)	FDR	MTA IDA	Chr	N. SNPs	Start	End	Length pb	N° SNPs totali
ER	SSI	S1_1504728	3.74	3.65	4	1	1	1093324	1518557	425233	66
AUC	SSI	S1_39879447	3.6	3.43	128	1	2	39511185	40401682	890497	147
G_{max}	SSI	S1_39931952	3.99	3.55	128	1	1	39511185	40401682	890497	147
$t_{50\%}$	Control	S1_40014192	4.53	3.73	128	1	15	39511185	40401682	890497	147
$t_{50\%}$	Salt	S1_40065735	4.81	3.55	128	1	11	39511185	40401682	890497	147
$t_{50\%}$	Control	S1_40610729	4.87	3.73	129	1	15	40412890	40619172	206282	95
$t_{50\%}$	Salt	S1_40571758	4.11	3.55	129	1	14	40412890	40619172	206282	95
$t_{50\%}$	Control	S1_40694665	3.7	3.73	130	1	4	40666313	40730493	64180	15
$t_{50\%}$	Salt	S1_40677794	4.11	3.55	130	1	3	40666313	40730493	64180	15
$t_{50\%}$	Control	S1_41161149	3.85	3.73	132	1	1	40737721	41172858	435137	69
G_{max}	Control	S2_24831269	3.69	3.53	275	2	1	24831214	24839365	8151	6
$t_{50\%}$	Control	S3_31256275	3.68	3.73	390	3	1	30647948	31592025	944077	11
ER	Salt	S5_3645628	3.81	3.63	559	5	12	3616945	3699657	82712	16
ER	Salt	S5_3858344	4.46	3.63	561	5	29	3765865	4611942	846077	66
ER	SSI	S5_3858344	3.85	3.65	561	5	9	3765865	4611942	846077	66
AUC	Control	S5_6880835	5.42	3.73	565	5	1	6503939	7359585	855646	113
G_{max}	Control	S5_13667220	3.66	3.53	570	5	5	13280433	14277516	997083	73
$t_{50\%}$	Salt	S5_15641006	4.43	3.55	572	5	1	14992834	15992831	999997	163
AUC	Salt	S5_16321058	4.02	3.56	575	5	1	16200617	17199988	999371	82
AUC	Control	S6_22360970	3.73	3.73	676	6	1	22225475	22363120	137645	20
AUC	Control	S6_22375931	3.89	3.73	678	6	1	22375722	22678707	302985	22
AUC	Control	S7_17357899	4.25	3.73	753	7	6	17215925	17847657	631732	14
AUC	Salt	S7_17357899	3.82	3.56	753	7	4	17215925	17847657	631732	14
ER	Salt	S7_17552808	3.75	3.63	753	7	1	17215925	17847657	631732	14
$t_{50\%}$	Control	S7_17435993	8.46	3.73	753	7	8	17215925	17847657	631732	14
$t_{50\%}$	Salt	S7_17435993	6.11	3.55	753	7	7	17215925	17847657	631732	14
AUC	Control	S7_18168356	3.91	3.73	757	7	1	18125797	18773583	647786	80
ER	Salt	S7_18728431	3.86	3.63	757	7	3	18125797	18773583	647786	80
ER	SSI	18728431	3.99	3.65	757	7	3	18125797	18773583	647786	80
$t_{50\%}$	Control	S7_18773583	4.74	3.73	757	7	1	18125797	18773583	647786	80
AUC	Control	S7_18875745	4.42	3.73	758	7	1	18775939	19101596	325657	67
AUC	Salt	S7_19087327	3.62	3.56	758	7	7	18775939	19101596	325657	67
$t_{50\%}$	Control	S7_19087327	7.55	3.73	758	7	58	18775939	19101596	325657	67
$t_{50\%}$	Salt	S7_19087327	3.66	3.55	758	7	7	18775939	19101596	325657	67
G_{max}	Control	S7_19952373	4.31	3.53	759	7	1	19105134	20104652	999518	228
G_{max}	SSI	S7_19529424	3.63	3.55	759	7	1	19105134	20104652	999518	228
$t_{50\%}$	Control	S7_19444927	3.7	3.73	759	7	3	19105134	20104652	999518	228
$t_{50\%}$	SSI	S8_ 3425045	3.84	3.63	829	8	1	3310091	3547971	237880	19
$t_{50\%}$	SSI	S8_21086229	4.11	3.63	830	8	1	20907303	21321794	414491	90
ER	Control	S8_24855219	3.7	3.61	841	8	1	24811631	25121782	310151	29
G_{max}	Salt	S8_26566266	3.73	3.59	847	8	1	26502275	26714693	212418	29
G_{max}	SSI	S8_26566266	3.95	3.55	847	8	2	26502275	26714693	212418	29
G_{max}	Control	S8_13678818	5.42	3.53	923	8	1	13033195	14033186	999991	122
$t_{50\%}$	Control	S9_13736588	3.68	3.73	1005	9	2	13337756	13935367	597611	29
G_{max}	Salt	S10_16621543	3.7	3.59	1123	10	1	16041577	16624807	583230	92
G_{max}	Control	S11_22427517	4.33	3.53	1270	11	1	37452726	37463444	10718	2
AUC	Control	S11_27259559	3.79	3.73	1372	11	1	27169302	27272703	103401	25

Table 4. MTAs redundancy among phenotypic parameters and chromosome.

Chr. N°	MTA Id	Condition or SSI
1	4	SS_ER
	128	SSI_AUC SSI_G_{max} Control_$t_{50\%}$ Salt_$t_{50\%}$
	129	Control_$t_{50\%}$ Salt_$t_{50\%}$
	130	Control_$t_{50\%}$ Salt-$t_{50\%}$
	132	Control_$t_{50\%}$
2	275	Control_G_{max}
3	390	Control_$t_{50\%}$
5	559	Salt_ER
	561	Salt_ER SSI_ER
	565	Control_AUC
	570	Control_ G_{max}
	572	Salt_ $t_{50\%}$
	575	Salt_AUC
6	676	Control_AUC
	678	Control_AUC
7	753	Control_AUC Salt_AUC Salt_ER Control_ $t_{50\%}$ Salt_$t_{50\%}$
	757	Control_AUC Salt_ER SSI_ER Control_ $t_{50\%}$
	758	Control_AUC Salt_AUC Control_ $t_{50\%}$ Salt_ $t_{50\%}$
	759	Control_ G_{max} SSI_G_{max} Control_ $t_{50\%}$
8	829	SSI_ $t_{50\%}$
	830	SSI_ $t_{50\%}$
	841	Control_ER
	847	Salt_ G_{max} SSI_ G_{max}
	923	Control_ G_{max}
9	1005	Control_ $t_{50\%}$
10	1123	Salt_ G_{max}
11	1270	Control_ G_{max}
	1372	Control_AUC

Table 5. Haplotype analyses

			AUC_SSI		AUC_C		AUC_S		$t_{50\%}$_C		$t_{50\%}$_S		$t_{50\%}$_SSI		ER_S		GMAX_SSI	
Allele1	Allele2	Marker	Allele1	Allele2	Allele1	Allele2	Allele1	Allele2	Allele1	Allele2	Allele1	Allele2	Allele1	Allele2	Allele1	Allele2	Allele1	Allele2
C	T	S1_39831573	0.28	-0.05					1.75	-0.55	4.70	-1.08					0.78	-0.10
G	A	S1_39852850	-0.05	0.27					-0.51	2.08	-1.08	5.21					-0.10	0.66
G	T	S1_39879447	-0.04	0.39					-0.44	2.71	-1.01	8.50					-0.08	1.01
C	G	S1_39886933	-0.05	0.29					-0.51	1.92	-1.09	4.99					-0.09	0.62
G	A	S1_39893250	0.28	-0.05					1.89	-0.52	4.95	-1.11					0.66	-0.10
C	T	S1_39902281	-0.05	0.28					-0.52	1.89	-1.11	4.95					-0.10	0.66
T	G	S1_39906510	0.28	-0.05					1.89	-0.52	4.95	-1.11					0.66	-0.10
A	G	S1_39911427	-0.05	0.28					-0.51	1.86	-1.07	4.82					-0.09	0.62
A	G	S1_39923186	0.28	-0.05					1.89	-0.52	4.95	-1.11					0.66	-0.10
T	C	S1_39926579	0.27	-0.05					2.04	-0.53	5.30	-1.13					0.63	-0.10
T	C	S1_39931952	0.35	-0.04					1.43	-0.34	4.43	-0.73					0.83	-0.07
T	C	S1_39946248	-0.05	0.28					-0.52	1.89	-1.11	4.95					-0.10	0.66
C	T	S1_39990699	0.28	-0.05					1.89	-0.52	4.95	-1.11					0.66	-0.10
T	C	S1_39991954	0.28	-0.05					1.89	-0.52	4.95	-1.11					0.66	-0.10
A	T	S1_40014192	0.28	-0.05					2.07	-0.53	5.30	-1.13					0.65	-0.10
A	C	S1_40019475	0.28	-0.05					2.07	-0.53	5.30	-1.13					0.65	-0.10
A	C	S1_40020146	0.28	-0.05					2.07	-0.53	5.30	-1.13					0.65	-0.10
G	A	S1_40026744	0.28	-0.05					2.07	-0.53	5.30	-1.13					0.65	-0.10
C	T	S1_40027070	0.28	-0.05					2.07	-0.53	5.30	-1.13					0.65	-0.10
G	C	S1_40031088	0.26	-0.05					1.92	-0.50	4.94	-1.06					0.56	-0.08
G	A	S1_40031180	0.26	-0.05					1.92	-0.50	4.94	-1.06					0.56	-0.08
T	C	S1_40034825	0.28	-0.05					2.07	-0.53	5.30	-1.13					0.65	-0.10
A	G	S1_40047705	0.28	-0.05					2.07	-0.53	5.30	-1.13					0.65	-0.10
C	T	S1_40059348	0.28	-0.05					2.07	-0.53	5.30	-1.13					0.65	-0.10
C	T	S1_40059994	0.28	-0.05					2.07	-0.53	5.30	-1.13					0.65	-0.10
G	C	S1_40065735	0.28	-0.05					2.36	-0.54	5.87	-1.13					0.60	-0.09
G	A	S1_40069878	0.28	-0.05					2.07	-0.53	5.30	-1.13					0.65	-0.10
T	C	S1_40089754	0.26	-0.05					1.98	-0.54	4.89	-1.14					0.61	-0.09
T	C	S1_40091118	-0.05	0.28					-0.53	2.07	-1.13	5.30					-0.10	0.65
C	T	S1_40093313	0.28	-0.05					2.24	-0.53	5.66	-1.13					0.62	-0.10
A	G	S1_40093635	0.28	-0.05					2.07	-0.53	5.30	-1.13					0.65	-0.10
T	C	S1_40096035	0.30	-0.05					2.11	-0.53	5.34	-1.11					0.61	-0.09
C	T	S1_40096987	0.28	-0.05					2.07	-0.53	5.30	-1.13					0.65	-0.10
T	C	S1_40119129	0.28	-0.05					2.07	-0.53	5.30	-1.13					0.65	-0.10
A	T	S1_40124297	0.27	-0.05					1.79	-0.51	4.86	-1.10					0.60	-0.09

T	C	S1_40124333	0.27	-0.05					1.79	-0.51	4.86	-1.10					0.60	-0.09
A	G	S1_40124579	0.27	-0.05					1.79	-0.51	4.86	-1.10					0.60	-0.09
C	T	S1_40142665	0.27	-0.05					1.79	-0.51	4.86	-1.10					0.60	-0.09
G	C	S1_40152051	0.26	-0.05					1.95	-0.52	5.20	-1.12					0.57	-0.09
A	T	S1_40159394	0.27	-0.05					1.79	-0.51	4.86	-1.10					0.60	-0.09
A	G	S1_40185824	0.27	-0.05					1.68	-0.48	4.86	-1.08					0.56	-0.09
A	G	S1_40193204	0.27	-0.05					1.68	-0.48	4.86	-1.08					0.56	-0.09
A	T	S1_40213307	-0.05	0.29					-0.51	1.97	-1.11	5.30					-0.09	0.62
C	T	S1_40228586	0.27	-0.05					1.68	-0.48	4.86	-1.08					0.56	-0.09
G	C	S1_40233789	0.27	-0.05					1.68	-0.48	4.86	-1.08					0.56	-0.09
C	T	S1_40250329	0.27	-0.05					1.68	-0.48	4.86	-1.08					0.56	-0.09
T	C	S1_40264587	0.27	-0.05					1.68	-0.48	4.86	-1.08					0.56	-0.09
T	G	S1_40285839	0.30	-0.04					3.09	-0.44	7.09	-0.95					0.56	-0.07
C	T	S1_40317727	0.27	-0.05					1.80	-0.50	5.11	-1.11					0.50	-0.08
A	T	S1_40317737	0.28	-0.05					1.66	-0.49	4.77	-1.09					0.52	-0.08
T	C	S1_40372283	0.24	-0.05					1.32	-0.44	4.20	-1.01					0.48	-0.08
T	C	S1_40389083	-0.05	0.24					-0.44	1.32	-1.01	4.20					-0.08	0.48
A	T	S1_40394306	0.24	-0.05					1.32	-0.44	4.20	-1.01					0.48	-0.08
G	T	S7_17215925							1.23	-3.49	0.18	-4.89						
C	T	S7_17332871			2.69	-2.84			-3.54	1.23	-0.85	1.58						
A	G	S7_17357899			-2.92	2.83			1.28	-3.67	0.22	-5.12						
C	T	S7_17361679			-2.92	2.83	-3.77	5.77	1.28	-3.67	0.22	-5.12						
G	A	S7_17366708			-2.92	2.83	-3.77	5.77	1.28	-3.67	0.22	-5.12						
T	C	S7_17435993			-2.90	1.64	-3.93	4.30	1.80	-3.49	0.00	-5.11						
G	A	S7_17552808							1.21	-3.42	0.27	-4.81			0.39	-0.86		
T	C	S7_17639290							1.18	-3.44	0.32	-4.98						
C	T	S8_3425045											-0.14	0.00				

4. Discussion

A large set of SNP markers obtained by Genotyping by Sequencing was used for the genomic characterization of the rice panel. The size of this set was very similar to that reported by Volante et al. (2017). About 52% of these SNPs markers and the average LD decay detected in the rice panel is 912 kbp. Considering the temperate and tropical japonica ecotypes individually, LD results to be 1,163 kbp and 1,150 kbp, respectively. These values are higher than those previously reported by Mather et al. (2007) of about 500 kbp and 150 kbp for temperate and tropical japonica rice, respectively. The discrepancies could be explained considering different factors such as SNP densities and/or kinship among accessions as previously discussed (Biscarini et al., 2016; Volante et al., 2017). However, higher LD values ranging from 600 kbp up to 2 Mbp were also observed in other researches for japonica and indica rice (Xu et al., 2011; Kumar et al., 2015). Moreover, for a germplasm collection of temperate japonica rice accessions related to the panel used in the present study, the values of LD decay of 1,250 kbp have been reported (Biscarini et al., 2016; Volante et al., 2017). The stratification analyses carried out clearly separated the population into two clusters, each one corresponding to the two main japonica rice ecotypes. Such clustering is comparable to that reported in previous studies (Biscarini et al., 2016; Volante et al., 2017: Orasen, 2018), that used a panel containing a large proportion of the accessions considered in the present work. Finally, Courtois et al. (2012) showed that the japonica subspecies clusters into tropical and temperate varieties also in a panel of 425 accessions belonging to four main rice varietal groups. The presence in the studied panel of varieties classified as admixed, i.e. not clustered in a defined group, suggests that these accessions were developed from interspecific breeding programs where a significant gene exchange between temperate and tropical japonica has occurred, as noticed in similar panel (Volante et al., 2017; Orasen et al., 2018).

Recently, the physiological mechanisms controlling rice adaptation to salt stress at the germination and early seedling establishment stages have been extensively reviewed on a panel of Asian varieties where a strong component of indica ones was present (Kumar et al., 2015; Shi et al., 2017). GWAS proved in the case of SSI significant association in the genomic regions including Saltol QTL on chromosome 01 and the genes of nitrate transporter family on chromosome 02, other than non-better-defined associations on chromosomes 04, 06 and 07. In our study, on chromosome 07 we found a cluster of QTLs for ER-SSI and ER-S between 18125797 bp and 18773583 bp, i.e., the same chromosomic region where Mohammadi et al. (2013) found a cluster of QTLs for yield-related

compounds under salt stress. In particular, in this 647786 kbp region is included the *OsTPP10* gene, whose transcripts are only reliably detected in the endosperm (Galland et al., 2017), putatively encoding for a TPP enzyme that, by regulating the T6P/tre level, may be involved in the regulation of the T6P/Suc/SnrK1 system that plays a key role in the sink-source carbon allocation during the seed germination and the seedling establishment (Morgutti et al., 2019). This finding may indicate a relationship between genes involved in trehalose metabolism in rice seeds and seed germination and seedling establishment in salt conditions. Moreover, the role of the TPP enzymes related to the tolerance to abiotic stresses as anaerobiosis in rice has been described, in particular referring to OsTPP7 (Kretszchmar et al., 2017). The GWAS analysis was conducted on the data deriving from test in salty, unsalted conditions, and from the SSI. The SSI data analysis shows a smaller number of signals but a more regular Q-Q plot, although it analyzes trough the integer values can also be considered reliable. The allelic effect is also more marked in GWAs conducted with integer values, compared to SSI.

In this study four traits concerning the salt response in early stage, where monitored in 274accessions. Despite the high LD value resulting, that is considered a limit in the resolution of GWAS studies, the purposed approach allowed the identification of 28 MTA. Accumulation of these alleles conferring small fractions of improved phenotypic values for a given trait. A similar output could be expected when loci showing associations detected in Salt and control conditions are pyramided in an improved rice line. Several MTAs have been identified in different traits, in particular the MTA in common between ER, $t_{50\%}$ and AUC, a MTA in common between AUC and $t_{50\%}$ and one MTA in common between $t_{50\%}$ and Gmax and a MTA on chromosome 01 in common between G_{max}, $t_{50\%}$ and AUC. The MTA 753 in common between ER, $t_{50\%}$, and AUC highlighted the *OSTTP10* gene. A member of the same gene family, the *OsTPP1* gene, resulted initially and transiently up-regulated after salt, osmotic and abscisic acid (ABA) treatments but slowly up-regulated under cold stress and it overexpression in rice enhanced tolerance to salt and cold stress (Ge et al., 2008). Analysis of the overexpression lines revealed that OsTPP1 triggered abiotic stress response genes, which suggests a possible transcriptional regulation pathway in stress induced reprogramming initiated by OsTPP1 (Ge et al., 2008). The possible involvement of the *OsTPP10* gene in a similar regulative picture in response to salt stress can be suggested.

5. Conclusion

Although all the accessions of the japonica rice panel considered showed a maximum of germinability (G_{max}) just below 100% and this value was not significantly altered even in the presence of a severe salt condition imposed at 150 mM NaCl, a quite large variability was observed concerning the parameters $t_{50\%}$, U_{25-75} , and AUC kinetically describing the germination cumulative curve of the accessions. This variability, evident also in control condition, resulted amplified by imposing salt stress. Among the 274 rice accessions analyzed, by expressing their responses to the salt treatment as SSI, two of them resulted, for each of the kinetic parameter evaluated, were always included in the 10^{th} percentile grouping the most tolerant and the 10^{th} percentile grouping the most sensitive: Olcenengo and SR113 respectively. The high H^2value resulting for the kinetic considered parameters made possible the use of the data for phenotype-genotype association studies, exploiting the already existing GBS information for the panel. In total, 28 significant MTAs resulted by the GWAs carried out in MLM mode. Some of them were highlighted in control or salt condition and several were referred to SSI results. Three very interesting gene i.e. *Os01g0911100*- like *OsBAT1DEAD-box ATP-dependent RNA helicase, Os07g0485000 -OsTPP10,* and *Os08g0157600*, known to be in some ways involved in rice responses to salt stress are present in the LD block including three significant MTAs. Deeper analyses aimed at evaluating the existence of allelic polymorphism and/or expression profile under stress condition between highly tolerant and highly sensitive rice accessions are suggested.

6. References

Appelo, C.A.J., and Postma, D. (2004). Geochemistry, groundwater and pollution. CRC press.

Barrett, J.C., Fry, B., Maller, J., and Daly, M.J. (2005). Haploview: analysis and visualization of LD and haplotype maps. *Bioinformatics* 21, 263–265, doi:10. 1093/bioinformatics/bth457.

Benjamini, Y., Hochberg, Y. (1995). Controlling the false discovery rate: a practical and powerful approach to multiple testing. *J. R. Stat. Soc.* Ser. B. 57, 289–300, doi: 10.2307/2346101.

Bewley, J.D. (1997) Seed germination and dormancy. *Plant Cell* 9, 1055–1066.

Biscarini, F., Cozzi, P., Casella, L., Riccardi, P., Vattari, A., Orasen, G., Perrini, R., Tacconi, G., Tondelli, A., Biselli, C., Cattivelli, L., Spindel, J., McCouch, S., Abbruscato, P., Valé, G., Piffanelli, P., and Greco, R. (2016). Genome-Wide Association Study for traits related to plant and grain morphology, and root architecture in temperate rice accessions. *PLoS ONE*, 11(5), e0155425. doi:10.1371/journal.pone.0155425.

Cleveland, W. S. (1979). Robust locally weighted regression and smoothing scatterplots. *J. Am. Stat. Assoc.*74, 829–836, doi:10.1080/01621459.1979.10481038.

Counce, P.A., Keisling, T.C., and Mitchell, A.J. (2000). Rice growth staging system. *Crop Sci*. 40, 436-443. doi:10.2135/cropsci2000.402436x.

Daszkowska-Golec, A. (2011). Arabidopsis seed germination under abiotic stress as a concert of action of phytohormones. *Omics: J. Integ. Biol.*, 15, 763-774, doi: 10.1089/omi.2011.0082.

El-Kassaby, Y.A., Moss, I., Kolotelo, D., and Stoehr, M. (2008). Seed germination: mathematical representation and parameters extraction. *Forest Sci.* 54, 220–227.

Earl, D., and von Holdt, B. (2012). STRUCTURE HARVESTER: a website and program for visualizing STRUCTURE output and implementing the Evanno method. *Conserv. Genet. Res.* 4:359. doi: 10.1007/s12686-011-9548-7.

Farooq, M., Siddique, K. H., Rehman, H., Aziz, T., Lee, D. J., and Wahid, A. (2011). Rice direct seeding: experiences, challenges and opportunities. *Soil Till. Res*., 111, 87-98, doi:10.1016/j.still.2010.10.008.

Fischer R.A., Maurer R. (1978). Drought resistance in spring wheat cultivars. Grain yield responses. *Aust. J. Agr. Res.* 29, 897–912.doi:10.1071/AR9780897.

Flowers, T.J., Yeo, A.R. (1981). Variability in the resistance of sodium chloride salinity within rice (*Oryza sativa* L.) varieties. *New Phytol.* 88, 363–373, doi:10.1111/j.1469-8137.1981.tb01731.x.

Gabriel, S.B., Schaffner, S.F., Nguyen, H., Moore, J.M., Roy, J., Blumenstiel, B., Higgins, J., DeFelice, M., Lochner, A., Faggart, M., Liu-Cordero, S.N., Rotimi, C., Adeyemo, A., Cooper, R., Ward, R., Lander, E.S., Daly, M.J., and Altshuler, D. (2002). The structure of haplotype blocks in the human genome. Science 296, 2225–2229, doi: 10.1126/science.1069424.

Galland, M., He, D., Lounifi, I., Arc, E., Clément, G., Balzergue, S., Huguet, S., Cueff, G., Godin, B., Collet, B., Granier, F., Morin, H., Tran, J., Valot, B., and Rajjou, L. (2017). An integrated "multi-omics" comparison of embryo and endosperm tissue-specific features and their impact on rice seed quality. *Front. Plant Sci.* 8, 1984, doi: 10.3389/fpls.2017.01984.

Ge, L-F., Chao, D-Y., Zhu, M-Z., Gao, J-P. and Lin H-X. (2008). Overexpression of the trehalose-6-phosphate phosphatase gene *OsTPP1* confers stress tolerance in rice and results in the activation of stress responsive genes. *Planta* 228, 191–201.

Heenan, D.P., Lewin, L.G. McCaffery, D.W. (1988). Salinity tolerance in rice varieties at different growth stages. *Aust. J. Exp. Agric.* 28, 343–349, doi.org/10.1071/EA9880343.

Hoang, T.M.L., Tran, T.N., Ngoc T., Nguyen, T.K.T., Williams, B., Wurms, P. Bellairs, S., Mundree S. (2016). Improvement of salinity stress tolerance in rice: Challenges and opportunities. *Agronomy* 6, 54, doi:10.3390/agronomy6040054.

Hannachi, S., van Labeke, M. C. (2018). Salt stress affects germination, seedling growth and physiological responses differentially in eggplant cultivars (*Solanum melongena* L.). *Sci. Hort*., 228, 56-65, doi.org/10.1016/j.scienta.2017.10.002.

Hardie, D.G. (2000). Plant protein serine/threonine protein kinases: classification into sub-families and overview of function. *Adv. Bot. Inc. Adv. Plant Pathol.* 32, 1-44.

Hatzig, S.V., Frisch, M., Breuer F., Nesi, N., Ducournau, S., Wagner, M-H., Leckband, G., Abbadi, A. Snowdon, R.J. (2015). Genome-wide association mapping unravels the genetic control of seed germination and vigor in *Brassica napus*. *Front. Plant Sci.* 6:221. doi: 10.3389/fpls.2015.00221.

Huang, X., Zhao, Y., Wei, X., et al. (2011). Genome-wide association study of flowering time and grain yield traits in a worldwide collection of rice germplasm. *Nat. Genet.*, 44, 32–9.

Jombart, T., and Collins, C. (2015). A tutorial for discriminant analysis of principal components (DAPC) using adegenet 2.0. 0. London: Imperial College London, MRC Centre for Outbreak Analysis and Modelling.

Joosen R.V.L., Kodde J., Willems L.A.J., Ligterink W., van der Plas L.H.W., and Hilhorst H.W.M. (2010). GERMINATOR: a software package for high-throughput scoring and curve fitting of Arabidopsis seed germination. *Plant J.* 62, 148-159, doi:10.1111/j.1365-313X.2009.04116.x.

Kawahara, Y., de la Bastide, M., Hamilton, J. P., Kanamori, H., McCombie, W. R., Ouyang, S., Schwartz, D.C., Tanaka, T., Wu, J. , Zhou, S. , Childs, K.L , Davidson, R.M , Lin, H., Quesada-Ocampo, L. , Vaillancourt, B., Sakai, H., Lee, S.S., Kim, J., Numa, H., Itoh, T., Buell, C.R., andTakashi, M. et al. (2013). Improvement of the *Oryza sativa* Nipponbare reference genome using next generation sequence and optical map data. *Rice* 6, 4. doi:10.1186/1939-8433-6-4.

Kretzschmar, T., Pelayo, M.A.F., Trijatmiko, K.R., Gabunada, L.F.M., Alam, R., Jimenez, R., Mendioro, M.S., Slamet-Loedin, I.H., Sreenivasulu, N., Bailey-Serres, J., Ismail, A. M. Mackill, D.J., and Septiningsih, E.M. (2015). A trehalose-6-phosphate phosphatase enhances anaerobic germination tolerance in rice. *Nature Plants* 1, 15124, doi: 10.1038/nplants.2015.124.

Kumar, V., Singh, A., Mithra, S., Krishnamurthy, S., Parida, S., Jain, S. and Mohapatra, T. (2015). Genome-wide association mapping of salinity tolerance in rice (*Oryza sativa*). *DNA Research*, 22(,133–145.

Li, D., Dossa, K., Zhang, Y., Wei, X., Wang, L., Zhang, Y., et al. (2018). GWAS uncovers differential genetic bases for drought and salt tolerances in sesame at the germination stage. *Genes* 9, 87, doi:10.3390/genes9020087.

Luan, Z., Xiao, M., Zhou, D., Zhang, H., Tian, Y., Wu, Y., Song, Y. (2014). Effects of salinity, temperature, and polyethylene glycol on the seed germination of sunflower (*Helianthus annuus* L.). *The Sci. World J*. 2014, doi.org/10.1155/2014/170418.

Machado, R.M.A., Serralheiro, R.P. (2017). Soil salinity: Effect on vegetable crop growth. Management practices to prevent and mitigate soil salinization. *Horticulturae* 3, 30; doi:10.3390/horticulturae3020030.

Magneschi, L., Perata, P. (2009). Rice germination and seedling growth in the absence of oxygen. *Ann. Bot.* 103, 181-196.

Mangin, B., Siberchicot, A., Nicolas, S., Doligez, A., This, P., and Cierco-Ayrolles, C. (2012). Novel measures of linkage disequilibrium that correct the bias due to population structure and relatedness. *Heredity* 108, 285–291. doi: 10.1038/hdy.2011.73.

Marroni, F., Pinosio, S., Zaina, G., Fogolari, F., Felice, N., Cattonaro, F., et al. (2011). Nucleotide diversity and linkage disequilibrium in *Populus nigra* cinnamyl alcohol dehydrogenase (*CAD4*) gene. *Tree Genet. Genom*. 7, 1011–1023. doi: 10.1007/s11295-011-0391-5.

Mei, H., Zhu, X. and Zhang, T. (2013) Favorable QTL Alleles for yield and its components identified by association mapping in Chinese Upland cotton cultivars. *PLoS One* 12:e82193.

Mohammadi, R., Mendioro, M.S., Diaz, G.Q., Gregorio, G.B. and Singh, R.K. (2013), Mapping quantitative trait loci associated with yield and yield components under reproductive stage salinity stress in rice (*Oryza sativa* L.), *J. Genet*.92, 433–43.

Morgutti, S., Negrini, N., Pucciariello, C., and Sacchi, G.A. (2019). Role of Trehalose and Regulation of its Levels as a Signal Molecule to Abiotic Stresses in Plants. *In* Plant Signaling Molecules, Woodhead Publishing, pp. 235-255.

Morton, M. J., Awlia, M., Al-Tamimi, N., Saade, S., Pailles, Y., Negrão, S., and Tester, M. (2019). Salt stress under the scalpel – dissecting the genetics of salt tolerance. *Plant J*. 97, 148-163, doi: 10.1111/tpj.14189.

Munnik, T., Ligterink, W., Meskiene, I., Calderini, O., Beyerly, J., Musgrave, A. and Hirt, H. (1999). Distinct osmo-sensing protein kinase pathways are involved in signalling moderate and severe hyper-osmotic stress. *Plant J.* 20, 381–388.

Munns R., Tester M. (2008). Mechanisms of salinity tolerance. *Annu. Rev. Plant. Biol.* 59, 651-681, doi:10.1146/annurev.arplant.59.032607.092911.

Muramaki, M., Rago, Y., Yamashimo, T., Mizuno, T. (2007). Comparative Overviews of Clock-Associated Genes of *Arabidopsis thaliana* and *Oryza sativa*. *Plant Cell Physiol.* 48, 110–121, doi:10.1093/pcp/pcl043,

Nakashima, K., Jan, A., Todaka, D., Maruyama, K., Goto, S., Shinozaki, K., Yamaguchi-Shinozaki, K. (2014). Comparative functional analysis of six drought-responsive promoters in transgenic rice. *Planta* 239, 47-60, doi:10.1007/s00425-013-1960-7.

Nghi, K. N., Tondelli, A., Valè, G., Tagliani, A., Marè, C., Perata, P., and Pucciariello, C. (2019). Dissection of coleoptile elongation in japonica rice under submergence through integrated genome-wide association mapping and transcriptional analyses. *Plant Cell Environ*. 42, 1832-1846, doi: 10.1111/pce.13540-

Nyquist, W.E. (1991). Estimation of heritability and prediction of selection response in plant populations. *Crit. Rev. Plant Sci.* 10, 235–322. doi: 10.1080/07352689109382313.

Orasen, G. (2018). Genome-wide analysis of *japonica* rice performances under alternate wetting and drying and permanent flooding conditions. PhD thesis, University of Milan, doi: 10.13130/orasen-gabriele_phd2018-01-19.

Pritchard, J. K., Stephens, M., and Donnelly, P. J. (2000). Inference of population structure using multilocus genotype data. *Genetics* 155, 945–959.

Rajjou, L., Duval, M., Gallardo, K., Catusse, J., Bally, J., Job, C., Job, D. (2012). Seed germination and vigor. *Annu. Rev. Plant Biol*. 63, 507-533, doi:10.1146/annurev-arplant-042811-105550-

Reddy, I.N.B.L., Kim, B-K., Yoon I-S, Kim K-H, Kwon, T-R. (2017). Salt tolerance in rice: focus on mechanisms and approaches. *Rice Sci.* 24, 123-144.

Rozema, J., Flowers, T. Crops for a salinized world (2008). *Science* 322, 1478-1480, doi: 10.1126/science.1168572

Shi, Y., Gao, L., Wu, Z., Zhang, X., Wang, M., Zhang, C., Zhang, F., Zhou, Y., and Li, Z. (2017). Genome-wide association study of salt tolerance at the seed germination stage in rice. *BMC Plant Biol*. 17, 92-103, doi: 10.1186/s12870-017-1044-0.

Shima, S., Matsui, H., Tahara, S. and Imai, R. (2007). Biochemical characterization of rice trehalose-6-phosphate phosphatases supports distinctive functions of these plant enzymes. *FEBS J*. 274, 1192–1201.

Tanji, K.K., Kielen, N.C. Agricultural Drainage Water Management in Arid and Semi-Arid Areas. *FAO* 2002.

Turner, S. D. (2014). qqman: an R package for visualizing GWAS results using QQ and Manhattan plots. *Biorxiv*, 005165, doi.org/10.1101/005165.

Tuteja, N., Sahoo, R.K., Huda, K.M.K., Tula, S. and Tuteja, R. (2015). *OsBAT1* augments salinity stress tolerance by enhancing detoxification of ROS and expression of stress-responsive genes in transgenic rice. *Plant Mol. Biol. Rep.* 33, 1192–1209. doi:10.1007/s11105-014-0827-9.

Volante A., Desiderio F., Tondelli A., Perrini R., Orasen G., Biselli C., Riccardi P., Vattari A., Cavalluzzo D., Urso S., Hassen M.B., Fricano A., Piffanelli P., Cozzi P., Biscarini F., Sacchi G.A., Cattivelli L., and Valè G. (2017), Genome-Wide Analysis of japonica rice performance under limited water and permanent flooding conditions. *Front. Plant Sci.* 8, 862, doi: 10.3389/fpls.2017.01862-

Xu, X., Liu, X., Ge, S., Jensen, J., Hu, F., Li, X. and Wang, W. (2011). Resequencing 50 accessions of cultivated and wild rice yields markers for identifying agronomically important genes. *Nature Biotechnology* 30, 105-111

Zhang, J., Song, Q., Cregan, P.B., and Jiang, G.-L. (2016). Genome-wide association study, genomic prediction and marker-assisted selection for seed weight in soybean (*Glycine max*). *Theor. Appl. Genet.* 129, 117–130, doi:10.1007/s00122-015-2614-x.

Zhao, K., Tung, C.W., Eizenga, G.C., Norton, G.J., Islam, M.R., Reynolds, A., Mezey, J., Bustamante, C.D. (2011). Genome-wide association mapping reveals a rich genetic architecture of complex traits in *Oryza sativa*. *Nat. Commun.* 2, 467, doi: 10.1038/ncomms1467.

Supplemental Material

Supplemental table 1. List of the rice accessions included in the considered panel. Their country of origin, subgroup, commercia class and population subgroup membership are reported.

Accession	Origin	Group	Commercial Class	Structure Group
A201	USA	tropical japonica	Long B	k2
A301	USA	tropical japonica	Long B	k2
ADAIR	USA	tropical japonica	Long B	k2
ADELAIDE CHIAPPELLI	ITALY	temperate japonica	Long A	k1
AGATA	ITALY	temperate japonica	Long A	k1
AGOSTANO	ITALY	temperate japonica	Long A	k1
AIACE	ITALY	tropical japonica	Long A	k2
AKITAKOMACHI	JAPAN	temperate japonica	Round	k1
ALAN	USA	tropical japonica	Long B	k2
ALEXANDROS	GREECE	tropical japonica	Long B	k2
ALICE	ITALY	temperate japonica	Long A	k1
ALLORIO	ITALY	temperate japonica	Long A	k1
ALPE	ITALY	temperate japonica	Long A	k1
ALPHA	ITALY	temperate japonica	Long A	k1
AMERICANO	ITALY	temperate japonica	Round	k1
ANSEATICO	ITALY	temperate japonica	Long A	admixed
ANTARES	ITALY	temperate japonica	Long A	admixed
ANTONI	BULGARIA	temperate japonica	Long A	k1
APOLLO	ITALY	tropical japonica	Long B	k2
ARBORIO	ITALY	temperate japonica	Long A	k1
ARGO	ITALY	temperate japonica	Medium	k1
ARSENAL	ITALY	tropical japonica	Long B	k2
ARTEMIDE	ITALY	tropical japonica	Long B	admixed
AUGUSTO	ITALY	temperate japonica	Long A	k1
BAHIA	SPAIN	temperate japonica	Medium	k1
BAIXET	SPAIN	temperate japonica	Long A	k1
BALDO	ITALY	temperate japonica	Long A	k1
BALILLA	ITALY	temperate japonica	Round	k1
BALZARETTI	ITALY	temperate japonica	Medium	k1
BARAGGIA	ITALY	temperate japonica	Round	k1
BEIRAO	PORTUGAL	temperate japonica	Long A	k1
BELLE PATNA	USA	tropical japonica	Long B	k2
BENGAL	USA	temperate japonica	Long A	admixed
BERTONE	ITALY	temperate japonica	Long A	k1
BIANCA	ITALY	temperate japonica	Long A	k1
BOMBILLA	SPAIN	temperate japonica	Medium	k1
BOMBON	SPAIN	temperate japonica	Medium	k1

BONNI	ITALY	temperate japonica	Long A	k1
BRAZOS	USA	tropical japonica	Long A	k2
BURMA	ITALY	tropical japonica	Long A	admixed
CALENDAL	FRANCE	temperate japonica	Long A	k1
CALMOCHI 101	USA	temperate japonica	Medium	k1
CAMPINO	PORTUGAL	temperate japonica	Medium	k1
CAPATAZ	SPAIN	temperate japonica	Long A	k1
CARINA	BULGARIA	temperate japonica	Round	k1
CARIOCA	ITALY	tropical japonica	Long B	admixed
CARMEN	ITALY	temperate japonica	Long A	k1
CARNAROLI	ITALY	temperate japonica	Long A	k1
CARNISE	ITALY	temperate japonica	Long A	k1
CARRICO	PORTUGAL	temperate japonica	Round	k1
CASTELMOCHI	ITALY	temperate japonica	Round	k1
CENTAURO	ITALY	temperate japonica	Round	k1
CHIPKA	BULGARIA	temperate japonica	Round	k1
CIGALON	FRANCE	temperate japonica	Medium	k1
CINIA 40	CILE	temperate japonica	Long A	k1
CLOT	SPAIN	temperate japonica	Medium	k1
COCODRIE	USA	tropical japonica	Long B	k2
COLINA	SPAIN	temperate japonica	Round	k1
CORBETTA	ITALY	temperate japonica	Medium	k1
CRESO	ITALY	temperate japonica	Long A	k1
CRIPTO	ITALY	temperate japonica	Round	k1
CT36	COLOMBIA	temperate japonica	Long B	k1
CT58	COLOMBIA	temperate japonica	Long A	k1
DELFINO	ITALY	temperate japonica	Long A	k1
DELLMONT	USA	tropical japonica	Long B	k2
DELLROSE	USA	tropical japonica	Long A	k2
DIMITRA	GREECE	temperate japonica	Long A	k1
DIXIEBELLE	USA	tropical japonica	Long A	k2
DOURADAO	BRAZIL	tropical japonica	Long A	k2
DRAGO	ITALY	temperate japonica	Long A	k1
DREW	USA	tropical japonica	Long B	k2
DUCATO	ITALY	temperate japonica	Round	k1
ERCOLE	ITALY	temperate japonica	Long A	k1
ERMES	ITALY	tropical japonica	Long B	admixed
ESCARLATE	PORTUGAL	temperate japonica	Round	k1
ESTRELA	PORTUGAL	temperate japonica	Long A	admixed
EUROPA	ITALY	temperate japonica	Long A	k1
EUROSE	ITALY	temperate japonica	Long A	k1
EUROSIS	ITALY	temperate japonica	Long A	admixed

FAMILIA 181	PORTUGAL	temperate japonica	Long A	k1
FAST		tropical japonica	Long B	k2
FIDJI	PHILIPPINES	tropical japonica	Long B	admixed
FLIPPER	ITALY	temperate japonica	Long B	k1
FRANCES	SPAIN	temperate japonica	Medium	k1
GALILEO	ITALY	temperate japonica	Long A	k1
GANGE	ITALY	tropical japonica	Long B	k2
GARDE SADRI	TURKEY	temperate japonica	Long A	k1
GIADA	ITALY	tropical japonica	Long B	k2
GIANO	ITALY	tropical japonica	Long B	admixed
GIGANTE VERCELLI	ITALY	temperate japonica	Long A	k1
GIOVANNI MARCHETTI	ITALY	temperate japonica	Medium	k1
GITANO	ITALY	temperate japonica	Long A	k1
GIZA 177	EGYPT	temperate japonica	Medium	k1
GLADIO	ITALY	tropical japonica	Long B	k2
GLORIA	AUSTRALIA	temperate japonica	Long A	k1
GOOLARAH	FRANCE	tropical japonica	Long B	k2
GRAAL	FRANCE	tropical japonica	Long B	admixed
GRALDO	ITALY	tropical japonica	Long B	admixed
GREGGIO	ITALY	temperate japonica	Long A	k1
GREPPI	ITALY	tropical japonica	Round	admixed
GRITNA	ITALY	temperate japonica	Long A	k1
GUADIAMAR	SPAIN	temperate japonica	Medium	k1
GZ8367	EGYPT	temperate japonica	Round	k1
HANDAO 11	CHINA	temperate japonica	Round	k1
HANDAO 297	CHINA	temperate japonica	Round	k1
HAREM	PORTUGAL	temperate japonica	Long A	k1
HARRA	AUSTRALIA	temperate japonica	Round	k1
HONDURAS	SPAIN	tropical japonica	Long A	k2
IAC32 52	BRAZIL	tropical japonica	Long B	k2
IBO 380-33	PORTUGAL	temperate japonica	Long A	k1
IBO 400	PORTUGAL	temperate japonica	Long A	k1
ITALMOCHI	ITALY	temperate japonica	Medium	k1
ITALPATNA 48	ITALY	temperate japonica	Long A	k1
ITALPATNAxMILYANG	PORTUGAL	temperate japonica	Long A	admixed
JACINTO	USA	tropical japonica	Long A	k2
JEFFERSON	USA	tropical japonica	Long A	k2
JUBILIENI	BULGARIA	temperate japonica	Round	k1
KARNAK	ITALY	temperate japonica	Long A	k1
KING	ITALY	tropical japonica	Long B	k2
KORAL	ITALY	temperate japonica	Long A	k1
KRYSTALLINO	ITALY	temperate japonica	Round	k1

KULON	RUSSIA	temperate japonica	Long A	k1
L201	USA	tropical japonica	Long B	k2
L202	USA	tropical japonica	Long B	k2
L204	USA	tropical japonica	Long B	k2
L205	USA	tropical japonica	Long B	k2
LACASSINE	USA	tropical japonica	Long B	k2
LAGRUE	USA	tropical japonica	Long A	k2
LAMONE	ITALY	tropical japonica	Long B	k2
LENCINO	ITALY	temperate japonica	Round	k1
LIDO	ITALY	temperate japonica	Medium	k1
LOMELLINO	ITALY	temperate japonica	Medium	k1
LORD	ITALY	temperate japonica	Long A	k1
LOTO	ITALY	temperate japonica	Long A	k1
LUNA	USA	temperate japonica	Medium	k1
LUSITO IRRADIADO	PORTUGAL	temperate japonica	Long A	k1
LUXOR	ITALY	temperate japonica	Long A	k1
M202	USA	temperate japonica	Medium	k1
M203	USA	temperate japonica	Long A	k1
M204	USA	temperate japonica	Long A	k1
M6	ITALY	temperate japonica	Long A	k1
MAIORAL	PORTUGAL	temperate japonica	Long A	admixed
MANTOVA	ITALY	temperate japonica	Long A	k1
MARATELLI	ITALY	temperate japonica	Medium	k1
MARENY	SPAIN	temperate japonica	Long A	k1
MARTE	ITALY	temperate japonica	Round	k1
MAYBELLE	USA	tropical japonica	Long B	k2
MECO	FRANCE	temperate japonica	Long A	admixed
MEJANES	FRANCE	temperate japonica	Long B	admixed
MELAS	GREECE	temperate japonica	Long B	k1
MIARA	ITALY	temperate japonica	Long B	k1
MILEV 21	BULGARIA	temperate japonica	Round	k1
MOLO	ITALY	temperate japonica	Long A	k1
MONTICELLI	ITALY	temperate japonica	Medium	k1
MUGA	PORTUGAL	temperate japonica	Round	k1
MUSA	ITALY	temperate japonica	Long A	k1
NANO	ITALY	temperate japonica	Round	admixed
NEMBO	ITALY	temperate japonica	Long A	k1
NILO	ITALY	temperate japonica	Long A	k1
NOVARA	ITALY	temperate japonica	Medium	k1
OLCENENGO	ITALY	temperate japonica	Long A	k1
ONICE	ITALY	temperate japonica	Long A	k1
OPALE	ITALY	temperate japonica	Long A	k1

ORIGINARIO	ITALY	temperate japonica	Round	k1
ORIONE	ITALY	temperate japonica	Long A	k1
OSCARxSUWEON	PORTUGAL	temperate japonica	Long A	admixed
OSTIGLIA	ITALY	temperate japonica	Round	k1
OTA	PORTUGAL	temperate japonica	Long A	k1
P6	ITALY	temperate japonica	Medium	k1
PADANO	ITALY	temperate japonica	Long A	k1
PANDA	ITALY	tropical japonica	Long B	admixed
PECOS	USA	tropical japonica	Medium	admixed
PEGONIL	SPAIN	temperate japonica	Medium	k1
PELDE	AUSTRALIA	temperate japonica		k1
PERLA	ITALY	temperate japonica	Round	k1
PIEMONTE	ITALY	temperate japonica	Long A	k1
PIERINA MARCHETTI	ITALY	temperate japonica	Long A	k1
PLOVDIV 22	BULGARIA	temperate japonica	Long A	k1
PLOVDIV 24	BULGARIA	temperate japonica	Round	k1
PLUS	ITALY	tropical japonica	Long B	k2
PREVER	ITALY	tropical japonica	Long B	admixed
PROMETEO	ITALY	temperate japonica	Medium	k1
PUNTAL	SPAIN	tropical japonica	Long B	k2
RANGHINO	ITALY	temperate japonica	Round	k1
RAZZA 77	ITALY	temperate japonica	Medium	k1
REDI	ITALY	temperate japonica	Long A	k1
REXMONT	USA	tropical japonica	Long B	k2
RIBE	ITALY	temperate japonica	Long A	k1
RINALDO BERSANI	ITALY	temperate japonica	Long A	k1
RINGO	ITALY	temperate japonica	Long A	k1
RIZZOTTO 51 1	ITALY	temperate japonica	Long A	k1
ROBBIO SEL1	ITALY	temperate japonica	Long A	k1
RODEO	ITALY	temperate japonica	Long A	k1
RODINA	BULGARIA	temperate japonica	Round	k1
ROMA	ITALY	temperate japonica	Long A	k1
RONCAROLO	ITALY	temperate japonica	Medium	k1
RONCOLO	ITALY	temperate japonica	Medium	k1
ROTUNDUS	HUNGARY	temperate japonica	Long A	k1
ROXANI	GREECE	temperate japonica	Long A	k1
RPC 12	CHINA	temperate japonica	Round	k1
RUBI	PORTUGAL	temperate japonica	Long A	k1
RUBINO	ITALY	temperate japonica	Round	k1
RUSSO	ITALY	temperate japonica		k1
S101	USA	temperate japonica	Medium	k1
S102	USA	temperate japonica	Medium	k1

S102 2	USA	temperate japonica	Medium	k1
SAEDINENIE	BULGARIA	temperate japonica	Long A	k1
SAFARI	PORTUGAL	temperate japonica	Long A	k1
SAGRES	PORTUGAL	temperate japonica	Long A	k1
SAKHA 102	EGYPT	temperate japonica	Medium	k1
SAKHA 103	EGYPT	temperate japonica	Round	k1
SALOIO	PORTUGAL	temperate japonica	Long B	k1
SALVO	ITALY	tropical japonica	Long B	admixed
SAMBA	ITALY	tropical japonica	Long A	admixed
SANDOCA	PORTUGAL	temperate japonica	Long B	k1
SANT ANDREA	ITALY	temperate japonica	Long A	k1
SANTERNO	ITALY	temperate japonica	Long B	admixed
SATURNO	ITALY	tropical japonica	Long B	k2
SAVIO	ITALY	temperate japonica	Long B	k1
SCUDO	ITALY	tropical japonica	Long B	k2
SELENIO	ITALY	temperate japonica	Round	k1
SELN 244A	AUSTRALIA	temperate japonica	Medium	k1
SENATORE NOVELLI	ITALY	temperate japonica	Long A	k1
SENIA	SPAIN	temperate japonica	Medium	k1
SEQUIAL	SPAIN	temperate japonica	Medium	k1
SESIA	ITALY	temperate japonica	Long A	k1
SESIAMOCHI	ITALY	temperate japonica	Long A - Round	k1
SETANTUNO	PORTUGAL	temperate japonica	Round	k1
SFERA	ITALY	temperate japonica	Round	k1
SHSS 381	SPAIN	temperate japonica	Long A	k1
SHSS 53	SPAIN	temperate japonica	Long A	k1
SILLA	ITALY	temperate japonica	Long A	k1
SIRIO CL	ITALY	tropical japonica	Long A	k2
SIS R215	ITALY	tropical japonica	Long A	k2
SLAVA	BULGARIA	temperate japonica	Medium	k1
SMERALDO	ITALY	temperate japonica	Long A	k1
SOURE	PORTUGAL	temperate japonica	Long A	k1
SPRINT	ITALY	tropical japonica	Long B	k2
SR 113	SPAIN	temperate japonica	Long A	k1
STRELLA	ITALY	temperate japonica	Long A	k1
SUPER	PORTUGAL	temperate japonica	Long A	k1
T757	INDIA	temperate japonica	Long A	k1
TAICHUNG 65	THAILAND	temperate japonica	Long A	k1
TEJO	ITALY	temperate japonica	Long A	admixed
TEXMONT	USA	tropical japonica	Long A	k2
THAIBONNET	ITALY	tropical japonica	Long B	k2
THAIPERLA		temperate japonica	Round	k1

TITANIO	ITALY	temperate japonica	Long A	k2
TOPAZIO	ITALY	temperate japonica	Medium	k1
TORIO	PORTUGAL	temperate japonica	Long A	k1
ULISSE	ITALY	temperate japonica	Long A	k1
ULLAL	SPAIN	temperate japonica	Round	k1
UPLA 32	ARGENTINA	tropical japonica	Long B	k2
UPLA 63	ARGENTINA	tropical japonica	Long B	admixed
UPLA 64	ARGENTINA	tropical japonica	Long B	admixed
UPLA 66	ARGENTINA	tropical japonica	Long B	admixed
UPLA 68	ARGENTINA	tropical japonica	Long B	k2
UPLA 75	ARGENTINA	tropical japonica	Long B	admixed
UPLA 77	ARGENTINA	tropical japonica	Long B	admixed
UPLA 91	ARGENTINA	tropical japonica	Long B	k2
VALTEJO	PORTUGAL	temperate japonica	Round	k1
VELA	ITALY	temperate japonica	Long A	k1
VENERE	ITALY	temperate japonica	Long B	k1
VENERIA	ITALY	temperate japonica	Long A	k1
VIALE	ITALY	temperate japonica	Long A	k1
VIALONE 190	ITALY	temperate japonica	Medium	k1
VIALONE NANO	ITALY	temperate japonica	Medium	k1
VIALONE NERO	ITALY	temperate japonica	Round	k1
VICTORIA	ARGENTINA	temperate japonica	Round	k1
VIRGO	ITALY	temperate japonica	Medium	k1
VOLANO	ITALY	temperate japonica	Long A	k1
VULCANO	ITALY	temperate japonica	Long A	k1
YRM 6 2	AUSTRALIA	temperate japonica	Medium	k1
ZENA	ITALY	tropical japonica	Long B	k2

Supplemental table 2. SSI values of G_{max}, $t_{50\%}$, U_{25-75}, AUC and ER for each accession of the japonica rice panel

Accession	SSI G_{max}	SSI t_{50}	SSI U_{25-75}	SSI AUC	SSI Emerg.
A 201	1.009456	1.466891	0.950878	1.272154	1.246849
A301	0.800603	0.668249	0.896529	0.659394	1.103248
Ad.Chiappelli	-1.25192	1.324066	0.543605	0.64268	0.810334
Adair	2.243487	0.411797	2.188144	0.802606	1.282668
Agata	-0.26997	0.78507	0.641758	0.750301	1.157124
AGOSTANO	0.533735	0.862418	1.523605	0.929572	1.030436
Aiace	2.401808	1.208229	1.689648	1.495198	1.068168
Akitakomachi	0	0.913853	1.362088	0.629028	0.749559
Alan	0.327007	1.058825	1.922056	0.737846	0.681418
ALEXANDROS	4.173928	1.243269	1.860326	1.877264	1.022126
ALICE	3.391317	0.856327	2.320908	1.183293	1.007313
Allorio	1.031888	1.770617	1.367739	1.468965	1.077591
Alpe	-0.2764	1.238823	1.734557	0.945956	0.809183
Alpha	0.521741	1.271381	0.837613	0.958336	1.208552
Americano	0.773916	0.928828	0.355931	0.960211	1.219379
Anseatico	0.81944	1.163554	1.549324	1.496847	0.82404
Antares	4.030812	1.33599	1.503294	1.629714	1.277658
ANTONI	1.304353	1.177776	0.767283	1.081752	1.040711
Apollo	1.365734	1.206917	0.945753	1.017725	1.192481
Arborio	0.784374	0.92536	0.619001	-2.62766	1.308322
ARGO	-0.33168	1.202884	0.788687	1.040474	1.096194
ARSENAL	0.84942	1.162401	0.874364	1.279368	0.991153
Artemide	1.06747	1.331074	2.076902	1.27954	0.9967
Augusto	-1.07988	1.017808	0.231199	0.714789	0.808462
BAHIA	1.319175	1.085248	1.157024	1.143568	1.065489
BAIXET	0.809912	0.644612	0.624111	0.776912	1.084073
Baldo	0.260871	0.971258	0.83477	0.710843	1.143023
Balilla	0.623288	0.897563	0.640709	1.002272	0.713866
Balzaretti	2.953516	1.12521	1.218299	1.569759	0.709421
Baraggia	1.766547	0.876014	0.568857	1.329652	0.617535
Beirao	-0.28314	1.207623	0.417784	0.919947	1.140978
BELLEPATNA	-7.9E-09	0.945907	0.114668	0.71043	1.015932
Bengal	-0.26087	0.567645	0.317012	0.448243	0.956376
Bertone	-0.53994	1.101619	1.295665	0.778803	0.930189
Bianca	2.935543	1.260348	0.91982	1.705895	1.127864
Bombilla	0.52767	1.048226	0.795101	1.125888	0.917293
Bombon	0.266868	0.947903	0.380922	0.838719	0.982043
BONNI	1.088183	1.055226	1.355383	0.969454	0.993734
Brazos	8.19E-09	1.159991	1.252827	0.744436	1.17156
Burma	0.515944	0.944477	0.419945	0.632978	1.00537
Calendal	0	0.928261	1.782145	0.585867	1.072395
Calmochi 101	3.913058	1.088171	1.572267	1.841401	1.192481
Campino	1.06747	1.003565	1.493145	1.360661	1.093855
Capataz	0.521741	1.010675	0.837166	0.730194	1.001267
Carina	1.263528	0.299168		0.625818	0.545134
CARIOCA	1.381993	0.774006	1.616185	0.837707	1.101867
CARMEN	0.773916	1.123343	0.472115	0.907284	1.040711
Carnaroli	0.941249	1.121865	0.834811	1.132306	0.740671
Carnise	-0.54629	0.854498	0.978308	0.833888	1.175779

Carrico	0.52767	1.174795	1.286917	1.358145	0.958244
Castelmochi	0.52767	0.866469	0.976421	0.86235	1.197643
Centauro	-0.5528	1.089729	1.129721	1.132176	1.070799
Chipka	2.321748	1.082258	0.832219	1.408309	0.916389
Cigalon	1.092587	0.83847	2.016333	1.164629	0.855112
Cinia40	5.070484	1.430403	3.004125	1.604139	1.000832
CLOT	-8.1E-09	1.318595	1.260331	0.883575	1.096194
COCODRIE	1.846845	1.018956	0.735342	1.052509	1.016352
Colina	0.263835	1.439	0.705753	1.222188	1.075923
CORBETTA	1.868073	0.632666	1.300823	0.671125	1.010378
Creso	-0.27315	1.584163	2.211809	1.500339	0.784663
Cripto	0.52767	1.014685	1.235092	0.906815	1.055098
CT36	1.319175	1.01591	0.580998	1.415797	1.027064
CT58	0.52767	0.885843	0.882954	0.736766	1.010378
DELFINO	-0.26383	0.997135	1.145303	0.681225	1.102293
Dellmont	1.552109	0.828581	4.190566	1.403443	0.465358
Dellrose	1.393049	0.761569	0.318949	0.809112	0.630942
Dimitra	0.52767	1.221915	1.158258	1.14103	0.982043
Dixiebelle	2.57972	0.850601	0.814351	1.234679	1.314163
Douradao	0.515944	0.845994	1.301895	0.688918	0.964468
Drago	4.536748	1.461539	0.964042	1.732941	0.886924
Drew	0.791505	1.136695	1.04907	1.032212	1.108747
Ducato	0.533735	1.207193	1.00784	1.152676	0.877758
Ercole	0.784374	0.998046	0.609084	0.947126	0.637455
Ermes	0.260871	1.034576	-0.49816	0.799672	0.841751
Escarlate	2.902185	1.083067	1.023047	1.695155	0.312782
Estrela	0.934932	1.0225	1.004813	0.925581	0.408851
Europa	2.321748	1.710697	1.331135	1.599893	1.221852
EUROSE	-0.26997	1.03048	1.661599	0.66293	1.022126
Eurosis	1.079883	1.466828	1.55759	1.356265	0.834389
Familia181	0	1.047841	0.935952	1.117451	1.127864
Fast	1.334338	1.176355	1.33687	1.309358	0.817701
Fidji	2.347835	1.11741	1.696155	1.533966	1.109284
FLIPPER	-0.26687	1.673134	0.679332	0.779524	1.03694
Frances	0.521741	1.15257	0.64711	0.78732	1.080869
Galileo	-0.54629	1.381324	0.752974	0.91369	1.135696
Gange	2.608705	1.232335	1.242045	1.509629	0.881835
Gardesadri	1.565223	1.056994	0.994396	1.342768	0.801668
Giada	0	0.878335	0.252202	0.558248	1.149892
Giano	1.031888	1.134435	1.194012	1.148867	0.811902
Gigantevercelli	-0.84942	0.803954	1.15399	0.344883	0.916004
Giovanni Marchetti	0.531233	0.942135	0.74648	0.710787	0.999412
Gitano	3.16602	1.33269	1.283209	1.789514	0.887908
GIZA 177	0.619133	0.785481	0.712899	0.865006	0.700346
Gladio	2.26512	1.080343	0.790749	1.223542	0.892892
Gloria	-1.8574	0.885719	1.149048	1.086146	1.070799
Goolarah	0.266868	1.011625	0.680961	0.947009	0.851772
GRAAL	1.868073	0.831288	0.613408	0.862764	1.032451
Graldo	2.837692	1.240533	1.643854	1.494993	1.055098
Greggio	3.130446	1.220949	0.92573	1.711766	0.848979

Greppi	0.464282	0.552886	0.20568	1.047293	0.42449
Gritna	0.77911	0.866419	0.954105	0.62811	1.26372
Guadiamar	0	0.877355	1.873218	0.937466	1.115047
GZ8367	1.638881	0.796703	1.396595	1.184149	0.932466
HANDAO11	2.057245	1.027352	1.042989	1.620834	1.031861
HANDAO297	1.381993	0.817356	1.097565	1.134337	1.048335
Harem	1.57942	0.634048	0.269872	0.890002	0.664798
Harra	0.947652	0.731439	0.986496	0.711073	0.747361
Honduras	0.154783	0.695444	0.310096	0.439406	0.746315
IAC 3252	2.166965	0.531572	-0.17271	0.815784	0.681418
IBO 38033	1.209244	0.77052	0.584078	0.978569	0.572391
IBO400	1.304353	0.928011	1.291437	0.867609	0.929206
Italmochi	6.433759	2.065278	1.02624	2.709426	1.104366
Italpatna x Milyang	1.601205	1.170975	1.391045	1.239583	1.209276
Italpatna48	-7.9E-09	0.846996	0.20778	0.70724	1.18246
Jacinto	-0.16236	0.516864	0.109604	0.559992	0.681418
Jefferson	3.391317	1.35721	1.593372	1.574994	1.099061
Jubilieni	-0.53374	0.961028	0.777705	0.641075	1.197643
Karnak	0.521741	0.656036	0.518673	0.698993	0.960179
King	1.565223	0.969785	0.451115	1.072109	1.188856
KORAL	1.381993	1.377478	2.372274	1.328688	1.048335
KRYSTALLINO	-0.84942	0.859325	0.3797	0.730954	1.028104
Kulon	-1.13256	1.192439	2.52629	0.647819	1.122335
L201	0.273147	0.86284	1.166363	0.749331	1.115047
L202	1.06747	0.558271	0.657253	0.82867	1.070799
L204	2.11068	1.436291	1.994097	1.51541	1.26549
L 205	2.487587	1.109642	2.33417	1.16044	1.178044
Lacassine	-0.15794	0.916268	2.278647	0.747268	1.231793
LAGRUE	0.839186	1.127889	0.988159	1.12103	1.050519
Lamone	1.118915	1.569305	0.860979	1.407206	1.084073
LENCINO	-1.7E-08	1.190791	2.132453	0.970072	1.103248
LIDO	1.05534	0.945614	0.878107	0.881888	1.022126
Lomellino	0.533735	0.968122	0.730283	0.71023	1.211409
LORD	1.638881	1.153931	0.636117	1.196235	1.097839
LOTO	0.800603	1.244031	0.818242	0.991489	0.991153
Luna	1.28986	0.835043	0.937485	0.917859	1.00537
LusitoIrradio859	0.539941	1.192867	1.399554	1.113432	0.865292
Luxor	-0.52767	1.300439	0.288385	0.776251	1.217853
M202	4.826572	1.077557	0.684731	2.174545	1.022126
M203	-0.26087	0.819995	0.291462	0.566442	0.99779
M204	0	0.809865	1.186149	0.992466	0.986881
M6	1.365734	0.816424	0.638647	1.276315	1.221852
Maioral	1.334338	0.757077	0.855091	0.999272	1.078911
Mantova	1.9581	1.152153	0.520064	1.353649	1.12696
Maratelli	-0.53374	1.224049	2.541075	1.023455	1.112982
MARENY	0.269971	1.020008	1.0251	0.678722	0.991153
MARTE	8.01E-09	0.947337	0.762284	0.75906	1.033117
Maybelle	1.381993	1.624453	0.406389	1.186776	1.219379
MECO	0.628632	0.895552	0.672341	0.89919	1.303581
Mejanese	0.52767	0.969609	-0.18618	0.711968	0.876108

Melas	1.031888	1.420909	0.355902	0.856608	0.867259
Miara	0.338941	0.885825	1.537301	0.800893	1.331141
Milev21	1.043482	1.058817	0.718475	1.150461	1.139826
MOLO	1.28986	0.880742	1.110922	1.050295	0.989155
Monticelli	0	1.005643	0.426128	1.014253	0.829552
Muga	0.266868	1.46997	1.723217	1.045368	0.781626
Musa	1.319175	0.765512	0.691456	0.860701	1.178044
Nano	1.737362	0.556219	0.376727	0.921432	0.561167
Nembo	0.552797	1.190071	1.59445	1.093187	1.101867
Nilo	1.043482	1.255188	-0.16607	0.891572	0.790049
Novara	1.105594	1.148099	0.809425	1.203942	0.711044
Olcenengo	-0.31588	0.610816	0.499527	0.528924	0.668561
Onice	0.782612	0.887471	0.94914	0.860425	1.178044
Opale	0.52767	1.442224	1.000965	1.050373	1.00537
Originario	0	0.940725	0.822747	0.824261	0.763188
Orione	2.487587	1.606811	2.052909	1.844961	0.923211
OscarXSuweon285	0.546294	0.763106	1.126186	0.663457	1.17156
Ostiglia	-0.54629	0.976187	0.582562	0.795882	0.838668
Ota	0.009202	1.200796	1.489757	0.946029	0.99779
P6	6.393218	0.787411	0.343647	-1.85385	1.30605
Padano	0	0.714211	0.635234	0.602525	0.772951
Panda	1.319175	0.727815	1.069868	0.790163	1.121042
PECOS	0.260871	0.686379	2.512698	0.475464	1.022126
Pegonil	0	0.478509	0.115452	0.691739	0.67182
Pelde	0.036926	0.712965	0.861441	0.421286	0.769342
Perla	1.28986	0.686152	0.538953	0.826173	0.884001
Piemonte	-0.83919	0.877047	0.913171	0.51745	1.117078
Pier.Marchetti	0.52767	1.560256	1.955578	1.319142	1.198355
Plovdiv22	-0.56628	0.932638	0.70554	0.645158	1.074543
PLOVDIV24	2.347835	0.876377	0.778077	1.318128	1.015932
Plus	0.627499	0.828572	0.774401	0.801826	1.333839
Prever	0.81944	0.83401	1.524858	0.990986	0.924781
Prometeo	0.286636	0.862227	0.748116	0.787796	1.168144
Puntal	-0.27315	0.902267	0.236779	0.727439	0.794987
Ranghino	2.699707	1.044155	1.457404	1.46563	0.943501
RAZZA77	0.800603	0.57504	0.252472	0.537937	1.029698
Redi	1.431214	1.444353	1.376337	1.494898	1.230948
Rexmont	2.211188	1.222234	2.033848	1.226826	1.258002
Ribe	1.254999	1.001984	1.13613	1.116539	1.320247
Rinaldo B.	0.260871	1.339381	1.511529	1.205541	1.228471
Ringo	5.276699	1.207337	1.162918	2.027216	0.927888
Rizzotto511	0.533735	0.533323	0.677944	0.645771	1.207968
ROBBIOSEL1	-0.81944	1.045816	1.209008	0.832871	0.878272
Rodeo	-0.16977	1.012383		0.826639	1.362835
Rodina	1.031888	0.722898	0.492041	0.787359	1.135696
Roma	1.238265	0.727936	0.484995	0.984747	1.282668
Roncarolo	0.52767	0.691992	0.571985	0.741637	0.938346
Roncolo	1.105594	1.000592	0.840621	1.228078	1.084706
Rotundus	1.031888	0.695651	0.07337	0.776551	0.887428
ROXANI	6.260893	1.220228	0.823197	2.12154	1.050519

RPC12	0.260871	0.91303	3.001433	0.889511	1.04484
Rubi	-1.19064	0.651802	0.660821	0.455219	1.12582
Rubino	0.81944	1.052595	0.553273	1.190864	1.168144
Russo1	2.44495	1.108136	1.030593	1.547506	1.15841
S. Andrea	-0.31805	0.669457	1.168027	0.696926	0.666919
S101	1.319175	0.985139	1.153767	1.03095	1.028555
S102	0.533735	0.663413	0.565358	0.681205	0.768779
S102.2	0.773916	0.962964	0.819152	0.853517	0.782905
SAEDINENIE	0.260871	1.101854	0.70991	1.334002	1.097839
Safari	0.800603	0.884062	0.581181	0.857216	0.98427
Sagres	1.319175	0.876245	1.061652	1.168372	0.891085
SAKHA102	7.92E-09	0.838477	2.481298	0.657052	1.043421
Sakha103	0.257972	0.935254	0.811668	0.792674	0.887908
Saloio	0.515944	0.768733	0.437543	0.706238	1.059983
Salvo	1.912028	1.102282	1.394974	1.479318	0.851772
Samba	0.52767	0.645912	0.01451	0.582924	1.226552
Sandoca	1.090754	0.762739	0.507897	0.945748	0.629001
Santerno	0.515944	0.071634	0.8601	0.213673	1.115047
Saturno	1.678372	1.373206	2.64137	1.772851	0.859179
Savio	0.916479	0.99602	1.511753	1.173617	1.165323
SCUDO	3.239648	1.102386	1.281738	1.693736	1.043874
Selenio	0.263835	0.68912	1.527112	0.855764	0.923211
SELN244A620	0.515944	0.970722	0.729624	0.845119	1.054269
Sen Novelli	0.627499	0.704334	0.503695	0.519164	1.315841
Senia	1.098124	1.067306	1.071117	0.929664	1.314163
Sequial	0.269971	1.144425	1.178133	0.937894	1.150839
Sesia	1.120844	0.808207	1.07552	0.655998	1.238941
Sesiamochi	0	0.968503	0.851274	0.767679	1.30605
Setantuno	0.809912	0.87948	1.177365	0.968869	1.195957
Sfera	0.260871	0.83463	0.821349	0.733541	0.965342
SHSS 381	-1.16087	0.659707	0.702078	0.431973	1.188113
SHSS53	0.809912	2.014858	1.22151	1.310202	1.208967
Silla	3.293251	0.833408		1.480236	1.362835
Sirio	0	1.174846	0.890816	0.767452	1.211409
SISR 215	2.11068	0.999913	0.977391	1.463072	1.304842
Slava	2.63835	0.959473	0.716535	1.093008	0.851772
Smeraldo	5.696242	1.454609	3.103552	2.178639	1.109284
Soure	-0.27973	0.803033	0.401928	0.625909	0.96833
SPRINT	-1.46946	1.136705	0.358733	0.832917	0.994501
SR113	2.945501	1.390756	2.099119	1.900781	1.302265
STRELLA	0.279729	1.115597	1.463395	1.314025	0.994501
Super	0.533735	0.892359	2.634313	0.758517	1.099832
T757	1.098124	1.014049	0.904532	1.038316	1.280239
Taichung65	-0.26383	1.601383	1.986398	1.191442	0.811902
TEJO	7.92E-09	0.798202	0.868046	0.852727	1.015446
Texmont	0	1.072667	1.13127	0.899077	1.168144
Thaibonnet	-0.16341	1.535622	1.283008	1.373625	1.27198
Thaiperla	0.515944	1.119796	0.578084	1.026409	0.908557
Titanio	1.469461	0.996185	0.605564	0.809462	0.926728
TOPAZIO	2.13494	1.005729	2.142332	1.26895	1.05133

Torio	0.521741	0.752642	0.918916	0.535425	0.931271
Ulisse	2.685014	1.315112	1.508489	1.656322	1.322752
Ullal	0.533735	0.805107	1.008111	0.763351	0.967173
UPLA 32	1.317304	0.956556	1.353459	0.893485	1.244328
UPLA 63	0.320241	0.756956	1.184384	0.528659	1.238941
UPLA 64	0.773916	0.334723	1.794375	0.553391	1.111787
UPLA66	2.763985	1.201032	1.784495	1.379644	1.226552
UPLA68	0	0.761152	0.982104	0.636303	1.230948
UPLA 75	0.640482	0.824147	0.876812	0.664075	0.726845
UPLA77	0.829196	1.504913	0.980343	0.927427	1.084706
Upla91	0.263835	1.137918	1.64428	0.758598	1.168144
Valtejo	8.39E-09	0.878561	1.300718	1.029445	0.963957
Vela	-0.26997	0.915207	0.765017	0.512273	1.075923
Venere	4.063059	1.338738	0.909987	2.24475	0.970154
Veneria	3.391317	0.978345	1.625316	1.50544	0.863129
Viale	0	0.659607	1.104588	0.507308	0.769342
Vialone Nano	2.797286	0.838078	1.318041	1.338201	0.849303
Vialone Nero	0	0.662995	1.363683	0.581354	0.900857
Vialone190	2.057245	1.24574	0.81479	1.533917	1.18246
Victoria	0.319446	0.89173	0.967574	0.748429	0.691015
Virgo	8.19E-09	0.832672	0.74069	0.764886	0.785363
Volano	-0.28314	0.831837	0.946969	0.520062	1.198355
Vulcano	1.441828	0.472589		1.333303	1.362835
YRM62	0.52767	0.863007	0.248883	0.843667	0.821709
Zena	2.731468	0.989703	1.414456	1.490983	1.186171
10^{th} percentile	-0.27315	0.686198	0.379403	0.625836	0.752285
90^{th} percentile	2.675681	1.370007	1.878102	1.514253	1.237512

Supplemental table 3. Broad-sense hereditability (H^2) of the values of the parameters recorded in control or salt condition

Trait	H^2	
	Control	Salt
G_{max} (%)	0.36	0.51
$t_{50\%}$ (h)	0.90	0.88
$U_{25\text{-}75}$ (h)	0.52	0.61
AUC (cm^2)	0.69	0.83
ER (%)	0.57	0.29

Supplemental table 4. Significance of variance estimates related to rice accession (A), treatment (T; control and salt) and their interactions on parameter describing seed germination kinetic and seedling emergence rate from soil Significance at P < 0.001 (***).

Trait	Accession (A)	Treatment (T)	AxT
G_{max} (%)	***	***	***
$t_{50\%}$ (h)	***	***	***
$U_{25\text{-}75}$ (h)	***	***	***
AUC (cm^2)	***	***	***
ER (%)	***	***	***

Supplemental table 5. Correlation between germination parameters in both control and salt conditions. The Spearman' s correlation coefficients are reported. Significance at P < 0.001 (***) or P<0.05 (**)

A)

Control		G_{max}	$t_{50\%}$	U_{25-75}	AUC	ER
Control	G_{max}	-	-0.157 **	0.545 ***	-0.364 ***	ns
	$t_{50\%}$		-	0.556 ***	-0.574 ***	ns
	U_{25-75}			-	-0.364 ***	ns
	AUC				-	ns
	ER					-

B)

Salt		G_{max}	$t_{50\%}$	U_{2575}	AUC	ER
Salt	G_{max}	-	-0.551 **	-0.471 ***	0.761 ***	ns
	$t_{50\%}$		-	0.645 ***	-0.898 ***	ns
	U_{25-75}			-	-0.650 ***	ns
	AUC				-	ns
	ER					-

C)

Control		G_{max}	$t_{50\%}$	U_{2575}	AUC	ER
Salt	G_{max}	0.421 ***	-	-	-	-
	$t_{50\%}$	-	0.823 ***	-	-	-
	U_{25-75}	-	-	0.588 ***	-	-
	AUC	-	-	-	0.677 ***	-
	ER	-		-	-	0577 ***

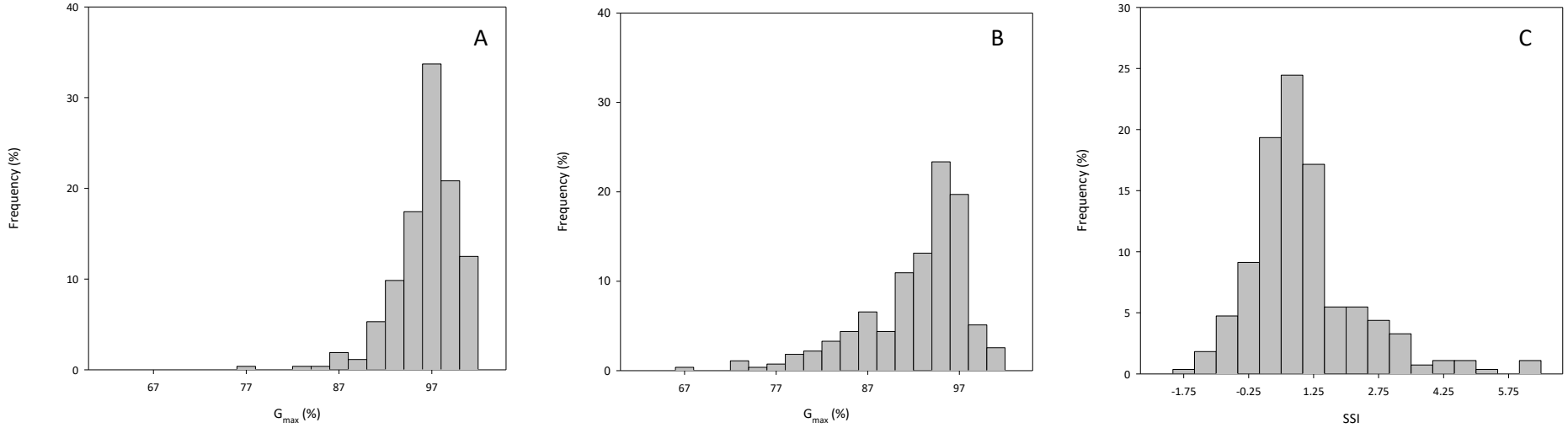

1

2

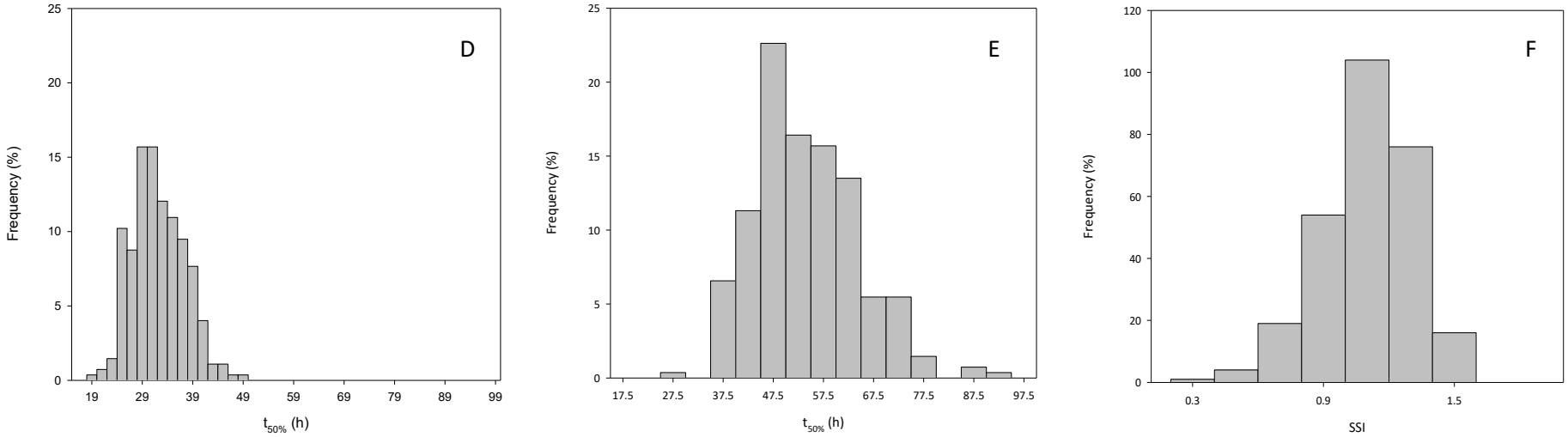

3

4

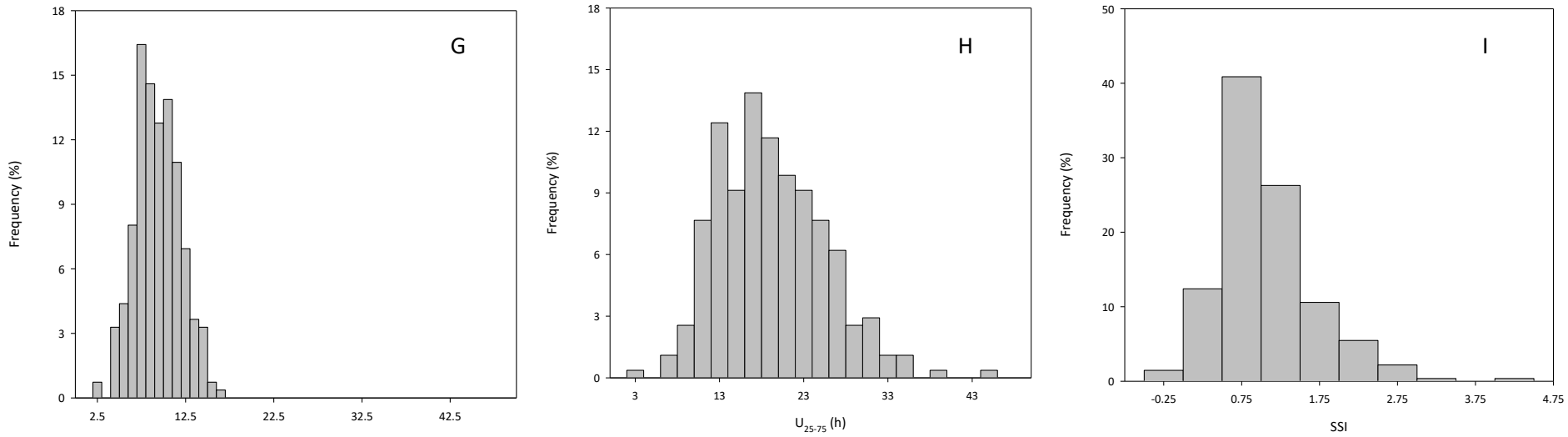

5

6

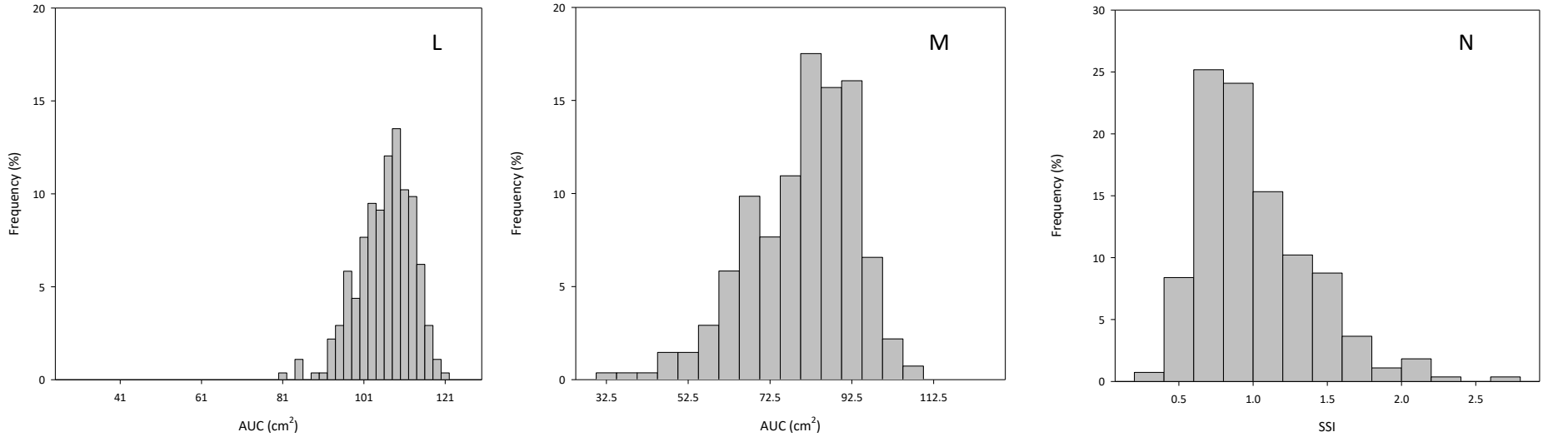

7

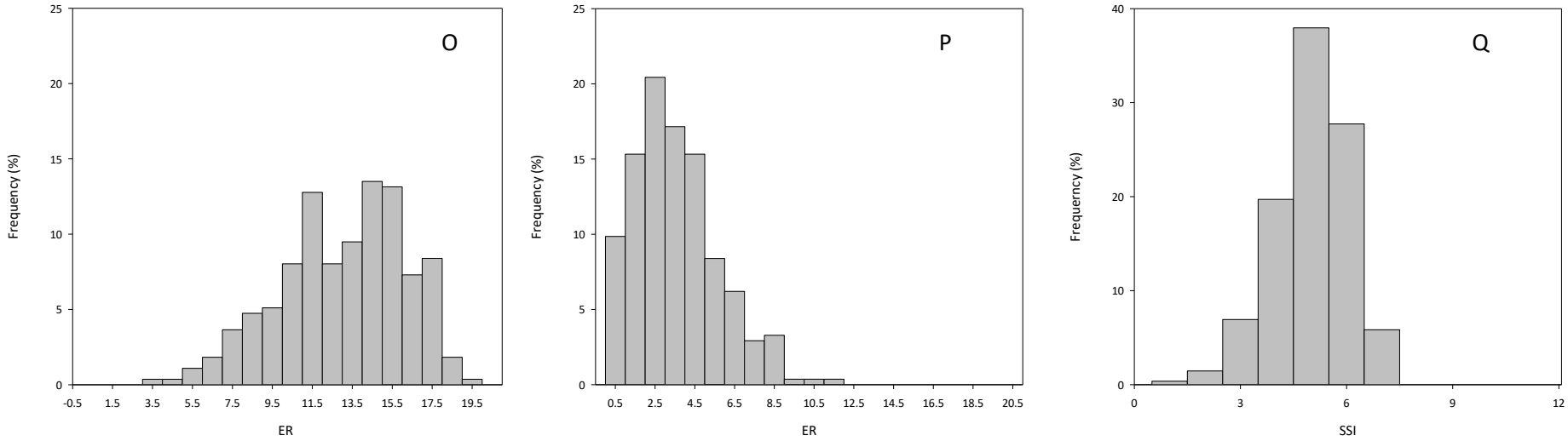

Supplemental figure 1. Frequency distribution for all the traits used for the genome-wide association study analysed in control (on the left) and salt (in the middle), as well as for the respective SSI values (on the right). A-B: Gmax; C-E: t50%; G-I: U_{25-75}; L-N: AUC

Genome-wide association study for salinity tolerance during growth in a panel of *japonica* rice (*Oryza sativa,* L.) accessions

Michele Pesenti[1], Gabriele Orasen[1‡], Alessandro Abruzzese[1], Giorgio Lucchini[1], Silvia Morgutti[1], Noemi Negrini[1], Luca Espen[1], Gian Attilio Sacchi[1]

[1]DiSAA – Dipartimento di Scienze Agrarie e Ambientali, Università degli Studi di Milano, via Celoria 2, I-20133 Milano, Italy. ‡ Bertone Sementi. Strada Cacciolo 35, Terruggia Monferrato I-15030, Italy (current address).

Abstract

The soil salt concentration of many European rice areas, where temperate rice cultivars are mainly grown, is increasing. In order to identify molecular markers and/or new *loci* related to salt tolerance, a Genome Wide Association Study (GWAS) was carried out using a panel of 277 *japonica* rice accessions. The panel, previously subjected to Genotyping by Sequencing, was phenotyped for tolerance to a mild-salt stress soil condition (5 dS m^{-1}). The parameters considered were Standard Evaluation Score (SES), plant height, flowering time, and chlorophyll content. The phenotyping results recorded under control and salt conditions and normalized as SSIs, allowed to define a core collection of most tolerant/sensitive genotypes. GWAS for the four traits uncovered a total of 21 significant MTAs. The analysis of genes annotated in the Nipponbare reference sequence and included in the regions associated to the traits allowed the identification of candidate genes whose functions could affect the respective traits. Among them, *Os01g0337500* encoding the vacuolar OsOVP6 H^+-PPase, *Os10g0438000* encoding a protein crucial for the assembly of KOR channels, and *Os10g0436900* encoding a CCX protein with the function of cation/Ca^{2+} exchanger, were identified to co-localize with three major traits MTAs. These findings indicate the importance of cellular Na^+ and K^+ homeostasis in the studied traits. Consequently, a physiological approach was undertaken to evaluate possible different effects of salt on Na^+ and K^+ fluxes in: i) two genotypes (Galileo and Virgo) assessed in the core collection as highly salt-tolerant, ii) a positive control (salt-tolerant FL478), and iii) a negative control (salt-sensitive PL12). Na^+ influx and the K^+ efflux, the cytosolic and vacuolar pH were evaluated in roots of the four rice genotypes. Root and shoot Na^+/K^+ ratios were also evaluated. The results obtained, consistent among Galileo and Virgo and the reference salt tolerant FL478, allowed to define a picture that may contribute to the salt tolerance phenotype observed. The results also suggest that the genes identified may represent putative promising candidates exploitable for selection of salt-tolerant rice lines.

Key words: *Oryza sativa* L., salt tolerance, growth, GWAS, ion transport.

1. Introduction

World agriculture faces a challenging task in order to produce by 2050 70% more food for an additional 2.3 billion people[1]. The lowering of crop productivity is mainly attributed to various abiotic stresses that represent a major concern for coping with the constantly increasing food requirement (Shanker and Venkateswarlu, 2011). Major abiotic stresses include soil salinity, drought, cold, and high temperature, all negatively influencing survival, biomass production, and yield of staple food crops, and a major threat to food security worldwide (Thakur et al., 2010; Mantri et al., 2012). Among abiotic stresses, soil salinity is one of the most severe environmental factors that in a complex way affects the phenotype and the physiology of a plant by imposing ion imbalance/disequilibrium, hyper-ionic and hyper-osmotic stress, and by altering the overall metabolic activities with limitation of the productivity of crop plants (Munns and Tester, 2008). More than 80 million hectares of irrigated land (representing 40% of total irrigated land) have already been damaged by salt worldwide (Xiong and Zhu, 2001).

The physiological and molecular mechanisms of tolerance to osmotic and ionic components of salinity stress involve different mechanisms from the cellular up to the whole-plant level. Plant growth responds to salinity in two phases: a rapid osmotic phase that inhibits growth of young leaves, and a slower ionic one that accelerates senescence of mature leaves. Plant adaptations to salinity comprise three distinct strategies: tolerance to osmotic stress, Na^+ or Cl^- exclusion, and tolerance to the excess of Na^+ or Cl^- accumulated in the tissues (Munns and Tester, 2008). In most plants, the part of the plant most sensitive to Na^+ toxicity is the leaf blade, where Na^+ accumulates after being deposited from the transpiration flow (Munns, 2002).

The cultivated areas subjected to salt stress are increasing due to many factors including climate change, rise in sea levels, excessive irrigation without proper drainage in inlands, underlying rocks rich in harmful salts, etc. It is estimated that if the current scenario of salinity stress will persist, by 2050 there may occur losses of 50% of the presently cultivated land for agriculture (Wang et al., 2003). In particular, the global temperature has increased over the last century, especially during the last 50 years (0.13 °C/decade). This warming, particularly intense in the Mediterranean region, has been especially evident in spring and summer. Temperature increases around the Mediterranean coasts are greater than those observed in other regions at the same latitude. In

[1] http://www.Fao.Org/wsfs/world-summit/wsfs-challenges/en/

addition, due to poor water availability and rise in sea levels, there is a clear tendency towards salinization in the river deltas where, in Europe, rice is grown.

Among cereals, rice is very sensitive to salinity stress and is currently listed as the most salt-sensitive cereal crop with a threshold of suffering symptoms at EC_e (Electrical Conductivity of its saturation extract) values of about 3 dSm^{-1} for most cultivated varieties (Hoang et al., 2016), whereas generally a soil is only considered saline (salt-affected) when the value of its EC_e is above 4 dS m^{-1} (Rengasamy, 2006). Even at an EC_e as low as 3.5 dSm^{-1}, rice loses about 10% of its yield, and a 50% yield loss has been recorded for rice at EC_e values of about 7.0 dS m^{-1}(Umali, 1993). Rice has been reported to be relatively tolerant to salinity stress during germination, active tillering and towards maturity, but sensitive during the early seedling and reproductive stages (Heenan et al., 1988; Zeng et al., 2001), with a delay in blooming time and a reduction in pollen viability with consequent negative effects on productivity. Additionally, there are nutritional as well as industrial qualitative traits threatened by salinity (Fitzgerald et al., 2009; Rao et al., 2013).

Plant response to salt stress is a multigenic trait, depending on many genes, involved in several metabolic pathways, and thus difficult to control and engineer. Exploiting the natural variation that occurs in worldwide genotypes may be a powerful approach to discover new traits (molecular markers, QTLs, genes and/or alleles) related to salt tolerance. A powerful approach increasingly used to identify molecular traits involved in the response to environmental stresses consists in the so-called Genome Wide Association Studies (GWAS). The basic approach in GWAS is the evaluation of the possibly existing association between each genotyped marker and a phenotype of interest scored across a large number of individuals in order to identify causative/predictive factors for a given trait. In this respect, several approaches have been undertaken (Kumar et al., 2015; Patishtan et al., 2018; Cui et al., 2018), but most of them concern *indica* rice germplasm and the intensity of the salt stress experimentally imposed is usually very high, not consistent with the mild-salt stress severity (EC_e 3.0-5.0 dS m^{-1}) that interests paddy field in temperate areas.

In this context, a *japonica* rice collection previously subjected to genotyping-by-sequencing (GBS; Biscarini et al., 2016; Volante et al., 2017) was subjected to a two-years phenotyping to analyze the natural variation in the response to mild-salt stress and obtained data were exploited in a genotype-phenotype association study. Specific objectives of the research were to a) evaluate the variability in salt tolerance in a large collection of worldwide *japonica* rice cultivars exposed to mild-salt stress conditions (soil EC_e about 5 dS m^{-1}); b) identify novel sources of salt tolerance-related in

japonica rice varieties; c) identify genomic regions harboring significant genetic effects for salt tolerance and, c) identify candidate genes in the rice *loci* involved in conferring salt tolerance.

2. Materials and Methods

2.1. Plant material and phenotyping

The panel of accessions used included 277 *Oryza sativa* L. varieties from the rice germplasm collection maintained at the CREA- Research Centre for Cereal and Industrial Crops (Vercelli, Italy). With respect to the panel described in the first part of the thesis (Table S1, Pesenti et al., 2020) three additional accessions (Lucero, Sandora and Xiangou2) were included (Tab- S1). The panel was composed of 68 tropical *japonica* and 209 temperate *japonica* accessions; most of these accessions (144) were developed in Italy, 32 from USA, 25 from Portugal, 19 from Spain, 10 from Bulgaria, 9 from Argentina, 6 from France and the remaining were developed elsewhere but considered well adapted to Italian agro-climatic conditions (Volante et al., 2017; Orasen et al., 2018).

Two-years (May 2016- October 2016 and May 2017 – October 2017) experiments were carried out for the phenotyping activity. Plants were grown to full maturity in a greenhouse (Tavazzano, Lodi, Italy, 45°18'35.60" N, 9°30'3.06"E) under submerged conditions in pots containing paddy soil. Twenty seeds per pot were sown in non-salinized soil maintained at about 70-80% of its water field capacity. When plants were at the 3^{rd}-4^{th} leaf stage, their number per pots was reduced to five and then pots for salt treatment were salinized until the soil reached, by adequate addition of a 100 mM NaCl solution, a value of electric conductance (EC_e) of about 5 dS m^{-1}. Throughout the growth period the EC_e of the soil was maintained at less than 1 dS m^{-1} (control) or about 5 dS m^{-1} (salt treatment) by addition of adequate amounts of water or NaCl solutions. A randomized block design, with three replicates of five plants each for both control- and salt-treated pots, was adopted. At the panicle initiation stage each pot was fertilized applying a commercial NPK fertilizer according to the usual agronomic rate.

Fourteen days after the salt treatment the morphological responses to the stress of each plant in each plot were evaluated using the Standard Evaluation System for Rice (SES) developed by the International Rice Research Institute (Gregorio et al., 1997). A SES value was assigned to each plant of a pot; for each pot a mean value of SES was calculated and then the average of the three replicates was calculated.

Days to flowering were counted starting from the date of sowing (Days After Sowing; DAS). For each accession the flowering time was recorded; an accession in a plot was considered flowered

when at least three out of the five plants in a pot were clearly in anthesis, with pollen release. When all the plants in a pot had flowered, their height was measured considering the maximum extension of the three longest leaves of all the five plants in each pot.

Twelve days after anthesis the plant flag leaf chlorophyll content was evaluated using the Dualex® ForceA sensor, a handy clip tool that allows to rapidly and accurately estimate the content of chlorophyll in the leaves by assessing their light transmission properties (Cerovic et al., 2012). Six measurements per plant were performed on the flag leaf: three on the upper page and three on the lower page of the leaf, respectively in the basal, median and apical part. The three best flag leaves of five plants were considered, for a total of 18 measurements per pot.

The responses of the genotypes to salt stress were also expressed in terms of Stress Susceptibility Index (Fischer and Maurer, 1978; Shi et al., 2017; Morton et al., 2019), calculated as: $SSI = 1 – (Y_s/Y_p) / D$, where

Y_s = mean performance of a genotype under stress;

Y_p = mean performance of the same genotype without stress;

D (stress intensity) = 1 - (mean Y_s of all genotypes / mean Y_p of all genotypes)

2.2. Statistical analysis of phenotyping data

Least Square Means

For all the measurements obtained from the two-years data, means were adjusted with Least Square Means (LSM) approach (Kaniel and Stein, 1974). A REML (REsidual Maximum Likelihood) model was used to evaluate random factors and fixed factors, and to minimize problems related to the different number of repetitions in the two years. The block effect and the year effect were considered as random factors; the variety effect was considered a fixed factor.

For each phenotypic trait evaluated, as well as for the relative SSI value, the broad-sense heritability (*H*) within the rice panel was calculated according to the following equation (Nyquist, 1991):

$$H = \sigma^2G/[\sigma^2G + (\sigma^2GE/E) + (\sigma^2e/rE)], \text{ where}$$

σ^2G = genetic variance;

σ^2GE = genotype x environment interaction variance;

σ^2e = residual variance;

E = number of environments;

r = number of replicates.

In the distribution of each phenotypic parameter, normalized as SSIs of the LSMs, the genotypes belonging to the 10th (salt-tolerant) or 90th (salt-sensitive) percentiles were identified (Supplemental Table 2) and the most interesting ones were used to define a core collection of the most tolerant and sensitive accessions.

2.3. Genotypic data, genetic diversity analysis and linkage disequilibrium analysis

The accessions included in the rice panel were Genotyped-By-Sequencing (GBS) following a pipeline described by Biscarini et al. (2016), except for the number of tags (one instead of five) required for the alignment to the Nipponbare reference sequence. As described in detail by Volante et al. (2017), a set of 246,084 SNPs was identified, mapped on the Os-Nipponbare-Reference-IRGSP-1.0 pseudomolecule assembly and intersected with the genome annotation (Kawahara et al., 2013) to define the percentage of markers in rice genes. The original SNP dataset was filtered with the program PLINK1 (Purcell et al., 2007) to avoid the biased detections due to rare alleles. Markers with a call rate value lower than 95% and with Minimum Allele Frequency (MAF) lower than 5% were discarded. After filtering for call rate and MAF, a total number of 31,421 SNPs was subsequently used for the GWAS analyses.

In order to investigate the population structure, three different approaches (Principal Component Analysis, phylogenetic clustering, and Bayesian model-based analysis), were adopted. The PCA analysis were developed with the Adegenet package 2.0.0 of R software (Jombart and Collins, 2015). A phylogenetic tree or Neighbour-joining tree was constructed using a shared allele index based on a dissimilarity matrix estimated from the SNP dataset through Ape and Phyclust R package. The Bayesian model-based analysis was performed with the Structure software v2.3.4 (Pritchard et al., 2000), with a sub-set of 5,000 random SNPs marker. The parameters used in this analysis were: presence of admixture, allele frequencies correlated, burn-in period of 10,000 iterations, followed by 20,000 Monte Carlo Markov Chain (MCMC) replications, K levels from 1 to 10, 5 runs per K value. For the choice of the best number of clusters (K), the Evanno method of Δk was used, implemented in the free software Structure Harvester (Earl and von Holdt, 2012). Once defined the most probable K value, a final single run was performed using the same parameters listed above, except for burn-in period of 100,000 iterations and 200,000 Monte Carlo Markov Chain (MCMC) replications. Accessions with a minimum membership of 0.7 were assigned to a subpopulation, while the remaining were considered as admixed. The phylogenetic tree,

represented with iTOL (http://itol.embl.de/) was implemented with the results of the Structure analysis, together with the information relative to the varieties of the panel.

The computation of pairwise Linkage Disequilibrium (R2) among 5000 randomly selected markers was performed with the R package "LDcorSV v1.3.1" (Mangin et al., 2012), using the Structure membership matrix as a covariate. The values were averaged in 10 kb windows (as in Biscarini et al., 2016). For each distance class, a mean value was obtained from the data of the 12 chromosomes; the resulting values were plotted against physical distance and fitted to a second-degree LOESS curve using an R script (Cleveland, 1979; Marroni et al., 2011). A critical value of 0.2 was set as R2 between unlinked loci. The physical distance corresponding to a LOESS curve value of 0.2 was assumed as LD decay in the rice panel (Volante et al., 2017).

2.4. Genome wide association studies

Association studies were carried out using the values measured directly on the salt-treated plants (SES) or using the calculated SSI values [flowering time, height, and chlorophyll index (CHL)]. A Mixed Linear Model (MLM) was used for GWAS, by including the Kinship matrix (K) as a random effect to consider the population stratification. Association analyses were performed with the Tassel v5.2.0 software adopting the following parameters: no compression, genetic and residual variance estimated for each marker (P3D OFF). For each SNP marker a p-value of the association to the phenotypic traits (Marker-Trait Association, MTA) was calculated. The significance threshold to declare a marker as associated was set at 0.05, after correction for multiple testing using the False Discovery Rate (FDR) method (Benjamini and Hochberg, 1995).

After identification of the significant MTAs, candidate genes were searched within genomic intervals defined based on local Linkage Disequilibrium (LD). The chromosome-wise LD was calculated with the program Haploview v4.2 software (Barrett et al., 2005). LD blocks were defined using the default settings, i.e. the method by (Gabriel et al., 2002), assuming 0.7 and 0.98 as D' lower and upper minima for strong LD, respectively. The regions associated to each trait were aligned with the results of the Haploview analysis, in order to detect adjacent associations possibly tagging a single LD block. The regions defined by the peak marker/region positions including 100 kbp upstream and downstream (corresponding to an average LD decay of 0.5 estimated on the LOESS curve described above, as a trade-off between accuracy and power of the analysis) were screened to search for candidate genes underlying each trait. The intervals were then explored on the *Oryza*

sativa reference genome (Os-Nipponbare-Reference-IRGSP-1.0[2]), and all the genes recorded or known in the literature (gene bank of Rice Annotation Project) within that LD block were analyzed for their possible involvement in the response to salt stress.

2.5. Plant hydroponic cultivation

Seeds of two accessions (Galileo and Virgo) of the panel included in the five most tolerant salt stress, the *indica* genotype FL478 well known as salt-tolerant (Gregorio et al, 1997; Walia et al., 2005) and the Spanish genotype PL12 known for extreme salt sensitivity (B. San Segundo, personal communication), were surface-sterilized by dipping them for 3 min in 70% (v/v) ethanol and for additional 30 min in a 2% (v/v) $NaClO_4$ solution supplemented with 0.02% (v/v) Tween-20. Seeds were then rinsed six times (5 min each) with distilled water. After sterilization, seeds were sown in Petri dishes (20 cm x 20 cm) on two layers of sterile filter paper wetted with 40 ml of sterile water. The dishes were incubated at 25°C for 7 d in the dark. Uniformly germinated seedlings, blocked on a floating polystyrene sheet, were transferred onto hydroponic medium (Table S21) in 5-L plastic containers. Plants were grown for 21 d up to the 4^{th}-5^{th} leaf stage. The hydroponic solution was renewed twice a week, and pH was checked and adjusted every two days.

2.6. Root transport activities (Na^+ and Rb^+ influxes and K^+ efflux) and assessment of tissue Na^+/K^+ ratios.

Plants were removed from the hydroponic solution and their roots were rapidly washed in distilled water followed by 0.5 mM $CaSO_4$. Roots of single plants were then dipped in 100 mL of 2-(N-Morpholino) Ethane Sulfonic acid (MES)-Bis-Tris-Propane (BTP), pH 6.2, 0.4 mM $CaSO_4$, and 2.5 mM Rb_2SO_4, in the absence or in the presence of 50 mM NaCl, in continuous agitation (60 shakes per minute) at 25 °C. For each treatment, four replicates were planned. After 10 min, a 1-mL aliquot of the external solution was sampled (time = 0) and roots were equilibrated for the subsequent 30 min; the external solution was then sampled again and replaced three times at intervals of 30 min. The amounts of K^+ released from the roots into the solution at the different times were then determined by ICP-MS (see below). At the end of the experiment, roots were washed (4 °C, 30 min with a change after 15 min) in MES-BTP, pH 6.2, 0.4 mM $CaSO_4$ added with 50 mM Cs_2SO_4 in order to remove Na^+ and Rb^+ from the apoplast. Roots were then rinsed with distilled water and oven

[2] http://rapdb.dna.affrc.go.jp/download/irgsp1.html

dried at 60 °C for about 72 h, i.e., until their weight was constant. Shoots were also rapidly rinsed in distilled water, weighed, and oven dried. Both dry roots and shoots were mineralized by a microwave digester system (MULTIWAVE-ECO, Anton Paar GmbH) in Teflon tubes containing 10 mL of 65% (v/v) HNO_3 by applying a two steps power ramp (Step 1: at 500 W in 10 min, maintained for 5 min − Step 2: at 1200 W in 10 min, maintained for 15 min). After 20 min cooling, the mineralized samples were transferred into polypropylene test tubes. Samples were diluted 1:40 with Milli-Q water and the concentrations of Na^+, K^+ and Rb^+ were measured by ICP-MS (Bruker Aurora M90 ICP-MS, Bruker Daltonik GmbH). An aliquot of an internal standard solution (2 mg L^{-1} ^{72}Ge, ^{89}Y, ^{159}Tb) was added to both samples and standards for calibration curves to give a final concentration of 20 mg L^{-1}. In the samples of the external solutions withdrawn at the desired times the concentrations of K^+ were directly evaluated by the same ICP-MS procedures.

2.7. ^{31}P-NMR analyses

The experiments were carried out on roots excised from plants grown for 21 d in hydroponic solution according to procedure previously described (Nocito et al., 2008). ^{31}P-NMR spectra were obtained with a Bruker AMX 600 spectrometer (Bruker Analytische Messtechnik GmbH, Rheinstetten-Forchheim, Germany) equipped with an X32 data system, running UX NMR software, version 920801. In vivo ^{31}P-NMR experiments were carried out by packing 1.5 g of vacuum-infiltrated root segments (20 mm) in a 10 mm diameter NMR tube (Wilmad Glass Co., Buena, NJ, USA) equipped with a perfusion system connected to a peristaltic pump where the aerated, thermoregulated (25 °C) basal medium (0.4 mM $CaSO_4$, 2 mM sucrose, 1 mM MES-BTP, pH 6.20), with or without 50 mM NaCl, was flowing (10 ml min^{-1}). To allow a complete recovery, prior to starting the experiments, the root segments were maintained in the absence of NaCl for 1 h. ^{31}P-NMR spectra were recorded at 242.9 MHz without lock, using a standard broad-band 10 mm probe and fast acquisition conditions (Kime et al., 1982) with a waltz-based broad-band proton decoupling and a spectral window of 16 kHz. The acquisition time was 0.386 s with a relaxation delay of 1 s and a pulse angle of 90°. Spectra were the results of 1500 scans, corresponding to a total acquisition time of 34 min 15 s. The whole experiment was carried out for 16 h. Resonance identification was obtained according to Roberts et al. (1980) and Kime et al. (1982) and the cytosolic and vacuolar pH estimated from the chemical shift (δ) of inorganic phosphate (P_i) resonance. Standard titration curves relating δ to pH were constructed according to Roberts et al. (1981). Chemical shifts were measured in ppm relative to the signal of 33 mM methylene-diphosphonic acid sealed in a coaxial

capillary tube included with the sample, which resonates at 18.5 ppm relative to the signal of 85% H_3PO_4.

3. Results

3.1. Phenotyping of the rice accessions panel

Table 1 reports the values of the phenotypic parameters observed under control and salt conditions in the rice panel. Concerning the average behavior of the genotypes, plant cultivation in salt conditions caused noticeable effects on all the parameters analyzed, even if it did not essentially amplify the range of the values compared to the controls.

Table 1. Summary statistics of phenotypic parameters (two-years LSM) during growth of the 277 *japonica* rice accessions grown in control or saline conditions. The data are the means ± SD of the LSM. CV: coefficient of variation.

	Mean values of LSM		Min-max range of LSM		CV	
	Control	Salt	Control	Salt	Control	Salt
SES	1.03 ± 0.17	2.33 ± 0.5	1	1.33-4.37	16.5	21.7
Plant height (cm)	86.5 ± 11.6	79.0 ± 10.8	62.6-117.0	56.0-108.9	13.4	13.7
Chlorophyll Index	36.9 ± 3.7	33.8 ± 3.9	26.3-46.7	19.4-43.6	10.0	11.5
Flowering time (d)	85.4 ± 8.2	90.6 ± 8.5	63.1-113.6	66.2-118.0	9.6	9.4

The observations concerning the phenotypic parameters considered were analyzed taking into consideration their dispersion. The distributions of phenotypic classes indicate that all the traits considered are quantitative and continuous, suggesting a complex genetic control (Figure S1). Figures 1-4 represent box plots of the values (Least Square Means; LSM) recorded in all the genotypes under control and salt conditions (left panels) or expressed as Stress Susceptibility Indexes (SSIs; right panels).

Concerning the SES parameter, no visible symptom of suffering was observed in the controls; in this case, the SES value was set at 1 for all genotypes. In the salt condition several stress symptoms, including leaf bleaching and rolling up to leaf death were detected in all the accessions, to different extents in the different genotypes (Tab. 1). SES allowed to discriminate with satisfactory clarity between tolerant and susceptible varieties (Supplemental Table S2). In major details, in the salt condition, the distribution of the SES values showed a median value of 2.2; the value of the 90th percentile was 3.0 and 40 accessions, indicated by the black dots (outliers) in the upper part of the figure, showed SES values higher that of 90th percentile indicating high sensitivity to the salt condition (Supplemental Table S3). Thirty-five accessions, indicated by the outliers in the lower part

of the figure, showed values lower than that (1.63) of the 10th percentile and close to the value of 1 (lack of symptoms), indicating poor sensitivity (tolerance) to salt based on SES (Fig. 1A). Figure 1B describes the dispersion of the SSI_{SES} that ranged from the lowest value of 0.053 to the highest one of 1.713.

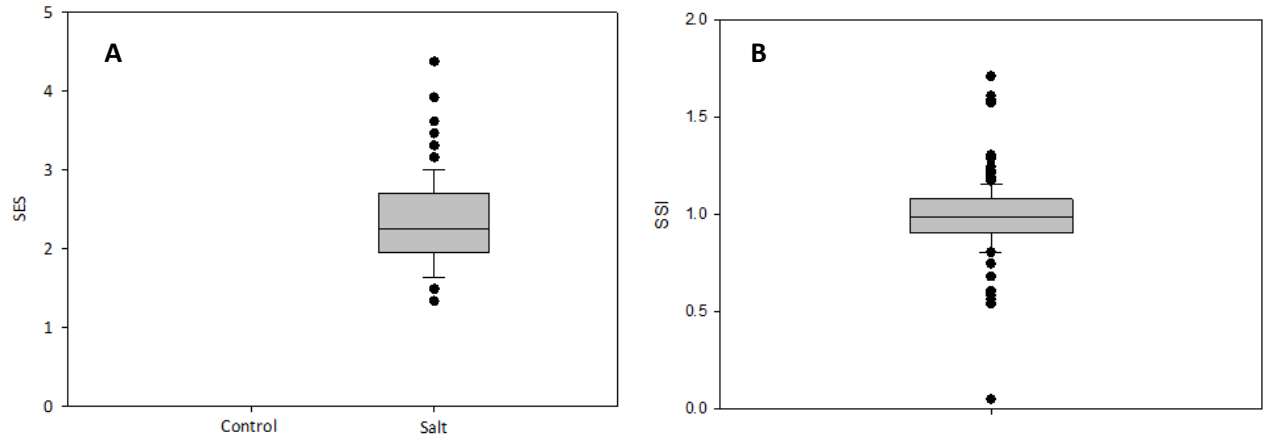

Figure 1. Box plots of the SES variability of the rice panel grown in control or salt conditions (A) and of the related SSI_{SES} (B). The plots show median, 25th, and 75th percentile (boxes) and 10th and 90th percentiles (indicated by the error bars). Black dots indicate outliers outside the 10th and 90th percentiles.

In rice, plant height/shoot length are influenced by salt stress. Many studies showed significant reductions in height between the controls and the salt-exposed plants (Rahman et al., 2016, 2017; Puvanitha and Mahendram, 2017). This effect has been ascribed to excess Na^+ entrance into the cells that causes ionic imbalances leading to non-regular cell division (Ogawa et al., 2011) and enlargement, with eventual reduction of the final size of the whole plant. In our rice panel, the values of plant height showed a large variability, in both control (63 cm plant^{-1} - 117 cm plant^{-1}) and salt (56 cm plant^{-1} - 109 cm plant^{-1}) conditions (see also Tab. 1). Salt negatively affected the growth of all the accessions inducing a reduction in height, although a few genotypes showed only slight effects of the salt stress (from -3.5% in the less sensitive genotype to -20% in the most sensitive one; Supplemental Table S2). As reported in Figure 2A, the median value of the controls was 84 cm plant^{-1}, while the median of the salt-treated plants was 77 cm plant^{-1}. The values of SSI_{Height} ranged from the lowest value of 0.4 (very slight inhibition of growth) to the highest value of 23 (strong reduction of growth in the presence of salt; Fig. 2B; Supplemental Table S3).

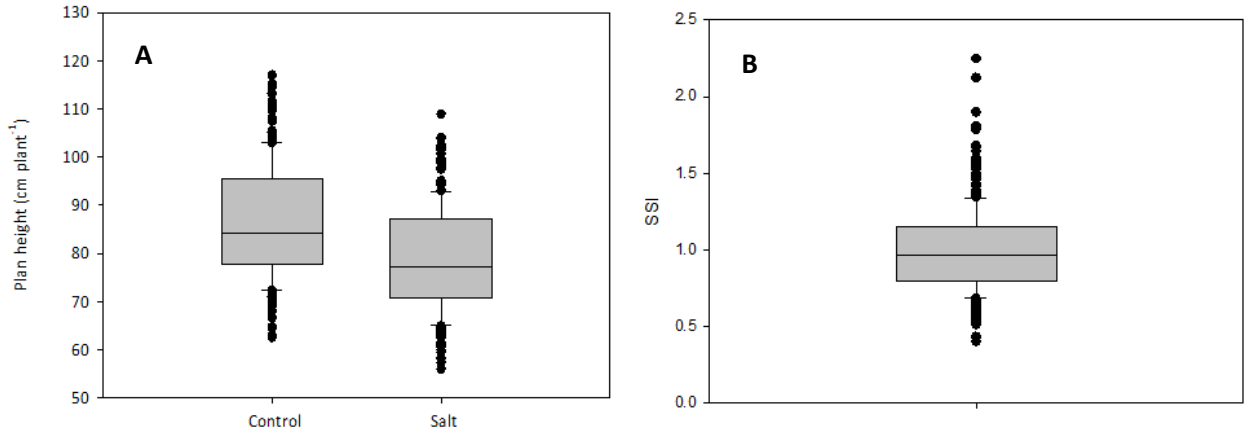

Figure 2. Box plots of plant height variability of the rice panel grown in control or salt conditions (A) and of the related SSI_{Height} (B). The plots show median, 25th, and 75th percentile (boxes) and 10th and 90th percentiles (indicated by the error bars). Black dots indicate outliers outside the 10th and 90th percentiles.

Different than most plant species that, when subjected to salt stress, shorten their life cycle by anticipating flowering, in saline conditions rice tends to lengthen its life cycle; a genotype is the more sensitive to salt the more it delays flowering in comparison with the control (Castillo et al., 2007; Lutts et al., 1995). In fact, the delay of flowering is often used to discriminate between sensitive and tolerant varieties (Castillo et al., 2007; Frouin et al., 2018). The flowering time showed a great variability in the rice panel, as shown by the broad dispersion of the outlier values. In the control condition, in fact, the flowering time covered a large time span (63-114 DAS; Tab. 1), with a median at 87 DAS. In all genotypes the salt treatment induced a delay in the flowering time, with a shift of the median value to 93 DAS and a salt-induced delay that ranged, in specific genotypes, from 1.4 d to 14 d. In a few genotypes the effect was indeed very small, less than 2 d (Fig. 3A, Supplemental Table S2).

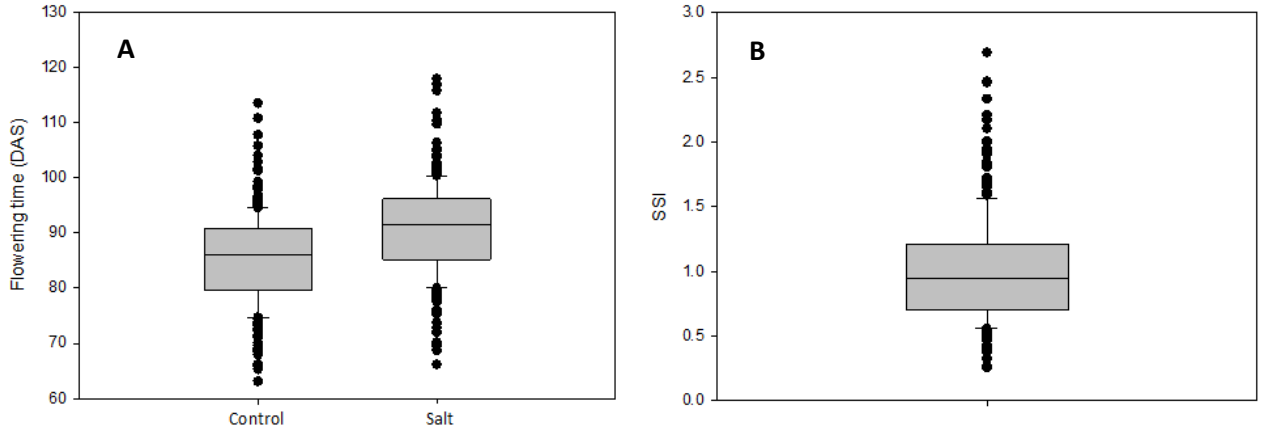

Figure 3. Box plots of the flowering time variability of the rice panel grown in control or salt conditions (A) and of the related $SSI_{Flowering\ time}$ (B). The plots show median, 25th, and 75th percentile (boxes) and 10th and 90th percentiles (indicated by the error bars). Black dots indicate outliers outside the 10th and 90th percentiles.

The dispersion of the values of $SSI_{Flowering\ time}$ (Fig. 3B) was also very high, as indicated by the high number of outliers**.** The values ranged from close to 0 (very poor sensitivity to salt stress) to more than 25 (high sensitivity). Variability appeared higher in the sensitive genotypes.

Salt stress affects the chlorophyll content (Ali et al., 2004; Chandramohanan, 2014; Gerona et al., 2019). The Dualex chlorophyll index (CHL) reliably reflects the chlorophyll content of plant tissues (Cerovic et al., 2012). A great variability of CHL was present in the flag leaves, 12 days after anthesis, of the considered panel of rice genotypes, in both control (26.3 to 46.7; Tab. 1) and salt (19.4 to 43.6) conditions. In the presence of salt, the median value of CHL diminished from 37.3 in the controls to 34.2 in salt-stressed plants (Fig. 4A). The values of SSI_{CHL} (Fig. 4B) also showed a very broad distribution; indeed, a few outliers had negative values of SSI_{CHL}. This observation may be explained by a lower leaf blade expansion and therefore lesser dilution of its components (at least until occurrence of senescence symptoms) under salinity.

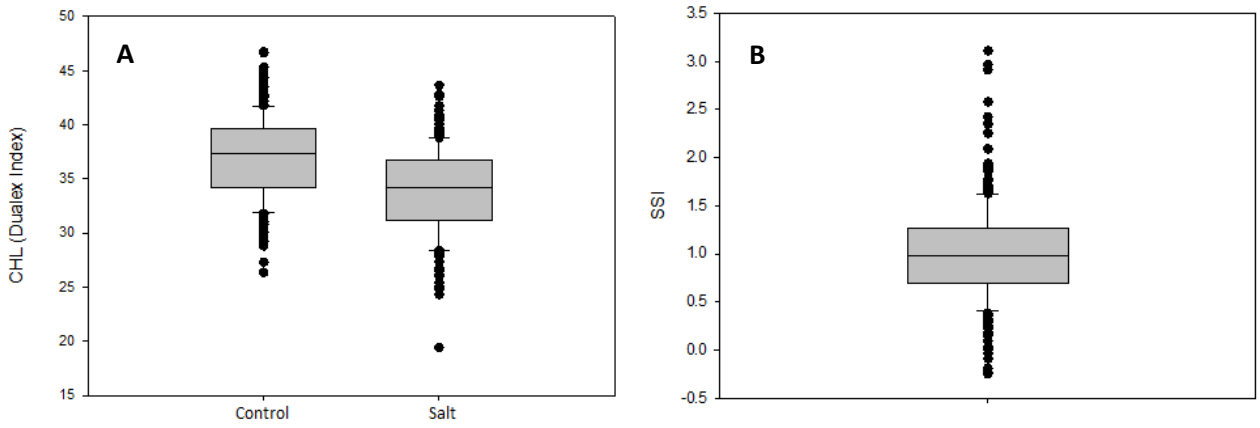

Figure 4. Box plots of CHL variability of the population grown in control or salt conditions (A) and of the related SSI_{CHL} (B). The plots show median, 25th, and 75th percentile (boxes) and 10th and 90th percentiles (indicated by the error bars). Black dots indicate outliers outside the 10th and 90th percentiles.

For each of the phenotypic parameters considered, the genotypes belonging to the 10th and 90th percentile were identified (Supplemental Table 3). Genotypes within the 10th and the 90th percentile for at least two parameters were chosen for the definition of a core collection, that in summary resulted composed respectively by the eight most tolerant and the 12 most sensitive accessions (Table 4).

Table 4. The core collection of most tolerant and most sensitive genotypes from the 277-accessions panel.

Developmental phase	MOST TOLERANT	MOST SENSITIVE
Vegetative	Samba Galileo Virgo Muga Orione Vulcano IBO38033	Ostiglia CT58 L201 L205 Agostano Carrico Pecos Zena Santerno Venere Vialone Nano Miara
Reproductive	Vulcano Muga IBO38033 Bengal	Ostiglia CT58 L201 L205 Agostano Carrico Pecos Zena

3.2. Genotypic effects in the rice accessions panel

For all the parameters considered and the relative SSI values, the broad-sense heritability (*H*) of traits was quite high in both control and salt conditions (0.853-0.995 range), indicating that genetic factors greatly contribute to the variance of measured traits (Table 2). Since no accession showed any visible symptom on the leaves when grown in the control condition, and thus the resulting SES values were therefore very close to 1, the related value of *H* was not evaluated, as well as that concerning the corresponding SSI value.

Table 2. Broad-sense heritability (*H*) of the population for the parameters considered.

Trait	*H*		
	Control	Salt	SSI
SES	-	0.91	0.91
Flowering time	0.99	0.99	0.91
Plant height	0.99	0.997	0.86
CHL	0.96	0.99	0.88

3.3. GWAS analysis for the identification of MTAs and putative candidate genes

The existence of relevant genotype-phenotype associations between the GBS data and the SSI values obtained for each of the four phenotypical parameters considered was tested in a GWAS

study in MLM configuration carried out through the Tassel program. The resulting Marker-Trait Associations (MTAs), Manhattan and Q-Q plots are reported in Table 3 and in Figure 5 (A-D).

A total of 21 significant MTAs were identified for the SSIs of the parameters considered (Table 3), with $-\log_{10}(p)$ values for these associations ranging from 3.56 to 5.50. The significant MTAs identified were four for plant height and CHL index, five for SES, and eight for flowering time. Two MTAs (MTA_{629} and MTA_{633}) were in common between SES and height.

Table 3. Relevant MTAs identified by GWAS on the basis of the SSIs of the four phenotypical parameters considered

	Peak marker	$-\log_{10}(p)$	MTA	Chr	SNPs	Associated region		
SES						Start	End	Length (bp)
	S1_13531175	3.63	51	1	2	13,353,630	13,584,196	230,566
	S1_37025529	3.62	119	1	1	36,460,838	37,352,694	991,856
	S6_10197901	4.78	629	6	4	10,147,151	10,198,065	50,914
	S6_10365586	3.92	633	6	3	10,273,907	10,379,493	105,586
	S12_19629112	3.71	1462	12	1	19,628,528	19,642,749	14,221
Height								
	S3_6000810	3.63	323	3	1	5,406,735	6,179,725	772,990
	S6_10197901	4.00	629	6	3	10,147,151	10,198,065	50,914
	S6_10365586	3.85	633	6	2	10,273,907	10,379,493	105,586
	S8_16443868	3.63	933	8	1	16,443,496	16,527,447	83,951
Flowering time								
	S2_4868913	4.62	173	2	1	4,376,965	4,959,227	582,262
	S6_21750763	4.88	670	6	4	21,736,417	21,981,213	244,796
	S7_13181978	3.93	742	7	1	12,759,825	13,759,665	999,840
	S9_3499607	3.69	964	9	1	3,359,172	4,359,129	999,957
	S10_18080257	5.50	1022	10	14	18,018,523	18,098,485	79,962
	S10_16612956	3.93	1123	10	1	16,041,577	16,624,807	583,230
	S11_2026499607	3.80	1233	11	1	19,986,703	20,356,814	370,111
	S11_26088884	3.64	1343	11	5	26,055,966	26,090,477	34,511
CHL								
	S1_11142970	3.56	46	1	1	10,939,343	11,208,711	269,368
	S1_31035257	3.92	91	1	1	30,739,571	31,475,181	735,610
	S7_22921045	3.79	784	7	1	22,560,826	22,937,275	376,449
	S7_24705699	4.14	792	7	1	24,648,627	24,758,577	109,950

A) SSI_SES

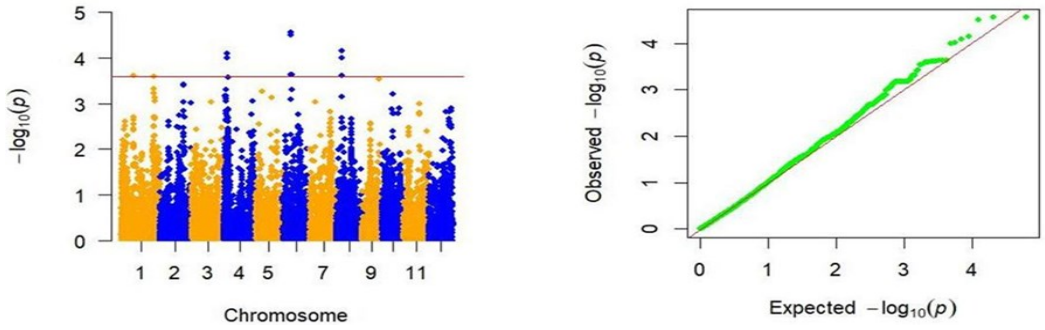

B) SSI_Height

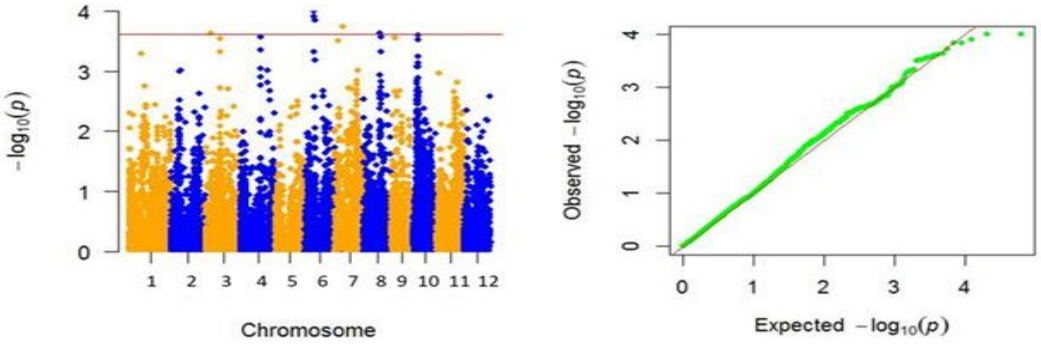

C) SSI_Flowering time

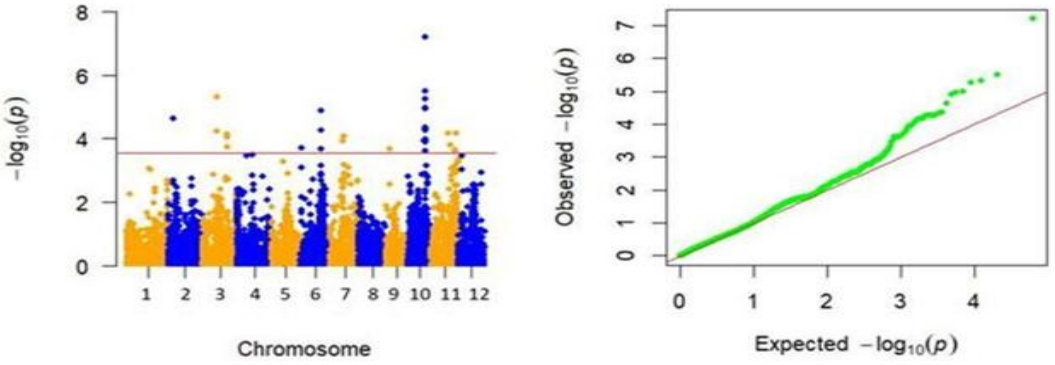

D) SSI_CHL

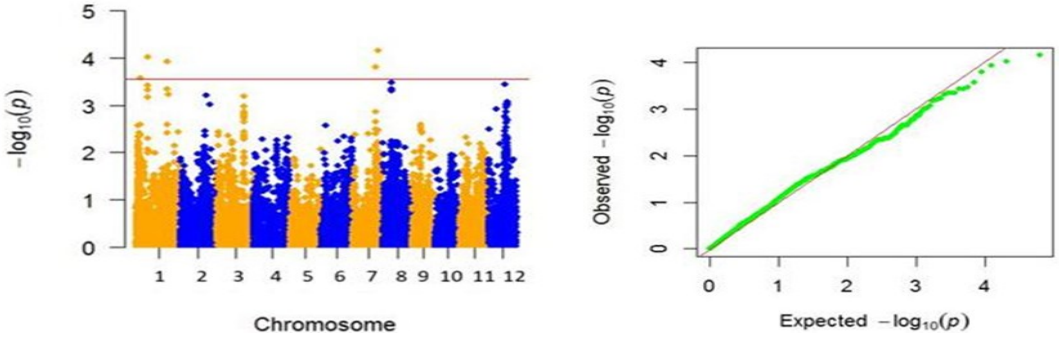

Figure 5. Manhattan (left panels) and Q-Q (right panels) plots of GWAS of SSI_{SES} (A), SSI_{Heigth} (B), $SSI_{Flowering\ time}$ (C) and SSI_{CHL} (D). The red straight horizontal line in the Manhattan plot shows the threshold for FDR (False Discovery Rate) ≤ 0.05.

Among the MTAs identified for the SSI_{SES} values, the MTA_{51} on chromosome 1 was particularly interesting. This MTA_{51} spans from bp 13,353,630 to bp 13,584,196 (length = 230,566 bp), with the most significant SNP marker at bp 13,531,175. Search for candidate genes in this MTA region led to the identification of *Os01g0337500*, that encodes a peptide of the vacuolar H^+-pyrophosphatase 6 (Plett et al., 2010), and *Os01g0338100*, encoding *OsTFIID*, one of the several transcription factors (TFs) localized within the major salinity tolerance-related QTL '*Saltol*' (Nutan et al., 2017).

Concerning SSI_{Height}, GWAS identified four significant MTAs, with the most interesting one (MTA_{933}: chromosome 8; spanning region bp 16,443,496 to bp 16,527,447; length = 83,951 bp) showing the peak SNP marker at bp 16,443,868. Search for candidate genes in this region led to the identification of *Os08g0357300*, encoding a *bZIP65* TF domain-containing protein related to stress conditions[3].

In the case of $SSI_{Flowering\ time}$, out of the eight significant MTAs identified, the MTA_{1123} (chromosome 10) resulted particularly interesting since in this genomic region (bp 16,041,577-16,624,807; length = 583,230 bp; most significant SNP marker at 16,612,956 bp) are present three interesting *loci*,candidates for their role in the response to salt conditions**:** *Os10g0436900* encoding the vacuolar Na^+/Ca^{2+} OsCCX3 transporter; *Os10g0438000* encoding a protein containing a tetramerization domain for K^+ channel structure; *Os10g0442600*, encoding a protein involved in the control of cell division (Yu et al., 2017) and rice plant survival (Shi et al., 2019).

GWAS for SSI_{CHL} uncovered four significant MTAs with the most interesting one (MTA_{46}; chromosome 1; range: bp 10,939,343 - bp 11,208,711; length: 269,368 bp; peak marker: bp 11,142,970). Search for candidate genes in this region led to the identification of *Os01g0705700* encoding a protein similar to ICE1 (Inducer of CBF Expression1), a basic helix-loop-helix DNA-binding protein in cold acclimation (Man et al., 2017 and references therein; Supplemental Table S4).

3.4. Preliminary activities for candidate gene confirmation

Among the putative candidate genes emerged from GWAS analyses concerning SSI_{SES}, particular attention was focused on *Os01g0337500* (LOC_Os01g23580), that encodes a peptide of the vacuolar H^+-pyrophosphatase 6 (OsOVP6; Plett et al., 2010). This PP_i-dependent H^+ pump located on the tonoplast contributes to generate the H^+ transmembrane electrochemical gradient that

[3] http://rice.plantbiology.msu.edu/cgi-bin/ORF_infopage.cgi?orf=LOC_Os08g26880

energetically drives the activity of the Na^+/H^+ NHX antiporters that, by accumulating excess Na^+ into the vacuole, limit its toxic effects in the cytoplasm (Kobayashi et al., 2017; Almeida et al., 2017; Fig. 6).

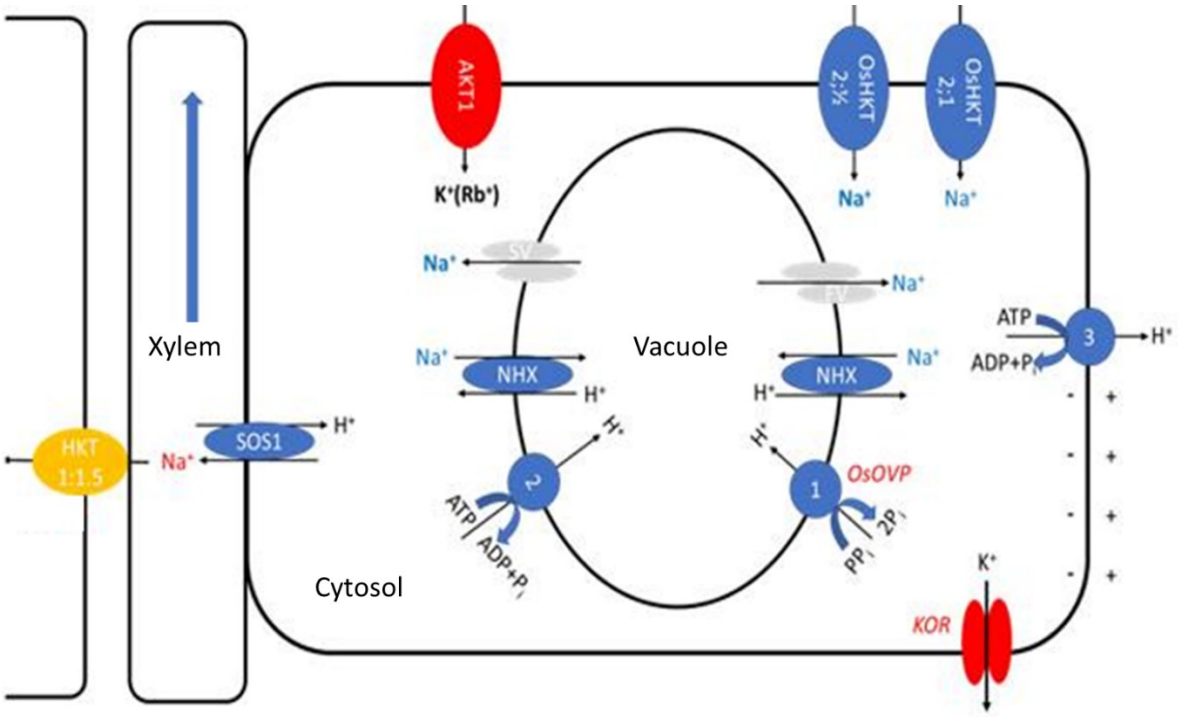

Figure 6. Transport mechanisms involved in cellular Na^+ and K^+ homeostasis.

The vacuolar H^+-PPase, together with the Na^+/H^+ exchanger NHX and the K^+ Outward Rectifying (KOR) channels, plays a key role in the complex network of the Na^+ and K^+ transport mechanisms (Figure 6) that contribute to the maintenance of the homeostasis of Na^+ and K^+ in the cytoplasm of plant cells, particularly relevant in salt stress conditions. In this framework, we assumed that by comparing the behavior, in terms of Na^+ and K^+ fluxes and of cell pH, of roots of rice genotypes with opposite behavior in salt stress, it could be possible to infer, directly or indirectly, differential operativity of H^+ and cation membrane transport activities in the absence or in the presence of salt stress. Therefore, both the K^+ efflux from roots and the H^+ transport activities at the tonoplast (indirectly evaluated as cellular pH changes) were compared in the genotypes Galileo, Virgo chosen from the core collection described above (Table 4). FL478, demonstrated to be highly tolerant (Thomson et al., 2010) was exploited as positive control, whereas PL12, well known as a highly sensitive genotype, was the negative control. Both the two control genotypes show these peculiar characteristics in the early vegetative phases (San Segundo, personal communication).

3.4.1. Na^+ and K^+ fluxes

Short-term experiments aimed at assessing potential differences in the membrane transport properties at the root cell level in the rice genotypes selected for different tolerance/sensitivity to saline conditions were conducted. Table 5 shows that very low (compared to those observed in the NaCl-treated roots) amounts of Na^+, different in the different genotypes, were present also in the root tissue of control plants, for the entry of the small concentration (85 µM) of Na^+ present in the composition of the hydroponic solution used (Supplemental Table 1). In the presence of 50 mM NaCl, the rates of Na^+ influx into the roots of the three salt-tolerant genotypes, expressed on a tissue dry weight basis, were quite different, ranging from the lowest value of 526 µmol g^{-1} DW h^{-1} in FL478 to 1170 µmol g^{-1} DW h^{-1} in Virgo. In the salt-sensitive PL12 the influx of Na^+ was much higher (about 2100 µmol g^{-1} DW h^{-1}) and about four-folds than in the salt-tolerant FL478. The values of influx of Rb^+ (indicative of K^+ uptake; Karim et al., 1971), in control conditions were very similar (at about 210 µmol g^{-1} DW h^{-1}) in the two tolerant genotypes Virgo and FL478 as well as in the sensitive one PL12, whereas in the tolerant Galileo the Rb^+ influx was lower (66 µmol g^{-1} DW h^{-1}). The presence of Na^+ in the incubation medium lowered Rb^+ influx in Virgo and FL478, without essentially any effect in the tolerant Galileo and in the sensitive PL12.

Table 5. Short-term influxes of Na^+ and Rb^+ (K^+) in roots of four rice genotypes with different tolerance/sensitivity to salt. Data are the means ± SD of four replicates. Asterisks indicate significant difference ($P \leq 0.05$) between salt-treated and control roots.

	Na^+_{root} influx (µmol g^{-1} DW h^{-1})		Rb^+_{root} influx (µmol g^{-1} DW h^{-1})	
Genotype	Control	50 mM NaCl	Control	50 mM NaCl
Galileo	1.13±0.56	783.53± 67.15*	166.00±9.22	108.65±14.79
Virgo	53.55±6.81	1168.82±113.78*	209.50±13.14	119.41±18.41*
FL478	16.67±1.71	525.97±24.91*	216.29±14.29	104.59±22.22*
PL12	7.23±1.39	2097.66±270.14	206.77±11.91	219.30±20.00

The efflux of K^+ from the roots into the incubation medium (without or with 50 mM NaCl) was also measured in the four rice genotypes in short-term (130 min) experiments. In the absence of NaCl in the medium (controls), the rates of efflux of K^+ were low in the tolerant Galileo and Virgo genotypes, where they rapidly diminished with the time, reaching in Virgo a null value at 120; in the tolerant FL478 and in the sensitive PL12 the rates of K^+ efflux were much higher, increasing with the time in FL478 and remaining essentially constant in PL12. Addition of salt to the medium induced, excluding FL478, an increase in the rates of K^+ efflux in all three genotypes Galileo, Virgo and in particular in PL12 up to the longest time interval (Fig. 7).

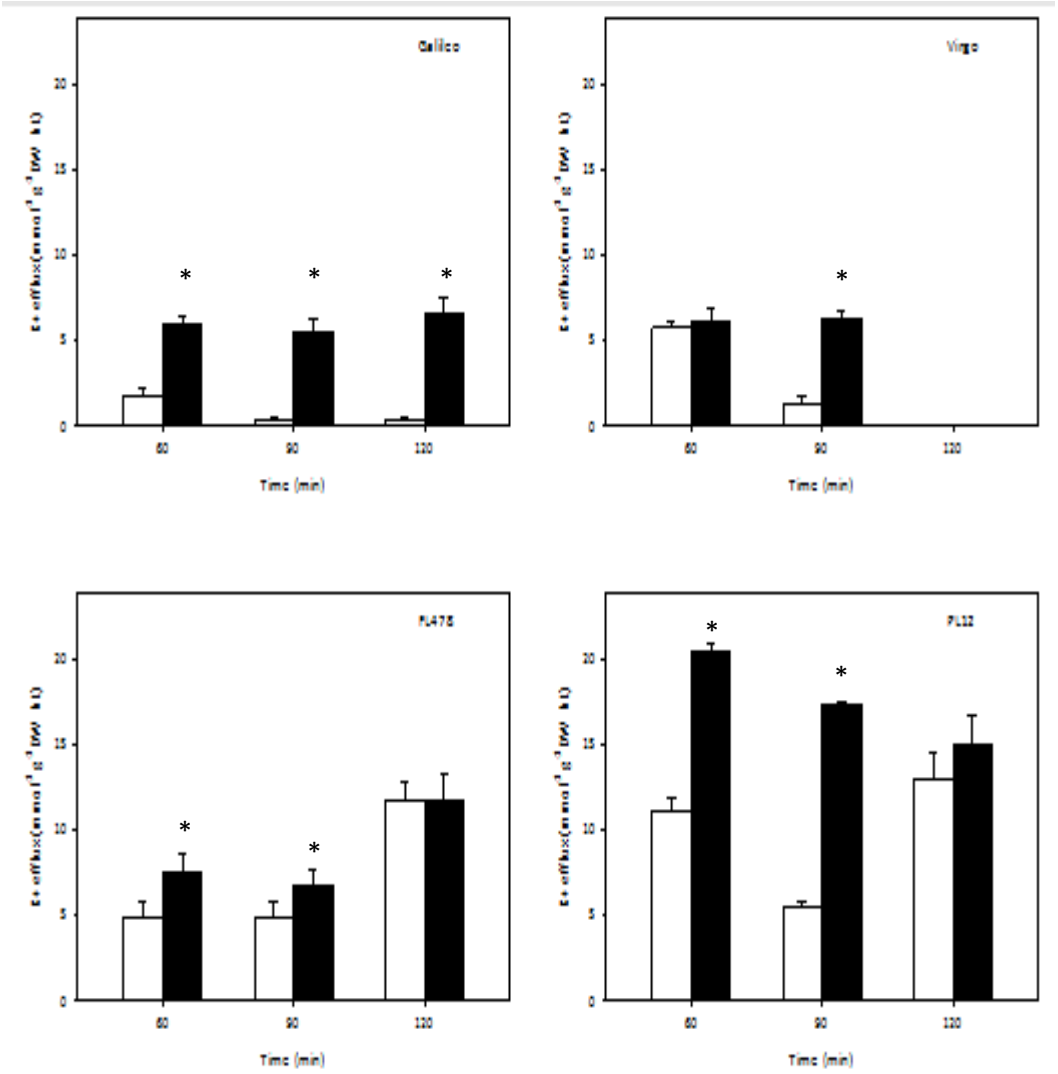

Figure 7. K^+ efflux from roots of four rice genotypes with different tolerance/sensitivity to salt. White bars: controls; black bars: 50 mM NaCl. Data, expressed as µmol K^+ g^{-1} DW h^{-1}, are the means ± SD of four replicates. Asterisks indicate significant difference ($P \leq 0.05$) between salt-treated and control roots.

The Na^+/K^+ ratio in the shoots is an important indicator of the plant capability for a long-term adaptation to salt conditions through the maintenance of efficient ionic homeostasis in photosynthetic tissues (Almeida et al., 2017). In particular, restriction of Na^+ accumulation in shoots has long been correlated with salt stress tolerance in rice (Lutts et al., 1996; Tester and Davenport, 2003). Table 6 shows the values of the Na^+/K^+ ratios determined in roots and shoots sampled after short-term exposure to 50 mM NaCl. In the roots, after exposure to salt, the Na^+/K^+ ratios increased, reaching very high values in PL12 and Virgo. In shoots, the Na^+/K^+ ratio was lowest in FL478.

Table 6. Na^+/K^+ molar ratios in roots and shoots of plants of four rice genotypes with different tolerance/sensitivity to salt exposed for 130 min to 50 mM NaCl. Data are the means ± SD of four replicates. Different letters indicate significance at $P \leq 0.05$.

	Na^+/K^+ ratio			
Genotype	Root		Shoot	
	Control	50 mM NaCl	Control	50 mM NaCl
Galileo	0.0006±0.0001	0.1588± 0.0137[b]	0.0004±0.0001	0.0425±0.0081
Virgo	0.0130±0.0044	0.1920±0.0093[ab]	0.0002±0.0001	0.0343±0.0057
FL478	0.0035±0.0011	0.1599±0.0072[b]	0.0006±0.0002	0.0296±0.0036
PL12	0.00006±0.0001	0.2480±0.0296[a]	0.0006±0.0001	0.0378±0.0021

3.4.2. Cytoplasmic and vacuolar pH

Removal of excess Na^+ from the cytoplasm by compartmentalization into the vacuole requires the driving force of an electrochemical H^+ gradient ($\Delta\mu_{H+}$) across the tonoplast generated by the activity of, amongst others, transport mechanisms identified as H^+-pyrophosphatases (H^+-PPases; Plett et al., 2010). Dissipation of the $\Delta\mu_{H+}$ is suggested to accompany the activity of the NHX Na^+/H^+ exchanger at the tonoplast (Almeida et al., 2017). Altogether, differential activation of these mechanisms may have obvious consequences on the values of both cytoplasmic and vacuolar pH when, under salt stress conditions, enhanced Na^+ compartmentalization is necessary. Figure 8 reports the results (ΔpH of salt-treated *vs* control roots) of ^{31}P-NMR experiments assessing the changes in cytoplasmic and vacuolar pH potentially induced by the salt treatment in roots of the tolerant Galileo, Virgo, and FL478 genotypes and of the sensitive PL12 one. Aalready after 1 h from the start of the salt treatment, a slight alkalinization of the vacuolar pH occurred in the tolerant genotypes Galileo, Virgo, and FL478, that was maintained also at longer experimental times (5 h). No salt-induced alkalinization of the vacuole was observed in the salt-sensitive PL12. The values of cytosolic pH showed early acidification of the cytoplasm upon salt addition in Galileo, FL478, and in PL12, but not in Virgo. This effect tended to be relieved at longer times.

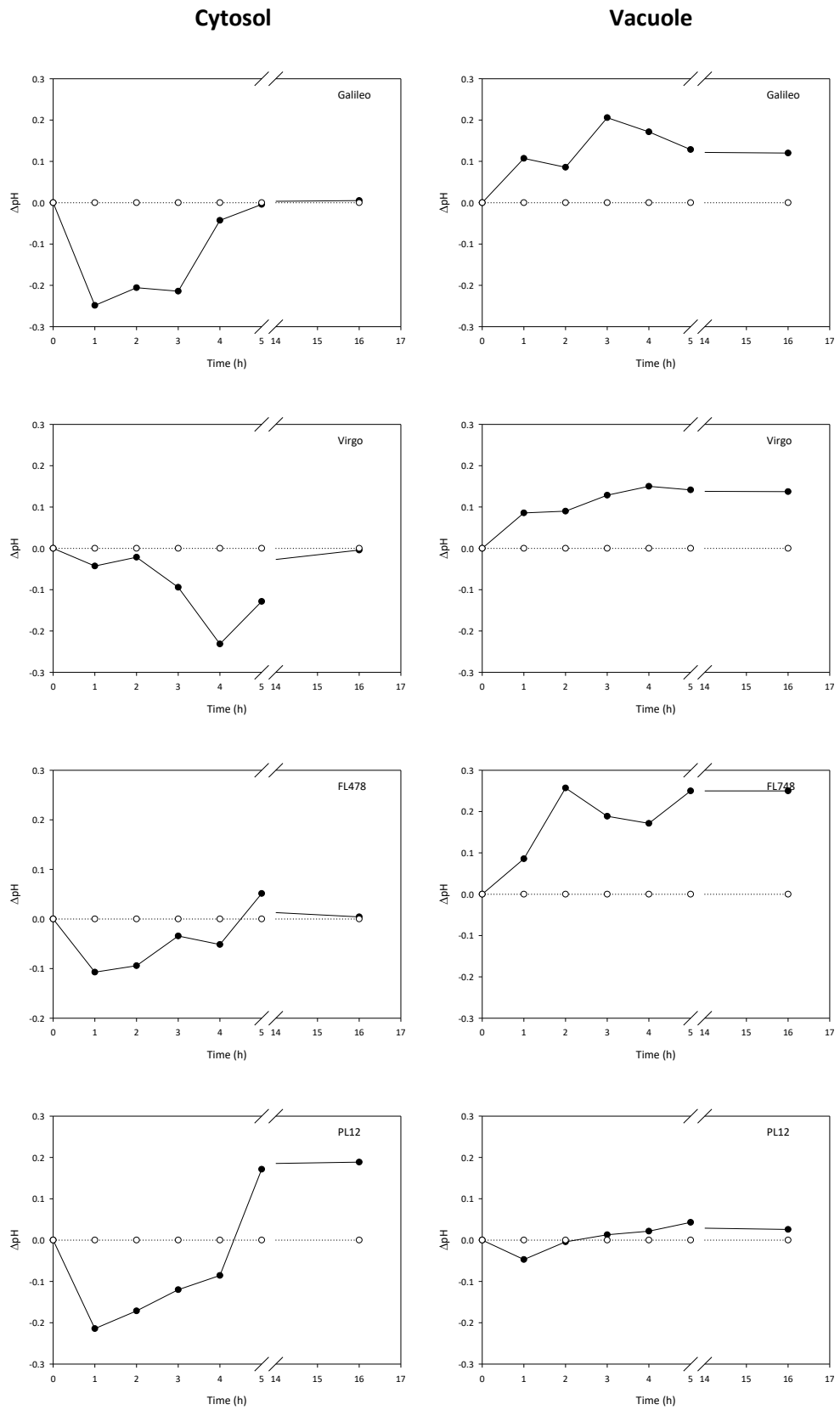

Figure 8. Time-course of cytosolic and vacuolar changes in pH of root cells of four rice genotypes with different tolerance/sensitivity to salt upon transfer into salt (50 mM NaCl) conditions. The dashed horizontal line at ΔpH = 0 refers to roots in control (no salt) conditions.

4. Discussion

Rice is relatively tolerant to salinity stress during germination, active tillering and towards maturity, but sensitive during early seedling establishment and reproductive stage (Heenan et al., 1988; Zeng et al., 2001). The molecular mechanisms and the underlying genes involved in the salt stress response may vary according to the specific phenological phase; moreover, different varieties may have different mechanisms to deal with salt stress. In fact, some are tolerant only in the initial stages of vegetative growth, others when approaching to the flowering phase (Zeng et al., 2001).

Genetic variability for salt tolerance within varieties is of paramount importance in crop improvement programs. Therefore, the choice of suitable germplasm in a breeding program is most crucial as its success relies on it. Concerning the *indica* subspecies, several QTLs and genes involved in the phenotypic variability in the response to salt stress have been identified and exploited for the genetic improvement of cultivated varieties (Naveed et al., 2018), but in the *japonica* subspecies fewer information is available. Furthermore, *indica* varieties are often grown in environments where salt stress is quite severe, different than in temperate areas, where salt stress is mild, and *japonica* is the most widely cultivated subspecies.

In this study we focused on the characterization of a large panel of *japonica* genotypes subjected to mild-salt stress condition (soil EC_e about 5 dS m^{-1}) considering: *i*) phenotyping during growth; *ii*) GWAS based upon previous GBS and the phenotyping results; *iii*) confirming the involvement of the membrane transport mechanisms potentially related to the control the Na^+/K^+ ratios in establishing the differences in salt tolerance observed in some accessions of the panel, in order to justify further investigation about the role of the OsVP6 in the variability observed within the rice panel.

In general, the genotype panel considered showed a broad range of the values of the four phenotypical parameters considered, in both control and salt conditions. The salt treatment did affect the behavior concerning all four parameters. Considering the SSI values, it resulted evident that the range of values delimiting the 10^{th} percentile of the most sensitive genotypes was generally markedly broader than that of the 90^{th} percentile defining the most tolerant ones. This observation suggests that the sensitivity response may involve a broader range of biochemical/physiological processes than the tolerance response.

The Standard Evaluation Score (SES), widely used to classify the visual symptoms of salt toxicity, allows to discriminate among susceptible, tolerant, and moderately tolerant genotypes (Batayeva et al., 2018; Chunthaburee et al., 2016; Naveed et al., 2018; Suriya-arunruj et al., 2004).

In general, in the panel studied, normalization of the response to salt by means of Stress Susceptibility Index (SSI) calculation of the four phenotypical parameters (SES, plant height, flowering time, and CHL), always yielded a broad variability in the response to salt (Figs. 1-4); in particular, a larger dispersion was generally observed for salt-sensitivity rather than for salt-tolerance.

The box plot graphical representation gives interesting indications on the variability within a population, but it does not allow to gain any information about the behavior of each specific genotype in the (stress) conditions imposed. Indeed, almost each genotype of the panel showed a different modulation in the response to salt condition for each of the four different parameters (Supplemental TableS2).

Within the core collection of most salt-sensitive and most salt-tolerant genotypes, two genotypes, Galileo and Virgo, resulted also among the most tolerant in a different panel characterized for salt-tolerance by Frouin et al. (2018). Upon this basis, Galileo and Virgo were chosen from our core collection, together with genotypes of assessed salt-tolerance (FL478) or salt-sensitivity (PL12), for the conduction of preliminary experiments specifically focused at validating the indication of GWAS analysis concerning the MTA_{51} LOC_Os01g23580 (Supplementary Table S4). In this framework, the aim was to assess the possible relationship between the physiological mechanism(s) and the gene individuated, and the possible role of these factors in the different response of rice to salt.

At the cell level, any mechanism able to limit the uncontrolled influx of Na^+, and/or remove efficiently its excess from the cytoplasm is expected to improve salt tolerance. The cytoplasmic concentration of Na^+ can be controlled by sequestering it in the vacuole and/or by controlling its net fluxes from/into the cell. The Na^+ ions that enter into root and leaf cells are removed from the cytoplasmic compartment by active pumping into the vacuole mainly controlled by vacuolar Na^+/H^+ antiporters (NHXs; Blumwald et al., 2000), in turn energized by the H^+ electrochemical potential difference to whose generation vacuolar H^+-PPase (OVPs) contributes, as shown also in rice (Plett et al., 2010). Overexpression of the vacuolar Na^+/H^+ antiporter NHX1 indeed increases the salinity tolerance of *Arabidopsis* (Mian et al., 2011 and references therein), tomato (Zhang and Blumwald, 2001), *Brassica napus* (Zhang et al., 2001), and rice (Fukuda et al., 2004; Chen et al., 2007). With these premises, among the different MTAs significantly associated with the analyzed traits in the rice panel considered, worth of particular attention is MTA_{51} (Tables 3 and S4), where it has been individuated the *Os01g0337500* (*OsOVP6*) gene, that encodes a vacuolar H^+-PPase. Indeed, the

expression of *OsOVP6* increases in transgenic rice lines, where the Na^+ selective transporter OsHKT1;5 (involved in the unloading of Na^+ in the xylem of leaf sheaths and in mediating Na^+ exclusion in the phloem to prevent Na^+ transfer to young leaf blades; Kobayashi et al., 2017) is upregulated (Plett et al., 2010). An indirect indication of the possible involvement of H^+-transport mechanisms at the membrane level in the determination of salt tolerance in rice comes from the results of the physiological ^{31}P-NMR experiments on the changes in cytoplasmic and vacuolar pH following exposure to 50 mM NaCl observed in roots of the salt-tolerant Virgo, Galileo, and FL478, and the salt-sensitive PL12 rice cultivars (Fig. 9). The early (detectable already after 1 h from salt addition) and persistent (up to 5 h) salt-induced alkalinization of the vacuolar pH in all three salt-tolerant genotypes is consistent with the hypothesis of a higher activity of vacuolar Na^+/H^+ exchange (probably supported by increased H^+ pumping by the H^+-PPase at the tonoplast) involving dissipation of the electrochemical H^+ gradient between vacuole and cytoplasm. This response, not observed in the salt-sensitive genotype PL12, appears compatible with a higher activity of the NHX Na^+/H^+ exchanger in tolerant genotypes. In Galileo, Virgo and FL478 this hypothesis seems to be coherently supported by the relatively high alkalinization of the vacuolar pH mirroring a higher dissipation of the H^+ gradient. The changes in the values of cytosolic pH consequent to salt addition may be explained by the pH buffering properties of this compartment, seemingly not efficient in the sensitive genotype PL12. Taken as a whole, the reported data seem to suggest that *OsOVP6* might play a role in salt tolerance representing a putative promising candidate gene exploitable for selection of salt-resistant rice lines. Further work is necessary to assess more directly, at the molecular and biochemical levels, the involvement of the OsOVP 6 H^+-PPase.

The control and maintenance of the complex balance between influx of Na^+ and efflux of K^+, that occur in the short term at the cell level, and of the concentrations of these ions, that are established in the plant in the long term, ultimately affect the ability to successfully cope with salt stress conditions. One significant effect of salt stress on K^+ homeostasis is the Na^+-induced K^+ efflux from root and leaf cells (Wang et al., 2009; Demidchik et al., 2014). This phenomenon is the result of excess Na^+ influx into the cytoplasm that leads to the depolarization of the membrane potential; as a consequence, activation of K^+ Outward Rectifier channels, that mediate the leakage of K^+ (Shabala and Cuin, 2008), counterbalances the entry of excessive amounts of positive charges. On the other hand, maintenance of the favorable low Na^+/K^+ ratios, particularly necessary in salt-stress conditions, requires enhanced intracellular K^+ retention (reduced K^+ efflux). Our results, obtained by short-term ion transport experiments at the root level, seem consistent with the

sensitivity/tolerance to salt of the four genotypes considered. The tolerant FL478 showed essentially no effect of salt on the efflux of K^+ compared to the controls, accompanied by low influx of Na^+, altogether determining a low Na^+/K^+ ratio in the roots. In the other two tolerant genotypes the presence of salt in the incubation medium did induce an increase in the efflux of K^+ that was much lower than in the sensitive PL12, consistent with the values of Na^+ influx and with those of root Na^+/K^+ ratios. It is interesting to stress out that the shoot Na^+/K^+ ratio was lowest in FL478, consistent with what described in the literature (*'Saltol'* QTL involved in Na^+/K^+ homeostasis during salt stress; Thomson et al., 2010) (Tables 5,6; Fig. 7).

GWAS analysis on data concerning Flowering time put in evidence that the MTA_{1123} also comprises the gene *Os10g0438000* that encodes a K^+ channel tetramerization domain-containing protein 9 involved in a network of proteins indeed reported to interact in determining salt tolerance[4]; Yu et al., 2017). The activity of Inward- and Outward rectifying K^+ channels that are involved at different tissue and organ levels in the regulation of the homeostasis of K^+ is regulated by the heteromerization of different polypeptidic subunits (Dreyer et al., 2004; Lebaudy et al., 2010; Ragel et al., 2019) that are therefore crucial for this function. It will be interesting to deepen the study of this aspect in the framework of salt resistance assessment in our rice panel.

It may be worth citing that in the same region defined by MTA_{1123} an *Os10g0436900* gene encoding an OsCCX3 was identified. CCX proteins are part of a superfamily of Ca^{2+} transporters, representing also in plants cation/Ca^{2+} and in particular Na^+/Ca^{2+} antiporters (*OsNCX11* Na^+/Ca^{2+} exchanger; Singh et al., 2015). Calcium is one of the most important secondary messengers in plants, and plays a key role in the response to biotic and abiotic stresses. NCX proteins play a pivotal role in Ca^{2+} homeostasis potentially participating in the physiological processes and stress (salt) responses that involve Ca^{2+} signaling (Yu et al., 2017). In rice, the expression of a few members of the *NCX* family (*OsNCX3*, *OsNCX10*, and *OsNCX15*) has been reported to be up-regulated in response, amongst others, to salinity stress, even if *OsNCX11* appears to be only slightly up-regulated (Singh et al., 2015). Other authors, on the other side, report that the expression profile of OsCCX3 is not significantly changed under salt stress (Yadav et al., 2015). In this context, the *Os10g0436900* gene individuated may be considered for future studies aimed at better clarifying the role of Ca^{2+} in the determination of salt tolerance in rice and at searching for possible candidate genes for this trait. In the same region defined by the MTA_{51} is located the OsTFIID (*Os01g0338100*), one of the 14

[4] https://shigen.nig.ac.jp/rice/oryzabase/gene/detail/21963

transcription factors included in the QTL '*SalTol*'. The expression of this gene is affected by salt differently in the tolerant Pokkali genotypes and in the sensitive one IR64 (Nutan et al., 2017).

Concerning the GWAS results on height phenotypic data, the region defined by MTA_{933} contained the gene *Os08g0357300* that encodes a bZIP TF. Seven transcript isoforms of bZIP family were identified related to a LOC_Os08g26880.1 over-expressed in the salt-tolerant FL478 and down-regulated in the salt-sensitive IR29 (Mirdar-Mansuri et al., 2019; Patishtan et al., 2018).

Concerning the GWAS results on flowering data, the region defined by MTA_{1123} contained the gene *Os10g0442600* that encodes a homologue of a Cell Division Cycle control protein 48 (CDC48), i.e., OsCDC48E (Yu et al., 2017; Shi et al., 2019). CDC48 belongs to the superfamily protein of ATPases associated with diverse cellular activities. OsCDC48 interacts with OsCDC48E to control plant survival in rice. OsCDC48E are likely to form a hetero-multimeric complex to control plant survival by regulating senescence-associated genes and the cell cycle progression in rice. OsCDC48E has a similar expression pattern to OsCDC48, and is constitutively expressed in different tissues including roots, culms of the second internode, flag leaf sheaths, flag leaves and panicles at the heading stage; rice OsCDC48E knockout plants exhibit similar behavior to the CDC48 mutant *psd128* with premature senescence and plant death. A GWAS study for salt-tolerance in rice suggested this gene as playing a roleis also involved in salt tolerance (Yu et al., 2017).

Concerning the GWAS results on CHL, the region defined by MTA_{46} contained the gene *Os01g0705700* encoding a protein similar to ICE1 (Inducer of CBF Expression1), a basic helix-loop-helix DNA-binding protein involved in cold acclimation. In rice, ectopic expression of a *Raphanus sativus ICE1* (*RsICE1*) gene confers tolerance to low-temperature stress based upon higher accumulation of soluble sugars and free proline, lesser electrolyte leakage and MDA levels, accompanied by higher chlorophyll levels in comparison to the control plants (Man et al., 2017). In *Arabidopsis*, *AtICE1* induces Dehydration-Responsive Element-Binding (DREB) protein/C-Repeat Binding Factors (CBFs) known to regulate the expression of stress-responsive genes. In rice, a number of *CBF*/*DREB1* homologues (*OsDREB*s) have been isolated and their overexpression has been found to upregulate the transcription levels of cold-regulated genes improving tolerance to, in addition to cold, also salt and drought (Man et al., 2017 and references therein).

5. Conclusion

The data obtained concerning the phenotyping of a wide panel of rice genotypes of the *japonica* ssp indicate a broad variability of this population for what concerns the response to mild

salinity condition, confirming its suitability for GWAS studies aimed at identifying MTAs potentially exploitable for selection of specific genotypes best suited to temperate environments.

The GWAS activity conducted allowed to identify a few interesting candidate genes; in detail: *Os01g0337500* that encodes the vacuolar OsOVP6 H^+-PPase, of *Os10g0438000* that encodes a protein crucial for the assembly of KOR channels, and of *Os10g0436900* that encodes a CCX protein with the function of cation/Ca^{2+} exchanger. All these activities are involved in the maintenance of proper Na^+/K^+ ratios under salt stress most probably playing a role in salt tolerance; they may therefore represent putative promising candidates exploitable for selection of salt-resistant rice lines.

6. References

Ali, Y., Aslam, Z., Ashraf, M. Y., and Tahir, G. R. (2004). Effect of salinity on chlorophyll concentration, leaf area, yield and yield components of rice genotypes grown under saline environment. *Int. J. Environ. Sci. Technol.* 1, 221–225. doi:10.1007/BF03325836.

Almeida, D. M., Oliveira, M. M., and Saibo, N. J. M. (2017a). Regulation of Na^+ and K^+ homeostasis in plants: towards improved salt stress tolerance in crop plants. *Genetics and Molecular Biology* 40, 326–345. doi:10.1590/1678-4685-gmb-2016-0106.

Barrett, J.C., Fry, B., Maller, J., and Daly, M.J. (2005). Haploview: analysis and visualization of LD and haplotype maps. Bioinformatics 21, 263–265, doi:10. 1093/bioinformatics/bth457.

Batayeva, D., Labaco, B., Ye, C., Li, X., Usenbekov, B., Rysbekova, A., et al. (2018). Genome-wide association study of seedling stage salinity tolerance in temperate japonica rice germplasm. *BMC Genetics* 19, 2. doi:10.1186/s12863-017-0590-7.

Benjamini, Y., and Hochberg, Y. (1995). Controlling the False Discovery Rate - A Practical and Powerful Approach to Multiple Testing. *J. Royal Statist. Soc., Series B* 57, 289–300. doi:10.2307/2346101.

Biscarini, F., Cozzi, P., Casella, L., Riccardi, P., Vattari, A., Orasen, G., et al. (2016). Genome-Wide Association Study for Traits Related to Plant and Grain Morphology, and Root Architecture in Temperate Rice Accessions. *PLOS ONE* 11, e0155425. doi:10.1371/journal.pone.0155425.

Blumwald, E., Aharon, G. S., and Apse, M. P. (2000). Sodium transport in plant cells. *Biochimica et Biophysica Acta (BBA) - Biomembranes* 1465, 140–151. doi:10.1016/S0005-2736(00)00135-8.

Castillo, E. G., Tuong, T. P., Ismail, A., and Inubushi, K. (2007). Response to Salinity In Rice: Comparative Effects of Osmotic and Ionic Stresses. *Plant Production Science* 10, 159–170. doi:10.1626/pps.10.159.

Cerovic, Z. G., Masdoumier, G., Ghozlen, N. B., and Latouche, G. (2012). A new optical leaf-clip meter for simultaneous non-destructive assessment of leaf chlorophyll and epidermal flavonoids. *Physiol Plant* 146, 251–260. doi:10.1111/j.1399-3054.2012.01639.x.

Chandramohanan, K. T., Radhakrishnan, V. V., Joseph, E. A., and Mohanan, K. V. (2014). A study on the effect of salinity stress on the chlorophyll content of certain rice cultivars of Kerala state of India. *Agriculture, Forestry and Fisheries* 3, 67-70. doi:10.11648/j.aff.20140302.13.

Chen, Z., Pottosin, I. I., Cuin, T. A., Fuglsang, A. T., Tester, M., Jha, D., et al. (2007). Root Plasma Membrane Transporters Controlling K^+/Na^+ Homeostasis in Salt-Stressed Barley. *Plant Physiology* 145, 1714–1725. doi:10.1104/pp.107.110262.

Chunthaburee, S., Dongsansuk, A., Sanitchon, J., Pattanagul, W., and Theerakulpisut, P. (2016). Physiological and biochemical parameters for evaluation and clustering of rice cultivars differing in salt tolerance at seedling stage. *Saudi J Biol Sci* 23, 467–477. doi:10.1016/j.sjbs.2015.05.013.

Cui, Y., Zhang, F., and Zhou, Y. (2018). The Application of Multi-Locus GWAS for the Detection of Salt-Tolerance Loci in Rice. *Front. Plant Sci.* 9. doi:10.3389/fpls.2018.01464.

Demidchik, V., Straltsova, D., Medvedev, S. S., Pozhvanov, G. A., Sokolik, A., and Yurin, V. (2014). Stress-induced electrolyte leakage: the role of K^+-permeable channels and involvement in programmed cell death and metabolic adjustment. *J Exp Bot* 65, 1259–1270. doi:10.1093/jxb/eru004.

Dreyer, I., Porée, F., Schneider, A., Mittelstädt, J., Bertl, A., Sentenac, H., et al. (2004). Assembly of Plant Shaker-Like Kout Channels Requires Two Distinct Sites of the Channel α-Subunit. *Biophys J* 87, 858–872. doi:10.1529/biophysj.103.037671.

Fischer, R. A., and Maurer, R. (1978). Drought resistance in spring wheat cultivars. I. Grain yield responses. *Aust. J. Agric. Res.* 29, 897–912. doi:10.1071/ar9780897.

Fitzgerald, M. A., McCouch, S. R., and Hall, R. D. (2009). Not just a grain of rice: the quest for quality. *Trends in Plant Science* 14, 133–139. doi:10.1016/j.tplants.2008.12.004.

Frouin, J., Languillaume, A., Mas, J., Mieulet, D., Boisnard, A., Labeyrie, A., et al. (2018). Tolerance to mild salinity stress in japonica rice: A genome-wide association mapping study highlights calcium signaling and metabolism genes. *PLOS ONE* 13, e0190964. doi:10.1371/journal.pone.0190964.

Fukuda, A., Nakamura, A., Tagiri, A., Tanaka, H., Miyao, A., Hirochika, H., et al. (2004). Function, Intracellular Localization and the Importance in Salt Tolerance of a Vacuolar Na^+/H^+ Antiporter from Rice. *Plant Cell Physiol* 45, 146–159. doi:10.1093/pcp/pch014.

Gerona, M. E. B., Deocampo, M. P., Egdane, J. A., Ismail, A. M., and Dionisio-Sese, M. L. (2019). Physiological Responses of Contrasting Rice Genotypes to Salt Stress at Reproductive Stage. *Rice Science* 26, 207–219. doi:10.1016/j.rsci.2019.05.001.

Gregorio, G., Senadhira, D., and Mendoza, R. (1997). Screening rice for salinity tolerance, vol 22, IRRI discussion paper series. *International Rice Research Institute*.

Heenan, D. P., Lewin, L. G., and McCaffery, D. W. (1988). Salinity tolerance in rice varieties at different growth stages. *Aust. J. Exp. Agric.* 28, 343–349. doi:10.1071/ea9880343.

Hoang, T. M. L., Tran, T. N., Nguyen, T. K. T., Williams, B., Wurm, P., Bellairs, S., et al. (2016). Improvement of Salinity Stress Tolerance in Rice: Challenges and Opportunities. *Agronomy* 6, 54. doi:10.3390/agronomy6040054.

Kaniel, S., and Stein, J. (1974). Least-square acceleration of iterative methods for linear equations. *J Optim Theory Appl* 14, 431–437. doi:10.1007/BF00933309.

Karim, M., Rahman, S., and Rahman, M. (1971). Rb^{86} as tracer for potassium: I. Uptake of Rb and K by rice plant in nutrient solution. *Plant Soil* 35, 179–181. doi:10.1007/BF01372642.

Kawahara, Y., de la Bastide, M., Hamilton, J. P., Kanamori, H., McCombie, W. R., Ouyang, S., et al. (2013). Improvement of the *Oryza sativa* Nipponbare reference genome using next generation sequence and optical map data. *Rice* 6, 4. doi:10.1186/1939-8433-6-4.

Kime, M. J., Ratcliffe, R. G., Williams, R. J. P., and Loughman, B. C. (1982). The Application of ^{31}P Nuclear Magnetic Resonance to Higher Plant Tissue. I. Detection of Spectra. *J Exp Bot* 33, 656–669. doi:10.1093/jxb/33.4.656.

Kobayashi, N. I., Yamaji, N., Yamamoto, H., Okubo, K., Ueno, H., Costa, A., et al. (2017). OsHKT1;5 mediates Na^+ exclusion in the vasculature to protect leaf blades and reproductive tissues from salt toxicity in rice. *The Plant Journal* 91, 657–670. doi:10.1111/tpj.13595.

Kumar, V., Singh, A., Mithra, S. V. A., Krishnamurthy, S. L., Parida, S. K., Jain, S., et al. (2015). Genome-wide association mapping of salinity tolerance in rice (*Oryza sativa*). *DNA Res* 22, 133–145. doi:10.1093/dnares/dsu046.

Lebaudy, A., Pascaud, F., Véry, A.-A., Alcon, C., Dreyer, I., Thibaud, J.-B., et al. (2010). Preferential KAT1-KAT2 Heteromerization Determines Inward K^+ Current Properties in Arabidopsis Guard Cells. *J. Biol. Chem.* 285, 6265–6274. doi:10.1074/jbc.M109.068445.

Lutts, S., Kinet, J. M., and Bouharmont, J. (1995). Changes in plant response to NaCl during development of rice (*Oryza sativa* L.) varieties differing in salinity resistance. *J Exp Bot* 46, 1843–1852. doi:10.1093/jxb/46.12.1843.

Lutts, S., Kinet, J. M., and Bouharmont, J. (1996). Effects of salt stress on growth, mineral nutrition and proline accumulation in relation to osmotic adjustment in rice (*Oryza sativa* L.) cultivars differing in salinity resistance. *Plant Growth Regul* 19, 207–218. doi:10.1007/BF00037793.

Man, L., Xiang, D., Wang, L., Zhang, W., Wang, X., and Qi, G. (2017). Stress-responsive gene RsICE1 from *Raphanus sativus* increases cold tolerance in rice. *Protoplasma* 254, 945–956. doi:10.1007/s00709-016-1004-9.

Mirdar Mansuri, R., Shobbar, Z.-S., Babaeian Jelodar, N., Ghaffari, M. R., Nematzadeh, G.-A., and Asari, S. (2019). Dissecting molecular mechanisms underlying salt tolerance in rice: a comparative transcriptional profiling of the contrasting genotypes. *Rice* 12, 13. doi:10.1186/s12284-019-0273-2.

Mantri, N., Patade, V., Penna, S., Ford, R., and Pang, E. (2012). "Abiotic Stress Responses in Plants: Present and Future," in *Abiotic Stress Responses in Plants: Metabolism, Productivity and Sustainability*, eds. P. Ahmad and M. N. V. Prasad (New York, NY: Springer New York), 1–19. doi:10.1007/978-1-4614-0634-1_1.

Mian, A.A., Senadheera, P., and Maathuis, F. (2011). Improving Crop Salt Tolerance: Anion and Cation Transporters as Genetic Engineering Targets. *Plant Stress* 5, 64–72.

Morton, M. J. L., Awlia, M., Al-Tamimi, N., Saade, S., Pailles, Y., Negrão, S., et al. (2019). Salt stress under the scalpel – dissecting the genetics of salt tolerance. *The Plant Journal* 97, 148–163. doi:10.1111/tpj.14189.

Munns, R. (2002). Comparative physiology of salt and water stress. *Plant, Cell & Environment* 25, 239–250. doi:10.1046/j.0016-8025.2001.00808.x.

Munns, R., and Tester, M. (2008). Mechanisms of Salinity Tolerance. *Annual Review of Plant Biology* 59, 651–681. doi:10.1146/annurev.arplant.59.032607.092911.

Naveed, S. A., Zhang, F., Zhang, J., Zheng, T.-Q., Meng, L.-J., Pang, Y.-L., et al. (2018). Identification of QTN and Candidate Genes for Salinity Tolerance at the Germination and Seedling Stages in Rice by Genome-Wide Association Analyses. *Sci Rep* 8, 1–11. doi:10.1038/s41598-018-24946-3.

Nyquist, W.E., and Baker, R.J. (1991). Estimation of heritability and prediction of selection response in plant populations. *Critical Reviews in Plant Sciences* 10, 235–322. doi:10.1080/07352689109382313.

Nocito, F., Espen, L., Crema, B., Cocucci, M., and Sacchi, G. (2008). Cadmium induces acidosis in maize root cells. *The New phytologist* 179, 700–11. doi:10.1111/j.1469-8137.2008.02509.x.

Nutan, K. K., Kushwaha, H. R., Singla-Pareek, S. L., and Pareek, A. (2017). Transcription dynamics of Saltol QTL localized genes encoding transcription factors, reveals their differential regulation in contrasting genotypes of rice. *Funct Integr Genomics* 17, 69–83. doi:10.1007/s10142-016-0529-5.

Ogawa, D., Abe, K., Miyao, A., Kojima, M., Sakakibara, H., Mizutani, M., et al. (2011). RSS1 regulates the cell cycle and maintains meristematic activity under stress conditions in rice. *Nat Commun* 2, 1–11. doi:10.1038/ncomms1279.

Orasen, G. (2018). Genome-Wide Analysis of Japonica Rice Performances under Alternate Wetting and Drying and Permanent Flooding Conditions. doi:10.13130/orasen-gabriele_phd2018-01-19.

Patishtan, J., Hartley, T. N., Carvalho, R. F. de, and Maathuis, F. J. M. (2018). Genome-wide association studies to identify rice salt-tolerance markers. *Plant, Cell & Environment* 41, 970–982. doi:10.1111/pce.12975.

Plett, D., Safwat, G., Gilliham, M., Møller, I. S., Roy, S., Shirley, N., et al. (2010). Improved Salinity Tolerance of Rice Through Cell Type-Specific Expression of AtHKT1;1. *PLOS ONE* 5, e12571. doi:10.1371/journal.pone.0012571.

Purcell, S., Neale, B., Todd-Brown, K., Thomas, L., Ferreira, M. A. R., Bender, D., et al. (2007). PLINK: A Tool Set for Whole-Genome Association and Population-Based Linkage Analyses. *The American Journal of Human Genetics* 81, 559–575. doi:10.1086/519795.

Puvanitha, S., and Mahendran, S. (2017). Effect of Salinity on Plant Height, Shoot and Root Dry Weight of Selected Rice Cultivars. *Sch. J. Agric. Vet. Sci.* 4, 126-131, doi:10.21276/sjavs.

Ragel, P., Raddatz, N., Leidi, E. O., Quintero, F. J., and Pardo, J. M. (2019). Regulation of K+ Nutrition in Plants. *Front Plant Sci* 10. doi:10.3389/fpls.2019.00281.

Rahman, A., Hossain, M. S., Mahmud, J. A., Nahar, K., Hasanuzzaman, M., and Fujita, M. (2016). Manganese-induced salt stress tolerance in rice seedlings: regulation of ion homeostasis, antioxidant defense and glyoxalase systems. *Physiol Mol Biol Plants* 22, 291–306. doi:10.1007/s12298-016-0371-1.

Rahman, A., Nahar, K., Mahmud, J. A., Hasanuzzaman, M., Hossain, M. S., and Fujita, M. (2017). Salt Stress Tolerance in Rice: Emerging Role of Exogenous Phytoprotectants. *Advances in International Rice Research*. doi:10.5772/67098.

Rao, P. S., Mishra, B., and Gupta, S. R. (2013). Effects of Soil Salinity and Alkalinity on Grain Quality of Tolerant, Semi-Tolerant and Sensitive Rice Genotypes. *Rice Science* 20, 284–291. doi:10.1016/S1672-6308(13)60136-5.

Rengasamy, P. (2006). World salinization with emphasis on Australia. *J Exp Bot* 57, 1017–1023. doi:10.1093/jxb/erj108.

Roberts, J. K. M., Ray, P. M., Wade-Jardetzky, N., and Jardetzky, O. (1980). Estimation of cytoplasmic and vacuolar p H in higher plant cells by ^{31}P NMR. *Nature* 283, 870–872. doi:10.1038/283870a0.

Roberts, J. K. M., Wade-Jardetzky, N., and Jardetsky, O. (1981). Intracellular pH measurements by phosphorus-31 nuclear magnetic resonance. Influence of factors other than pH on phosphorus-31 chemical shifts. *Biochemistry* 20, 5389–5394. doi:10.1021/bi00522a006.

Shabala, S., and Cuin, T. (2008). Potassium transport and plant salt tolerance. *Physiologia plantarum* 133, 651–69. doi:10.1111/j.1399-3054.2007.01008.x.

Shanker, A., and Venkateswarlu, B. (2011). *Abiotic Stress in Plants - Mechanisms and Adaptations*. doi:10.5772/895.

Shi, L., Zhang, X., Shi, Y., Xu, X., He, Y., Shao, G., et al. (2019). OsCDC48/48E complex is required for plant survival in rice (Oryza sativa L.). *Plant Mol Biol* 100, 163–179. doi:10.1007/s11103-019-00851-9.

Shi, Y., Gao, L., Wu, Z., Zhang, X., Wang, M., Zhang, C., et al. (2017). Genome-wide association study of salt tolerance at the seed germination stage in rice. *BMC Plant Biol* 17, 92. doi:10.1186/s12870-017-1044-0.

Singh, A. K., Kumar, R., Tripathi, A. K., Gupta, B. K., Pareek, A., and Singla-Pareek, S. L. (2015). Genome-wide investigation and expression analysis of Sodium/Calcium exchanger gene family in rice and Arabidopsis. *Rice (N Y)* 8, 54. doi:10.1186/s12284-015-0054-5.

Suriya-arunruj, D., Supapoj, N., Toojinda, T., and Vanavichit, A. (2004). Relative leaf water content as an efficient method for evaluating rice cultivars for tolerance to salt stress. *Science Asia*, 30, 411, doi.org/10.2306/scienceasia1513-1874.2004.30.411.

Tester, M., and Davenport, R. (2003). Na^+ tolerance and Na^+ transport in higher plants. *Ann. Bot.* 91, 503–527. doi:10.1093/aob/mcg058.

Thakur, P., Kumar, S., Malik, J. A., Berger, J. D., and Nayyar, H. (2010). Cold stress effects on reproductive development in grain crops: An overview. *Environmental and Experimental Botany* 67, 429–443. doi:10.1016/j.envexpbot.2009.09.004.

Thomson, M. J., Ocampo, M. de, Egdane, J., Rahman, M. A., Sajise, A. G., Adorada, D. L., et al. (2010). Characterizing the Saltol Quantitative Trait Locus for Salinity Tolerance in Rice. *Rice* 3, 148–160. doi:10.1007/s12284-010-9053-8.

Umali, D. L. (1993). Irrigation induced salinity : a growing problem for development and the environment. The World Bank doi:10.1596/0-8213-2508-6. Available at: http://documents.worldbank.org/curated/en/486611468766779740/Irrigation-induced-salinity-a-growing-problem-for-development-and-the-environment [Accessed October 18, 2019].

Volante, A., Desiderio, F., Tondelli, A., Perrini, R., Orasen, G., Biselli, C., et al. (2017). Genome-Wide Analysis of japonica Rice Performance under Limited Water and Permanent Flooding Conditions. *Front. Plant Sci.* 8. doi:10.3389/fpls.2017.01862.

Walia, H., Wilson, C., Condamine, P., Liu, X., Ismail, A.M., Zeng, L., Wanamaker, S.I., Mandal, J., Xu, J. Cui, X., Close, T.J. (2005). Comparative transcriptional profiling of two contrasting rice genotypes under salinity stress during the vegetative growth stage. *Plant Physiol.* 139, 82-835. doi:10.1104/pp.105.065961.

Wang, C.-M., Zhang, J.-L., Liu, X.-S., Li, Z., Wu, G.-Q., Cai, J.-Y., et al. (2009). Puccinellia tenuiflora maintains a low Na+ level under salinity by limiting unidirectional Na^+ influx resulting in a high selectivity for K^+ over Na+. *Plant, Cell & Environment* 32, 486–496. doi:10.1111/j.1365-3040.2009.01942.x.

Wang, W., Vinocur, B., and Altman, A. (2003). Plant responses to drought, salinity and extreme temperatures: towards genetic engineering for stress tolerance. *Planta* 218, 1–14. doi:10.1007/s00425-003-1105-5.

Xiong, L., and Zhu, J.-K. (2001). Abiotic stress signal transduction in plants: Molecular and genetic perspectives. *Physiologia Plantarum* 112, 152–166. doi:10.1034/j.1399-3054.2001.1120202.x.

Yadav, A. K., Shankar, A., Jha, S. K., Kanwar, P., Pandey, A., and Pandey, G. K. (2015). A rice tonoplastic calcium exchanger, OsCCX2 mediates Ca^{2+}/cation transport in yeast. *Sci Rep* 5. doi:10.1038/srep17117.

Yu, J., Zao, W., He, Q., Kim, T.-S., and Park, Y.-J. (2017). Genome-wide association study and gene set analysis for understanding candidate genes involved in salt tolerance at the rice seedling stage. *Mol. Genet. Genomics* 292, 1391–1403. doi:10.1007/s00438-017-1354-9.

Zeng, L., Shannon, M. C., and Lesch, S. M. (2001). Timing of salinity stress affects rice growth and yield components. *Agricultural Water Management* 48, 191–206. doi:10.1016/S0378-3774(00)00146-3.

Zhang, H.-X., and Blumwald, E. (2001). Transgenic salt-tolerant tomato plants accumulate salt in foliage but not in fruit. *Nat Biotechnol* 19, 765–768. doi:10.1038/90824.

Zhang, H.-X., Hodson, J. N., Williams, J. P., and Blumwald, E. (2001). Engineering salt-tolerant Brassica plants: Characterization of yield and seed oil quality in transgenic plants with increased vacuolar sodium accumulation. *PNAS* 98, 12832–12836. doi:10.1073/pnas.231476498.

SUPPLEMENTAL MATERIAL

Supplemental Table 1. Additional rice accessions included in the panel

Accession	Origin	Group	Commercial Class	Structure Group
LUCERO	ITALY	temperate japonica	Round	k1
SANDORA	HUNGARY	temperate japonica	Long A	k1
XIANGOU2	CHINA	tropical japonica	Medium	admixed

Supplemental Table 2. Composition of the hydroponic solution for rice growth (pH 6.2)

Macronutrient	Concentration	Micronutrient	Concentration
KNO_3	1.5 mM	$Na_2O_3Si \bullet 9\ H_2O$	30 µM
$Ca(NO_3)_2 \bullet 4\ H_2O$	1 mM	H_3BO_3	46 µM
$MgSO_4$	500 µM	$MnCl_2 \bullet 4\ H_2O$	9 µM
$NH_4H_2PO_4$	250 µM	$ZnSO_4 \bullet 7\ H_2O$	0.8 µM
		$CuSO_4 \bullet 5\ H_2O$	0.3 µM
		$(NH_4)_6Mo_7O_{24} \bullet 4\ H_2O$	0.1 µM
		$C_{10}H_{12}FeN_2NaO_8$ - Fe(III)EDTA	25 µM

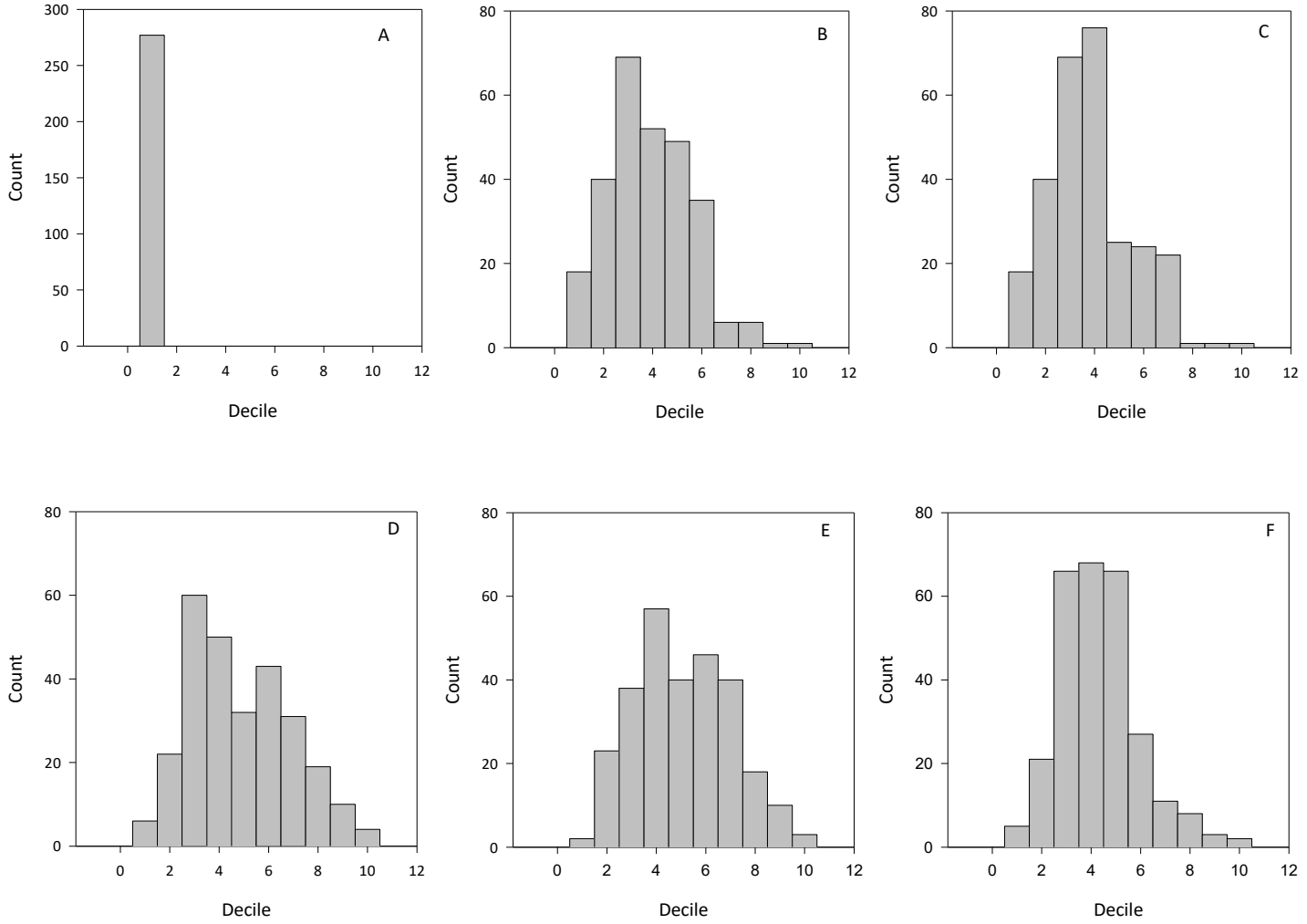
A
B
C
D
E
F
Count
Decile
0
2
4
6
8
10
12
20
40
50
60
80
100
150
200
250
300

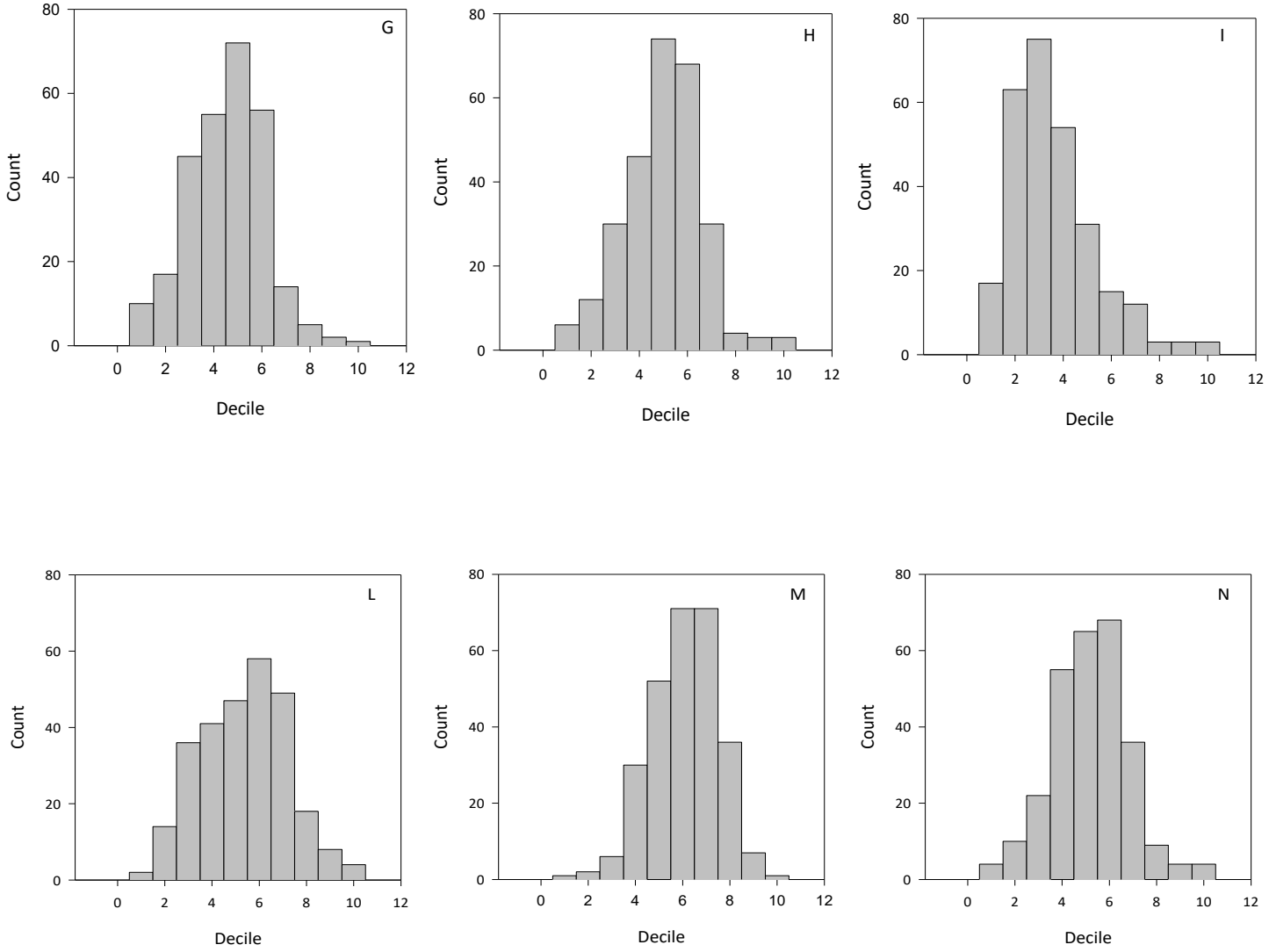

Supplemental figure 1. Frequency distribution for all the traits used for the genome-wide association study analysed in control (on the left) and salt (in the middle), as well as for the respective SSI values (on the right). A-C: SES; D-F: plant height; G-I: flowering time; L-N: CHL index

Supplemental Table S3. List of all the genotypes of the panel with associated SSIs of the Least Square Means for the four phenotypical parameters considered. Green-highlighted block: genotypes with SSI values ≤ to the 10th percentile (salt-tolerant). Pink-highlighted block: genotypes with SSI values ≥ to the 90th percentile (salt-sensitive). Within each highlighted block, gray cells indicate genotypes with four parameters in the percentile, red cells indicate genotypes with three parameters in the percentile, yellow cells indicate genotypes with two parameters in the percentile. 10th percentile: SSI_SES = 0.808; SSI_Height = 0.690; SSI_FLOWERING = 0.566; SSI_CHL = 0.424; 90th percentile SSI_SES = 1.155; SSI_Height = 1.336; SSI_Flowering = 1.532; SSI_CHL = 1.604.

Growth phase							
Vegetative				Reproductive			
Genotype	SSI_SES	Genotype	SSI_Height	Genotype	SSI_Flowering	Genotype	SSI_CHL
SAMBA	0.053	GZ8367	0.405	M203	0.258	ITALPATNAxMILYANG	-0.249
ITALPATNAxMILYANG	0.544	SAKHA102	0.433	SENATORENOVELLI	0.271	L202	-0.236
SAFARI	0.566	ORIONE	0.435	UPLA68	0.323	A201	-0.192
VIALONENERO	0.588	CARNISE	0.514	VULCANO	0.330	ALEXANDROS	-0.092
S1022	0.609	SUPER	0.515	YRM62	0.379	REXMONT	-0.036
BAIXET	0.684	RUBI	0.535	AUGUSTO	0.392	THAIBONNET	0.007
BALDO	0.684	PERLA	0.546	SAFARI	0.418	PANDA	0.029
LOMELLINO	0.684	UPLA64	0.554	IBO38033	0.426	ROBBIOSEL1	0.033
MUGA	0.684	GALILEO	0.566	HANDAO297	0.427	REDI	0.091
NANO	0.684	DIMITRA	0.568	P6	0.470	DELLMONT	0.093
OPALE	0.684	UPLA91	0.576	RINALDOBERSANI	0.474	JACINTO	0.148
RINALDOBERSANI	0.684	MECO	0.578	JUBILIENI	0.489	MAYBELLE	0.160
DREW	0.750	CALMOCHI101	0.579	SOURE	0.491	DIXIEBELLE	0.183
GALILEO	0.750	MUGA	0.581	MUGA	0.493	BENGAL	0.225
GITANO	0.750	SESIA	0.600	SANDORA	0.501	L204	0.241
HONDURAS	0.750	VULCANO	0.603	IBO400	0.501	LACASSINE	0.248
LUXOR	0.750	DELFINO	0.616	GITANO	0.507	ARTEMIDE	0.252
MARTE	0.750	IBO38033	0.625	TAICHUNG65	0.520	SUPER	0.286
ONICE	0.750	IAC3252	0.641	M204	0.523	GZ8367	0.292
PANDA	0.750	RONCAROLO	0.645	HAREM	0.524	DELLROSE	0.308
VULCANO	0.750	GIZA177	0.652	OSCARxSUWEON	0.528	UPLA75	0.325
XIANGOU2	0.750	GIADA	0.658	FAMILIA181	0.530	UPLA32	0.351

BENGAL	0.808
BIANCA	0.808
DIXIEBELLE	0.808
FLIPPER	0.808
GRITNA	0.808
JEFFERSON_1	0.808
L204	0.808
ORIONE	0.808
PIEMONTE	0.808
ROMA	0.808
SETANTUNO	0.808
SLAVA	0.808
SR113	0.808
TEXMONT	0.808
VIALE	0.808
VIRGO	0.808
A301	0.860
ARSENAL	0.860
CARNAROLI	0.860
CENTAURO	0.860
DOURADAO	0.860
FAMILIA181	0.860
GANGE	0.860
GIADA	0.860
GIOVANNIMARCHETTI	0.860
IBO38033	0.860
KULON	0.860
LOTO	0.860
LUCERO	0.860
MANTOVA	0.860
MARENY	0.860

M203	0.661
VOLANO	0.661
ARGO	0.684
VIRGO	0.685
MUSA	0.685
SEQUIAL	0.689
SAMBA	0.691
XIANGOU2	0.702
VENERIA	0.707
SILLA	0.708
ROMA	0.714
KRYSTALLINO	0.715
JUBILIENI	0.716
S102	0.719
PELDE	0.720
SIRIO	0.720
PADANO	0.722
CARINA	0.726
UPLA68	0.735
CENTAURO	0.742
ITALMOCHI	0.748
SANTANDREA	0.752
SATURNO	0.753
PLUS	0.754
BRAZOS	0.756
CRIPTO	0.758
SAFARI	0.761
ADELAIDECHIAPPELLI	0.763
TAICHUNG65	0.764
SOURE	0.765
SELN244A	0.767

CT36	0.531
SANTERNO	0.540
ITALMOCHI	0.554
RIZZOTTO511	0.558
BENGAL	0.559
GIANO	0.565
REDI	0.566
ERCOLE	0.569
FIDJI	0.571
TORIO	0.573
CRIPTO	0.578
RUBI	0.581
JACINTO	0.584
GZ8367	0.599
TEJO	0.602
S102	0.605
THAIPERLA	0.606
BALZARETTI	0.606
UPLA64	0.610
CARNISE	0.613
ADELAIDECHIAPPELLI	0.613
PUNTAL	0.616
SR113	0.621
UPLA63	0.624
A301	0.626
ORIONE	0.626
EUROPA	0.628
LUCERO	0.633
GIZA177	0.634
VOLANO	0.643
ARTEMIDE	0.646

LAMONE	0.353
IBO38033	0.364
CARMEN	0.364
MAIORAL	0.375
UPLA64	0.381
L201	0.414
MARENY	0.431
TEXMONT	0.433
COCODRIE	0.435
FIDJI	0.436
NANO	0.448
GREPPI	0.449
L205	0.468
LOMELLINO	0.471
RUBI	0.483
CARIOCA	0.486
SLAVA	0.486
SOURE	0.488
GIOVANNIMARCHETTI	0.490
CALENDAL	0.522
SESIA	0.531
RODEO	0.532
MECO	0.548
IBO400	0.556
RIZZOTTO511	0.558
SANDORA	0.567
ULLAL	0.580
M203	0.589
SETANTUNO	0.590
VOLANO	0.598
BALZARETTI	0.606

MOLO	0.860	GRAAL	0.768	SELN244A	0.661	VIALE	0.608
NILO	0.860	VALTEJO	0.769	SAKHA102	0.664	VALTEJO	0.618
OTA	0.860	PANDA	0.771	CARMEN	0.669	EUROPA	0.621
SCUDO	0.860	BONNI	0.774	SISR215	0.676	GUADIAMAR	0.621
SEQUIAL	0.860	ADAIR	0.774	AIACE	0.676	MUGA	0.625
SESIA	0.860	ALLORIO	0.776	MAIORAL	0.677	CORBETTA	0.632
YRM62	0.860	RIBE	0.778	SALVO	0.677	SAEDINENIE	0.637
ALLORIO	0.907	BAIXET	0.778	ROXANI	0.689	GLORIA	0.646
ANTARES	0.907	L204	0.781	KORAL	0.690	SR113	0.658
ARBORIO	0.907	PREVER	0.781	ALEXANDROS	0.691	FAMILIA181	0.661
BRAZOS	0.907	PIERINAMARCHETTI	0.781	NANO	0.692	GRITNA	0.662
CARMEN	0.907	ANSEATICO	0.786	MARTE	0.693	DELFINO	0.677
CARNISE	0.907	LIDO	0.787	RINGO	0.694	GRAAL	0.679
CRIPTO	0.907	PUNTAL	0.788	SLAVA	0.695	LIDO	0.681
DRAGO	0.907	LOMELLINO	0.790	SCUDO	0.696	SATURNO	0.683
GLORIA	0.907	IBO400	0.797	CENTAURO	0.700	ALPE	0.691
IAC3252	0.907	HAREM	0.797	RPC12	0.701	FAST	0.692
ITALMOCHI	0.907	OPALE	0.797	ERMES	0.709	VIALONENERO	0.695
KARNAK	0.907	BIANCA	0.798	DIXIEBELLE	0.713	ADAIR	0.698
KORAL	0.907	ORIGINARIO	0.799	MECO	0.720	JUBILIENI	0.704
KRYSTALLINO	0.907	UPLA63	0.801	SFERA	0.722	RONCAROLO	0.710
LAGRUE	0.907	RONCOLO	0.811	ALPHA	0.726	UPLA66	0.712
M6	0.907	TORIO	0.813	RODEO	0.727	GALILEO	0.717
NEMBO	0.907	HONDURAS	0.814	OTA	0.729	JEFFERSON_1	0.720
OLCENENGO	0.907	SAEDINENIE	0.820	PLUS	0.731	APOLLO	0.723
ORIGINARIO	0.907	MARENY	0.828	DIMITRA	0.735	BRAZOS	0.733
PEGONIL	0.907	CARMEN	0.829	DRAGO	0.760	ULISSE	0.734
PUNTAL	0.907	SENIA	0.829	OPALE	0.762	MARATELLI	0.739
REDI	0.907	MOLO	0.830	SUPER	0.770	T757	0.739
REXMONT	0.907	SETANTUNO	0.832	SANDOCA	0.783	BERTONE	0.745
RIBE	0.907	GOOLARAH	0.833	ORIGINARIO	0.784	SISR215	0.752
RINGO	0.907	KULON	0.833	RUSSO1	0.786	SCUDO	0.753
RODEO	0.907	CASTELMOCHI	0.835	T757	0.787	ROMA	0.754

SELN244A	0.907	CARIOCA	0.837	ITALPATNAxMILYANG	0.793	UPLA68	0.762
SHSS381	0.907	ROXANI	0.838	PADANO	0.796	LAGRUE	0.762
SILLA	0.907	SALOIO	0.843	COLINA	0.797	PIERINAMARCHETTI	0.768
VOLANO	0.907	RINALDOBERSANI	0.844	KING	0.799	AUGUSTO	0.770
SALOIO	0.936	ERCOLE	0.844	KARNAK	0.801	KARNAK	0.774
ALPE	0.949	BENGAL	0.852	CIGALON	0.802	GANGE	0.777
BOMBON	0.949	NOVARA	0.856	TEXMONT	0.807	KRYSTALLINO	0.778
CAPATAZ	0.949	RIZZOTTO511	0.857	DELLMONT	0.811	ADELAIDECHIAPPELLI	0.782
CARIOCA	0.949	GITANO	0.859	OLCENENGO	0.811	TEJO	0.790
CLOT	0.949	S101	0.859	SAGRES	0.811	PLUS	0.801
DELFINO	0.949	UPLA66	0.863	EUROSIS	0.812	UPLA63	0.802
DELLROSE	0.949	SAKHA103	0.864	XIANGOU2	0.814	PUNTAL	0.803
DUCATO	0.949	MARTE	0.866	HARRA	0.815	A301	0.808
ERMES	0.949	SMERALDO	0.866	M202	0.815	ONICE	0.809
EUROSIS	0.949	CHIPKA	0.866	SAVIO	0.816	SILLA	0.811
GIGANTEVERCELLI	0.949	SCUDO	0.870	BIANCA	0.817	M6	0.811
GRAAL	0.949	ULLAL	0.871	SETANTUNO	0.821	ALAN	0.818
GRALDO	0.949	DELLMONT	0.879	UPLA32	0.821	ARBORIO	0.818
HANDAO_11	0.949	ONICE	0.879	LUXOR	0.825	MUSA	0.820
M202	0.949	RUBINO	0.882	GLORIA	0.826	IAC3252	0.826
MAYBELLE	0.949	REDI	0.883	ULLAL	0.836	XIANGOU2	0.826
OSCARxSUWEON	0.949	KING	0.888	GIOVANNIMARCHETTI	0.840	ANTARES	0.829
PADANO	0.949	GLADIO	0.890	MOLO	0.845	SHSS381	0.832
PIERINAMARCHETTI	0.949	NILO	0.896	GARDESADRI	0.848	KING	0.833
PLOVDIV24	0.949	COLINA	0.896	BEIRAO	0.855	CRIPTO	0.840
PREVER	0.949	RINGO	0.906	KRYSTALLINO	0.856	ESTRELA	0.841
RIZZOTTO511	0.949	CLOT	0.907	FAST	0.857	GIGANTEVERCELLI	0.853
RONCAROLO	0.949	JACINTO	0.908	CALENDAL	0.859	NILO	0.876
ROXANI	0.949	SHSS381	0.918	BOMBILLA	0.868	BOMBILLA	0.876
RUBINO	0.949	GIGANTEVERCELLI	0.919	SPRINT	0.869	DREW	0.886
SIRIO	0.949	GRALDO	0.921	L204	0.874	SELN244A	0.887
SISR215	0.949	TEJO	0.921	CINIA40	0.874	ITALPATNA48	0.889
SMERALDO	0.949	GIOVANNIMARCHETTI	0.929	VALTEJO	0.883	M202	0.892

TAICHUNG65	0.949	SANDORA	0.929	ULISSE	0.889	LUXOR	0.899
TITANIO	0.949	HARRA	0.931	TITANIO	0.892	DRAGO	0.907
TORIO	0.949	FLIPPER	0.934	BOMBON	0.892	MILEV21	0.919
UPLA63	0.949	BALDO	0.934	DUCATO	0.894	MARTE	0.923
UPLA75	0.949	DIXIEBELLE	0.936	UPLA66	0.897	CAPATAZ	0.930
A201	0.987	OTA	0.940	GOOLARAH	0.897	CARNAROLI	0.936
AIACE	0.987	LUNA	0.948	ROMA	0.898	SAFARI	0.937
AUGUSTO	0.987	COCODRIE	0.948	RANGHINO	0.903	SALOIO	0.940
BARAGGIA	0.987	THAIBONNET	0.948	ANTONI	0.904	CLOT	0.943
BELLEPATNA	0.987	ESCARLATE	0.950	ALPE	0.906	ORIGINARIO	0.943
BONNI	0.987	ARSENAL	0.951	PEGONIL	0.907	LENCINO	0.944
CALENDAL	0.987	SISR215	0.954	RIBE	0.910	GIZA177	0.946
CHIPKA	0.987	MONTICELLI	0.954	BERTONE	0.914	GRALDO	0.951
COCODRIE	0.987	FAMILIA181	0.956	S1022	0.914	GARDESADRI	0.960
CORBETTA	0.987	MANTOVA	0.956	CORBETTA	0.919	CRESO	0.961
CT36	0.987	RAZZA77	0.957	MUSA	0.920	ROTUNDUS	0.961
DELLMONT	0.987	SALVO	0.964	VIALONENERO	0.929	LUSITOIRRADIADO	0.963
DIMITRA	0.987	SAGRES	0.964	HANDAO_11	0.930	BELLEPATNA	0.963
ERCOLE	0.987	ARBORIO	0.966	SMERALDO	0.939	RINALDOBERSANI	0.970
ESTRELA	0.987	CRESO	0.966	GANGE	0.943	BALDO	0.972
FIDJI	0.987	GLORIA	0.969	VICTORIA	0.946	FLIPPER	0.973
GIZA177	0.987	AUGUSTO	0.972	THAIBONNET	0.948	P6	0.984
KING	0.987	OSCARxSUWEON	0.973	LUNA	0.948	VULCANO	0.985
M203	0.987	CARNAROLI	0.977	VIALONENANO	0.949	SIRIO	0.992
MONTICELLI	0.987	ROTUNDUS	0.978	MIARA	0.950	OPALE	1.005
PELDE	0.987	VIALONENERO	0.981	SHSS53	0.952	ROXANI	1.008
PLUS	0.987	BARAGGIA	0.983	CARNAROLI	0.960	BAIXET	1.018
RONCOLO	0.987	GARDESADRI	0.985	PANDA	0.966	GIANO	1.036
SATURNO	0.987	DRAGO	0.986	GUADIAMAR	0.966	SFERA	1.037
SENATORENOVELLI	0.987	SFERA	0.990	M6	0.973	HANDAO_11	1.040
SENIA	0.987	LOTO	0.994	SHSS381	0.973	DOURADAO	1.042
SPRINT	0.987	LAMONE	0.997	ALLORIO	0.979	BAHIA	1.048
UPLA91	0.987	BELLEPATNA	1.000	PREVER	0.980	SAKHA102	1.050

GARDESADRI	0.998	ALAN	1.004	GRALDO	0.983	TAICHUNG65	1.051
SANDORA	1.002	PEGONIL	1.007	FRANCES	0.986	TORIO	1.051
ADAIR	1.006	EUROPA	1.009	ANTARES	0.987	SESIAMOCHI	1.063
ALEXANDROS	1.021	MELAS	1.010	MILEV21	0.988	MEJANES2	1.071
ALPHA	1.021	M202	1.017	UPLA91	0.996	CT58	1.074
APOLLO	1.021	ESTRELA	1.018	ARSENAL	1.001	HANDAO297	1.075
BAHIA	1.021	GRITNA	1.020	RAZZA77	1.003	HARRA	1.079
BEIRAO	1.021	RPC12	1.020	LOMELLINO	1.003	ARSENAL	1.080
BERTONE	1.021	CORBETTA	1.022	GIGANTEVERCELLI	1.004	CT36	1.088
BOMBILLA	1.021	VICTORIA	1.023	APOLLO	1.006	VIALONENANO	1.090
GREGGIO	1.021	TEXMONT	1.036	AMERICANO	1.017	MOLO	1.098
GZ8367	1.021	CAPATAZ	1.041	PLOVDIV24	1.018	ITALMOCHI	1.103
JACINTO	1.021	ANTARES	1.042	GREGGIO	1.025	ANTONI	1.114
LUNA	1.021	RUSSO1	1.046	PIERINAMARCHETTI	1.025	ERMES	1.115
LUSITOIRRADIADO	1.021	NEMBO	1.047	MELAS	1.026	SHSS53	1.125
MECO	1.021	LUCERO	1.048	RONCOLO	1.032	PIEMONTE	1.127
PERLA	1.021	ALPE	1.050	RUBINO	1.033	VIRGO	1.128
ROBBIOSEL1	1.021	DUCATO	1.052	PELDE	1.036	ERCOLE	1.129
S101	1.021	MAYBELLE	1.053	NILO	1.037	TITANIO	1.129
SFERA	1.021	AIACE	1.054	LIDO	1.038	CAMPINO	1.131
SUPER	1.021	VIALE	1.055	RONCAROLO	1.040	RIBE	1.135
THAIPERLA	1.021	PIEMONTE	1.055	PROMETEO	1.041	SENATORENOVELLI	1.137
ULLAL	1.021	ROBBIOSEL1	1.060	BAHIA	1.042	GITANO	1.138
VALTEJO	1.021	RODEO	1.062	UPLA77	1.045	RINGO	1.140
VENERIA	1.021	A201	1.063	SESIAMOCHI	1.045	RUBINO	1.143
SAEDINENIE	1.041	SLAVA	1.066	LACASSINE	1.062	GLADIO	1.144
ARGO	1.053	BURMA	1.067	BALILLA	1.065	LOTO	1.146
BALZARETTI	1.053	ALEXANDROS	1.067	ANSEATICO	1.068	OSCARxSUWEON	1.146
BURMA	1.053	DOURADAO	1.069	LOTO	1.072	PELDE	1.149
CAMPINO	1.053	UPLA32	1.070	REXMONT	1.074	VIALONE190	1.152
CASTELMOCHI	1.053	M6	1.072	ARBORIO	1.075	SAMBA	1.153
COLINA	1.053	UPLA77	1.074	ALAN	1.078	ORIONE	1.157
CRESO	1.053	ARTEMIDE	1.076	VIRGO	1.080	UPLA77	1.172

GIANO	1.053	STRELLA	1.080	BALDO	1.089	ESCARLATE	1.175
IBO400	1.053	LACASSINE	1.083	BAIXET	1.091	VENERIA	1.175
LAMONE	1.053	APOLLO	1.085	CARINA	1.095	PROMETEO	1.181
M204	1.053	GREGGIO	1.085	BURMA	1.103	CARINA	1.184
MEJANES2	1.053	SENATORENOVELLI	1.092	GRAAL	1.112	SENIA	1.185
P6	1.053	OLCENENGO	1.092	MONTICELLI	1.119	PLOVDIV22	1.188
PECOS	1.053	SANDOCA	1.100	SAKHA103	1.122	RAZZA77	1.194
RUBI	1.053	BERTONE	1.101	S101	1.123	M204	1.195
SAVIO	1.053	FIDJI	1.101	KULON	1.132	DIMITRA	1.199
SHSS53	1.053	SR113	1.106	MANTOVA	1.139	ALPHA	1.205
SOURE	1.053	KARNAK	1.107	SANTANDREA	1.143	RONCOLO	1.221
TEJO	1.053	LORD	1.125	SATURNO	1.147	BARAGGIA	1.228
THAIBONNET	1.053	BALZARETTI	1.125	LAMONE	1.156	GIADA	1.230
UPLA64	1.053	BAHIA	1.129	GIADA	1.160	ARGO	1.237
UPLA68	1.053	LUXOR	1.130	PIEMONTE	1.165	SMERALDO	1.240
UPLA77	1.053	BOMBON	1.134	SESIA	1.166	FRANCES	1.242
SANDOCA	1.068	SHSS53	1.135	MEJANES2	1.169	MONTICELLI	1.248
ALICE	1.081	SESIAMOCHI	1.136	ROBBIOSEL1	1.179	ALLORIO	1.249
AMERICANO	1.081	RANGHINO	1.139	HONDURAS	1.194	GOOLARAH	1.260
BALILLA	1.081	FAST	1.141	MARENY	1.202	NEMBO	1.262
CALMOCHI101	1.081	KORAL	1.143	IAC3252	1.206	SEQUIAL	1.263
EUROPA	1.081	RODINA	1.144	GLADIO	1.207	CARNISE	1.263
GREPPI	1.081	CAMPINO	1.152	SELENIO	1.212	SAGRES	1.269
HARRA	1.081	CIGALON	1.155	SEQUIAL	1.213	LUNA	1.274
L201	1.081	EUROSIS	1.158	MAYBELLE	1.220	BIANCA	1.285
L202	1.081	L202	1.161	ESTRELA	1.226	SANDOCA	1.294
LACASSINE	1.081	DELLROSE	1.171	L202	1.229	CASTELMOCHI	1.299
LIDO	1.081	S1022	1.172	ALICE	1.231	PADANO	1.304
MAIORAL	1.081	T757	1.173	ITALPATNA48	1.243	RUSSO1	1.314
MELAS	1.081	EUROSE	1.176	JEFFERSON_1	1.244	GREGGIO	1.318
MUSA	1.081	TITANIO	1.178	CAPATAZ	1.258	DUCATO	1.334
NOVARA	1.081	CT36	1.179	DELFINO	1.266	THAIPERLA	1.353

PROMETEO	1.081	SAVIO	1.180	LENCINO	1.270	CINIA40	1.356
RAZZA77	1.081	M204	1.193	CLOT	1.271	SAVIO	1.358
RODINA	1.081	DREW	1.196	PERLA	1.273	YRM62	1.360
T757	1.081	LUSITOIRRADIADO	1.198	SIRIO	1.273	VENERE	1.367
ULISSE	1.081	GANGE	1.203	BONNI	1.274	VELA	1.373
VELA	1.081	SELENIO	1.204	GREPPI	1.276	PREVER	1.379
VICTORIA	1.081	MILEV21	1.204	AGATA	1.276	NOVARA	1.381
AGOSTANO	1.108	ULISSE	1.204	VENERIA	1.310	S1022	1.394
ANSEATICO	1.108	VELA	1.205	A201	1.327	OLCENENGO	1.415
CIGALON	1.108	MEJANES2	1.210	VIALONE190	1.340	BURMA	1.435
EUROSE	1.108	PLOVDIV24	1.212	BRAZOS	1.345	RPC12	1.439
FAST	1.108	GIANO	1.217	ONICE	1.351	SAKHA103	1.450
GLADIO	1.108	AGATA	1.222	DELLROSE	1.352	EUROSIS	1.459
HANDAO297	1.108	PROMETEO	1.224	CRESO	1.352	EUROSE	1.459
LENCINO	1.108	GUADIAMAR	1.233	RODINA	1.356	SPRINT	1.469
SAGRES	1.108	BOMBILLA	1.233	MARATELLI	1.363	AIACE	1.473
AKITAKOMACHI	1.132	ITALPATNA48	1.234	SILLA	1.377	AKITAKOMACHI	1.485
ANTONI	1.132	AMERICANO	1.244	VENERE	1.386	CENTAURO	1.491
ARTEMIDE	1.132	REXMONT	1.262	AKITAKOMACHI	1.413	BALILLA	1.496
CARRICO	1.132	NANO	1.268	CALMOCHI101	1.423	CALMOCHI101	1.499
FRANCES	1.132	VIALONE190	1.270	FLIPPER	1.441	RANGHINO	1.500
GOOLARAH	1.132	CINIA40	1.277	ROTUNDUS	1.444	MELAS	1.500
GUADIAMAR	1.132	HANDAO_11	1.285	SALOIO	1.444	VICTORIA	1.520
HAREM	1.132	LAGRUE	1.286	NOVARA	1.447	PEGONIL	1.521
LORD	1.132	LENCINO	1.292	ARGO	1.466	KORAL	1.521
PLOVDIV22	1.132	YRM62	1.298	CASTELMOCHI	1.477	SANTANDREA	1.528
RUSSO1	1.132	THAIPERLA	1.299	LUSITOIRRADIADO	1.478	SANTERNO	1.530
ZENA	1.132	SPRINT	1.301	CARIOCA	1.481	STRELLA	1.545
S102	1.137	HANDAO297	1.301	STRELLA	1.499	COLINA	1.559
AGATA	1.155	MARATELLI	1.305	GRITNA	1.501	SALVO	1.562
JUBILIENI	1.155	UPLA75	1.309	BARAGGIA	1.505	TOPAZIO	1.567
MILEV21	1.155	VIALONENANO	1.334	ESCARLATE	1.509	OTA	1.590

OSTIGLIA	1.155
RANGHINO	1.155
ROTUNDUS	1.155
RPC12	1.155
SELENIO	1.155
STRELLA	1.155
TOPAZIO	1.155
CARINA	1.176
CINIA40	1.176
MIARA	1.176
SESIAMOCHI	1.176
UPLA32	1.176
UPLA66	1.176
ADELAIDECHIAPPELLI	1.188
ALAN	1.196
CT58	1.196
SANTERNO	1.196
VENERE	1.196
MARATELLI	1.214
VIALONE190	1.230
ESCARLATE	1.247
L205	1.290
SAKHA103	1.294
SANTANDREA	1.309
SAKHA102	1.578
VIALONENANO	1.594
SALVO	1.613
ITALPATNA48	1.713

CALENDAL	1.339
CT58	1.345
FRANCES	1.370
MIARA	1.380
ANTONI	1.393
P6	1.420
ERMES	1.431
L201	1.434
BALILLA	1.459
GREPPI	1.460
ITALPATNAxMILYANG	1.476
JEFFERSON_1	1.482
BEIRAO	1.488
AKITAKOMACHI	1.502
TOPAZIO	1.526
MAIORAL	1.539
A301	1.551
AGOSTANO	1.568
ALICE	1.572
PLOVDIV22	1.600
ALPHA	1.646
VENERE	1.676
CARRICO	1.681
OSTIGLIA	1.787
PECOS	1.810
L205	1.901
SANTERNO	2.124
ZENA	2.249

CT58	1.555
CHIPKA	1.592
TOPAZIO	1.595
OSTIGLIA	1.620
DREW	1.650
GALILEO	1.668
ADAIR	1.675
COCODRIE	1.701
SENIA	1.716
LORD	1.719
PECOS	1.726
EUROSE	1.808
UPLA75	1.814
VELA	1.815
SAEDINENIE	1.831
SAMBA	1.844
NEMBO	1.906
VIALE	1.919
AGOSTANO	1.948
BELLEPATNA	2.001
CARRICO	2.009
PLOVDIV22	2.106
L205	2.174
DOURADAO	2.212
LAGRUE	2.336
ZENA	2.463
CAMPINO	2.469
L201	2.693

BOMBON	1.617
SELENIO	1.628
S102	1.631
S101	1.632
ZENA	1.637
OSTIGLIA	1.641
UPLA91	1.664
AGATA	1.684
MANTOVA	1.694
ANSEATICO	1.711
BEIRAO	1.713
AMERICANO	1.756
CIGALON	1.766
HAREM	1.775
CARRICO	1.858
PLOVDIV24	1.868
RODINA	1.887
HONDURAS	1.912
BONNI	1.937
PERLA	1.938
ALICE	2.092
MIARA	2.256
KULON	2.352
CHIPKA	2.424
LORD	2.580
AGOSTANO	2.912
PECOS	2.968
LUCERO	3.110

Supplemental Table S4. Relevant genes and putative functions associated to MTAs identified by GWAS for different phenotypic parameters.

Phenotypic parameter	MTA	Chromosome	Gene	Putative function	Reference
SES	51	1	*Os01g0337500* LOC_Os01g23580	Peptide of the vacuolar H^+-PPase (OsOVP6)	Plett et al., 2010
	51	1	*Os01g0338100* LOC_Os01g23630	*OsTFIID*, TFs within the QTL '*Saltol*'	Nutan et al., 2017
Height	933	8	*Os08g0357300* LOC_Os08g26880	*bZIP* TF domain-containing protein	Hirano et al., 2013; Mansuri et al., 2019; Patishtah et al., 2018
Flowering time	1123	10	*Os10g0436900* LOC_Os10g30070	Na^+/Ca^{2+} exchanger membrane region domain-containing protein; OsCCX3 cation/Ca^{2+} exchanger 3	Singh et al., 2015; Yadav et al., 2015; Yu et al., 2017
	1123	10	*Os10g0438000* LOC_Os10g30190	K^+ channel tetramerisation domain-containing protein 9	Yu et al., 2017
	1123	10	*Os10g0442600* LOC_Os10g30580	Cell Division Cycle control protein 48 (CDC48)-like protein (homologue)	Shi et al., 2019; Yu et al., 2017
CHL	46	1	*Os01g0705700* LOC_Os01g50940	Protein similar to ICE1, basic HLH DNA-binding protein involved in cold acclimation	Man et al., 2017; Zhao et al., 2017

Possible involvement of *OsTPP* genes in trehalose metabolism and starch mobilization during rice germination and seedling emergence under salt condition

Michele Pesenti, Gabriele Orasen‡, Noemi Negrini, Silvia Morgutti, Patrizia De Nisi, Fabio Francesco Nocito, Federico Colombo and Gian Attilio Sacchi

DiSAA – Dipartimento di Scienze Agrarie e Ambientali, Università degli Studi di Milano, via Celoria 2, I-20133 Milano, Italy. ‡Bertone Sementi. Strada Cacciolo 35, Terruggia Monferrato I-15030, Italy (current adress).

Abstract - Soil salinity represents an increasing problem for agriculture exacerbated by the ongoing climate changes that limit the supply of good quality water. Rice (*Oryza sativa* L.), and particularly the ssp. *japonica*, is highly sensitive to saline conditions that affect the seed germination and seedling emergence phases. In cereal grains, at these developmental stages, signaling-based source-to-sink communication has a major role in the mobilization of nutrients from the endosperm to the elongating embryonic axis. Plant salt tolerance requires reprogramming of sugar allocation and energy metabolism also involving changes in source-sink relationships. The ratio trehalose-6-P (T6P)/Trehalose (Tre) modulates the activity of Snf1-Related protein Kinase-1 (SnRK1), the principal metabolic sugar sensor for maintenance of C homeostasis under stress. Aim of the work was to clarify the possible role of the Suc/T6P/SnRK1 system in the response to salt stress during seed germination and early seedling development of two *japonica* rice accessions with opposite behavior in salt stress (Olcenengo, tolerant, and SR113, sensitive), with particular focus to the role of two genes, *OsTPP7* and *OsTPP10*, encoding T6P phosphatase (TPP), that plays a key role in the regulation of the T6P/Tre ratio. In rice seeds grown in control (water) or salt (150 mM NaCl) conditions, biochemical and molecular analyses assessed: *i*) in embryos, the levels of T6P, Tre, Suc, *OsTPP7* and *OsTPP10* expression; *ii*) in endosperms, the α-amylase activity. The results highlighted differential salt responses in the two accessions, that included lower concentrations of T6P and Suc and lower T6P/Suc ratios, while maintaining higher α-amylase activity, in the tolerant accession in comparison to the susceptible one. An early higher expression of *OsTPP10* in the tolerant genotype under salt condition allowed to suggest, in the two genotypes, a different temporal cascade of events between the early changes in the levels of *OsTPP10* transcripts and the later changes in the levels of substrate (T6P) and product (Tre) of the reaction catalyzed by the encoded enzyme. The observed higher vigor (coleoptile elongation rate, α-amylase timing of appearance and specific activity) of Olcenengo compared to SR113 under salt is suggested to involve *OsTPP10* and the regulation of its expression.

Keywords: Rice, salinity, trehalose metabolism, OsTPP, sugar signalling, seed germination, seedling emergence

1. Introduction

Soil salinity represents the most severe and yield-limiting abiotic stress on a worldwide basis. The widespread diffusion of the salinity problem, together with salt sensitivity of crop species, that mostly belong to the glycophyte group, appears counterproductive for the important objectives of both enhancing food supply to the increasing world population and containing the progressive abandonment of land (Ghosh and Gantait, 2016; Hoang et al., 2016; Horie et al., 2012). Among cereals, barley shows maximum tolerance to salinity, which decreases in wheat and even more so in rice (*Oryza sativa* L.; Munns and Tester, 2008), that is reported to have a threshold (i.e., the highest permissible salt level without reduction in yield) of 3.0 dS m^{-1} (Reddy et al., 2014).

Soil salinity interferes heavily on plant physiology up to the definition of morpho-physiological and phenological traits that ultimately affect crop yield and production. In rice, salinity affects pollen viability, fertility, heading time, seed germination, seedling growth, leaf size, shoot and root length, shoot dry and fresh weight, number of tillers per plant, spikelet number, percent of sterile florets and productivity (Hoang et al., 2016).

In all plants, the mechanisms involved in salt tolerance strategies (mainly osmotic adjustment, ion flux regulation, and Na^+ and Cl^- exclusion/compartmentalization) have a high-energy cost that competes with the energy requirements of the plant biochemical and physiological processes all over the whole life span, from germination to plant vegetative and reproductive growth (Zhang et al., 2009; Munns and Gilliham, 2015).

Between the two main subspecies of rice, *japonica* genotypes are reported to be less tolerant than the *indica* ones (Lee et al., 2003); in particular, tolerant *indica* varieties are capable to maintain low Na^+/K^+ ratios in the shoot, being Na^+ excluders and capable to absorb high amounts of K^+. Unfortunately, most salt-tolerant rice landraces and cultivars show tall plant stature, poor grain quality, low yield, altogether determining poor agronomic characteristics (Reddy et al., 2014). The ability to respond to salt conditions may change during the life cycle of the plant; for rice, a specific line may be tolerant in one stage and sensitive in another (Hoang et al., 2016 and references therein). The different responses are also genotype-related: different genotypes can be more tolerant to salinity stress at reproductive and grain filling stages than at the germination and vegetative ones, or relatively tolerant during germination, active tillering, and towards maturity, but sensitive during early seedling and reproductive stages (Flowers and Yeo, 1981; Heenan et al., 1988). Concerning in particular the early stages of seedling establishment, the complex developmental/physiological processes involved are crucial also in determining the success of the

subsequent phases of plant growth. In agriculture, a prerequisite for obtainment of satisfactorily productive crops is a rapid and uniform seed germination.

High soil salinity affects the germination process by diminishing the external water osmotic potential, in turn decreasing the seed capability to absorb water, and consequently affecting the metabolic reactivation that accompanies the early phases of germination (Luan et al., 2014; Hannachi and van Labeke, 2018). In addition to the osmotic effect, in glycophytes the accumulation of ions (with particular regard to Na^+) negatively affects cell functionality also through specific toxic effects (Daszkowska-Golec, 2011). Overall, plant salt tolerance requires the activation of the most cost-efficient strategies, in any case based upon the use of C reserves and energy (Munn and Gilliham, 2015), that include the perception of unbalanced C metabolism followed by the onset of metabolic changes aimed at restoring an adequate energy level even at the cost of a growth slowdown. In this context, development and growth are supported by time- and organ-specific metabolic changes that reprogram the source-sink relationships. During cereal germination and seedling establishment, signaling-based source-to-sink communication has a major role in the mobilization of nutrients from the endosperm (source) to the elongating embryonic axis (sink; Yu et al., 2015), and sensing of adequate availability of C sources is necessary for sustaining a balanced development in either optimal or stressful conditions (Wingler, 2018).

In plants, two regulatory networks related to the sugar signaling system are involved in the response to changes in nutrient and energy status (Wingler, 2018): the high-C and the low-C availability signaling pathways. An important component of the latter one is the sucrose (Suc)/trehalose-6-P (T6P)/Snf1-Related protein Kinase-1 (SnRK1) system. Trehalose biosynthesis is a two-step process that occurs in the cytosol and involves the enzymes T6P synthase (TPS) and T6P phosphatase (TPP) that catalyze the condensation reaction of uridine diphosphate glucose and Glu6P to T6P and the subsequent dephosphorylation of T6P to Tre, respectively. Tre is eventually hydrolyzed by trehalase into two glucose molecules. The intermediate T6P plays important functional roles, including the regulation of plant development and growth, and of the plant responses to several stresses (Fernandez et al., 2010). The presence of active TPSs and TPPs is widespread among all the major plant taxa including monocots (Martínez-Barajas et al., 2011). In rice, 13 putative *OsTPP* genes (Ge et al., 2008; Dong et al., 2019) have been identified. Different abiotic stresses transiently induce expression of *OsTPP1* and *OsTPP2* (Shima et al., 2007). More recently, Kretzschmar and coworkers reported increased expression of an *OsTPP7* gene and activity of the recombinant encoded protein in rice seedlings under anaerobiosis (Kretzschmar et al., 2015).

In any case, the presence of multiple *TPP* genes strongly suggests the need of a fine regulation, at different histological and/or cellular levels, of the levels of the substrate (T6P) and/or the product (Tre) of the encoded activities. Trehalose-6-P is a regulator of the activity of SnRK1. This Ser/Thr kinase regulates the cell energy homeostasis activating catabolic energy-producing pathways and inhibiting the anabolic energy-consuming ones when intrinsic or environmental factors impact with the overall cell energy availability (Polge and Thomas, 2007; Wurzinger et al., 2018). Under low-energy conditions, SnRK1 triggers a cascade of events that repress the anabolic pathways limiting developmental and growth processes. The activity of SnRK1 is downregulated when T6P is high ("feast metabolism"), and upregulated when T6P is low and a starvation response ("famine metabolism", leading to an energy saving program) is triggered (Wurzinger et al., 2018; Morgutti et al., 2019 and references therein). SnRK1 plays a key role in the regulation of starch metabolism. In cereal grains, starch is the major reserve providing a C source to generate energy and metabolites for embryo growth until the photoautotrophic stage is achieved. Therefore, the regulation of expression/activity of *α-amylase* genes and corresponding enzymes in the endosperm is of primary importance. Active SnRK1 regulates the Myeloblastosis Sugar Response Complex 1 (MYBS1) transcription factor that in the nucleus binds to sugar-responsive elements on the promoters of *α-amylase* (*RAmy3D*) genes (Lu et al., 2002, 2007). In rice, enhanced starch mobilization for increased expression of *OsTPP7* and activity of OsTPP7 with possible activation of SnRK1 would support early seedling growth in anaerobic conditions, enhancing tolerance to such stress (Kretzschmar et al., 2015). Rice varieties that do harbor the *OsTPP7* gene appear more effective in supporting coleoptile elongation under O_2 shortage through the activation of starch hydrolysis, even if the possible involvement of other genes in coleoptile elongation under anaerobiosis is suggested (Nghi et al., 2019). Trehalose and T6P metabolism and SnRK1 are therefore components of a very complex, multifactorial, integrated regulatory system that gives the cell the ability to adequate its metabolism to the needs imposed by internal (developmental) processes and/or external (environmental) conditions (Yu et al., 2015).

In this context, main objective of the present study was the biochemical and molecular characterization of two rice (ssp. *japonica*) accessions showing different behavior under salt stress (Olcenengo, tolerant and SR113, sensitive), with the aim of investigating the possible role of the Suc/T6P/SnRK1 system and its involvement in starch mobilization in the salt response during germination and early seedling emergence. The final goal was to gain advancement in the

knowledge of the biochemical-physiological mechanisms involved in the control of rice salt tolerance potentially useful for rice breeding programs.

2. Materials and Methods

2.1. Coleoptile elongation and plant material collection

Coleoptile growth and elongation rate under saline conditions were assessed in two genotypes, Olcenengo and SR113, with very different response of tolerance or sensitiveness, respectively, to salt stress at germination and emergence stages (Pesenti et al. 2020a,b). Twenty seeds per each genotype were germinated in square Petri dishes (Pesenti et al., 2020a), in the absence (control) or in the presence of salt. Briefly, surface-sterilized seeds were sown on two layers of filter paper wetted with 40 mL of ddH_2O or 150 mM NaCl and placed at 26 °C in the dark at 95% relative humidity. Growth of individual seedlings was monitored by measuring the coleoptile length with an electron digital calliper gauge (Blinky 5850810 Calibri Stainless Vernier Calliper Gauge) at fixed times, from the 24th to the 96th h after sowing. Trials were conducted in triplicate per each condition. At different times (16, 24, 30, 48, 72, and 96 h) of incubation, embryos were excised from all (germinated and not germinated) 20 seeds of Olcenengo and SR113 grown in either condition. Embryos at 0 h were obtained from seeds soaked in ddH_2O at 4 °C for 12 h. Embryos and the starchy endosperm were collected, immediately frozen in liquid N_2 and stored at -80 °C until use for the biochemical and molecular determinations.

2.2. Biochemical analyses

2.2.1. Analysis of sugars

Profiling of disaccharides (Suc and Tre) in Olcenengo and SR113 embryos grown in the different conditions was conducted by gas chromatography-mass spectrometry (GC-MS), according to the literature (Roessner-Tunali et al., 2003; Lisec et al., 2006; Xia et al., 2018) with slight modifications. Frozen material (50-100 mg fresh weight) was powdered with liquid N_2 in a pre-cooled mortar with pestle. The powder was suspended in 1.4 mL of 100% (v:v) methanol (MeOH) with the addition, as an internal quantitative standard, of 60 µL of 0.02% (v:v) Ribitol aqueous solution, extracted for 10 min at 70 °C in a thermomixer (ThermoCell Mixing Block MB-102, Bioer, Hanzhou, P.R. China) at 900 rpm and centrifuged for 10 min at 11,000 *g* (Centrifuge Z 300 K, Hermle LaborTecnik GmbH, Wehingen, Germany). The supernatant was mixed with 0.75 mL of chloroform and 1.5 mL of ddH_2O,

vigorously shaken and centrifuged for 15 min at 2,200 *g*. The MeOH:water upper phase, containing the polar metabolites, was recovered and portioned in aliquots (150 µL each) that were vacuum-dried and stored at -80 °C. For derivatization, the dry residues were dissolved with 40 µL of freshly prepared methoxyamination reagent (20 mg mL^{-1} methoxyamine-HCl in pure pyridine), shaken for 2 h at 37 °C, and subsequently treated with 70 mL of N-methyl-N-(trimethylsilyl) trifluoroacetamide for 30 min at 37 °C. Eight microliters of a retention time standard mixture (Alcane Standard Mixture, Supelco, Merck, Darmstadt, Germany) were added before trimethylsilylation. Sample volumes of 1 µL were then injected onto the GC column using a hot needle technique. The GC-MS system used comprised a CTC-PAL autosampler (Agilent Technologies, Cernusco s/N, Italy), a GC-MS Agilent Technologies Series 5975C gas chromatograph, and a quadrupole mass spectrometer (Agilent). The chromatographic separation was conducted on a DB-35 silica capillary column (30 m × 0.25 mm × 0.25 µm; Agilent). The temperature was set at 230 °C for injection and at 250 °C for the interface, the ion source temperature was adjusted to 200 °C. Helium was used as the carrier gas at a flow rate of 1 mL min^{-1}. The analysis was performed using the following temperature profile: 5 min of isothermal heating at 80 °C, followed by a 5 °C min^{-1} oven temperature ramp to 320 °C, and a final 5-min heating at 330 °C. The system was equilibrated for 1 min at 80 °C before injection of the next sample. Mass spectra were recorded at 2 scans s^{-1} with a mass-to-charge ratio of 50 to 600 scanning range. The absolute concentrations of disaccharides were determined by comparison with calibration standard curve response ratios of various concentrations of standard solutions, including the internal standard ribitol, that were derivatized concomitantly to tissue samples.

Determination of T6P in embryos was conducted by liquid chromatography–mass spectrometry (LC-MS), according to the literature (Delatte et al., 2009; Toraño et al., 2012). The frozen material (50-100 mg fresh weight) was ground in liquid N_2; the powder was dispersed and protein precipitated with 500 µL of chloroform:acetonitrile (3:7, v:v) by shaking the mixture at −10 °C for 2 h. Phosphorylated sugars were extracted twice from the organic phase with 400 µL of ddH_2O at 4 °C under vigorous shaking for 5 min, followed by centrifugation at 13,000 *g* for 4 min. The aqueous supernatants containing acetonitrile were pooled and evaporated to dryness with a centrifugal vacuum dryer at room temperature. The dried extracts were reconstituted in 200 µL of water and subsequently cleaned up by solid phase extraction using Oasis MAX cartridges (Waters S.p.A., Sesto S.G., Italy). The cartridges were preconditioned with MeOH and water and, after sample loading, washed with 1 mL of water followed by 1 mL of MeOH. The phospho-disaccharides were desorbed with 1 mL of freshly prepared 2% (v:v) formic acid in MeOH and the eluate was

injected directly into the LC system or, alternatively, evaporated to dryness and reconstituted in 200 µL of water:MeOH:acetonitrile 8:7:85 (v:v:v) before injection. Separations were performed on an Acquity ultra-performance liquid-LC BEH amide column (3.0 × 100 mm, packed with 3.5 µm particles of Ethylene Bridged Hybrid; Waters, Milford, MA, USA) maintained at 25 °C during separation. A 5-µL injection volume was used for both standards and plant extracts. Hydrophilic Interaction Liquid Chromatography (HILIC) analyses were carried out with a high-performance 1260 Infinity LC system (Agilent Technologies) consisting of a standard auto-sampler, a thermostated column compartment, a variable-wavelength detector and a quaternary pump operated at a flow rate of 400 µL min^{-1}. The system was controlled by the Agilent Technologies Chemstation software. The optimum gradient used water:acetonitrile with 0.2% (v:v) trimethylamine as eluent. The optimized gradient conditions were as follows: 3% water for 1 min, 3% to 14% water in 2 min, 14% to 17% water in 12 min, 17% to 40% water in 1 min, 40% water for 9 min, and 40% to 3% water in 3 min. Detection was performed with an Agilent 6130 Series Quadrupole LC-MS System equipped with an ElectroSpray Ionization (ESI) source and liquid chromatography sprayer and operated in the negative-ion mode. The MS settings were optimized for T6P signal-to-noise ratio. The capillary voltage for the HILIC-MS system was + 5.0 kV, the nebulizer pressure 1.7 bar, the drying gas flow 9.0 L min^{-1}, the drying temperature 350 °C, and the single ion monitoring (SIM) scan mode was set at mass value m/z=421. For the LC-HILIC-MS system the capillary voltage was 3.5 kV, the nebulizer pressure 4.8 bar, the drying gas flow 11.0 L min^{-1}, and the drying temperature 350 °C. Compounds were detected as negative ions ($[M–H]^-$) at mass value m/z=421 for T6P. The T6P standard solution was prepared in water; a calibration T6P solution was freshly prepared daily by dissolving the standard in water:MeOH:acetonitrile 8:7:85 (v:v:v). The calibration curve was then constructed using linear regression on five points (2.5-100 nM T6P).

2.2.2. α-amylase assay

The activity of α-amylase (E.C. 3.2.1.1.) was assessed in the starchy endosperms of both non-germinated and germinated seeds. The crude extracts were prepared according to the literature (Guglielminetti et al., 1995) with slight modifications. Each sample, consisting of endosperms (approx. 1 g fresh weight) from 20 seeds, was ground to a fine powder (mortar and pestle) with liquid N_2 and homogenized with four volumes of 100 mM Hepes [4-(2-hydroxyethyl)piperazine-1-ethanesulfonic acid]-KOH buffer, pH 7.5, containing 1 mM EDTA (ethylenediaminetetraacetic acid), 1 mM $MgCl_2$, 5 mM DTT (1,4-dithiothreitol) and 5 mM $Na_2S_2O_5$. The homogenate was centrifuged

at 13,000 *g* for 30 min at 4 °C (Centrifuge Sorvall RC-5B, Rotor Sorvall SM-24; Fisher Scientific, Rodano, Italy) and the resulting supernatant was heated at 70 °C for 15 min in the presence of 3 mM $CaCl_2$ to inactivate β-amylase, debranching enzyme and β-glycosidase (Sun and Henson, 1991). The heat-treated crude extract was used as α-amylase source. Enzyme activity was determined by quantifying the reducing sugars (glucose equivalents) released from soluble starch (Bernfeld, 1955). The assay mixture contained 0.4 mL of (2 x) Na-acetate buffer (100 mM Na-acetate, pH 5.2 plus 20 mM $CaCl_2$) and 0.4 mL of boiled 2.5% (w:v) soluble starch in 50 mM Na-acetate buffer as a substrate. The reaction was started by addition of 0.4 mL of the heat-treated extract, conducted at 37 °C for 20 and 30 min, and stopped with 0.5 mL of DNS reagent (40 mM 3,5-dinitrosalycilic acid, 0.4 mM NaOH, 1 M K-Na tartrate heated at 50 °C and filtered through filter paper). For the blank (0 min incubation), the DNS reagent was added immediately after the enzymatic extract. Samples were then boiled at 105 °C for 5 min and cooled. Aliquots were then diluted with ddH_2O up to 3 mL and Abs_{530} was measured (Spectrophotometer Secoman UviLine 9400, Biosigma, Cona, Italy). The reducing sugars produced by the enzymatic reaction were quantified by comparing the Abs_{530} of the samples with those of a standard curve of glucose (0-3 µmol). One unit (U) of enzyme activity was defined as the amount of enzyme required to release from soluble starch 1 µmol of glucose min^{-1} under the assay conditions.

2.2.3. Protein content determination

The protein content of the extracts was determined colorimetrically (Bradford, 1976) using bovine serum albumin as a standard (Micro-Bio-Rad Protein Assay; Bio-Rad Laboratories, Segrate, Italy).

All chemicals, except where otherwise indicated, were from Sigma Aldrich, Milan, Italy.

2.3. Gene expression analyses

Total RNA was extracted from embryos (50-100 mg fresh weight) according to the method described for high-quality RNA isolation from seeds containing high levels of starch (Li and Trick, 2005). Contaminant DNA was removed from RNA extracts with Deoxyribonuclease I (Invitrogen-Thermo Fisher Scientific, Monza, Italy) following the manufacturer's instructions. First-strand cDNA synthesis was carried out using the SuperScript® III First-Strand Synthesis SuperMix for qRT-PCR (Invitrogen), according to the manufacturer's instructions.

qRT-PCR analysis of *OsTPP10* (LOC_*Os07g30160*/*Os07g0485000*) and *OsTPP7* (LOC_*Os09g20390*/*Os09g0369400*) was performed on first-strand cDNA in a 20 µL reaction mixture

containing GoTaqR qPCR Master Mix (Promega, Milano, Italy) and the specific primers, using an ABI 7300 Real-Time PCR system (Applied Biosystems Europe B.V., Monza, Italy). The relative transcript level of each gene was calculated by the $2^{-\Delta Ct}$ method using the expression of the *S16* gene as a reference. Primers for qRT-PCR are listed in Table 1.

Table 1. Sequences of the PCR primers used.

Primer name	Sequence 5'→3'	bp	Gene amplified
qTPP7_L	GGGAGGATGGTGTTCGAG	18	*OsTPP7*
qTPP7_R	AGCGAGTCGAGGAGGAACT	19	(LOC_*Os09g20390*/*Os09g0369400*)
qTPP10_L	CACTGTCGCCAATTGTCGAT	20	*OsTPP10*
qTPP10_R	CTCGCGCATCTGGTCAGA	18	(LOC_*Os07g30160*/*Os07g0485000*)
*S16*_L	ACGTCGACGAGGCATCCA	18	*S16*
*S16*_R	CGCGACCACCGAACTTCTT	19	

3. Results

3.1. Effect of saline conditions on coleoptile length in Olcenengo and SR113 embryos

Among the collection of the rice genotypes (ssp. *japonica*) phenotyped under saline conditions during the germination and emergence phases, the genotypes Olcenengo and SR113 were previously identified for extreme behavior concerning tolerance/sensitivity to salt stress (Pesenti et al. 2020a,b). Olcenengo (tolerant) and SR113 (sensitive) were therefore used as models in the present study.

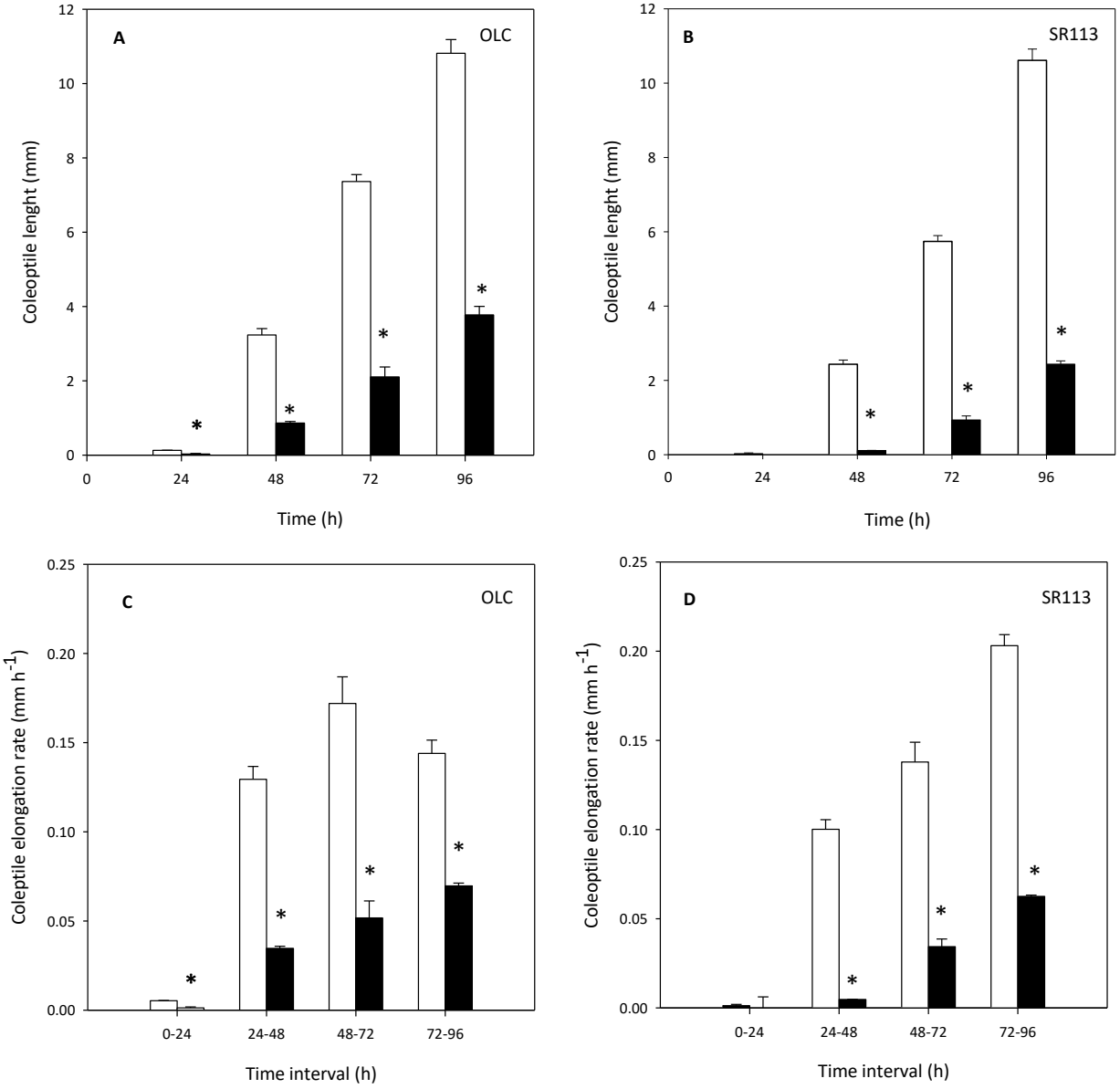

Figure 1. Coleoptile lengths (mm; A,B) and elongation rates (mm h^{-1}; C,D) in Olcenengo (OLC; A,C) and SR113 (B,D) rice embryos grown under control (water, white columns) or saline (150 mM NaCl, black columns) conditions. Values are means ± SE (n=6). Asterisks indicate significant difference ($P \leq 0.05$) between salt-treated and control seedlings.

Figure 1 reports the values of coleoptile length measured after 24, 48, 72, and 96 h in Olcenengo and SR113 seedlings grown in Petri dishes on filter paper wetted with water (control) or 150 mM NaCl (saline condition). Such procedure may simulate with good approximation the environment experienced by rice seeds when sown in the field under dry conditions (aerobiosis). In the controls, the coleoptiles of both genotypes increased their length steadily from 24 to 96 h, even if to different extents. In particular, in SR113 the coleoptile elongation was lower than in Olcenengo up to 72 h (- 76%, - 25%, and - 22%, respectively, at 24, 48, and 72 h) becoming equal at 96 h. Salt

strongly reduced coleoptile elongation in both genotypes, to a greater extent in SR113 (Fig. 1A,B). To better describe the behavior of the genotypes under control and saline conditions, absolute coleoptile length values were used to calculate the coleoptile elongation rates (mm h^{-1}) over 24-h intervals in the time span considered (Fig. 1C,D). In the control condition, in both genotypes, a boost in elongation rate occurred between the 24^{th} and the 48^{th} h, but while in Olcenengo the elongation rates on an hourly basis were essentially constant between 24 and 96 h, in SR113 the elongation rates increased steadily up to 96 h. Salt induced a dramatic reduction of coleoptile elongation rate in both genotypes at all times considered. In Olcenengo, the salt-induced inhibition of the coleoptile elongation rate was lower than in SR113 (- 76% vs - 100% at 24 h, - 73% vs - 95% at 48 h, -70% vs – 75% at 72 h, and – 52% vs - 69% at 96 h).

3.2. Effect of saline conditions on the concentrations of key components related to Tre metabolism in Olcenengo and SR113 embryos

Salt stress affects carbohydrate production and mobilization/use of C storage compounds altering the sink-source relationships, sugar allocation and energy metabolism (Yu et al., 2015). In this framework, the regulation of the Tre and T6P concentrations/ratios, together with that of the levels/activities of the enzymes involved in their metabolism, play an important role. The very low cellular concentrations of Tre and even more so of T6P strengthen the idea of their function in signaling networks (Paul et al., 2017). In particular, T6P acts as a sensor of Suc availability directly affecting the response to changes of environmental conditions. T6P is reported to regulate the activity of SnRK1, a metabolic sensor able to control α-amylase and fundamental in maintaining C homeostasis under stress. Changes in Tre and T6P levels are indeed described to be related to different tolerance to stresses (Delorge et al., 2014; Fernandez et al., 2010).

On this basis we focused our interest on a few components (T6P, Tre, Suc) of the general C metabolism involved in the early seedling growth. Figure 2 reports the changes in cellular concentrations of T6P (Fig. 2A,B), Tre (Fig. 2C,D), Suc (Fig. 2E,F), and of the T6P/Suc ratios (Fig. 2G,H) in embryos of Olcenengo and SR113 at the different times of germination under control or saline conditions.

The concentrations of T6P (Fig. 2A,B) in the embryos of quiescent seeds and after 24 h of incubation were higher in SR113 than in Olcenengo and increased in both genotypes up to 48 h of germination in both water and NaCl remaining essentially constant later on. In the controls the T6P concentrations were similar in both Olcenengo and SR113 throughout the whole time period

considered. However, the salt condition determined a higher increase in T6P concentration in SR113 with respect to Olcenengo from 24 h thereafter. In particular, salt did affect the T6P concentration in Olcenengo only in the first 24 h (+ 51% compared to the controls), whereas in SR113 the T6P levels were always dramatically higher (+ 81%, + 120%, + 100% after 24, 48, and 72 h respectively) than in the controls. The high solubility and low chemical reactivity of Tre allow its accumulation in the cells of all major groups of organisms (except vertebrates) without significant interference with metabolism (Figueroa and Lunn, 2016). Therefore, Tre plays roles as osmolyte, osmoprotectant and C storage compound (Morgutti et al., 2019 and references therein). Figure 2C,D shows the changes in Tre concentrations in Olcenengo and SR113 embryos grown in water or saline conditions. In the controls, the Tre concentrations of both genotypes increased with time after 24 h achieving at 48 h higher values in Olcenengo than in SR113, while at 72 h the values were approximately equalized in the two genotypes. The saline condition resulted in a lower accumulation of Tre compared to the controls, and the effect was most pronounced in SR113 at 72 h.

The concentrations of Suc (Fig. 2E,F) were high in quiescent seeds (t=0); at this stage, Olcenengo showed higher Suc content than SR113. In control conditions, Suc promptly (at 24 h) and steadily decreased in Olcenengo, whereas in SR113 the decrease was delayed (at 48 h). Also in the saline condition the levels of Suc decreased with time, but whereas in Olcenengo they were lower than in the controls already at 24 h, in SR113 they remained generally higher than in the controls. T6P contents are reported to correlate to Suc levels. In fact, T6P accumulates when Suc is high in the cell, acting as a specific signal for Suc availability (Nunes et al., 2013; Figueroa and Lunn, 2016). Moreover, changes in the T6P/Suc ratios have been hypothesized to act as indicators of a different use of C resources as related to sink-source relationships (Lunn et al., 2014; Yadav et al., 2014). In control embryos, the T6P/Suc ratios increased with time in both genotypes reaching absolute values that tended to be higher in SR113 than in Olcenengo up to 48 h, whereas at 72 h the values of the T6P/Suc ratios were very similar in both genotypes. The saline condition induced in both Olcenengo and SR113 up to 48 h a further increase of the T6P/Suc ratios, that in SR113 was still apparent at 72 h. In Olcenengo, at these two time points the T6P/Suc ratio in the saline condition was lower than in SR113 (Figure 2G,H). Since it is reported that low values of the T6P/Suc ratio would activate, while high ratios would inhibit, the mobilization of starch in rice seedlings (Wingler, 2018), the observed results are in agreement with a different attitude of the two genotypes to respond to salt stress and support active growth.

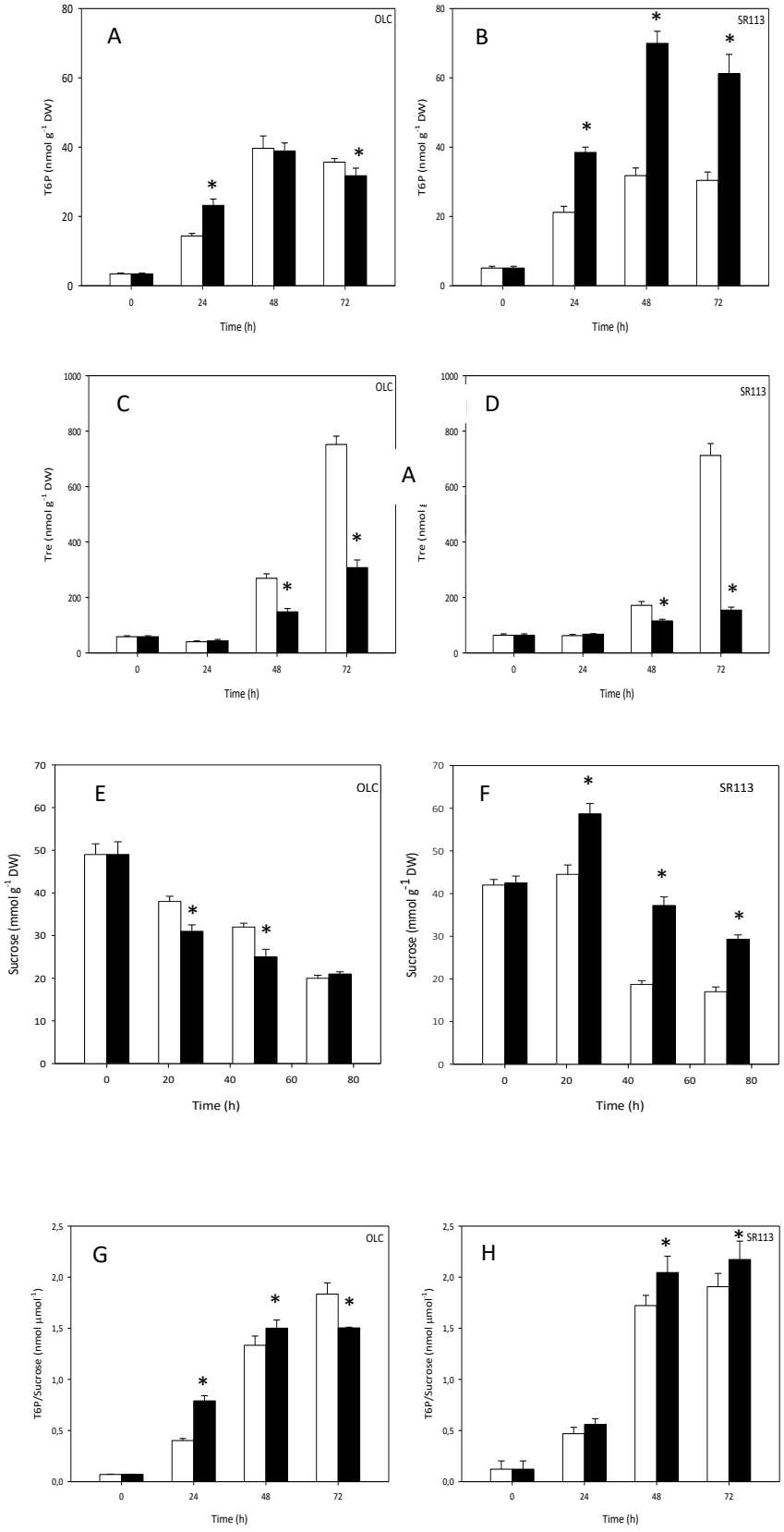

Figure 2. Concentrations of T6P (A,B), Tre (C,D), Suc (E,F) and T6P/Suc ratios (G,H) in embryos of Olcenengo (OLC) and SR113 accessions grown under control (water, white columns) or saline (150 mM NaCl, black columns) conditions. Values are means ± SE (n=6). Asterisks indicate significant difference ($P \leq 0.05$) between salt-treated and control seedlings.

3.3. Effect of saline conditions on α-amylase activity in Olcenengo and SR113 endosperms

The changes in T6P/Suc homeostasis are suggested to reduce the repressive action of T6P on SnRK1 (Kretzschmar et al., 2015). In rice germinating in anaerobiosis, SnRK1A activates the expression of the starvation-induced *α-amylase RAmy3D* gene with consequent appearance of α-amylase protein for starch hydrolysis in the endosperm; this action is realized through the sugar starvation-responsive MYBS1 transcription factor that in turn interacts with a key TA-box Sugar Responsive Element located on the Sugar Responsive Complex of the *α-amylase* promoter region (Lu et al., 2002, 2007; Damaris et al., 2019).

Figure 3 shows the changes in the values of α-amylase specific activity in endosperms of Olcenengo and SR113 during the first 96 h in water or saline conditions. In the controls, α-amylase activity was extremely low at 24 h and increased only at 48 h, consistent with what reported for the appearance of α-amylase protein in rice embryos (Lu et al., 2007). In Olcenengo the activity was high already at 48 h (with a 73-fold increase between 24 h and 48 h) and the values remained constant thereafter. In SR113 in control conditions, the activity was lower than in Olcenengo up to 72 h, with a 10-fold increase between 24 h and 48 h and reached at 96 h a value similar to Olcenengo. Salt delayed the appearance of α-amylase activity, that was barely detectable at 48 h in both genotypes but significantly increased at 72 h. At 96 h, the α-amylase activity increased very strongly (ca + 150%) compared to the controls in Olcenengo, whereas in SR113 the salt stimulation effect did not occur and the activity was similar to that observed in the water control. In addition, at 72 h and 96 h in salt, α-amylase activity was by 2- and 2.8-fold higher in Olcenengo than in SR113, respectively.

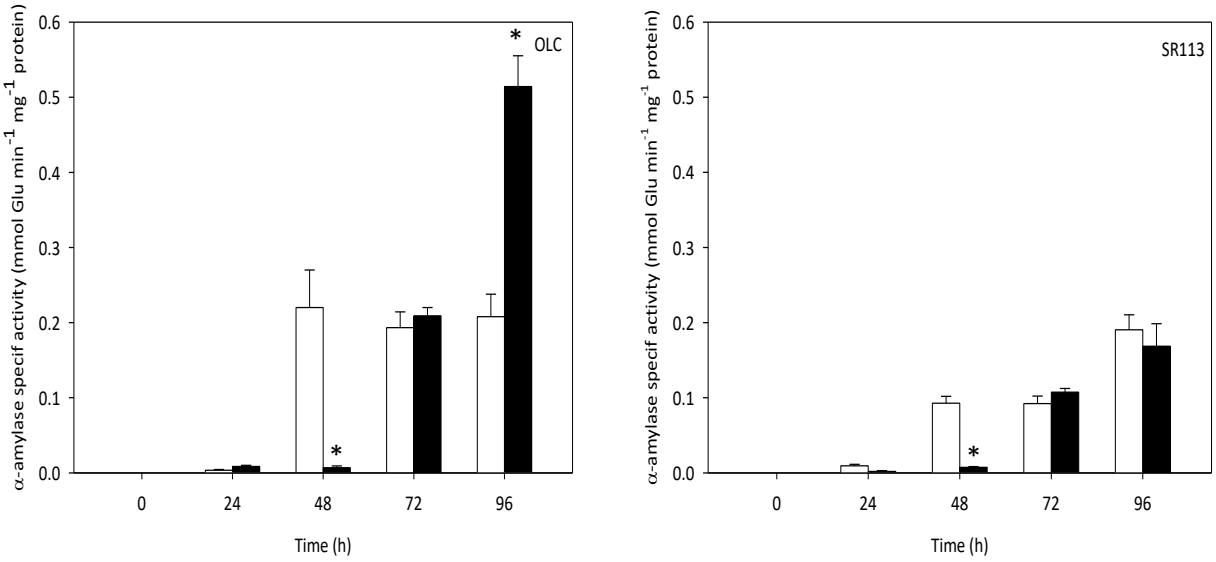

Figure 3. α-amylase specific activity in endosperms of Olcenengo (OLC) and SR113 grown under control (water, white columns) or saline (150 mM NaCl, black columns) conditions. Values are means ± SE (n=6). Asterisks indicate significant difference ($P \leq 0.05$) between salt-treated and control seedlings.

3.4. Effect of saline conditions on the relative expression of two OsTPP genes in Olcenengo and SR113 embryos

A previous GWAS analysis was conducted on a rice germplasm panel of temperate and tropical *japonica* accessions by considering parameters related to the behavior in the early stages of germination and seedling growth under control and saline conditions (Pesenti et al., 2020a,b). The study identified, amongst others, an *OsTPP* gene potentially related to salt tolerance: *OsTPP10* (LOC_*Os07g30160/Os07g0485000*; chromosome 07, from bp 17,816,192 to bp 17,820,602), that was localized within a genomic region (chromosome 07, from bp 17,215,925 to bp 17,847,657) where MTAs for several salt-related traits were positioned. *OsTPP10* belongs to a large family of *TPP* genes encoding isoforms of TPP, that catalyze the dephosphorylation of T6P to Tre, and are therefore important in the modulation of the reciprocal levels of both compounds. Among these, *OsTPP7* (LOC_*Os09g20390*/*Os09g0369400*) was previously described as a determinant of the coleoptile ability to elongate in submersion (Kretzschmar et al., 2015; Nghi et al., 2019). On this basis, we studied the salt-induced changes in the expression profiles of both genes in the very early phases (16, 24, 30, and 48 h) of seed germination (Figs. 4,5). In both genotypes, the transcripts of *OsTPP7* were present already at 16 h of incubation in the controls, at higher levels in SR113 than in Olcenengo, and progressively decreased with time reaching minimum levels at 48 h. Under salt stress, in both genotypes the accumulation of *OsTPP7* transcripts was always higher than in the controls, and particularly so at 16 h of incubation.

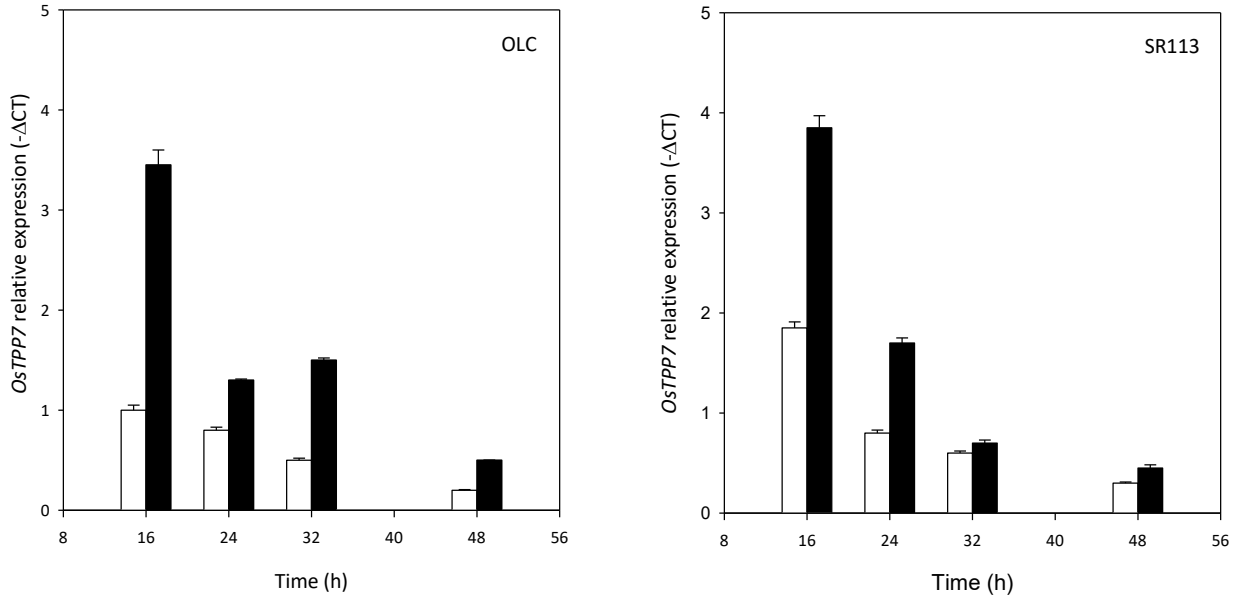

Figure 4. Relative expression profiles of *OsTPP7* in Olcenengo (OLC) and SR113 embryos under control (water, white columns) or saline (150 mM NaCl, black columns) conditions. Values are means ± SE (n=6).

The transcript levels of *OsTPP10* resulted lower than those of *OsTPP7*, but the time course of their expression, highest at the earliest time (16 h) and decreasing thereafter, was similar. In Olcenengo in the control condition the time course of expression of *OsTPP10* was similar to that of *OsTPP7*. Salt induced a very early increase in the transcript levels that was maintained all over the time span investigated. In SR113, in the controls the *OsTPP10* transcript levels were much higher than in Olcenengo and the effect of salt in the first 30 h was different, with a trend leading to a reduction in transcript accumulation; a salt-induced increase in *OsTPP10* expression appeared only at 48 h (Figure 5). Under salt-stress, an outstanding higher expression level was observed in Olcenengo with respect to SR113 in the first time point (16 h).

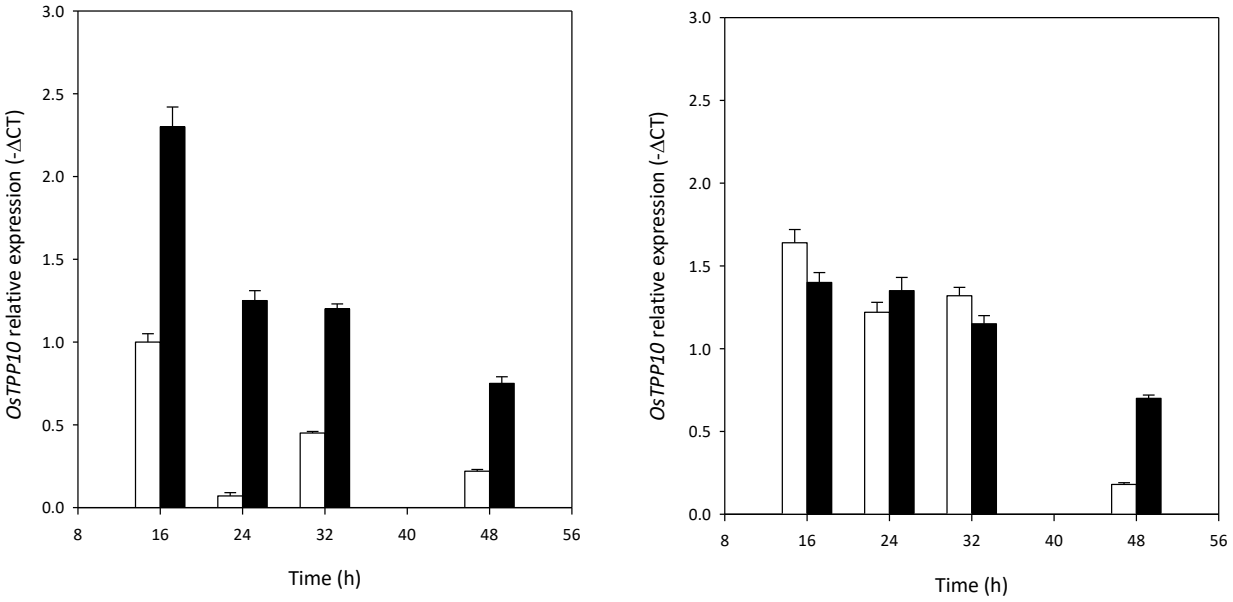

Figure 5. Relative expression profiles of *OsTPP10* in Olcenengo (OLC) and SR113 embryos under control (water, white columns) or saline (150 mM NaCl, black columns) conditions. Values are means ± SE (n=6).

4. Discussion

4.1. Phenotypic responses to salt stress

A previous phenotyping for salt tolerance during germination and emergence of the panel of *japonica* rice accessions (Pesenti et al., 2020a,b) highlighted opposite behaviors of Olcenengo and SR113 that resulted, respectively, tolerant and sensitive to salt stress. The results on coleoptile elongation during the first 96 h of seedling growth confirm these characteristics. In fact, when subjected to salt stress, coleoptile elongation was lower and delayed in SR113 compared to Olcenengo. In particular, whereas Olcenengo was able to elongate in salt already at 48 h, SR113 suffered of a substantial delay (by ca + 24 h) accompanied by a stronger growth inhibition (Fig. 1A,B).

4.2. Differences in metabolic and physiological responses to salt in the two contrasting accessions Olcenengo and SR113

The early phases of seed germination and seedling establishment depend on a heterotrophic metabolism that relies on the adequate supply of C compounds for energy and biosynthetic uses, made available through the hydrolysis of storage reserves, among which starch. In cereals, starch is stored in the endosperm and its hydrolysis is under the hormonal control by the embryo, that in turn will absorb and utilize the monomers produced by the action of the different hydrolytic

enzymes. The endosperm can therefore be regarded to as a source and the embryo as a sink (Fig. 6; Yu et al., 2015).

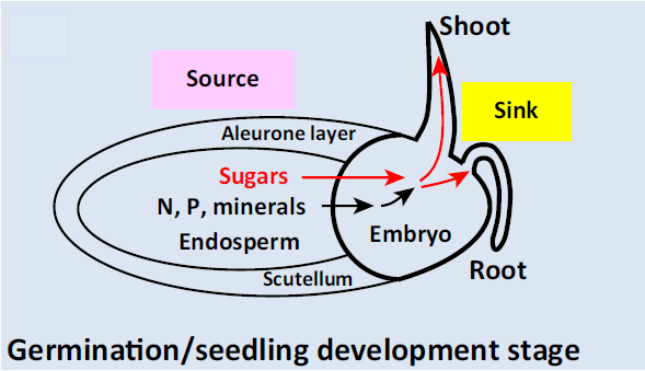

Figure 6. Scheme of relationship between different tissues/organs during cereal grain germination (after Yu et al., 2015).

In plants, developmental transitions and growth are supported by time- and organ-specific metabolic changes that reprogram the source-sink relationships. The sensing of adequate availability of C sources, and the consequent trigger of signaling cascades leading to specific metabolic changes, must be highly coordinated to ensure that the C sink is capable to sustain a developmental program (Wingler, 2018).

In plants, SnRK1 is an important actor of the regulation of energy metabolism, homolog of animal AMP-activated protein kinase and yeast sucrose non-fermenting 1 kinase (Wurzinger et al., 2018). These protein kinases monitor the cell carbohydrate and energetic status for the homeostasis of sugar and energy production/consumption for optimal growth in higher eukaryotes (Polge and Thomas, 2007). Concerning particularly rice, sugar shortage induces the mobilization of starch in the endosperm towards the growing embryo upon expression of SnRK1A, which activates *α-amylase* genes by the mediation, through a complex series of events, of bZIP11 (O'Hara et al., 2013) and MYBS1 (Lu et al., 2007) transcription factors. Although the regulation of SnRK1 is complex, it is important to stress that its activity is downregulated when T6P is high, and the contrary happens when the T6P level of is low and a starvation response (energy-saving program) is triggered (Lastdrager et al., 2014; Nunes et al., 2013; Zhang et al., 2009). The higher concentrations of T6P observed in SR113 embryos grown in the saline condition with respect to Olcenengo suggest a limitation of the SnRK1 activity, whose consequent possible effects would be, through the inhibition of *α-amylase* transcription and synthesis of the corresponding enzyme, the inhibition of starch mobilization and in turn low availability of sucrose for coleoptile growth. The picture appears consistent with the observed strong inhibition of coleoptile elongation in SR113 in saline conditions in comparison to Olcenengo (Fig. 1A,B). In our material, the absolute values of the tissue

concentrations of Tre reached a maximum of ca 700 nmol g^{-1} DW (control embryos of Olcenengo and SR113 at 72 h), the same order of magnitude of what observed (ca 500 nmol g^{-1} DW) in shoots of 9-week old rice plantlets, although in that material the salt treatments appeared to increase (+ 50%) the Tre concentrations compared to the untreated plants (Garg et al., 2002). Since in the germinating embryos of Olcenengo and SR113 lower concentrations of Tre were observed in the salt condition than in the controls, it seems that in this material at the developmental stage considered Tre does not play osmotic or osmo-protectant roles. In general, the lower Tre concentrations observed in SR113 in salt conditions (Figure 2D) appear consistent with the higher concentrations of T6P (Figure 2B), even if the very different amounts of Tre (range 80-700 nmol g^{-1} DW) and T6P (range 5-70 nmol g^{-1} DW) make it very difficult to conduct a stringent comparison between the levels of the two compounds.

During germination and early seedling establishment, adequate availability of sucrose is the prerequisite for the obtainment of hexoses to be conveyed into the energetic metabolism that sustains the heterotrophic embryo growth. The lower Suc concentrations observed in Olcenengo in the saline condition compared to the controls, and their early and progressive decrease with time (Figure 2E), suggest that this genotype may use efficiently the available Suc in this stress condition. On the contrary, the consumption of Suc seemed impaired in SR113 (Fig. 2F) where the levels Suc, while decreasing, remained at all the times considered much higher under salt stress than in the controls, suggesting a lower capability of SR113 in exploiting Suc for growth in this unfavorable condition. Interestingly, we observed in both Olcenengo and SR113 embryos, during the stress period considered, that the changes of T6P concentrations appeared in general coherent with those observed for Suc and in agreement with the evidence indicating a high correlation between the levels of these two sugars in the tissues (Lunn et al., 2014; Yadav et al., 2014). In this context, it was also suggested that the T6P/Suc ratio acts as a signal and is part of a homeostatic mechanism that controls, in a complex way, the Suc levels in the cell and finely tunes its availability during development and in different environmental conditions (Yadav et al., 2014). The T6P/Suc ratios depend, on one side, on the levels of Suc (as regulated by the balance between its production, upon mobilization of C reserves, and consumption by metabolic activities), and, on the other side, on those of T6P (as regulated by the balance between its synthesis by TPS and its dephosphorylation by TPP). The values of the T6P/Suc ratio were hypothesized to activate (low ratios) or inhibit (high ratios) the starch mobilization in rice seedlings with different attitude to respond to the unfavorable condition of anaerobiosis and support coleoptile growth; a specific role of an *OsTPP* isogene, i.e.

OsTPP7, was forwarded for the control and adequate buffering of T6P levels in turn involved in its regulatory function (Kretzschmar et al., 2015). In our material, in SR113 the constantly higher values of T6P/Suc ratios observed in the salt condition compared to the controls seem consistent with the inhibited growth of this genotype under salt stress. Moreover, at least at 48 h and 72 h under salt, the T6P/Suc ratios were lower in Olcenengo than in SR113, supporting a higher capability to mobilize C resources in this tolerant accession consistent with lesser growth inhibition (Fig. 2G,H).

For a successful germination, a finely tuned and balanced communication and exchange of energy substrates between source and sink tissues/organs is necessary. In this context, the Suc/T6P/SnRK1 system has been suggested to be involved in the regulation of sink strength in germinating seeds (Yu et al., 2015). A good consistency between the values of T6P/Suc ratios in embryonic axes (sinks) and α-amylase activity in the endosperm (source) could be observed, in our material, in the seeds germinated for 48 h (Figs. 2G,H and 3). Interestingly, in the embryos of both genotypes the changes in the values of the signaling component T6P/Suc ratio were apparent already at 24 h of germination in both water and salt conditions, even if at different extents (Fig. 2G,H). In the endosperms, α-amylase activity, one of the targets of this multi-component regulatory mechanism (Damaris et al., 2019), showed changes only later on (48 h). At this time, in the control condition, the T6P/Suc ratio was lower in Olcenengo embryos than in SR113, corresponding to higher α-amylase activity in the endosperm of Olcenengo. It is interesting to stress out that a consistent shift in the timing of appearance of SnRK1A (at 24 h of germination) and α-amylase (at 48 h) proteins has been described in rice embryos germinating in water (Lu et al., 2007). Concerning the salt condition, it is interesting to notice that the signal of the T6P/Suc ratio was clearly detectable at 48 h in both genotypes, but it was not accompanied by a response in terms of α-amylase activity, that remained at this time barely detectable (Figs. 2G,H and 3). In this framework, in our system salt appears to possibly further delay, through unidentified mechanism(s), the perception/transduction of the Suc/T6P/(SnRK1) signal. It may then be speculated that, in the early phases of rice germination in salt, some other components of the complex multi-actor sugar signaling pathway may be involved. The literature reports the presence in rice of two SnRK1-Interacting Negative regulators (SKINs) able to antagonize the function of SnRK1A at a double level, i.e., by inhibiting the expression of *MYBS1* and/or by interfering with the correct distribution of both SnRK1A and MYB1 between nucleus and cytoplasm. The final result would be, in both cases, a lack of activation of *α-amylase* transcription, and eventual stunted seedling growth because of the inhibition of starch and nutrient mobilization from the endosperm (Lin et al., 2014). The fine tuning of this dynamic balance would

also be affected by the phytoregulators ABA and GA (Lin et al., 2014; Yu et al., 2015). Moreover, GA deficiency due to NaCl treatment has been reported to inhibit rice seed germination for decreased α-amylase activity *via* down-regulation of *α-amylase* gene expression (Liu et al., 2018). In our system, at 72 h the effect of salt on the T6P/Suc ratios was different in Olcenengo and in SR113 (Fig. 2G,H): the value of the T6P/Suc ratio was diminished by salt in Olcenengo while it remained high in SR113; this signal was accompanied, at the following time (96 h), by a different activity of α-amylase, that resulted dramatically increased in Olcenengo, with an activity approximately three times higher than in SR113 at the same time and condition (Fig. 3). Lower T6P/Suc ratios are in fact interpreted as signal of sugar starvation, a cellular status that affects SnRK1 at the levels of both gene expression and lower repression of activity by T6P (Lu et al. 2007), eventually enhancing α-amylase production.

The overall picture of *OsTPP7* expression appeared essentially similar in both genotypes and in both growth conditions. *OsTPP7 e*xpression was increased in the presence of salt, suggesting that this specific *OsTPP* may indeed be involved in the salt response, but not in the determination of tolerance/sensitivity to salt stress in seeds grown in aerobiosis (Fig. 4), differently to what described for anaerobic stress (Kretzschmar et al., 2015; Nghi et al., 2019). Different profiles of accumulation of *OsTPP10* transcripts in response to the saline condition were observed up to 30 h, including: *i*) higher accumulation of transcripts than in the controls in Olcenengo; *ii*) generally lower accumulation of transcripts than in the controls in SR113; *iii*) a relevant higher accumulation of transcripts at 16 h in Olcenengo with respect to SR113 in the salt condition. These differential responses do suggest a possible role of this gene, and likely of its protein product, in the determination of the different salt tolerance/sensitivity in the two genotypes during germination in aerobic conditions.

It appears possible to speculate a temporal cascade of events between the changes in the levels of *OsTPP10* transcripts (within 30 h and higher in Olcenengo in the early 16 h time point) and the subsequent (24-48 h) changes of the substrate (T6P)-product (Tre) of the reaction catalyzed by the protein encoded by this gene (OsTPP; Figs. 2A-D and 4).

The picture here described can be discussed also in terms of the so-called “T6P-sucrose nexus” (Yadav et al., 2014), that hypothesizes that high levels of Suc may both activate TPS (T6P synthesis) and inhibit TPP (T6P dephosphorylation). Overall, these effects would induce an increase in the T6P levels upon high availability of Suc. TPS1 is indeed reported to be stimulated by high sucrose levels in turn accompanied by high T6P levels. Moreover, the T6P/Suc relationship is mediated by still unidentified protein(s) that may stimulate the activity of TPS and/or reduce that

of TPP (Yadav et al., 2014). Indeed, in SR113 the Suc levels in salt condition were generally higher than in the controls and than those observed in Olcenengo in the same condition (Fig. 2G,H), allowing to hypothesize a similar regulation mechanism also in our material.

5. Conclusions

The Suc/T6P/SnRK1 signaling system is part of an extremely complex metabolic network in which each component is subjected to own regulatory mechanism(s) that also foresee a different cell/tissue localization depending on specific developmental phases and environmental conditions (Yu et al., 2015). For this reason, it is not possible to exclude that other factors may affect the finely tuned and dynamically balanced levels of the single components considered in the present work.

The observed higher vigor of Olcenengo compared to SR113 in the presence of salt seems to involve, with an active role, the *OsTPP10* gene with particular regard to the mechanisms(s) that regulate its expression under salt stress. Additional work is necessary to assess whether some allelic variation concerning *OsTPP10* exists between the varieties here considered, and in general between salt-tolerant and salt-sensitive groups in *japonica* rice. Isolation and sequencing of the *OsTPP10* gene in Olcenengo and SR113 is foreseen in order to highlight possible polymorphisms in coding or regulatory regions. The necessary parallel functional characterization of the OsTPP10 enzyme will allow to verify the possible existence of structural and in turn kinetic differences in rice genotypes differing for salt tolerance at the germination and seedling establishment stages. Work is currently in progress to assess possible different patterns of expression of other components (SnRK1, MYBS1, bZIP11) of the Suc/T6P/SnRK1 system.

6. References

Bernfeld, P. (1955). Amylase alpha and beta. Methods Enzymol. 1, 149-158.

Bradford, M.M. (1976). A rapid and sensitive method for the quantitation of microgram quantities of protein utilizing the principle of protein-dye binding. *Anal. Biochem.* 72, 248-254.

Damaris, R. N., Lin, Z., Yang, P., and He, D. (2019). The rice alpha-amylase, conserved regulator of seed maturation and germination. *Int. J. Mol. Sci.* 20, 450. doi:10.3390/ijms20020450.

Daszkowska-Golec, A. (2011). *Arabidopsis* seed germination under abiotic stress as a concert of action of phytohormones. *Omics* 15, 763-774. doi: 10.1089/omi.2011.0082.

Delatte, T.L., Selman, M.H.J., Schluepmann, H., Somsen, G.W., Smeekens, S.C.M., and de Jong, G.J. (2009). Determination of trehalose-6-phosphate in *Arabidopsis* seedlings by successive extractions followed by anion exchange chromatography–mass spectrometry. *Anal. Biochem.* 389, 12-17. doi: 10.1016/j.ab.2009.03.003.

Delorge, I., Janiak, M., Carpentier, S., and Van Dijck, P. (2014). Fine tuning of trehalose biosynthesis and hydrolysis as novel tools for the generation of abiotic stress tolerant plants. *Front. Plant Sci.* 5, 147. doi: 10.3389/fpls.2014.00147.

Dong, J., Zhao, J., Zhang, S., Yang, T., Liu, Q., Mao, X., et al. (2019). Physiological and genome-wide gene expression analyses of cold-induced leaf rolling at the seedling stage in rice (Oryza sativa L.). *Crop J.* 7, 431–443. doi: 10.1016/j.cj.2019.01.003.

Fernandez, O., Béthencourt, L., Quero, A., Sangwan, R.S., and Clément, C. (2010). Trehalose and plant stress responses: friend or foe? *Trends Plant Sci.* 15, 409-417. doi: 10.1016/j.tplants.2010.04.004.

Figueroa, C.M., and Lunn, J.E. (2016). A tale of two sugars: trehalose 6-phosphate and sucrose. *Plant Physiol.* 172, 7-27. doi: 10.1104/pp.16.00417.

Flowers, T.J., and Yeo, A. R. (1981). Variability in the resistance of sodium chloride salinity within rice (*Oryza sativa* L.) varieties. *New Phytol. 88*, 363–373. doi: 1 0.1111/j.1469-8137.1981.tb01731.x.

Garg, A.K., Kim, J.K., Owens, T.G., Ranwala, A.P., Do Choi, Y., Kochian, L.V., and Wu, R.J. (2002). Trehalose accumulation in rice plants confers high tolerance levels to different abiotic stresses. *Proc. Natl. Acad. Sci. USA* 99, 15898-15903. doi: 10.1073/pnas.252637799.

Ge, L.-F., Chao, D.-Y., Shi, M., Zhu, M.-Z., Gao, J.-P., and Lin, H.-X. (2008). Overexpression of the trehalose-6-phosphate phosphatase gene OsTPP1 confers stress tolerance in rice and results in the activation of stress responsive genes. Planta 228, 191–201. doi: 10.1007/s00425-008-0729-x.

Ghosh, B., Md, N.A., and Gantait, S. (2016). Response of rice under salinity stress: a review update. *J. Res. Rice* 4, 167. doi: 10.4172/2375-4338.1000167.

Guglielminetti, L., Yamaguchi, J., Perata, P., and Alpi, A. (1995). Amylolytic activities in cereal seeds under aerobic and anaerobic conditions. *Plant Physiol.* 109, 1069–1076. doi: 10.1104/pp.109.3.1069.

Hannachi, S., and Van Labeke, M.C. (2018). Salt stress affects germination, seedling growth and physiological responses differentially in eggplant cultivars (*Solanum melongena* L.). *Sci. Hort.* 228, 56–65. doi: 10.1016/j.scienta.2017.10.002.

Heenan, D.P., Lewin, L.G, and McCaffery, D.W. (1988). Salinity tolerance in rice varieties at different growth stages. *Aust. J. Exp. Agric.* **28**, 343-349. doi: 10.1071/EA9880343.

Hoang, T.M.L., Tran, T.N., Nguyen, T.K.T., Williams, B., Wurm, P., Bellairs, S., et al. (2016). Improvement of salinity stress tolerance in rice: Challenges and opportunities. *Agronomy* 6, 54. doi:10.3390/agronomy6040054.

Horie, T., Karahara, I., and Katsuhara, M. (2012). Salinity tolerance mechanisms in glycophytes: An overview with the central focus on rice plants. *Rice* 5, 11. doi: 10.1186/1939-8433-5-11.

Kretzschmar, T., Pelayo, M.A.F., Trijatmiko, K.R., Gabunada, L.F.M., Alam, R., Jimenez, R., et al. (2015). A trehalose-6-phosphate phosphatase enhances anaerobic germination tolerance in rice. *Nature Plants* 1, 15124. doi: 10.1038/nplants.2015.124.

Lastdrager, J., Hanson, J., and Smeekens, S. (2014). Sugar signals and the control of plant growth and development. *J. Exp. Bot.* 65, 799-807. doi: 10.1093/jxb/ert474.

Lee, K.-S., Choi, W.-Y., Ko, J.-C., Kim, T.-S., and Gregorio, G.B. (2003). Salinity tolerance of japonica and indica rice (*Oryza sativa* L.) at the seedling stage. *Planta* 216, 1043–1046. doi: 10.1007/s00425-002-0958-3.

Li, Z., and Trick, H.N. (2005). Rapid method for high-quality RNA isolation from seed endosperm containing high levels of starch. *BioTechniques* 38, 872-876. doi: 10.2144/05386BM05

Lin, C.R., Lee, K-W., Chen, C-Y., Hong, Y-F., Chen, J-L., Lu, C-A., et al. (2014). SnRK1A-interacting negative regulators modulate the nutrient starvation signaling sensor SnRK1 in source-sink communication in cereal seedlings under abiotic stress. *Plant Cell* 26, 808-827. doi: 10.1105/tpc.113.121939.

Lisec, J., Schauer, N., Kopka, J., Willmitzer, L., and Fernie, A.R. (2006). Gas chromatography mass spectrometry–based metabolite profiling in plants. *Nat. Protoc.* 1, 387-396. doi: 10.1038/nprot.2006.59.

Liu, L., Xia, W., Li, H., Zeng, H., Wei, B., Han, S., and Yin, C. (2018). Salinity inhibits rice seed germination by reducing α-amylase activity via decreased bioactive gibberellin content. *Front. Plant Sci.* 9, 275. doi: 10.3389/fpls.2018.00275.

Lu, C-A., Ho, T.H.D., Ho, S.L., and Yu, S.M. (2002). Three novel MYB proteins with one DNA binding repeat mediate sugar and hormone regulation of α-amylase gene expression. *Plant Cell 14*, 1963-1980. doi: 10.1105/tpc.001735.

Lu, C-A., Lin, C-C., Lee, K-W., Chen, J-L., Huang, L-F., Ho, S-L., et al. (2007). The SnRK1A protein kinase plays a key role in sugar signaling during germination and seedling growth of rice. *Plant Cell* 19, 2484-2499. doi: 10.1105/tpc.105.037887.

Luan, Z., Xiao, M., Zhou, D., Zhang, H., Tian, Y., Wu, Y., et al. (2014). Effects of salinity, temperature, and polyethylene glycol on the seed germination of sunflower (*Helianthus annuus* L.). *Sci. World J.* 2014. doi: 10.1155/2014/170418.

Lunn, J.E., Delorge, I., Figueroa, C.M., Van Dijck, P., and Stitt, M. (2014). Trehalose metabolism in plants. *Plant J.* 79, 544-567. doi: 10.1111/tpj.12509.

Martínez-Barajas, E., Delatte, T., Schluepmann, H., de Jong, G.J., Somsen, G.W., Nunes, C., et al. (2011). Wheat grain development is characterized by remarkable trehalose 6-phosphate accumulation pregrain filling: tissue distribution and relationship to SNF1-related protein kinase1 activity. *Plant Physiol.* 156, 373–381. doi. org/10.1104/pp.111.174524

Morgutti, S., Negrini, N., Pucciariello, C., and Sacchi, G.A. (2019). "Role of Trehalose and Regulation of its Levels as a Signal Molecule to Abiotic Stresses in Plants". *In* Plant Signaling Molecules, eds. M.I.R. Khan, P.S. Reddy, A. Ferrante, N. Khan (Woodhead Publishing, Sawston, UK), 235-255.

Munns, R., and Gilliham, M. (2015). Salinity tolerance of crops–what is the cost? *New Phytol.* 208, 668-673. doi: 10.1111/nph.13519.

Munns, R., and Tester, M. (2008). Mechanisms of salinity tolerance. *Annu. Rev. Plant Biol.* 59, 651–681. doi: 10.1146/annurev.arplant.59.032607.092911.

Nghi, K.N., Tondelli, A., Valè, G., Tagliani, A., Marè, C., Perata, P., and Pucciariello, C. (2019). Dissection of coleoptile elongation in japonica rice under submergence through integrated genome-wide association mapping and transcriptional analyses. *Plant Cell Environ.* 42, 1832-1846. doi: 10.1111/pce.13540

Nunes, C., O'Hara, L.E., Primavesi, L.F., Delatte, T.L., Schluepmann, H., Somsen, G.W., et al. (2013). The trehalose 6-phosphate/SnRK1 signaling pathway primes growth recovery following relief of sink limitation. *Plant Physiol.* 162, 1720-1732. doi: 10.1104/pp.113.220657.

O'Hara, L.E., Paul, M.J., and Wingler, A. (2013). How do sugars regulate plant growth and development? New insight into the role of trehalose-6-phosphate. *Mol. Plant.* 6, 261-274. doi: 10.1093/mp/sss120.

Paul, M. J., Oszvald, M., Jesus, C., Rajulu, C., and Griffiths, C.A. (2017). Increasing crop yield and resilience with trehalose 6-phosphate: targeting a feast–famine mechanism in cereals for better source–sink optimization. J. Exp. Bot. 68, 4455–4462. doi: 10.1093/jxb/erx083.

Pesenti, M., Orasen, G., Negrini, N., Morgutti, S., Nocito, F.F., Colombo, F., et al. (2020a) Genome-wide association study of salinity tolerance during germination and seedling emergence from soil in rice (*Oryza sativa* L.). Submitted for publication.

Pesenti, M., Orasen, G., Abruzzese, A., Lucchini, G., Morgutti, S., Negrini, N., et al. (2020b) Genome-wide association study for salinity tolerance during growth in a panel of *japonica* rice (*Oryza sativa* L.) accessions. Submitted for publication.

Polge, C., and Thomas, M. (2007). SNF1/AMPK/SnRK1 kinases, global regulators at the heart of energy control? *Trends Plant Sci.* 12, 20–28. doi: 10.1016/j.tplants.2006.11.005

Reddy, A.M., Francies, R.M., Rasool, S.N., and Reddy, V.R.P. (2014). Breeding for tolerance stress triggered by salinity in rice. *Int. J. Appl. Biol. Pharm. Technol.* 5, 167–176. doi: 10.1016/j.rsci.2016.09.004

Roessner-Tunali, U., Hegemann, B., Lytovchenko, A., Carrari, F., Bruedigam, C., Granot, D., and Fernie, A.R. (2003). Metabolic profiling of transgenic tomato plants overexpressing hexokinase reveals that the influence of hexose phosphorylation diminishes during fruit development. *Plant Physiol.* 133, 84-99. doi: 10.1104/pp.103.023572.

Shima, S., Matsui, H., Tahara, S., and Imai, R. (2007). Biochemical characterization of rice trehalose-6-phosphate phosphatases supports distinctive functions of these plant enzymes. *FEBS J*. 274, 1192-1201. doi: 10.1111/j.1742-4658.2007.05658.x

Sun, Z., and Henson, C.A. (1991). A quantitative assessment of importance of barley seed α-amylase, β-amylase, debranching enzyme, and α-glucosidase in starch degradation. *Arch. Biochem. Biophys.* 284, 298–305. doi: 10.1016/0003-9861(91)90299-x.

Toraño, J.S., Delatte, T.L., Schluepmann, H., Smeekens, S.C.M., de Jong, G.J., and Somsen, G.W. (2012). Determination of trehalose-6-phosphate in *Arabidopsis thaliana* seedlings by hydrophilic-interaction liquid chromatography–mass spectrometry. *Anal. Bioanal. Chem.* 403, 1353–1360. doi: 10.1007/s00216-012-5928-4.

Wingler, A. (2018). Transitioning to the next phase: the role of sugar signaling throughout the plant life cycle. *Plant Physiol.* 176, 1075-1084. doi: 10.1104/pp.17.01229

Wurzinger, B., Nukarinen, E., Nägele, T., Weckwerth, W., and Teige, M., 2018. The SnRK1 kinase as central mediator of energy signaling between different organelles. *Plant Physiol.* 176, 1085-1094. doi: 10.1104/pp.17.01404

Xia, Y-G., Sun, H-M., Wang, T-L., Liang, J., Yang, B-Y., and Kuang, H-X. (2018). A modified GC-MS analytical procedure for separation and detection of multiple classes of carbohydrates. *Molecules* 23, 1284-1303. doi:10.3390/molecules23061284.

Yadav, U.P., Ivakov, A., Feil, R., Duan, G.Y., Walther, D., Giavalisco, P., et al. (2014). The sucrose–trehalose 6-phosphate (Tre6P) nexus: specificity and mechanisms of sucrose signalling by Tre6P. *J. Exp. Bot.* 65, 1051-1068. doi: 10.1093/jxb/ert457.

Yu, S.M., Lo, S.F., and Ho, T.H.D. (2015). Source–sink communication: regulated by hormone, nutrient, and stress cross-signaling. *Trends Plant Sci.* 20, 844-857. doi: 10.1016/j.tplants.2015.10.009.

Zhang, Y., Primavesi, L.F., Jhurreea, D., Andralojc, P.J., Mitchell, R.A.C., Powers, S.J., et al. (2009). Inhibition of SNF1-related protein kinase1 activity and regulation of metabolic pathways by trehalose-6-phosphate. *Plant Physiol.* 149, 1860-1871. doi: 10.1104/pp.108.133934.

General conclusions

The existence of wide genetic variability for salt tolerance within rice genotypes is a prerequisite of paramount importance in genetic improvement programs. The establishment of suitable germplasm collections is crucial for the success of breeding programs.

Concerning the rice *indica* subspecies, several QTLs genes and molecular markers related to the phenotypic variability in the response to salt stress have been identified and exploited for the marker assisted breeding programs. (Naveed et al., 2018). Within the rice *japonica* subspecies far fewer information are available. The reason of this difference resides in the fact that *indica* varieties are often grown in environments where salt stress is quite severe, different than in temperate areas, where salt stress is mild, and *japonica* is the most widely cultivated subspecies.

Rice is relatively tolerant to salinity stress during germination, active tillering and towards maturity, but sensitive during early seedling establishment and reproductive stage (Heenan et al., 1988; Zeng et al., 2001). The molecular mechanisms and the underlying genes involved in the salt stress response may vary according to the specific phenological phase. Moreover, different varieties may have different mechanisms to deal with salt stress. In fact, some are tolerant only in the initial stages of vegetative growth, others when approaching to the flowering phase (Zeng et al., 2001).

Taking into account the aforementioned considerations it is clear that in order to be able to identify molecular tools useful to counteract salt stress in rice area where japonica cultivars are cultivated, investigations on the natural variation existing in large germplasm collections concerning tolerate mild salt stress are suggested. Moreover, it is important that the studies are carried out both at specific phenological stages of the crop, as well as throughout its whole growth period. The research activities here described and commented had been developed according to this logic.

In this study we focused on the characterization of a large panel of *japonica* genotypes subjected to mild-salt stress condition considering: *i*) phenotyping during germination, emergence, and vegetative growth, up to flowering stage; *ii*) GWAS based upon previous GBS and the phenotyping results; *iii*) identification of several molecular markers significantly associated to the phenotypic variability observed in term of salt tolerance; iv) a list of candidate genes included in the MTAs highlighted by the positive genotype-phenotype associations; *v*) preliminary validation of the involvement of two of these candidate genes, i.e. *OsTPP10* and *OsOVP6* involved in the processes regulating seedling vigor under stress and in the control of the Na^+/K^+ ratio in plant tissues, respectively.

The conclusions emerging from the results obtained are listed below.

- The rice accession panel considered showed a broad range of the values for the different phenotypical parameters considered, both in control and salt conditions. Although, it is not normally distributed the variability within the accession panel of each parameter in both control and salt conditions, as well as that of the tolerance index considered (SSI) is continuous and thus, due to quantitative and not simply qualitative mechanisms. Moreover, almost all the traits measured show significant broad sense hereditability within the rice panel.

  Thus, phenotyping activities indicate that the rice accession panel defined can be reasonably used in GWAS aimed at identifying molecular markers, MTAs and/or alleles potentially useful in breeding programs with the objective to develop new japonica rice genotypes showing tolerance to mild salt stress conditions in different phenological stages.
- Grouping the rice accessions according their SSI values it has been possible to define cores of genotypes particularly tolerant (belonging to the 10^{th} percentile) or sensitive (belonging to the 90^{th} percentile) to mild salt stress during seed germination and early seedling growth, as well as during vegetative growth stages up to till to flowering.

  Concerning seed germination and seedling growth two accessions were clearly identified as strongly tolerant or sensitive: Olcenengo and SR113, respectively. Concerning vegetative stages, the results were less clear, but choosing genotypes within the 10^{th} and the 90^{th} percentile for at least two parameters a core collection including eight more tolerant (Samba, Galileo, Virgo, Muga, Orione, Vulcano, IBO3003 and Bengal) and twelve more sensitive (Ostiglia, CT58, L201, L205, Agostano, Carrico, Pecos, Zena, Santerno, Venere, Vialone Nano and Miara) accession was defined.
- Adopting GWAS approaches 28 significant genotype-phenotype associations were identified concerning seed germination and early seedling growth phases, whereas other 21 significant genotype-phenotype associations resulted considering the vegetative and the early reproductive (12 days after flowering) phases. Only the MTAs 1123, located on the chromone 10, emerged from both the GWAS. The large differences observed between the results emerging from the GWAS are coherent with the complexes molecular basis of the salt tolerance trait that, moreover, involves different mechanisms depending on the plant developmental stage considered.

- The preliminary haplotypes analysis carried out did not allow to link unequivocally specific allele configurations of the SNP markers identified to salt tolerance traits. This could be due to the relatively low marker coverage (32.5 k SNPs) of the GBS analysis adopted.
- The results on coleoptile elongation during the first 96 h of seedling growth under salt stress confirm that Olcenengo is a relatively tolerant rice accessions and SR113 a sensitive one. The observed higher vigor of Olcenengo compared to SR113 under salt condition involve the timing pattern of stress is temporally related to the expression pattern of the the *OsTPP10* gene involved in the SnRK1-mediated regulation of energy metabolism is plant cells under different abotic stresses (Lastdrager et al., 2014; Nunes et al., 2013; Zhang et al., 2009). the Snf1-related protein kinase. Further work is necessary to assess whether some allelic variation concerning *OsTPP10* exists between the two varieties here considered, and in general between salt-tolerant and salt-sensitive groups in the rice panel studied. Isolation and sequencing of the *OsTPP10* gene in Olcenengo and SR113 is foreseen in order to individuate the possible presence of significant sequence polymorphisms is in progress. Moreover, the results obtained make it interesting to verify, once obtained the purified OsTPP10 proteins from the two rice accessions, the possible existence of structural and kinetic differences between them.
- Among the putative candidate genes emerged from GWAS analyses, particular attention was payed to *Os01g0337500*, coding one of the peptides constituting the vacuolar H^+-pyrophosphatase 6 (OsOVP6; Plett et al., 2010). This PP_i-dependent H^+ pump located on the tonoplast contributes to generate the H^+ transmembrane electrochemical gradient that energetically drives the activity of the Na^+/H^+ NHX antiporters that, by accumulating excess Na^+ into the vacuole, limit its toxic effects in the cytoplasm (Kobayashi et al., 2017; Almeida et al., 2017). Vacuolar H^+-PPase, together with the Na^+/H^+ exchanger NHX and the K^+ Outward Rectifying (KOR) channels, plays a key role in the complex network of the Na^+ and K^+ transport mechanisms that contribute to the maintenance of the homeostasis of Na^+ and K^+ in the cytoplasm of plant cells, particularly relevant in salt stress conditions. Indirect observations obtained measuring by in vivo ^{31}P-NMR approaches the

  GWAS allowed to identify other interesting candidate genes: *Os10g0438000* coding for a protein crucial for the assembly of KOR channels, and *Os10g0436900* coding a CCX protein with the function of cation/Ca^{2+} exchanger. All these activities are involved in the maintenance of proper Na^+/K^+ ratios under salt stress most probably playing a role in salt

tolerance; they may therefore represent putative promising candidates exploitable for the future selection of salt-resistant rice lines.